



**Università
di Genova**



Quasiparticles in Exotic Phases of Matter

Advisors

Prof. Nicola Maggiore

Prof. Maura Sassetti

Prof. Niccolò Traverso Ziani

Candidate

Daniel Sacco Shaikh

Thesis submitted to Università degli Studi di Genova for the degree of
Doctor of Philosophy in Physics and Nanosciences, Curriculum Physics

Abstract

Phases of matter have always attracted great interest within the scientific community, as they represent emergent phenomena arising from the collective behavior of a large number of interacting degrees of freedom. Their macroscopic properties, often impossible to predict directly from the microscopic scale, can be effectively captured in terms of quasiparticles, *i.e.* particle-like low-energy excitations that emerge from interactions among the underlying microscopic constituents and may exhibit properties entirely different from those of any fundamental particle, reflecting the rich structure of the many-body system. In this Thesis, we investigate two classes of quasiparticles that arise in distinct exotic phases of matter.

The first class appears in antiferromagnetic quantum spin chains with discrete symmetries and frustrated boundary conditions, namely periodic boundary conditions with an odd number of sites. In this setting, the competition between global and local orders produces exotic gapless, non-relativistic excitations above the ground state, which can dramatically modify the physics even in the thermodynamic limit. In particular, we focus on how this specific choice of boundary conditions profoundly modifies the phase diagram of one of the most famous integrable models, the XY chain.

The second class consists of subdimensional quasiparticles, excitations whose mobility is restricted to lower-dimensional subspaces and which characterize the low-energy sector of emerging fracton phases of matter. Quasiparticles with restricted mobility first appeared in exactly solvable quantum spin models, and it was later realized that they can also emerge from higher-rank gauge theories. In this part of the Thesis, we develop Lorentz-covariant gauge field theories for

fractons in $2 + 1$ dimensions, starting from the first principles of Quantum Field Theory (fields and symmetries), with the aim of embedding the features observed in the condensed matter literature into a more formal field theoretical framework.

Acknowledgements

First of all, I wish to thank my supervisors Nicola Maggiore, Maura Sassetti, and Niccolò Traverso Ziani, for their constant guidance and for introducing me to the world of research. I have learned so much from all of you, and your enthusiasm and support have deeply fuelled my passion for theoretical physics.

I would then like to acknowledge all the other people with whom I interacted during these three years: the many collaborators and the professors in Genoa. Among the latter, a very special thanks goes to Dario Ferraro, Nicodemo Magnoli and Aldo Conca.

A very special thanks also goes to my officemates in the legendary *Stanzino*. With each of you, I have shared a different part of the journey that has brought me to where I am today.

A very special acknowledgment goes to Matteo Carrega: a great physicist, a wonderful collaborator and - most importantly for me - an even greater friend. Thank you for believing in me more than I often believe in myself, and for supporting me every single day, especially during this last year of postdoctoral applications. Thank you for your patience and for always helping me see the glass half full during difficult moments. You are an example well beyond physics. My PhD journey would not have been the same without you.

I would also like to express my deepest gratitude to all the people outside the academic world who allowed me to enjoy my free time with chillness and enthusiasm. First and foremost, I thank all my friends, among whom I must especially mention my travel companions in Vienna (Cala, Gughi and Luci), my padel partners (Lapo, Nico, Nicco and Ste), my longtime friends (Sam, Gagy and Gianlu), my Magic mates (Davide and Willy) and the big FitLove family.

Among friends, a very special thanks goes to Brus, probably the closest one. Thank you for always being there for me, for always understanding me, for the games of

Magic, the padel and basketball matches, and, more generally, for making Via Crispi an even more chill place.

Then, I must thank the people without whom none of this would have been possible: my parents (and Athos, of course). Thank you for your constant support, for your trust, and for always allowing me to follow my passions and my dreams.

Last, but certainly not least, a huge thanks goes to Silvia, who has been by my side through every single moment of writing this Thesis. Thank you for always taking care of me, for helping me reason through difficulties, and, above all, for loving me. I am very lucky.

List of Publications

This Thesis is based on the following publications:

- [1] **D. Sacco Shaikh**, M. Sassetti, N. Traverso Ziani. *Parity-Dependent Quantum Phase Transition in the Quantum Ising Chain in a Transverse Field*. *Symmetry* 14, 996 (2022).
- [2] **D. Sacco Shaikh**, A. G. Catalano, F. Cavaliere, F. Franchini, M. Sassetti and N. Traverso Ziani. *Phase diagram of the topologically frustrated XY chain*. *The European Physical Journal Plus* 139 (8), 1-14 (2024).
- [3] E. Bertolini, A. Blasi, N. Maggiore, **D. Sacco Shaikh**. *Hall-like behavior of higher rank Chern-Simons theory of fractons*. *Journal of High Energy Physics* 2024 (10), 1-29 (2024).
- [4] E. Bertolini, A. Blasi, M. Carrega, N. Maggiore, **D. Sacco Shaikh**. *Fractons from covariant higher-rank three-dimensional BF theory*. *Physical Review B* 111 (8), 085126 (2025).
- [5] E. Bertolini, M. Carrega, N. Maggiore and **D. Sacco Shaikh**. *Covariant field theory of 3D massive fractons*. *The European Physical Journal C* 85, 1222 (2025).

Other publications to which I contributed as a co-author, but which are not included in this Thesis, are:

- [6] F. R. De Filippi, A. F. Mello, **D. Sacco Shaikh**, M. Sassetti, N. Traverso Ziani and M. Grossi. *Few-Body Precursors of Topological Frustration*. *Symmetry* 16 (8), 1078 (2024).
- [7] R. Grazi, **D. Sacco Shaikh**, M. Sassetti, N. Traverso Ziani and D. Ferraro. *Controlling Energy Storage Crossing Quantum Phase Transitions in an Integrable Spin Quantum Battery*. *Physical Review Letters* 133 (19), 197001 (2024).

Contents

1. Introduction	1
2. Quasiparticles in Quantum Spin Models	15
2.1. Heisenberg model	16
2.1.1. Ferromagnetic case	17
2.1.2. Antiferromagnetic case	21
2.1.3. Why $d = 1$ is special?	24
2.2. XY chain	25
2.2.1. Jordan-Wigner transformation	27
2.2.2. Diagonalization	29
2.3. Ferromagnetic XY chain	35
2.3.1. Vacuum states	36
2.3.2. Ground state	37
2.3.3. Phase transitions	42
2.3.4. Correlation functions and magnetization	46
3. Topologically Frustrated XY Chain	51
3.1. Topologically frustrated quantum spin chains	52
3.2. The model and its solution	57
3.3. Signatures of topological frustration on the GS	58
3.3.1. In the absence of frustration	59
3.3.2. The frustrated case	59
3.4. First order b-QPTs	62
3.5. Second order b-QPTs	63
3.5.1. Analytical approach	64
3.5.2. Numerical analysis	65
3.6. Conclusions	69

4. Fractons	73
4.1. X-cube	74
4.2. Higher-rank $U(1)$ gauge theories	78
4.2.1. Vector Charge Theory	81
4.2.2. Traceless Vector Charge Theory	82
4.2.3. Scalar Charge Theory	83
4.2.4. Traceless Scalar Charge Theory	84
4.3. Scalar Charge Theory: generalized electromagnetism	85
4.3.1. Electrostatics and Magnetostatics	87
4.3.2. Lorentz force	88
4.4. Covariant approach	89
4.4.1. Gauge fixing	91
4.4.2. Higher-rank field strength	93
4.4.3. Higher-rank Maxwell theory of fractons	96
4.5. 3D fractons	103
5. Covariant Field Theories for 3D Fractons	107
5.1. Higher-rank Chern-Simons theory of fractons	108
5.1.1. The model	108
5.1.2. Currents and fractons	112
5.1.3. Gauge-fixing and propagators	116
5.1.4. Energy momentum tensor	117
5.2. Higher-rank BF theory of fractons	119
5.2.1. The model	119
5.2.2. Currents and fractons	124
5.2.3. Symmetric tensor fields	130
5.3. Covariant field theory of 3D massive fractons	132
5.3.1. The general model	132
5.3.2. Propagator	134
5.3.3. Degrees of freedom	135
5.3.4. Physical interpretation	137
5.3.5. Coupling to matter	142
5.4. Summary	142
6. Conclusions and follow-ups	145

A. Proof of some equations	153
A.1. Proofs of (2.73)-(2.76)	153
A.2. Proofs of (2.93)-(2.95)	154
B. Partition function of the XY chain	155
C. Calculation of the two-spin correlators in the ferromagnetic XY chain	159
D. Level quantization of rank-2 Chern-Simons theory	165
D.1. Flux quantization	166
D.2. Shift of the action and the large gauge transformation	167
D.3. An example on the torus	168
E. Propagators	171
E.1. Rank-2 Chern-Simons theory	171
E.2. Rank-2 BF theory	176
E.3. Covariant massive fractons	187
F. Degrees of Freedom	191
F.1. Rank-2 Chern-Simons	191
F.2. Rank-2 BF	193
F.3. Massive gauge theories	195
F.3.1. Maxwell-Chern-Simons	195
F.3.2. Massive fractons	197
G. Rank 2 BF: symmetric case	201
H. Massive fractons: coupling to matter	205
I. 3D covariant massive fractons: energy momentum tensor	209
Bibliography	215
List of figures	235
List of tables	239

Chapter 1.

Introduction

Matter as we encounter it in everyday life is composed of extraordinarily large numbers of elementary constituents. The typical scale in this context is set by Avogadro's number. Moreover, each element of this multitude interacts with all the others, giving rise to the diversity and complexity that characterize the macroscopic world [8]. It is therefore not a surprise that the study of *phases of matter* has attracted the interest of the scientific community.

The present work takes as its starting point the concept introduced by Philip Anderson in [9], encapsulated in the phrase "*more is different*", or, in Xiao-Gang Wen's evocative reformulation, "*a quantitative change can lead to a qualitative change*" [10]. At the heart of [9] lies the recognition that the physical laws governing a system of only a few particles may differ profoundly from those that dictate the behavior of a many-body system. In other words, new physical concepts, laws and principles can emerge from the interaction of many particles. This perspective has been repeatedly confirmed, both theoretically and experimentally, in the study of many-body systems, which are composed of a large number of particles or, more generally, of a vast collection of interacting degrees of freedom. Solids and liquids—the so-called *condensed* states—offers an exciting arena where this principles manifest and form the core of the rich and fascinating field of *condensed matter physics*, a term itself introduced by Anderson in 1967. Condensed matter physics is extraordinarily diverse: it spans problems ranging from materials science to particle physics, passing through statistical mechanics, and its richness and beauty stem from this diversity.

What about the theoretical description and the mathematical methods? In principle, one could determine all the properties of a many-body system by solving its Schrödinger equation. However, the computing power required to solve this equation

for a system of 10^{23} particles is beyond our imagination, and even a hypothetical classical computer built from all of the atoms in the observable universe would not possess enough memory to store a single state vector of such a system. Thus a generic many body interacting system is an extraordinarily complex object.

Furthermore, even if one could solve the Schrödinger equation exactly, it would often be extremely difficult—or completely impossible—to extract from the solution the physical properties of interest [10]. Exact results are typically far too intricate to yield transparent physical insight, and the sheer complexity of the many-body wavefunction makes it an impractical tool for understanding the emergent behavior of condensed matter systems. Moreover, and perhaps even more importantly, the exact solution may be so complicated that it becomes experimentally inaccessible: verifying its predictions could require energy resolutions or measurement capabilities far beyond what is achievable in practice.

Hence, we must construct a low-energy effective theory for the many-body system, that captures the relevant degrees of freedom and provides a coherent framework connecting different experimental observations. Importantly, we cannot assume that the theory describing the low-energy excitations bears any resemblance to the underlying microscopic description. Notice that this approach shares deep rooted similarities with the one adopted in high-energy physics. The key distinction is that, in condensed matter physics, the underlying “microscopic world” varies from material to material, whereas in high-energy physics we have only one “material”: the vacuum itself. The existence of infinitely many distinct condensed matter systems thus provides an enormous variety of physical playgrounds, making it possible to observe phenomena that would be unimaginable within particle physics.

Historically, since the earliest stages of human civilization, philosophers (most notably in ancient China and Greece) and later scientists sought to divide matter into smaller and smaller constituents in order to discover the fundamental building blocks of our universe, the so-called “elementary” particles. This viewpoint lies at the heart of the “reductionist” hypothesis which, as Anderson emphasizes at the beginning of [9], does not in any way guarantee a corresponding “constructionist” one, which breaks down when confronted with the issues of scale and complexity. In other words, even if we succeed in identifying the fundamental constituents of nature and the laws governing them, such knowledge does not automatically provide an understanding of the behavior of complex systems composed of a large number of elementary particles.

Anderson classified the sciences in a linear hierarchy: many-body physics is not merely applied particle physics, even though its fundamental constituents obey the laws of particle theory. Likewise, chemistry is not simply applied many-body physics, and molecular biology is not merely applied chemistry, and so on. At each level of this hierarchy, new behaviors and properties emerge, requiring the formulation of new laws and concepts. Research at every stage is therefore fundamental in its own right, not a simple secondary extension of the level below.

Let us now consider a many-body system. At high energies (or high temperatures), its properties are governed by the microscopic interactions among the constituent atoms, which are in general extremely complicated. As the temperature is lowered, however, the system undergoes qualitative changes: it may crystallize into an ordered lattice or form a superfluid, depending on the nature of its constituents and interactions. In these phases of matter, the only low-energy excitations are the *sound waves*, which arise from the collective vibration of the atoms. In the corresponding quantum theory, the same dispersion relation as in the classical description is recovered, but the energy is now discretized into quanta—called *phonons*—which behave as particles associated with sound waves. In other words, at low energies a new world emerges, governed by a new kind of particles, one that is profoundly different from the original microscopic atomic system. Crystals support two broad classes of phonons: *acoustic modes*, which are gapless and possess a linear dispersion at small momenta, and *optical modes*, which are gapped and do not propagate with a sound velocity. In what follows, the term “phonons” will refer to the acoustic modes, which provide the simplest example of collective excitations in a many-body system. Remarkably, not only the phonons themselves are emergent, but so too are the physical laws that govern their world, which are simpler and universal despite the underlying atomic interactions being specific and complicated. For instance, the sound velocity depends only on the atomic masses and the elastic constants, and phonons behave as nearly free particles even though the atoms interact strongly.

To summarize, the low-energy physics of a many-body system is governed by emergent low-energy *collective excitations* that behave like particles, obey simple emergent physical laws and have universal properties. Crucially, these collective excitations are not elementary in the sense of photons or electrons: if we probed them at sufficiently short length scales, we would uncover an extremely complicated and non-universal atomic system. In other words, unlike elementary particles, the collective excitations of a many-body system are not the fundamental building blocks of the model at high

energies and short distances. For all these reasons, these low-energy excitations arising from the collective behavior of a large number of microscopic degrees of freedom in a many-body system are known as *quasiparticles*, and they will be the protagonists of this Thesis. The term was introduced for the first time by Lev Davidovič Landau in [11], in the context of his Fermi liquid theory, where quasiparticles arise through the adiabatic continuation of particle–hole excitations of the free Fermi gas, retaining coherence and long lifetimes despite interactions [11, 12, 13].

Another cornerstone of traditional condensed matter and statistical physics that helps us understand the origin of gapless phonons is the Ginzburg–Landau theory [14]. According to this theory, phases separated by a *phase transition* can be distinguished by a change in the behavior of a *local* order parameter, allowing one to characterize the macroscopic order of a system. For example, the order parameter for the ferromagnet–paramagnet transition is the magnetization, while in the liquid–gas transition it is the density difference between the two phases. In particular, a non-zero local order parameter signals the emergence of a macroscopic order that explicitly violates one of the symmetries of the underlying Hamiltonian. This framework successfully describes almost all familiar phases of matter—such as solids, magnets, and superfluids—and the phase transitions between them.

Qualitatively, a phase transition occurs when a small variation in temperature causes an aggregate of elementary constituents to undergo a radical change in its macroscopic properties. Common examples include changes of state such as the freezing of water, magnetic transitions between ferromagnetic and paramagnetic phases, and the metal–superconductor transition. Beyond the intrinsic interest of a system changing dramatically under small temperature variations, a key feature of phase transitions—especially those known as continuous (or second-order) transitions—is their *universality* [8, 15]. In this context, universality means that, near the critical temperature T_c , the properties of the system depend only on a few coarse features: the range of interactions, the symmetries of the order parameter, and the dimensionality of the system. All continuous phase transitions can therefore be grouped into a small number of *universality classes* [8, 15], within which microscopic details of the constituents or of the specific material become irrelevant. For example, the width of the coexistence region between liquid and gas in a density–temperature diagram and the magnetization of a ferromagnet as a function of temperature exhibit the same scaling behavior near T_c : both vary as $(T - T_c)^{0.32}$ [8]. The theoretical foundation

for understanding such universality in critical phenomena lies in the concept of the Renormalization Group [16, 17], which earned Kenneth Wilson the 1982 Nobel Prize.

In Ginzburg–Landau theory, the emergence of a non-zero local order parameter is intimately tied to *spontaneous symmetry breaking* [18, 19], which takes place upon crossing a critical point, where the system reorganizes itself and undergoes a qualitative change in its macroscopic behavior. In simple terms, spontaneous symmetry breaking occurs whenever a physical state possesses less symmetry than the laws of nature that govern it [20]. More formally, it refers to the situation in which a system is in a stable state—such as the ground state or a thermal equilibrium state—that is not invariant under a symmetry of its underlying Hamiltonian, Lagrangian, or action [20]. Moreover, if a *global, continuous* symmetry is spontaneously broken in the absence of long-ranged interactions, while leaving a discrete subgroup of translations intact, then *gapless* excitations, known as *Goldstone bosons*, arise in the system. This result, known as *Goldstone’s theorem* [21], explains why gapless phonons emerge in a solid at low energies: they are the Goldstone modes associated with the spontaneous breaking of continuous translational symmetries. The Hamiltonian of a crystal is invariant under continuous spatial translations, but the crystalline ground state preserves only a discrete subgroup of these translations. As a consequence, in three spatial dimensions the breaking of continuous translations gives rise to three Goldstone modes, which manifest as the (acoustic) phonons of the crystal.

Because of its success, Landau theory was initially applied without modification to the study of *quantum phases of matter* [22]. Closely related to the notion of a phase transition is that of a *quantum phase transition* (QPT) [22]. In this case, the focus shifts from abrupt changes in the properties of many-particle systems as temperature varies to abrupt changes in the ground state energy as a function of the parameters of the Hamiltonian. Quantum phase transitions are of great interest because they can strongly influence the properties of quantum systems even at finite temperature. As with classical transitions, quantum phase transitions may be characterized by order parameters or may be topological in nature. The prototypical example of a QPT was studied in 1970 in the one-dimensional *Ising model* in a transverse magnetic field [23], the most iconic model in quantum statistical mechanics. As the magnetic field is lowered below a critical value, the system transitions from a disordered phase to an ordered one that spontaneously breaks the model’s discrete \mathbb{Z}_2 symmetry. Relevantly, QPTs have now been observed experimentally. Examples include transitions inferred in bosonic systems on periodic lattices [24], driven by the amplitude of the periodic

potential, and in the magnetic phases of high-temperature superconductors as a function of doping [25]. In the former case, the transition occurs between a Bose–Einstein condensate and a Mott insulator; in the latter, between an antiferromagnetic and a paramagnetic phase. It is worth noting that quantum phase transitions also exhibit universality in the same sense described above [22]. These developments extended the reach of Landau’s paradigm into the quantum domain, but they did not exhaust the range of possible phenomena in many-body systems...

A fundamentally different phenomenon emerges when a spontaneously broken global symmetry is promoted to a (local) *gauge symmetry*, as first understood by Anderson in 1963 in the context of superconductivity [26]. He showed that in the superconducting phase the phase mode of the condensate is “eaten” by the electromagnetic $U(1)$ gauge field, which thereby acquires a mass. This mechanism anticipates the Higgs mechanism of particle physics. In other words, the *Anderson–Higgs mechanism* [26, 27] arises when a spontaneously broken global symmetry is gauged: coupling the system to a dynamical gauge field enforces the symmetry locally, and the *would-be Goldstone mode* becomes the longitudinal component of a now massive gauge field. Remarkably, the mechanism that gives mass to the W and Z bosons [27] is conceptually the same as the one that gives mass to the electromagnetic field inside a superconductor [26].

Now it is natural to ask whether gapless gauge bosons and fermions themselves could arise as emergent quasiparticles through spontaneous symmetry breaking. The answer is no, and this is one of the reasons why many particle physicists regard our vacuum—containing gapless gauge bosons and Dirac fermions—as fundamentally different from the vacuum of an ordinary many-body system. Conventional solids and liquids do not appear to host such excitations, reinforcing the view that the structure of the particle physics vacuum is qualitatively distinct from that of familiar condensed matter system. For this reason, light and electrons have traditionally been regarded as *elementary* and introduced by hand in our theoretical descriptions of nature. In other words, elementary particles were thought to exist simply because of the special properties of our vacuum. Yet the very existence of light and fermions suggests that our understanding of possible phases of matter was incomplete and needed to be deepened and expanded, ultimately revealing a new, rich, and exciting world beyond Landau’s theories.

In the late 1970s, major advances in semiconductor technology led to the fabrication of heterostructures in which a two-dimensional electron gas forms at the

interface between different materials. In 1980, by measuring the Hall voltage of such a two-dimensional electron gas, von Klitzing [28] observed a striking result: the Hall resistance $R_H = \frac{h}{e^2} \frac{1}{\nu}$, with h the Planck constant, e the electron charge, and ν a positive integer, displayed extremely precise plateaus (in his experiment, the relative error was of order 10^{-5}). This discovery, which earned von Klitzing the 1985 Nobel Prize, was in clear disagreement with classical expectations and marked the birth of a new field in condensed matter physics, now known as the *integer quantum Hall effect* (IQHE). Crucially, this phenomenon lies entirely beyond Landau's theory, since the system exhibits distinct zero-temperature phases without spontaneous symmetry breaking or local order parameters, and its quantized response is instead rooted in a topological invariant [29]. In 1982, Tsui and Stormer [30], using samples prepared by Gossard, observed the existence of plateaus even for non-integer values of ν . This phenomenon, known as the *fractional quantum Hall effect* (FQHE), has a theoretical explanation—proposed by the 1998 Nobel laureate Robert Laughlin—in which electron–electron interactions play a fundamental role [31]. Astonishingly, the low-energy theory of this system hosts emergent quasiparticles with fractional charge [31] and anyonic statistics [32, 33]. These discoveries revealed that the landscape of possible phases of matter was far richer than previously imagined

What about methods? Traditional condensed matter theory had no tools capable of describing these new phenomena. As a result, entirely new mathematical techniques and physical concepts had to be developed or borrowed from other areas of theoretical and mathematical physics. This is the case of *Chern–Simons theories* [34], which, before the discovery of the quantum Hall effect (QHE), were regarded as a beautiful piece of mathematical physics [35] and a curiosity of field theories in fewer than four spacetime dimensions (4D) [36, 37], but without apparent relevance to the real world [38]. Astonishingly, Chern–Simons theories were later recognized as the natural theoretical framework for describing the FQHE [39, 40].

In 1989, Wen proposed that the states of the FQHE realize a new kind of order, which he termed *topological order* [41, 42]. Topological order represented a profound novelty in condensed matter theory, as it cannot be described by any of the usual theoretical tools, such as symmetry breaking, long-range correlations, or local order parameters [10]. New diagnostic tools are therefore required, including the ground state degeneracy on manifolds with nontrivial topology [41], the quasiparticle statistics [32], and the structure of chiral edge states [43]. Notably, the ground state degeneracy of a topologically ordered state is robust against any local perturbation [44], making it

not only a powerful property for characterizing such phases but also a key ingredient for fault tolerant quantum computation [45]. Finally, we remark that the low-energy effective description of a topologically ordered phase is given by a *topological quantum field theory* [37].

In 2002, Wen generalized the concept of topological order to the broader notion of *quantum order* [46], with the goal of describing new kinds of order in gapless quantum states. Quantum order can be divided into three subclasses, the first of which is the topological one discussed previously. The second class appears in free-fermion systems, whose states are classified by the topology of the Fermi surface [46]. The third class consists of the so-called *string-net condensations* [47], which are classified by mathematical structures known as *projective symmetry groups* [46]. String-nets are collective degrees of freedom of an underlying microscopic bosonic lattice model, whose ground state forms a condensate of fluctuating extended strings. Remarkably, within the string-net condensation framework, photons and massless fermions can emerge as quasiparticle excitations arising from fluctuations of the underlying string-nets that permeate space [48]. In particular, light corresponds to fluctuations of the condensed string-nets, while fermions appear as their endpoints. This mechanism allows one to construct complicated spin models whose low-energy effective theories reduce to simpler gauge theories such as quantum electrodynamics or quantum chromodynamics [48, 10]. As Wen evocatively puts it [10], “*Our vacuum is more like an ‘ocean’ which is not empty. Light and fermions are collective excitations that correspond to certain patterns of ‘water’ motion*”. This perspective has even led to the proposal that string-net condensation may provide a microscopic framework from which the Standard Model itself emerges as an effective field theory.

In summary, quasiparticles are emergent, effective particle-like excitations arising from the collective behavior of a large number of microscopic degrees of freedom—features that are not apparent at the microscopic scale [9]. Crucially, quasiparticles can exhibit properties that differ significantly from those of any fundamental particle, reflecting the rich structure of the underlying many-body system. The key idea is that when many fundamental particles interact, their collective dynamics can give rise to macroscopic phenomena that cannot be inferred from the properties of the individual constituents alone. Hoping this Introduction has conveyed that understanding such complex physical behavior requires a continuous interplay between quantum field theory, condensed matter physics, and statistical mechanics [38], in this Thesis we will investigate two distinct classes of quasiparticles that emerge in different exotic

phases of matter. In keeping with the spirit of this Introduction, a variety of theoretical tools will be employed, ranging from integrability to gauge theory techniques. To set the stage for the results presented in this Thesis, we now introduce the two research areas that constitute its core and outline the main contributions of my work.

The first class of quasiparticles arises in *one-dimensional integrable quantum systems* [49], with particular emphasis on quasiparticles appearing in the so-called *topologically frustrated quantum spin chains*, which constitute a new and intriguing exotic phase of matter. To understand why, let us take a step back to Ginzburg–Landau theory, which is based on the implicit assumption that microscopic changes in a system are negligible in determining its thermodynamic properties. Consequently, one is instructed to take the thermodynamic limit before performing any calculation. As a result, any change in the boundary conditions is expected to be irrelevant for the bulk, macroscopic behavior. Recently, however, it has been shown that at the quantum level this assumption misses part of the physics—specifically in antiferromagnetic quantum spin chains with discrete symmetries and *frustrated boundary conditions* [50], namely periodic boundary conditions with an odd number of sites. Such a choice of boundary conditions prevents the simultaneous minimization of all local interactions in the Hamiltonian, giving rise to a form of geometrical frustration.

For instance, it was recently demonstrated that the ground state of the antiferromagnetic Ising-like quantum spin chains with periodic boundary conditions is *gapped* when the chain contains an even number of spins and *gapless* otherwise [51, 52]. Moreover, in the odd case, additional *boundary quantum phase transitions* appear that are absent in the even case [53]. By boundary QPTs we mean non-analyticities of the ground-state energy in the thermodynamic limit that are *non-extensive* in the number of particles [54]. These phase transitions differ from ordinary bulk QPTs [22], which are associated with a non-analytic behavior of the ground state energy *density* in the thermodynamic limit and are therefore insensitive to the choice of boundary conditions. When frustrated boundary conditions are imposed, however, the quantum phases exhibit an unexpected sensitivity to the parity of the chain length [53]. The physical argument underlying the peculiarity of the odd case is simple. When antiferromagnetic interactions, periodic boundary conditions, and an even number of spins are present (as in Figure 1.1 (a)), the ground state resembles a *Néel state* [55], with spins on adjacent sites aligned antiparallel. In the anisotropic spin chains of interest, the excited levels are separated from the ground state by an energy gap. In the odd case, by contrast, at least one antiferromagnetic bond is necessarily unsatisfied (see Figure 1.1 (b)). Because

the system is translationally invariant, this unsatisfied bond can be located anywhere along the chain, giving rise classically to a highly degenerate ground state and, quantum mechanically, to a *gapless* energy band. In quasiparticle language, the frustrated boundary condition effectively injects a single delocalized topological excitation into the ground state [56]. Remarkably, this excitation influences the low-energy sector of the entire system, even in the thermodynamic limit [51, 52]. In particular, it can suppress local order on both sides of a quantum phase transition [57, 58] and, more generally, modify the nature of the associated quantum critical point [59]. Although the physical idea underlying this phenomenon is simple, demonstrating the presence of different orders in the even and odd cases, as well as the emergence of additional quantum phase transitions [53], is far from straightforward. Prior to the beginning of my PhD, only a very specific scenario had been analyzed in the literature: spin chains not subjected to external magnetic fields, where the quantum phase transition is driven solely by anisotropies in the spin couplings. This Thesis aims to address this gap. It will be shown that the *XY quantum spin chain* in an external magnetic field—the most famous generalization of the Ising model—exhibits, in the case of an odd number of spins, distinct boundary quantum phase transitions as functions of both the applied field and the anisotropy parameter, transitions that are entirely absent in the even case.

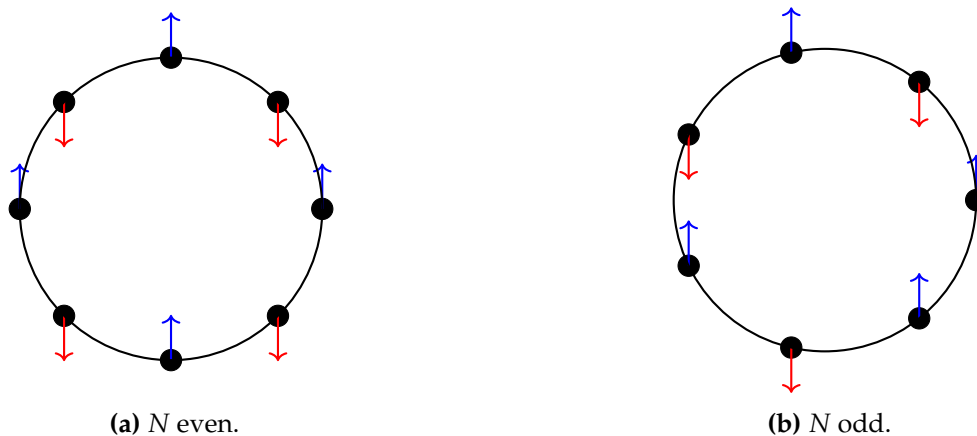


Figure 1.1.: Ground state configurations of the classical antiferromagnetic Ising chain with periodic boundary conditions. For even N , the ground state is doubly degenerate and spanned by the two Néel state (a). For odd N case, the ground state is $2N$ -fold degenerate and spanned by the kink states (b), characterized by the presence of two nearest-neighbour spin which are ferromagnetically aligned.

The second class consists of the so-called *subdimensional quasiparticles*, excitations whose mobility is restricted to lower-dimensional subspaces [60] and which characterize the low-energy sector of the emerging *fracton phases of matter* [61, 62, 63].

More precisely, quasiparticles constrained to move only within zero-, one-, or two-dimensional subspaces are known respectively as *fractons*, *lineons*, and *planons*, as illustrated in Figure 1.2. In particular, a fracton is completely immobile in isolation.

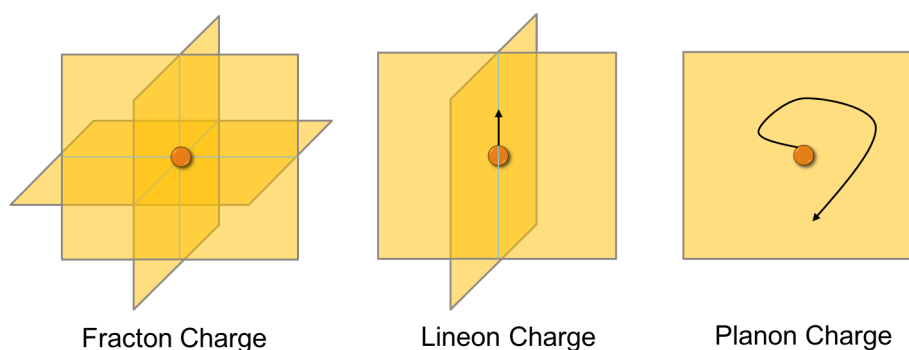


Figure 1.2.: Subdimensional quasiparticles. Figure taken from [64].

The first theoretical realization of such fractonic behavior appeared in 2004 in the context of exactly solvable quantum spin models with discrete symmetries in three spatial dimensions [65]. Subsequently, *gapped* fracton models were discovered in the setting of quantum error-correcting codes in quantum information theory, whose prototypical examples are the *X-cube* model [66, 67] and Haah’s code [68]. These belong, respectively, to the “type I” and “type II” classes: the former supports all three types of subdimensional excitations, while the latter hosts fractons only.

In 2017, Michael Pretko showed that *gapless* subdimensional quasiparticles can also emerge in the low-energy sector of higher-rank $U(1)$ quantum spin liquids [60]. Their effective descriptions take the form of higher-rank $U(1)$ tensor gauge theories [69], whose Gauss-law constraints both encode generalized spin-ice rules that characterize their low-energy sectors and determine the gauge transformations of the emergent tensor gauge field. Crucially, high-energy states host gapless emergent quasiparticle excitations that violate these lowest-energy constraints. Such emergent matter obeys higher-moment conservation laws [60], which in turn impose severe mobility restrictions, analogous to those previously found in gapped fracton models.

The simplest rank-2 fracton tensor gauge theory is the *Scalar Charge Theory* [60], which, once matter is introduced, exhibits immobile fractons together with freely propagating dipolar bound states composed of oppositely charged fractons. Moreover, this theory is characterized by a linear dispersion relation and can therefore be described, in its low-energy limit, by a Lorentz covariant quantum field theory. This connection

makes fracton phases of matter a particularly intriguing point of contact between condensed matter physics and high-energy physics.

It was not long before high-energy theorists became interested in exploring restricted mobility within the framework of relativistic quantum field theories. In 2022, the authors of [70, 71], starting from the Lorentz covariant 4D extension of the gauge transformation—known as *longitudinal diffeomorphisms* [72]—that characterizes the Scalar Charge Theory, derived and subsequently analyzed the most general 4D, power-counting-compatible, gauge invariant action using standard gauge theory techniques. Remarkably, this action turned out to be a combination of *Linearized Gravity* [73] and an additional term representing the genuine novelty of the theory. The latter provides a covariant embedding of the Scalar Charge Theory and thus defines a higher-rank covariant Maxwell theory for fractons [74].

Subsequently, numerous motivations emerged in the literature for studying fractons in $2 + 1$ spacetime dimensions (3D). To me, the most stimulating is the following: given the power of 3D topological quantum field theories [75] in describing topological orders in two spatial dimensions, one may ask whether there exists a higher-rank class of Chern–Simons or BF theories capable of capturing fractonic behavior [76]. From a more physical perspective, one may also wonder whether dipolar analogues of the QHE or of topological insulators can exist. Several theories describing the dipolar QHE and topological dipole insulators have indeed been proposed [77, 76, 78, 79, 80], but all within a non-covariant framework.

This Thesis aims to fill this gap by developing 3D covariant gauge field theories for fractons, with the dual goal of embedding the features observed in condensed matter models into a more formal field-theoretical framework and of shedding light on new fractonic behaviors that have not been proposed before.

The Thesis is organized as follows. In Chapter 2, we review two of the most famous quantum spin models—the Heisenberg model and the XY chain—which can be mapped onto systems of free bosons and free fermions, respectively. These mappings allow for a clear characterization of their low-energy quasiparticle excitations. In Chapter 3, based on [1, 2], we introduce topological frustration and investigate how it modifies the zero-temperature phase diagram of the XY quantum spin chain in a transverse magnetic field, with particular attention to the QPTs. In Chapter 4, we review some of the main developments in the young literature on fracton phases of matter, focusing in particular on the X-cube model, higher-rank gauge theories

together with their 4D covariant generalization, and several motivations for studying fractons in 3D. Chapter 5, which is based on [3, 4, 5], presents our results on 3D covariant gauge field theories for fractons. Finally, Chapter 6 concludes the Thesis with a summary and a discussion of possible future directions.

Chapter 2.

Quasiparticles in Quantum Spin Models

Understanding the nature of collective quasiparticle excitations is a crucial theme in the study of quantum phases of matter. In quantum spin models, emergent quasiparticles—such as magnons, effective fermions, or topological modes—provide an efficient and often remarkably accurate description of low-energy physics, revealing properties that are not immediately apparent from the microscopic Hamiltonian. In this Chapter, I examine a set of paradigmatic spin models that illustrate how dimensionality, integrability, and interaction structure affect the excitation spectrum and the resulting physical behavior.

Section 2.1 is devoted to the Heisenberg model [81] in generic spatial dimension d . This model provides the prototypical description of a quantum magnet with isotropic exchange interactions. Importantly, it does not admit an exact solution in $d \geq 2$, while in $d = 1$ it can be solved using the *Bethe Ansatz* [82], one of the most celebrated techniques in the theory of one-dimensional integrable quantum systems [49]. However, independently of its spatial dimension, in the semiclassical large-spin limit the model can be mapped onto a system of free bosons through the Holstein-Primakoff transformation [83]. This mapping allows for a clear characterization of the low-energy quasiparticles excitations and highlights a fundamental distinction between ferromagnets and antiferromagnets: while the former exhibit a quadratic dispersion relation at low momenta [84], the latter display a linear one [85], signaling the emergence of a Lorentz-invariant effective quantum field theory [86, 87]. Only at the end of the Section do I turn to the special case $d = 1$, where quantum fluctuations become so strong that they can destroy magnetic order, giving rise to non-trivial and sometimes counterintuitive emergent

behaviors. This observation motivates the focus, in the remainder of the Chapter, on integrable one-dimensional quantum spin systems [49], where exact methods allow for a controlled analysis even in strongly correlated regimes.

Section 2.2, which constitutes the core of this Chapter, deals with the XY chain in a transverse magnetic field [88, 89, 90, 91], arguably the simplest non-trivial one-dimensional integrable model. Thanks to the Jordan-Wigner transformation [92], the model can be mapped onto a system of free spinless fermions [88], enabling an exact diagonalization. Since this procedure will play a central role also in the next Chapter, I present it here in detail. I then focus, finally, in Section 2.3 on the ferromagnetic regime and on the corresponding zero-temperature phase diagram, where the model exhibits two second-order quantum phase transitions separating ordered and disordered phases [93, 94]. The behavior of the excitations across these phases provides a clear example of how integrability and reduced dimensionality lead to a rich and universal quasiparticle structure.

2.1 Heisenberg model

The Heisenberg model is defined by the Hamiltonian

$$H = -J \sum_{\langle i, j \rangle} \mathbf{S}_i \cdot \mathbf{S}_j, \quad (2.1)$$

where S_i^α ($\alpha = x, y, z$) are the spin operator on the i -th site, defined by the commutation rules ($\hbar = 1$)

$$[S_j^\alpha, S_k^\beta] = i\epsilon^{\alpha\beta\gamma} S_j^\gamma \delta_{jk}, \quad (2.2)$$

$\langle i, j \rangle$ denotes the sum over nearest-neighbor spins and J is an energy scale, positive in the ferromagnetic case and negative in the antiferromagnetic one. Moreover, in the following, periodic boundary conditions will be assumed for convenience.

The Hamiltonian (2.1) is not exactly solvable in spatial dimensions $d > 1$ whereas in one dimension it was exactly solved by Hans Bethe [82] in 1931 using an integrable technique that would later become known as Bethe Ansatz [49]. Thus, we will study the model (2.1) in the large-spin limit [85] which corresponds to the semi-classical regime since, in order to obtain a finite magnetization (a classical observable) in the classical limit $\hbar \rightarrow 0$, it is necessary that each spin $s \rightarrow \infty$. We will therefore consider the semi-classical limit and focus our attention on the low-energy quasiparticle excita-

tions. Before doing so, it is useful to examine the symmetries of the Hamiltonian (2.1). Since it possesses $SU(2)$ rotational invariance, the generator

$$S^\alpha \equiv \sum_i S_i^\alpha \quad \alpha = x, y, z \quad (2.3)$$

of such rotations is a symmetry, *i.e.*

$$[H, S^\alpha] = 0, \quad (2.4)$$

implying also

$$[H, \mathbf{S}^2] = 0. \quad (2.5)$$

In the following, we will use only the $U(1)$ rotational symmetry about the z -axis, *i.e.*

$$[H, S^z] = 0, \quad (2.6)$$

and we will denote with $|S, M\rangle$ the state such that

$$\mathbf{S}^2 |S, M\rangle \equiv S(S+1) |S, M\rangle \quad S^z |S, M\rangle \equiv M |S, M\rangle. \quad (2.7)$$

2.1.1 Ferromagnetic case

Let us begin by studying the ferromagnetic case, *i.e.* $J > 0$, and start by determining the ground state. To this end, it is useful to rewrite the Hamiltonian (2.1) as

$$H = \sum_{\langle i, j \rangle} H_{ij}, \quad (2.8)$$

with

$$H_{ij} \equiv -J \mathbf{S}_i \cdot \mathbf{S}_j = -\frac{J}{2} (\mathbf{S}_i + \mathbf{S}_j)^2 + Js(s+1), \quad (2.9)$$

where we use the fact that, by construction,

$$\mathbf{S}_i^2 = s(s+1). \quad (2.10)$$

From (2.9) we observe that H_{ij} is minimized when $(\mathbf{S}_i + \mathbf{S}_j)^2$ is maximum, *i.e.* equal to $2s(2s + 1)$, implying $H_{ij} = -Js^2$. Hence, given a state $|\psi\rangle$,

$$\langle\psi|H|\psi\rangle \geq -Js^2N_b, \quad (2.11)$$

with N_b the number of nearest-neighbor bonds in the lattice. Now it is useful to rewrite the Hamiltonian as

$$H = -J \sum_{\langle i,j \rangle} \left[\frac{1}{2}(S_i^+ S_j^- + S_i^- S_j^+) + S_i^z S_j^z \right], \quad (2.12)$$

where S_i^\pm are the spin-flip operators, defined as

$$S_i^\pm \equiv S_i^x \pm iS_i^y, \quad (2.13)$$

and satisfy the $SU(2)$ algebra

$$[S_i^z, S_j^\pm] = \pm S_j^\pm \delta_{ij} \quad [S_i^+, S_j^-] = 2S_i^z \delta_{ij}. \quad (2.14)$$

If we now choose $|\psi\rangle$ as the state such that $S_i^z |\psi\rangle = s |\psi\rangle$ for all $i = 1, \dots, N$, then we observe from (2.12) that it is an eigenstate of H , whose energy is exactly $-Js^2N_b$. In other words, on this ferromagnetic state we have all the H_{ij} simultaneously minimized and, since every nearest-neighbor pair is therefore in the maximal two-spin sector, the entire connected lattice must have all spins aligned, implying that the total spin of the state is the maximal one $S^z = Ns$. Since the Heisenberg Hamiltonian (2.1) is $SU(2)$ invariant, the ground space is given by the whole $S = Ns$ multiplet, given by the states $|Ns, M\rangle$ with $M = -Ns, \dots, Ns$, which is thus $2Ns + 1$ degenerate.

Let us consider the ferromagnetic state $|Ns, Ns\rangle$, where the notation introduced in (2.7) has been used. Intuitively, we expect to obtain a low-energy excitation by lowering the spin on a single site by one unit, which is the smallest possible change and is an integer. Consequently, we expect that the resulting excitations should exhibit a bosonic character. This intuition would suggest that when $M = Ns$ there are no bosonic quasiparticle excitations, whereas one appears when $M = Ns - 1$, and so on. Hence we are led to write

$$S_i^z = s - a_i^\dagger a_i \quad S_i^- = \sqrt{2s} a_i^\dagger, \quad (2.15)$$

where a_i is a bosonic operator on the i -th site, satisfying

$$[a_i, a_j^\dagger] = \delta_{ij} \quad [a_i, a_j] = 0, \quad (2.16)$$

and the prefactor $\sqrt{2s}$ follows from the observation that, at low energies in the semiclassical limit one has

$$[S_i^+, S_i^-] \approx 2s. \quad (2.17)$$

However, the transformation (2.15) cannot be exact since the spin and bosonic Hilbert spaces have different dimensions. The correct canonical transformation is

$$S_i^z = s - a_i^\dagger a_i \quad S_i^- = \sqrt{2s} a_i^\dagger \left(1 - \frac{a_i^\dagger a_i}{2s} \right)^{1/2}, \quad (2.18)$$

also known as *Holstein-Primakoff transformation* [83], where the correction $(2s - a_i^\dagger a_i)^{1/2}$ restricts the dimension of the bosonic Hilbert space. Notice that, in constructing the transformation (2.18), we began by analyzing the nature of the low-energy excitations above the ferromagnetic state $|Ns, Ns\rangle$. The resulting transformation is exact, *i.e.* it is canonical without requiring the semiclassical limit. However, it will be very useful to describe the low-energy excitations with respect to $|Ns, Ns\rangle$ since, in this case, the number of Holstein-Primakoff bosons remains small. By expanding the square root in the definition of S_i^- (2.18) at the lowest order in $a_i^\dagger a_i / (2s) \ll 1$, one recovers

$$S_i^- \approx \sqrt{2s} a_i^\dagger, \quad (2.19)$$

which allows us to rewrite the Hamiltonian (2.1) in terms of the bosons as

$$H \approx -JN_b s^2 - Js \sum_{\langle i,j \rangle} \left(-a_i^\dagger a_i - a_j^\dagger a_j + a_i^\dagger a_j + a_j^\dagger a_i \right). \quad (2.20)$$

Since the Heisenberg model (2.1) is translationally invariant, it is convenient to diagonalize the quadratic Hamiltonian (2.20) by going to Fourier space. We define

$$a_j \equiv \frac{1}{\sqrt{N_c}} \sum_{\mathbf{q} \in \text{BZ}} e^{i\mathbf{q} \cdot \mathbf{r}_j} a_{\mathbf{q}}, \quad (2.21)$$

where N_c is the number of primitive unit cells, \mathbf{q} runs over the first Brillouin zone (BZ), and \mathbf{r}_j denotes the position of the j -th lattice site. From now on we will focus on

hypercubic lattices of spatial dimension d , so that $N_c = N$ and

$$\mathbf{q} \in \Gamma \equiv \left\{ \frac{2\pi}{L}(k_1, \dots, k_d) : k_i = 0, \dots, L-1 \right\}, \quad (2.22)$$

where L is the linear size of the lattice in each direction. In momentum space, the Hamiltonian (2.20) reads

$$H = -\frac{JzN}{2}s^2 + \sum_{\mathbf{q} \in \Gamma} \epsilon(\mathbf{q}) a_{\mathbf{q}}^\dagger a_{\mathbf{q}}, \quad (2.23)$$

where z is the coordination number of the hypercubic lattice, and $\epsilon(\mathbf{q})$ is the dispersion relation

$$\epsilon(\mathbf{q}) = Js z (1 - \gamma_{\mathbf{q}}) \quad (2.24)$$

with

$$\gamma_{\mathbf{q}} \equiv \frac{1}{z} \sum_{\delta} e^{i\mathbf{q} \cdot \delta} = \frac{1}{z} \sum_{\delta} \cos(\mathbf{q} \cdot \delta), \quad (2.25)$$

where δ are the translation vectors to the neighboring lattice sites. We notice that, for small \mathbf{q} , one has $\gamma_{\mathbf{q}} \simeq 1 - |\mathbf{q}|^2/z$ and, as a consequence,

$$\epsilon(\mathbf{q}) \simeq Js |\mathbf{q}|^2, \quad (2.26)$$

which corresponds to a gapless, non-relativistic (Galilean) dispersion relation. These low-energy bosonic quasiparticle excitations are known as *magnons* [84].

But is our theory still consistent at nonzero temperature? In other words, are the Holstein–Primakoff bosons still few when $T \neq 0$? To answer this, we must compute the total number of bosons in the thermodynamic limit:

$$\sum_j \langle a_j^\dagger a_j \rangle = \sum_{\mathbf{q} \in \Gamma} \langle a_{\mathbf{q}}^\dagger a_{\mathbf{q}} \rangle = \frac{N}{(2\pi)^d} \int_{-\pi}^{\pi} \dots \int_{-\pi}^{\pi} d^d q \langle a_{\mathbf{q}}^\dagger a_{\mathbf{q}} \rangle = \frac{N}{\pi^d} \int_0^{\pi} \dots \int_0^{\pi} d^d q \frac{1}{e^{\beta \epsilon(\mathbf{q})} - 1}, \quad (2.27)$$

where β is the inverse temperature, $\epsilon(\mathbf{q})$ is the magnon dispersion relation (2.26), and in the first step we used the identity

$$\sum_j e^{-i(\mathbf{q}-\mathbf{q}')\cdot\mathbf{r}_j} = N\delta_{\mathbf{q},\mathbf{q}'}. \quad (2.28)$$

Importantly, the integral (2.27) diverges only for $d = 1, 2$, *i.e.* the density of magnons becomes infinite at finite T when $d \leq 2$. Since the magnetization is

$$m \equiv \frac{1}{N} \sum_j \langle S_j^z \rangle = s - \frac{1}{N} \sum_j \langle a_j^\dagger a_j \rangle, \quad (2.29)$$

thermal fluctuations destroy ferromagnetism in $d = 1, 2$. This constitute the first historical application of the *Mermin–Wagner theorem* [95], according to which a global continuous symmetry cannot be spontaneously broken at finite temperature in a system with short-range interactions in $d \leq 2$. In our case, the magnons are precisely the Goldstone bosons associated with the spontaneous breaking of the global $SU(2)$ continuous symmetry to its $U(1)$ subgroup, and their quadratic dispersion (2.26) leads to the infrared divergence responsible for the destruction of long-range order in $d \leq 2$.

2.1.2 Antiferromagnetic case

Let us now study the Hamiltonian (2.1) for $J < 0$, *i.e.* when the coupling between nearest-neighbor spins is antiferromagnetic. From the outset, we will consider a hypercubic lattice with lattice spacing equal to 1. This lattice can be viewed as the union of two hypercubic sublattices with lattice spacing 2. Following the same strategy we adopted in the ferromagnetic case, we now want to make an assumption about the ground state. From the expression (2.12) of the Hamiltonian, it becomes clear that the Néel state [55], namely the configuration in which nearest-neighbor spins are antiferromagnetically aligned along the z axis (chosen as our quantization axis), is not an eigenstate. This contrasts with the ferromagnetic case, where the fully aligned ferromagnetic state belonged to the ground state manifold. We would therefore like to know whether, and under which circumstances, the Néel state provides a qualitatively correct approximation to the ground state. To address this question, it is convenient to study small perturbations of the large- s limit. Indeed, when $s \rightarrow \infty$ the Néel state becomes exactly the ground state, since the spins become substantially classical objects. In other words, spins are up on sublattice A and down on sublattice B . Following [85], on the spins belonging to sublattice A we perform the ferromagnetic

Holstein–Primakoff transformation (2.18), written in terms of bosons a_i , while for those on sublattice B we use¹

$$S_j^z = -s + b_j^\dagger b_j \quad S_j^+ = \sqrt{2s} b_j^\dagger \left(1 - \frac{b_j^\dagger b_j}{2s}\right)^{1/2}, \quad (2.30)$$

where b_j are another set of bosonic operators, satisfying

$$[b_i, b_j^\dagger] = \delta_{ij} \quad [b_i, b_j] = [b_i, a_j] = [b_i, a_j^\dagger] = 0. \quad (2.31)$$

In terms of the two types of bosons just introduced, the Hamiltonian (2.12), in the regime where $\langle a_i^\dagger a_i \rangle \ll s$ and $\langle b_j^\dagger b_j \rangle \ll s$, can be written in the following quadratic form²:

$$H \approx \frac{JNz}{2} s^2 - Js \sum_{\langle i,j \rangle} \left(a_i^\dagger a_i + b_j^\dagger b_j - a_i b_j - b_j^\dagger a_i^\dagger \right), \quad (2.32)$$

where the sum runs over nearest-neighbor pairs with i and j belonging to sublattices A and B , respectively. Now we write the bosonic operators in Fourier series on each sublattice

$$a_i \equiv \frac{1}{\sqrt{\frac{N}{2}}} \sum_{\mathbf{q}} e^{i\mathbf{q}\cdot\mathbf{r}_i} a_{\mathbf{q}} \quad b_i \equiv \frac{1}{\sqrt{\frac{N}{2}}} \sum_{\mathbf{q}} e^{i\mathbf{q}\cdot\mathbf{r}_i} b_{\mathbf{q}}, \quad (2.33)$$

where

$$\mathbf{q} \in \Gamma' \equiv \left\{ \frac{2\pi}{L} (k_1, \dots, k_d) : k_i = -\frac{L}{4}, \dots, \frac{L}{4} - 1 \right\}, \quad (2.34)$$

with L the linear size of the hypercubic lattice in each direction³. In momentum space, the Hamiltonian reads

$$H = \frac{JNz}{2} s^2 - zJs \sum_{\mathbf{q}} \left[\gamma_{\mathbf{q}} \left(a_{\mathbf{q}}^\dagger b_{-\mathbf{q}}^\dagger + b_{-\mathbf{q}} a_{\mathbf{q}} \right) + a_{\mathbf{q}}^\dagger a_{\mathbf{q}} + b_{-\mathbf{q}}^\dagger b_{-\mathbf{q}} \right], \quad (2.35)$$

¹Notice that this corresponds, first, to performing on the spins of sublattice B the canonical transformation $S_i^x \rightarrow -S_i^x$, $S_i^y \rightarrow S_i^y$, and $S_i^z \rightarrow -S_i^z$, which implies $S_i^\pm \rightarrow -S_i^\mp$, and then applying the Holstein–Primakoff transformation (2.18).

²Working in this semi-classical regime allows us to neglect the $a_i^\dagger a_i b_j^\dagger b_j$ term in the sum over $\langle i, j \rangle$.

³For definiteness, we take L to be a multiple of 4, which is standard in this context since L is assumed large in spin wave theory.

where $\gamma_{\mathbf{q}}$ is given by (2.25). In order to diagonalize the Hamiltonian we perform a Bogoliubov transformation

$$\begin{pmatrix} \alpha_{\mathbf{q}} \\ \beta_{\mathbf{q}}^\dagger \end{pmatrix} \equiv \begin{pmatrix} u_{\mathbf{q}} & -v_{\mathbf{q}} \\ -v_{\mathbf{q}} & u_{\mathbf{q}} \end{pmatrix} \begin{pmatrix} a_{\mathbf{q}} \\ b_{-\mathbf{q}}^\dagger \end{pmatrix}, \quad (2.36)$$

where $u_{\mathbf{q}}$ and $v_{\mathbf{q}}$ are real. In order to preserve the bosonic commutation relations, they must satisfy the condition

$$u_{\mathbf{q}}^2 - v_{\mathbf{q}}^2 = 1. \quad (2.37)$$

Now, plugging the inverse of (2.36) into (2.35), one finds that the Hamiltonian is diagonal only if

$$\gamma_{\mathbf{q}}(u_{\mathbf{q}}^2 + v_{\mathbf{q}}^2) + 2u_{\mathbf{q}}v_{\mathbf{q}} = 0, \quad (2.38)$$

which, remembering (2.37), is solved by

$$u_{\mathbf{q}} = \sqrt{\frac{1}{2} \left(\frac{1}{\sqrt{1 - \gamma_{\mathbf{q}}^2}} + 1 \right)}. \quad (2.39)$$

Substituting this expression into the Hamiltonian, we finally arrive at

$$H = \frac{JNz}{2}s^2 + zJs \sum_{\mathbf{q}} \left(1 - \sqrt{1 - \gamma_{\mathbf{q}}^2} \right) + \sum_{\mathbf{q}} \epsilon(\mathbf{q}) \left(\alpha_{\mathbf{q}}^\dagger \alpha_{\mathbf{q}} + \beta_{\mathbf{q}}^\dagger \beta_{\mathbf{q}} \right), \quad (2.40)$$

where the dispersion relation reads

$$\epsilon(\mathbf{q}) = -Jzs \sqrt{1 - \gamma_{\mathbf{q}}^2}. \quad (2.41)$$

The excitations created by $\alpha_{\mathbf{q}}^\dagger$ and $\beta_{\mathbf{q}}^\dagger$ correspond to infinitesimal deviations from the Néel state. For small \mathbf{q} , (2.41) vanishes at $\mathbf{q} = 0$ as

$$\epsilon(\mathbf{q}) \simeq v|\mathbf{q}|, \quad (2.42)$$

which is a linear dispersion relation with effective velocity equal to

$$v = -Js\sqrt{z}. \quad (2.43)$$

As a consequence, the low-energy effective physics can be captured by a relativistic quantum field theory. In particular, in spatial dimensions $d \geq 2$ the appropriate continuum description is the $O(d)$ *non-linear sigma model* [38]. In the long-wavelength limit, spin-wave excitations correspond to states that are locally indistinguishable from a Néel-ordered configuration, while the staggered magnetization field undergoes smooth spatial rotations over distances much larger than the lattice spacing. These slowly varying rotations define the continuum field of the non-linear sigma model [96], whose dynamics well captures the low-energy, long-wavelength behavior of the Heisenberg antiferromagnet. In $d = 1$, the situation is more subtle due to strong quantum fluctuations. The low-energy relativistic quantum field theory is still a non-linear sigma model, but supplemented by a topological θ -term whose coefficient is proportional to the so called *Pontryagin index* of the field configuration [38, 86, 87]. This topological term underlies the *Haldane conjecture* [86], predicting a gapped spectrum for integer-spin chains and gapless behavior for half-integer spins.

2.1.3 Why $d = 1$ is special?

To conclude, following [96], we compute the z-magnetization in the ground state of the antiferromagnetic Heisenberg when $\langle a_i^\dagger a_i \rangle, \langle b_j^\dagger b_j \rangle \ll s$, which, from Eq. (2.40), is the vacuum of the bosons α and β . On the sublattice A we have

$$m_A \equiv s - \frac{2}{N} \sum_i \langle a_i^\dagger a_i \rangle = s - \frac{2}{N} \sum_{\mathbf{q}} \langle a_{\mathbf{q}}^\dagger a_{\mathbf{q}} \rangle = s - \frac{2}{N} \sum_{\mathbf{q}} v_{\mathbf{q}}^2 \simeq s - \int_{\text{BZ}} \frac{d^d q}{(2\pi)^d} v^2(\mathbf{q}), \quad (2.44)$$

where Eq. (2.36) has been used. Thus we find

$$\Delta s \equiv m_A - s = \frac{1}{2} \int_{-\frac{\pi}{2}}^{\frac{\pi}{2}} \cdots \int_{-\frac{\pi}{2}}^{\frac{\pi}{2}} \frac{d^d q}{(2\pi)^d} \left(\frac{1}{\sqrt{1 - \gamma^2(\mathbf{q})}} - 1 \right), \quad (2.45)$$

which gives [96]

$$\Delta s \approx -0.1 + \mathcal{O}\left(\frac{1}{s}\right) \quad \text{for } d = 3, \quad (2.46)$$

$$\Delta s \approx -0.2 + \mathcal{O}\left(\frac{1}{s}\right) \quad \text{for } d = 2, \quad (2.47)$$

while for $d = 1$ one finds [96]

$$\Delta s \approx - \int_0^{\frac{\pi}{2}} \frac{dq}{2\pi} \frac{1}{q}, \quad (2.48)$$

which is divergent. This means that, however large s is, the Néel state is destroyed by quantum fluctuations. From the quantum field theory point of view, this follows from *Coleman's theorem* [97], which states that, due to infrared divergences associated with Goldstone bosons, the spontaneous breaking of a continuous symmetry is not possible in a two dimensional spacetime (2D). In summary, the study of quantum models in $d = 1$ is particularly special because quantum fluctuations are so strong that they overwhelm semiclassical intuition, giving rise to phenomena with no analogue in higher dimensions.

2.2 XY chain

The purpose of this Section is to introduce the XY chain in a transverse magnetic field, exactly diagonalize its Hamiltonian, and discuss its phase diagram in the ferromagnetic case. The reason why this particular system is chosen is that it represents the simplest non-trivial integrable model. The key point is that the excitations are non-local spinless fermions, whose non-locality gives rise to a non-trivial zero temperature phase diagram, characterized by the presence of two quantum phase transitions [22]. The model is defined by the following Hamiltonian [49]

$$H = J \sum_{j=1}^N [(1 + \gamma) S_j^x S_{j+1}^x + (1 - \gamma) S_j^y S_{j+1}^y + h S_j^z], \quad (2.49)$$

where N is the number of sites, S_j^α with $\alpha = x, y, z$ are the spin operators on the j -th site, defined by the commutation rules (2.2) and satisfying *periodic boundary conditions* (PBC)

$$S_{N+1}^\alpha = S_1^\alpha. \quad (2.50)$$

Moreover, J is a real parameter representing the natural energy scale and which is negative in the ferromagnetic case and positive in the antiferromagnetic one. Finally, γ is a parameter quantifying the anisotropy of nearest neighbour spins interactions, h is an external magnetic field along z direction. In order to analyze the model it is useful to choose a base for the Hilbert space on the j -th site \mathcal{H}_j . In the following, we

will take $\{|\uparrow_j\rangle, |\downarrow_j\rangle\}$ as an orthonormal basis for \mathcal{H}_j , which is defined by

$$S_j^z |\uparrow_j\rangle \equiv \frac{1}{2} |\uparrow_j\rangle \quad S_j^z |\downarrow_j\rangle \equiv -\frac{1}{2} |\downarrow_j\rangle \quad \langle \uparrow_i | \uparrow_j \rangle = \langle \downarrow_i | \downarrow_j \rangle \equiv \delta_{ij} \quad \langle \downarrow_i | \uparrow_j \rangle \equiv 0, \quad (2.51)$$

in such a way to represent

$$S_j^\alpha \rightarrow \frac{\sigma_j^\alpha}{2} \quad \alpha = x, y, z, \quad (2.52)$$

where $\{\sigma_j^\alpha\}$ are the Pauli matrices defined on the j -th site satisfying ($\hbar = 1$)

$$[\sigma_j^\alpha, \sigma_k^\beta] = 2i\epsilon^{\alpha\beta\gamma}\sigma_j^\gamma\delta_{jk}. \quad (2.53)$$

As a consequence, the Hamiltonian (2.49) can be rewritten as

$$H = \frac{J}{2} \sum_{j=1}^N \left[\left(\frac{1+\gamma}{2} \right) \sigma_j^x \sigma_{j+1}^x + \left(\frac{1-\gamma}{2} \right) \sigma_j^y \sigma_{j+1}^y + h \sigma_j^z \right]. \quad (2.54)$$

Relevantly, when $\gamma = h = 0$ the model (2.54) reduces to the XX chain while when $\gamma = 1$ we recover the *Ising chain* in a transverse magnetic field [23]

$$H|_{\gamma=1} = \frac{J}{2} \left(\sum_{j=1}^N \sigma_j^x \sigma_{j+1}^x + h \sigma_j^z \right), \quad (2.55)$$

which is probably the most famous integrable model. To reduce the parameter space (h, γ) , we observe that

- sending $\gamma \rightarrow -\gamma$ is equivalent to perform a rotation of an angle $\pi/2$ on the xy spin plane;
- sending $h \rightarrow -h$ is equivalent to perform a reflection with respect to the xy spin plane, *i.e.* $\sigma_j^z \rightarrow -\sigma_j^z$.

Thanks to these two symmetries, in the following, it will be sufficient to study the model (2.54) in the region $h, \gamma \geq 0$ of the parameter space without loss of generality. The main reference we will use in this Section is [49].

2.2.1 Jordan-Wigner transformation

To solve the model, we would like to map it onto an equivalent system of bosonic or fermionic quasiparticles. If we aim for an exact solution, the mapping to bosons does not seem promising since the bosonic Hilbert space is infinite on each lattice site, whereas \mathcal{H}_j is two-dimensional. Hence, let us try to map the model (2.54) onto one of spinless fermions ψ_j , defined by the anticommutation rules

$$\{\psi_i, \psi_j^\dagger\} = \delta_{ij} \quad \{\psi_i, \psi_j\} = 0. \quad (2.56)$$

Let $\{|0_j\rangle, |1_j\rangle\}$ be the orthonormal basis of \mathcal{H}_j defined by

$$\psi_j |0_j\rangle \equiv 0 \quad \psi_j^\dagger |0_j\rangle \equiv |1_j\rangle \quad \psi_j |1_j\rangle \equiv |0_j\rangle \quad \psi_j^\dagger |1_j\rangle \equiv 0, \quad (2.57)$$

for which we choose the following representation

$$|0_j\rangle \rightarrow \begin{pmatrix} 1 \\ 0 \end{pmatrix}_j \quad |1_j\rangle \rightarrow \begin{pmatrix} 0 \\ 1 \end{pmatrix}_j. \quad (2.58)$$

Thus it follows that

$$\psi_j \rightarrow \begin{pmatrix} 0 & 1 \\ 0 & 0 \end{pmatrix}_j = \sigma_j^+ \quad \psi_j^\dagger \rightarrow \begin{pmatrix} 0 & 0 \\ 1 & 0 \end{pmatrix}_j = \sigma_j^-, \quad (2.59)$$

where

$$\sigma_j^\pm \equiv \frac{\sigma_j^x \pm i\sigma_j^y}{2}. \quad (2.60)$$

The argument just given would lead us to define the mapping as

$$\sigma_j^+ \equiv \psi_j \quad j = 1, \dots, N, \quad (2.61)$$

that is, more explicitly,

$$\sigma_j^+ \equiv \psi_j \quad \sigma_j^- = \psi_j \quad \sigma_j^z = 1 - 2\psi_j^\dagger \psi_j, \quad (2.62)$$

where we used

$$[\sigma_j^+, \sigma_j^-] = \sigma_j^z. \quad (2.63)$$

Unfortunately, the mapping (2.62) is not correct since it would imply

$$0 \neq [\psi_i, \psi_{j \neq i}^\dagger] = [\sigma_i^+, \sigma_{j \neq i}^-] = 0.$$

In order to satisfy the spin commutation rules (2.53), we therefore need to refine the transformation (2.62) with a non-local term. The correct mapping is given by the so called *Jordan-Wigner transformation* [92]

$$\sigma_j^+ \equiv \exp \left\{ i\pi \sum_{l=1}^{j-1} \psi_l^\dagger \psi_l \right\} \psi_j \quad j = 1, \dots, N. \quad (2.64)$$

Using (2.64) and (2.63), one has

$$\sigma_j^z = \left[e^{i\pi \sum_{l=1}^{j-1} \psi_l^\dagger \psi_l} \psi_j, \psi_j^\dagger e^{-i\pi \sum_{l=1}^{j-1} \psi_l^\dagger \psi_l} \right] = [\psi_j, \psi_j^\dagger] = 1 - 2\psi_j^\dagger \psi_j, \quad (2.65)$$

hence

$$e^{-i\pi \psi_j^\dagger \psi_j} = e^{-i\pi \frac{1-\sigma_j^z}{2}} = e^{-i\frac{\pi}{2}} e^{i\frac{\pi}{2} \sigma_j^z} = e^{-i\frac{\pi}{2}} \left[\cos\left(\frac{\pi}{2}\right) + i\sigma_j^z \sin\left(\frac{\pi}{2}\right) \right] = \sigma_j^z, \quad (2.66)$$

where we also used

$$\exp\{i\theta \sigma^z\} = I \cos \theta + i\sigma^z \sin \theta \quad \theta \in \mathbb{R}. \quad (2.67)$$

To resume, the Jordan-Wigner transformation (2.64) can be rewritten, more explicitly, as

$$\sigma_j^+ = \prod_{l=1}^{j-1} (1 - 2\psi_l^\dagger \psi_l) \psi_j \quad \sigma_j^- = \psi_j^\dagger \prod_{l=1}^{j-1} (1 - 2\psi_l^\dagger \psi_l) \quad \sigma_j^z = 1 - 2\psi_j^\dagger \psi_j, \quad (2.68)$$

which maps, up to a non-local string (which is necessary in order to satisfy the fermionic anticommutation relations (2.56)), the spin ladder operators onto the fermionic creation and destruction operators while the Pauli matrix not present in the ladder operators is written in terms of the fermion number.

From the Jordan-Wigner transformation (2.68) one has

$$\psi_j = \sigma_j^+ \prod_{l=1}^{j-1} \sigma_l^z, \quad (2.69)$$

implying that the vacuum state $|0\rangle$ of the Jordan–Wigner fermions, defined as

$$\psi_j |0\rangle \equiv 0 \quad j = 1, \dots, N, \quad (2.70)$$

is given by

$$|0\rangle = |\uparrow_1 \uparrow_2 \dots \uparrow_N\rangle. \quad (2.71)$$

2.2.2 Diagonalization

To proceed, we express the Hamiltonian (2.54) in terms of the spin ladders operators

$$H = \frac{J}{2} \sum_{j=1}^N [\sigma_j^+ \sigma_{j+1}^- + \sigma_j^- \sigma_{j+1}^+ + \gamma \sigma_j^+ \sigma_{j+1}^+ + \gamma \sigma_j^- \sigma_{j+1}^- + h \sigma_j^z]. \quad (2.72)$$

Here, using (2.68) and (2.56), we observe that (see Appendix A.1 for the detailed calculations)

$$\sigma_j^+ \sigma_{j+1}^- = \psi_{j+1}^\dagger \psi_j \quad (2.73)$$

$$\sigma_j^- \sigma_{j+1}^+ = \psi_{j+1} \psi_j \quad (2.74)$$

$$\sigma_N^+ \sigma_1^- = -\Pi^z \psi_1^\dagger \psi_N \quad (2.75)$$

$$\sigma_N^- \sigma_1^+ = -\Pi^z \psi_1 \psi_N, \quad (2.76)$$

where we defined the z -parity operator

$$\Pi^z \equiv \prod_{j=1}^N \sigma_j^z, \quad (2.77)$$

which will play a crucial role throughout the Thesis. As it is evident from the Jordan-Wigner transformation (2.68), the operator (2.77) represents the parity of the Jordan-Wigner fermion number in the system, being $+1$ and -1 on states with, respectively, an even and odd number of fermions.

Thus Hamiltonian (2.72) can be written in terms of the Jordan-Wigner fermions as

$$H = \frac{J}{2} \sum_{j=1}^{N-1} (\psi_{j+1}^\dagger \psi_j + \psi_j^\dagger \psi_{j+1} + \gamma \psi_{j+1} \psi_j + \gamma \psi_j^\dagger \psi_{j+1}^\dagger) + \frac{JhN}{2} - Jh \sum_{j=1}^N \psi_j^\dagger \psi_j + \frac{J}{2} \Pi^z (\psi_1^\dagger \psi_N + \psi_N^\dagger \psi_1 + \gamma \psi_1 \psi_N + \gamma \psi_N^\dagger \psi_1^\dagger), \quad (2.78)$$

which appears favorable for obtaining the exact solution as it is essentially bilinear in the fermionic operators but with the crucial exception of the boundary term on the second line, which is, however, extremely complicated being Π^z highly nonlinear in the fermions. As is evident from (2.75) and (2.76), the boundary term originates from the choice of PBC (3.16) and would be absent with open boundary conditions. From one hand, the ferromagnetic phase diagram does not depend on the boundary term which, in accordance both with Landau theory [98] and with our intuition, can be neglected in determining the macroscopic properties of the system in the thermodynamic limit, which is therefore implicitly taken at the beginning. This approximation, corresponding to the so called *c-cycle* problem [88], reduces the Hamiltonian (2.78) to a quadratic form in the Jordan-Wigner fermions and thus simplifies the model to a free fermionic one. Otherwise, if we preserve the boundary term, we have to deal with the so called *a-cycle* problem, where the thermodynamic limit will be taken only at the end of the diagonalization. For more than fifty years from [88], the effects of the boundary term on the phase diagram of the antiferromagnetic model have not been investigated deeply and only recently it has surprisingly been demonstrated that the c-cycle and a-cycle antiferromagnetic problems with odd N do not lead to the same physics [52], thus marking the onset of the scientific community's interest in the study of the so called *topologically frustrated spin chains*, which will be the subject of the next Section. In the following, we will review the a-cycle problem for the XY chain [49] since it serves both to determine exactly the degeneracy of the model in the ordered phase and also as a starting point for the frustrated case, which will be analyzed in detail in the next Chapter.

We observe that the Hamiltonian (2.54) commutes with $\sum_j \sigma_j^z$ if and only if $\gamma = 0$, meaning that the total number of Jordan-Wigner fermions is not conserved. However, we notice that

$$[H, \Pi^z] = 0, \quad (2.79)$$

i.e. what is conserved is the parity of the number of Jordan-Wigner fermions in the system. Thus, one can decompose the Hamiltonian as

$$H = \frac{1 + \Pi^z}{2} H^+ \frac{1 + \Pi^z}{2} + \frac{1 - \Pi^z}{2} H^- \frac{1 - \Pi^z}{2}, \quad (2.80)$$

where $(1 \pm \Pi^z)/2$ are the projectors to the states with an even/odd number of Jordan-Wigner fermions and H^\pm are quadratic, being H (2.78) with $\Pi^z = \pm 1$, respectively, *i.e.*

$$\begin{aligned} H^\pm &= \frac{J}{2} \sum_{j=1}^{N-1} (\psi_{j+1}^\dagger \psi_j + \psi_j^\dagger \psi_{j+1} + \gamma \psi_{j+1} \psi_j + \gamma \psi_j^\dagger \psi_{j+1}^\dagger) + \frac{JhN}{2} - Jh \sum_{j=1}^N \psi_j^\dagger \psi_j + \\ &\mp \frac{J}{2} (\psi_1^\dagger \psi_N + \psi_N^\dagger \psi_1 + \gamma \psi_1 \psi_N + \gamma \psi_N^\dagger \psi_1^\dagger), \end{aligned} \quad (2.81)$$

and hence writable in a free-fermionic form. Moreover, we observe that we can write the two Hamiltonians in the following compact form

$$H^\pm \equiv \frac{J}{2} \sum_{j=1}^N (\psi_{j+1}^{(\pm)\dagger} \psi_j^{(\pm)} + \psi_j^{(\pm)\dagger} \psi_{j+1}^{(\pm)} + \gamma \psi_{j+1}^{(\pm)} \psi_j^{(\pm)} + \gamma \psi_j^{(\pm)\dagger} \psi_{j+1}^{(\pm)\dagger} - 2h \psi_j^{(\pm)\dagger} \psi_j^{(\pm)}) + \frac{JhN}{2}, \quad (2.82)$$

where we defined

$$\psi_j^{(\pm)} \equiv \psi_j \quad \psi_{j+N}^{(\pm)} \equiv \mp \psi_j^{(\pm)} \quad j = 1, \dots, N, \quad (2.83)$$

which corresponds to imposing antiperiodic boundary conditions and PBC on the fermions in the parity sectors $\Pi^z = +1$ and $\Pi^z = -1$, respectively.

We are now in the position of diagonalizing the Hamiltonian and, to do that, it is useful to switch to Fourier space. The fermions $\psi_j^{(-)}$ satisfy PBC, therefore their Fourier transform can be defined without difficulty. We adopt the following convention

$$\psi_j^{(-)} \equiv \frac{1}{\sqrt{N}} e^{i\frac{\pi}{4}j} \sum_{k=0}^{N-1} e^{i\frac{2\pi}{N}kj} \tilde{\psi}_k^{(-)}. \quad (2.84)$$

On the other hand, regarding $\psi_j^{(+)}$, one must keep in mind, from (2.83), that they satisfy antiperiodic boundary conditions. Consequently, we define their Fourier transform as

$$\psi_j^{(+)} \equiv \frac{1}{\sqrt{N}} e^{i\frac{\pi}{4}} \sum_{k=0}^{N-1} e^{i\frac{2\pi}{N}(k+\frac{1}{2})j} \tilde{\psi}_k^{(+)} . \quad (2.85)$$

Equations (2.84) and (2.85) can be compactly written as

$$\psi_j^{(\pm)} \equiv \frac{1}{\sqrt{N}} e^{i\frac{\pi}{4}} \sum_{q \in \Gamma^\pm} e^{iqj} \tilde{\psi}_q, \quad (2.86)$$

where we defined the sets

$$\Gamma^+ \equiv \left\{ \frac{2\pi}{N} \left(k + \frac{1}{2} \right) \right\} \quad \Gamma^- \equiv \left\{ \frac{2\pi}{N} k \right\} \quad k = 0, \dots, N-1, \quad (2.87)$$

which will play a crucial role throughout the Thesis.

We observe that the definition (2.86) can be, equivalently, written as

$$\tilde{\psi}_{q \in \Gamma^\pm} \equiv \frac{1}{\sqrt{N}} e^{-i\frac{\pi}{4}} \sum_{j=1}^N e^{-iqj} \psi_j^{(\pm)}, \quad (2.88)$$

which can be obtained starting from (2.86) by invoking two properties: let $n \in \mathbb{Z}$, then⁴

$$\frac{1}{N} \sum_{q \in \Gamma^+} e^{iqn} = \begin{cases} (-1)^m & \text{if } n = mN \text{ with } m \in \mathbb{Z} \\ 0 & \text{otherwise} \end{cases} \quad (2.89)$$

and

$$\frac{1}{N} \sum_{q \in \Gamma^-} e^{iqn} = \begin{cases} 1 & \text{if } n = mN \text{ with } m \in \mathbb{Z} \\ 0 & \text{otherwise.} \end{cases} \quad (2.90)$$

From (2.88), we observe that

$$\tilde{\psi}_{q+2\pi n} = \tilde{\psi}_q \quad q \in \Gamma^\pm, n \in \mathbb{Z}, \quad (2.91)$$

⁴The proofs can be easily obtained by using the finite geometric series $\sum_{k=0}^n r^k = (1-r^{n+1})/(1-r)$ where $r \in \mathbb{C} : |r| < 1$.

meaning that we can extend the Fourier transform definition from Γ^\pm to $\Gamma^\pm + 2\pi\mathbb{Z}$. By using (2.88), (2.83) and (2.56), one can simply check that $\tilde{\psi}_q$ are fermionic operators, *i.e.*

$$\{\tilde{\psi}_q, \tilde{\psi}_{q'}^\dagger\} = \delta_{q,q'} \quad \{\tilde{\psi}_q, \tilde{\psi}_{q'}\} = 0. \quad (2.92)$$

Now we have to write H^\pm in terms of $\tilde{\psi}_q$ and, in order to proceed, one needs to evaluate⁵ (see Appendix A.2 for the explicit calculations)

$$\sum_{j=1}^N \psi_{j+1}^{(\pm)\dagger} \psi_j^{(\pm)} = \sum_{q \in \Gamma^\pm} e^{-iq} \tilde{\psi}_q^\dagger \tilde{\psi}_q \quad (2.93)$$

$$\sum_{j=1}^N \psi_j^{(\pm)\dagger} \psi_j^{(\pm)} = \sum_{q \in \Gamma^\pm} \tilde{\psi}_q^\dagger \tilde{\psi}_q \quad (2.94)$$

$$\sum_{j=1}^N \psi_{j+1}^{(\pm)} \psi_j^{(\pm)} = i \sum_{q \in \Gamma^\pm} e^{iq} \tilde{\psi}_q \tilde{\psi}_{-q}, \quad (2.95)$$

where we used

$$\frac{1}{N} \sum_{j=1}^N e^{i(q-q')j} = \delta_{q,q'}, \quad (2.96)$$

and

$$\frac{1}{N} \sum_{j=1}^N e^{i(q+q')j} = \begin{cases} \delta_{q', 2\pi-q} & \text{if } q, q' \in \Gamma^+, \Gamma^- \setminus \{0\} \\ \delta_{q', q} & \text{if } qq' = 0. \end{cases} \quad (2.97)$$

Upon substituting (2.93), (2.94), and (2.95) into (2.82), one arrives at

$$H^\pm = -J \sum_{q \in \Gamma^\pm} (h - \cos q) \tilde{\psi}_q^\dagger \tilde{\psi}_q - \frac{J\gamma}{2i} \sum_{q \in \Gamma^\pm} (e^{iq} \tilde{\psi}_q \tilde{\psi}_{-q} - \text{h.c.}) + \frac{JhN}{2}. \quad (2.98)$$

Here we observe that

$$\sum_{q \in \Gamma^\pm} e^{iq} \tilde{\psi}_q \tilde{\psi}_{-q} = \sum_{p \in \Gamma^\pm} e^{i(2\pi-p)} \tilde{\psi}_{2\pi-p} \tilde{\psi}_{p-2\pi} = \sum_{q \in \Gamma^\pm} (-e^{-iq}) \tilde{\psi}_q \tilde{\psi}_{-q}, \quad (2.99)$$

⁵Although the calculations are rather cumbersome, they are retained in the main body of the Thesis since they are prototypical for many effects that will be discussed later. For readers wishing to bypass the intermediate steps, the final result is given in Equations (2.115), (2.116), (2.112) and (2.106).

where, in the second equality, (2.91) has been used. From (2.99), one has

$$\sum_{q \in \Gamma^\pm} e^{iq} \tilde{\psi}_q \tilde{\psi}_{-q} = \frac{1}{2} \sum_{q \in \Gamma^\pm} (e^{iq} - e^{-iq}) \tilde{\psi}_q \tilde{\psi}_{-q} = i \sum_{q \in \Gamma^\pm} \sin q \tilde{\psi}_q \tilde{\psi}_{-q}, \quad (2.100)$$

which, upon substitution into (2.98), yields

$$H^\pm = -J \sum_{q \in \Gamma^\pm} (h - \cos q) \tilde{\psi}_q^\dagger \tilde{\psi}_q - \frac{J\gamma}{2} \sum_{q \in \Gamma^\pm} \sin q (\tilde{\psi}_q \tilde{\psi}_{-q} + \tilde{\psi}_{-q}^\dagger \tilde{\psi}_q^\dagger) + \frac{JhN}{2}. \quad (2.101)$$

We ultimately obtain the Bogoliubov–de Gennes representation of the Hamiltonian, written in matrix form as

$$H^\pm = \frac{J}{2} \sum_{q \in \Gamma^\pm} \begin{pmatrix} \tilde{\psi}_q^\dagger & \tilde{\psi}_{-q} \end{pmatrix} \begin{pmatrix} -h + \cos q & \gamma \sin q \\ \gamma \sin q & h - \cos q \end{pmatrix} \begin{pmatrix} \tilde{\psi}_q \\ \tilde{\psi}_{-q}^\dagger \end{pmatrix}. \quad (2.102)$$

In order to diagonalize the Hamiltonian, we define new fermionic operators χ_q via the $SO(2)$ rotation

$$\begin{pmatrix} \chi_q \\ \chi_{-q}^\dagger \end{pmatrix} \equiv \begin{pmatrix} \cos \theta_q & -\sin \theta_q \\ \sin \theta_q & \cos \theta_q \end{pmatrix} \begin{pmatrix} \tilde{\psi}_q \\ \tilde{\psi}_{-q}^\dagger \end{pmatrix}, \quad (2.103)$$

where the angle θ_q must obey the constraint

$$\theta_{0,\pi} \equiv 0, \quad (2.104)$$

since the 2×2 matrix at the right hand side of (2.101) is already diagonal for $q = 0$ and $q = \pi$, and the constraint

$$\begin{cases} \sin \theta_{-q} = -\sin \theta_q \\ \cos \theta_{-q} = \cos \theta_q, \end{cases} \quad (2.105)$$

in order to be well defined. It is straightforward to check that the transformation (2.103) with (2.105) is canonical, *i.e.*

$$\{\chi_q, \chi_{q'}\} = 0 \quad \{\chi_q, \chi_{q'}^\dagger\} = \delta_{q,q'}. \quad (2.106)$$

Furthermore, notice that, from (2.103) and (2.91), one has the periodicity

$$\chi_{q+2\pi n} = \chi_q \quad q \in \Gamma^\pm, n \in \mathbb{Z}. \quad (2.107)$$

In terms of these new quasiparticles χ_q , the Hamiltonian reads

$$H^\pm = \frac{J}{2} \sum_{q \in \Gamma^\pm} \begin{pmatrix} \chi_q^\dagger & \chi_{-q} \end{pmatrix} \tilde{H}_q \begin{pmatrix} \chi_q \\ \chi_{-q}^\dagger \end{pmatrix} \quad (2.108)$$

with

$$\tilde{H}_q \equiv \begin{pmatrix} (-h + \cos q) \cos(2\theta_q) - \gamma \sin q \sin(2\theta_q) & \gamma \cos(2\theta_q) \sin q + (-h + \cos q) \sin(2\theta_q) \\ \gamma \cos(2\theta_q) \sin q + (-h + \cos q) \sin(2\theta_q) & (h - \cos q) \cos(2\theta_q) + \gamma \sin q \sin(2\theta_q) \end{pmatrix}. \quad (2.109)$$

This form brings us to the final step of the diagonalization. Here, one needs to distinguish between the most common ferromagnetic case with $J < 0$ and the antiferromagnetic case $J > 0$. Since the latter will be the subject of the next Chapter, now we will focus on the former [49].

2.3 Ferromagnetic XY chain

It is convenient to chose θ_q such that

$$e^{i2\theta_q} = \frac{h - \cos q + i\gamma \sin q}{\sqrt{(h - \cos q)^2 + \gamma^2 \sin^2 q}} \quad q \neq 0, \pi, \quad (2.110)$$

implying

$$\tilde{H}_{q \neq 0, \pi} = \begin{pmatrix} -\epsilon(q) & 0 \\ 0 & \epsilon(q) \end{pmatrix} \quad (2.111)$$

where we introduced the dispersion relation

$$\epsilon(q) \equiv \sqrt{(h - \cos q)^2 + \gamma^2 \sin^2 q}, \quad (2.112)$$

the analysis of which will prove to be of central importance throughout the Thesis. Moreover, it is useful to observe that

$$\epsilon(0) = \begin{cases} -h+1 & \text{if } 0 \leq h < 1 \\ h-1 & \text{if } h \geq 1, \end{cases} \quad \epsilon(\pi) = h+1 \quad \text{if } h \geq 0, \quad (2.113)$$

thus, upon substitution into (2.109), one has

$$\tilde{H}_0 = \begin{cases} \begin{pmatrix} \epsilon(0) & 0 \\ 0 & -\epsilon(0) \end{pmatrix} & \text{if } 0 \leq h < 1 \\ \begin{pmatrix} -\epsilon(0) & 0 \\ 0 & \epsilon(0) \end{pmatrix} & \text{if } h \geq 1, \end{cases} \quad \tilde{H}_\pi = \begin{pmatrix} -\epsilon(\pi) & 0 \\ 0 & \epsilon(\pi) \end{pmatrix} \quad \text{if } h \geq 0. \quad (2.114)$$

Finally, plugging (2.111) and (2.114) into (3.18), we obtain, independently from the parity of N ,

$$H^+ = \sum_{q \in \Gamma^+} \epsilon(q) \left(\chi_q^\dagger \chi_q - \frac{1}{2} \right) \quad (2.115)$$

$$H^- = \begin{cases} \sum_{q \in \Gamma^- \setminus \{0\}} \epsilon(q) \left(\chi_q^\dagger \chi_q - \frac{1}{2} \right) - \epsilon(0) \left(\chi_0^\dagger \chi_0 - \frac{1}{2} \right) & \text{if } 0 \leq h < 1 \\ \sum_{q \in \Gamma^-} \epsilon(q) \left(\chi_q^\dagger \chi_q - \frac{1}{2} \right) & \text{if } h \geq 1, \end{cases} \quad (2.116)$$

where, for future convenience, we set $J = -1$.

2.3.1 Vacuum states

To write the energy levels, we have previously to establish the z -parity of the fermionic vacuum states $|0^\pm\rangle$, defined as

$$\chi_{q \in \Gamma^\pm} |0^\pm\rangle \equiv 0. \quad (2.117)$$

In order to do that, we have to write them in terms of the vacuum state $|0\rangle$ (2.71) of the Jordan–Wigner fermions, which has z -parity equal to 1, *i.e.*

$$\Pi^z |0\rangle = |0\rangle. \quad (2.118)$$

We observe that

$$\chi_q \left(\cos \theta_q + \sin \theta_q \tilde{\psi}_q^\dagger \tilde{\psi}_{-q}^\dagger \right) |0\rangle = 0, \quad (2.119)$$

which can be proved by direct computation using (2.103), (2.92), (2.104) and

$$\tilde{\psi}_q |0\rangle = 0, \quad (2.120)$$

with the latter immediately following from (2.88) and (2.70). Moreover, from (2.119) it follows that

$$\chi_{-q} \left(\cos \theta_q + \sin \theta_q \tilde{\psi}_q^\dagger \tilde{\psi}_{-q}^\dagger \right) |0\rangle = 0, \quad (2.121)$$

where (2.107), (2.104) and (2.92) have also been used. Putting (2.119) and (2.121) together, we can conclude that

$$|0^+\rangle = \prod_{k=0}^{\lfloor \frac{N-1}{2} \rfloor} \left(\cos \theta_{q_k} + \sin \theta_{q_k} \tilde{\psi}_{q_k}^\dagger \tilde{\psi}_{-q_k}^\dagger \right) |0\rangle \quad \text{where} \quad q_k \equiv \frac{2\pi}{N} \left(k + \frac{1}{2} \right) \quad (2.122)$$

$$|0^-\rangle = \prod_{k=0}^{\lfloor \frac{N}{2} \rfloor} \left(\cos \theta_{q_k} + \sin \theta_{q_k} \tilde{\psi}_{q_k}^\dagger \tilde{\psi}_{-q_k}^\dagger \right) |0\rangle \quad \text{where} \quad q_k \equiv \frac{2\pi}{N} k, \quad (2.123)$$

which can be readily proven to be both normalized to unity. From (2.122) and (2.123) and remembering (2.88) and (2.118), we conclude that

$$\Pi^z |0^\pm\rangle = |0^\pm\rangle, \quad (2.124)$$

since $|0^+\rangle$ and $|0^-\rangle$ are linear combinations of states with even numbers of Jordan-Wigner fermions ψ . Moreover, since, from (2.103), χ_q^\dagger is a linear combination of $\tilde{\psi}_q^\dagger$ and $\tilde{\psi}_{-q}$, then states with an even (odd) number of χ fermions have definite z-parity equal to $+1$ (-1).

2.3.2 Ground state

We will denote by $|GS'^\pm\rangle$, $|GS^\pm\rangle$ and $|GS\rangle$ the ground states, with energies $E_0'^\pm$, E_0^\pm and E_0 , of H^\pm , $\frac{1\pm\Pi^z}{2} H^\pm \frac{1\pm\Pi^z}{2}$ and H , respectively. The strategy to obtain $|GS\rangle$ is the following: after having identified $|GS'^\pm\rangle$, the states $|GS^\pm\rangle$ can be found applying $\frac{1\pm\Pi^z}{2}$. This in turn allows to find the GS energy $E_0 = \min\{E_0^+, E_0^-\}$ and the corresponding set of $|GS\rangle$.

We begin by determining $|GS^+\rangle$, namely the lowest-energy state in the even sector (that is, with an even number of Jordan-Wigner fermions). From (2.115) we observe that the ground state of H^+ is its vacuum $|0^+\rangle$, which also has the right z -parity. Thus

$$|GS^+\rangle = |GS'^+\rangle = |0^+\rangle, \quad (2.125)$$

with energy

$$E_0^+ = -\frac{1}{2} \sum_{q \in \Gamma^+} \epsilon(q). \quad (2.126)$$

Let us now find the ground state of the odd sector $|GS^-\rangle$. From (2.116), it becomes clear that the cases $h \geq 1$ and $0 \leq h < 1$ must be handled independently.

When $h \geq 1$, in analogy with the even sector, the ground state of H^- is its vacuum $|0^-\rangle$ which, however, has the wrong parity (since we are now in the odd sector). As a consequence, $|GS^-\rangle$ will be given by the lowest-energy quasiparticle excitation over the vacuum $|0^-\rangle$. Since in this region of the parameter space the dispersion relation (2.112) has an absolute minimum at $q = 0$ (as you can see from Figure 2.1), then

$$|GS^-\rangle = \chi_0^\dagger |0^-\rangle. \quad (2.127)$$

When $0 \leq h < 1$, from (2.116) we observe that the energy of H^- is minimized by the state (2.127), *i.e.* $|GS'^-\rangle = \chi_0^\dagger |0^-\rangle$, which, having the right parity, constitutes the ground state $|GS^-\rangle$ of the odd sector. To resume, the ground state of the odd sector is given by (2.127) for all $h \geq 0$, with energy

$$E_0^- = \begin{cases} -\frac{1}{2} \sum_{q \in \Gamma^-} \epsilon(q) & \text{for } 0 \leq h < 1 \\ -\frac{1}{2} \sum_{q \in \Gamma^-} \epsilon(q) + \epsilon(0) & \text{for } h \geq 1. \end{cases} \quad (2.128)$$

The excited states in the even sector are constructed by applying pairs of creation operators $\chi_q^\dagger \chi_{q'}^\dagger |0^+\rangle$ with $q, q' \in \Gamma^+$. In contrast, the excited states in the odd sector are generated by applying an odd number of creation operators to the vacuum $|0^-\rangle$. Moreover, the lowest excited states in the two parity sectors are separated from $|0^\pm\rangle$ by energy gaps of order J .

Now, in order to find the ground state $|GS\rangle$ of the full Hamiltonian H (2.80), we have to compare the energies E_0^\pm as the point (h, γ) varies in the parameter space. In the thermodynamic limit $N \rightarrow \infty$ this procedure is fully analytical, while at finite N one

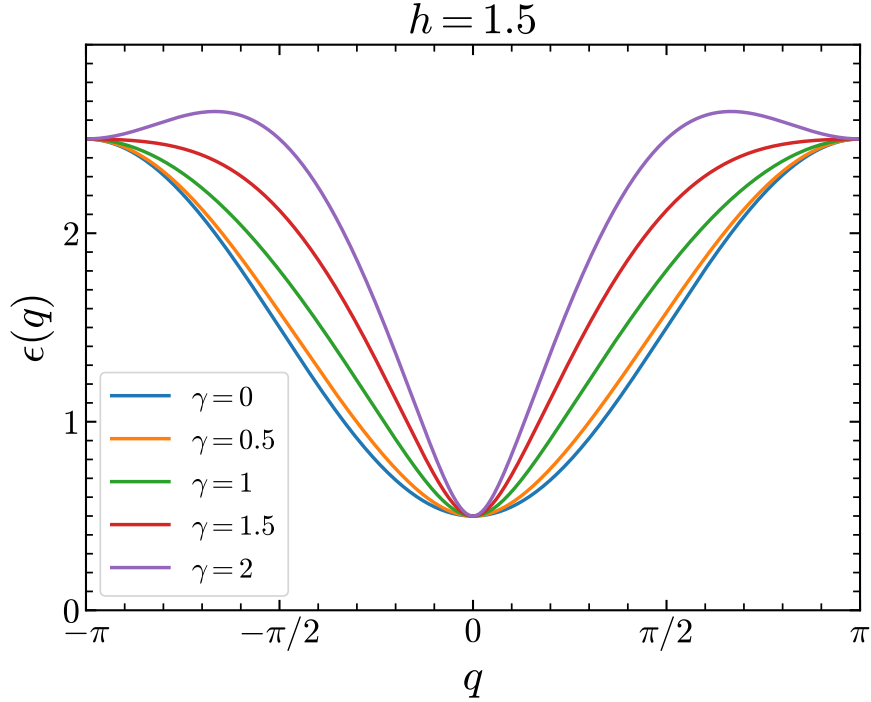


Figure 2.1.: Plot of the dispersion relation $\epsilon(q)$ as a function of $q \in [-\pi, \pi]$ for $h = 1.5$ and different values of the anisotropy parameter: $\gamma = 0$ (blue), $\gamma = 0.5$ (orange), $\gamma = 1$ (green), $\gamma = 1.5$ (red) and $\gamma = 2$ (purple).

has to resort to numerical methods.

At finite N , the states $|GS^+\rangle$ and $|GS^-\rangle$ alternate as the ground state $|GS\rangle$ of the full Hamiltonian H as we move in the parameter space (h, γ) . Figure 2.2 illustrates the curves of exact double degeneracy of the ground state for different values of N . We underline that although we only focused on a few particular values of N , the analysis can be straightforwardly extended to the general values of the number of sites. First of all, we observe that the number of level crossings grows with the chain length and, more precisely, there are exactly $\lceil N/2 \rceil$ degeneracy lines. Subsequently, we observe that the circle $h^2 + \gamma^2 = 1$ is common to all values of N , which can also be seen easily from an analytical point of view [94]. Indeed, on this curve, the dispersion relation (2.112) reads

$$\epsilon = 1 - h \cos q, \quad (2.129)$$

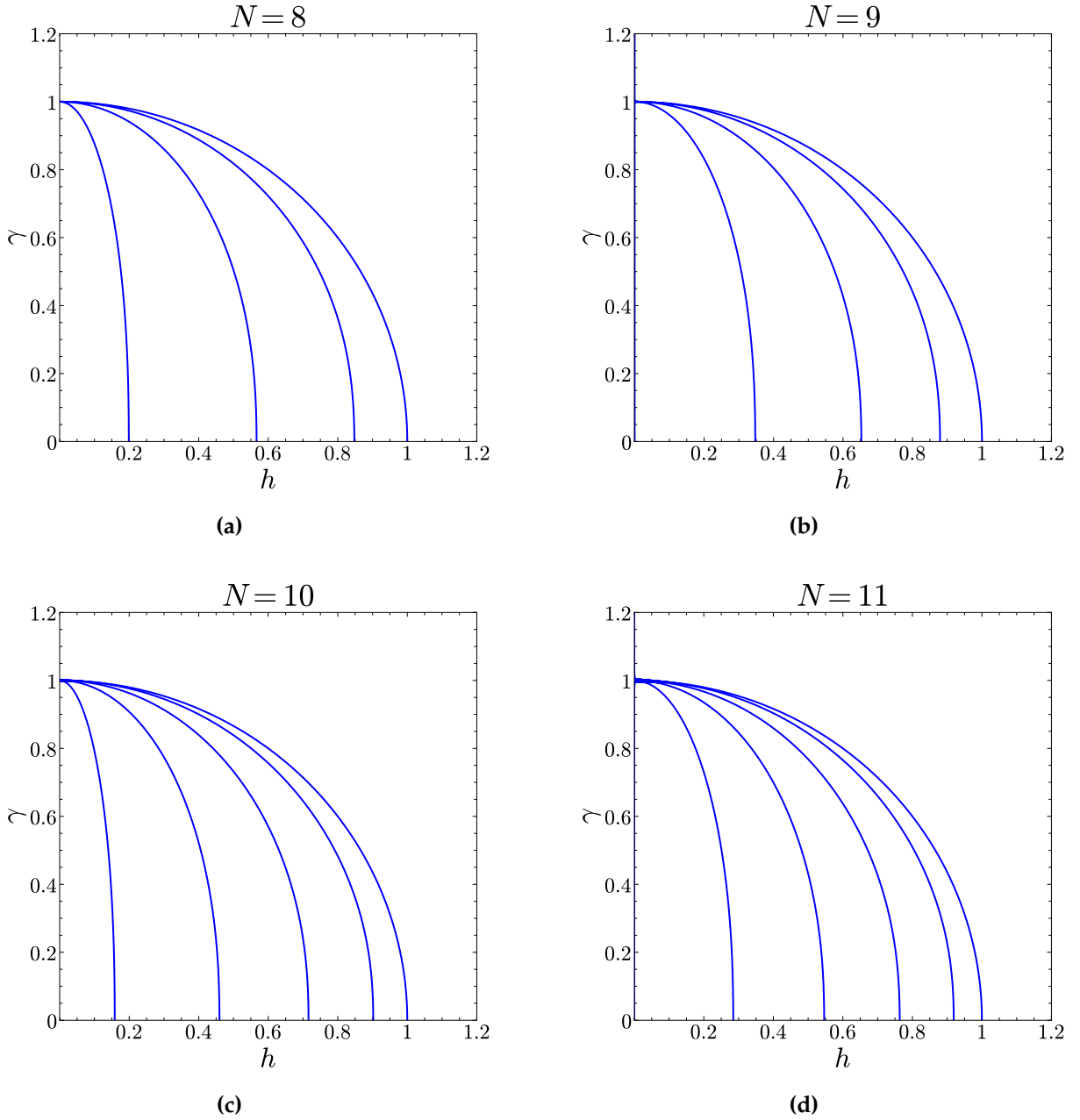


Figure 2.2.: Curves (in blue) where $E_0^+ = E_0^-$, *i.e.* where $|GS^\pm\rangle$ are degenerate, for different values of the chain length: $N = 8$ (a), $N = 9$ (b), $N = 10$ (c) and $N = 11$ (d).

which, once substituted into (2.126) and (2.128), yields

$$E_0^\pm = -\frac{N}{2}, \quad (2.130)$$

where (2.89) and (2.90) have also been used. In particular, at the point $(0, 1)$ in the (h, γ) plane we recover the 1D Ising chain in the absence of an external field, which is

a classical model. The ground state of the system at this point is, of course, a linear combination of the two following states:

$$|GS_1\rangle = \prod_{j=1}^N |\rightarrow_j\rangle = \prod_{j=1}^N \frac{1}{\sqrt{2}} (|\uparrow_j\rangle + |\downarrow_j\rangle) \quad (2.131)$$

$$|GS_2\rangle = \prod_{j=1}^N |\leftarrow_j\rangle = \prod_{j=1}^N \frac{1}{\sqrt{2}} (|\uparrow_j\rangle - |\downarrow_j\rangle), \quad (2.132)$$

where $|\rightarrow_j\rangle$ and $|\leftarrow_j\rangle$ are normalized eigenvectors of σ_j^x with eigenvalues, respectively, $+1$ and -1 . If instead we consider the Hamiltonian of the XY chain (2.54) in the limit $h \gg 1$, the dominant contribution is given by $-h \sum_{j=1}^N \sigma_j^z$. In this regime, the ground state is

$$|GS\rangle = \prod_{j=1}^N |\uparrow_j\rangle, \quad (2.133)$$

we thus observe that by varying only h the nature of the ground state can be completely modified, interpolating between (2.131), or (2.132), and (2.133). This naturally raises the question of whether a critical value of h exists at which the system undergoes a phase transition, an issue that will be examined in the following Sections.

From Figure 2.2, we observe that the ground states of the two parity sectors are exactly degenerate along the line $h = 0$ if and only if N is odd. This fact can also be established analytically: indeed, when $h = 0$ the dispersion relation reads

$$\epsilon = \sqrt{(1 - \gamma^2) \cos^2 q + \gamma^2}, \quad (2.134)$$

and, only for odd N , one has for each $q \in \Gamma^+$ there exists a $q' \in \Gamma^-$ such that

$$\cos^2 q = \cos^2 q', \quad (2.135)$$

where (2.89) and (2.90) have also been used. This concludes the proof. Finally, the analysis at finite N shows that in the region $h^2 + \gamma^2 > 1$ with $h \neq 0$ the ground state is always given by $|GS^+\rangle$. This result is consistent with the analytical proof in [99], where it was shown that in the Ising chain (a particular case of the XY chain with $\gamma = 1$) one has $E_0^- > E_0^+$ for $h > 0$.

In the thermodynamic limit, *i.e.* $N \rightarrow \infty$, one has

$$E_0^+ = E_0 \equiv -\frac{N}{4\pi} \int_0^{2\pi} \epsilon(q) dq, \quad (2.136)$$

and

$$E_0^- = \begin{cases} E_0 & \text{for } 0 \leq h < 1 \\ E_0 + h - 1 & \text{for } h \geq 1, \end{cases} \quad (2.137)$$

hence, for $h \leq 1$, the lowest-energy states in the two parity sectors become degenerate, giving rise to a doubly degenerate manifold that spontaneously breaks the \mathbb{Z}_2 symmetry and remains separated from the first excited level by an energy gap which does not close in the thermodynamic limit. More precisely, in [99] it has been shown analytically that the gap between $|GS^+\rangle$ and $|GS^-\rangle$ closes exponentially with the chain length N . For $h > 1$, as previously noted, one has $E_0^+ < E_0^-$. Hence, the ground state in this region is non-degenerate and gapped.

2.3.3 Phase transitions

As the next step, we now show that at finite temperature no phase transitions occur. To this end, we proceed with the calculation of the partition function. Although in the following Sections we will focus exclusively on the properties of the XY chain at $T = 0$, we now compute the partition function (and hence the free energy per site) of the XY chain. From the free energy, all thermodynamic quantities can be derived. From the explicit form obtained, it will be clear that the model does not exhibit thermal phase transitions. The calculation, reported in Appendix B, essentially reduces to that of the partition function of free fermions. One finds that the free energy per site in the thermodynamic limit is given by

$$f = -\frac{1}{\beta} \log 2 - \frac{1}{\pi\beta} \int_0^\pi \log \cosh \left[\frac{\beta}{2} J \epsilon(q) \right] dq. \quad (2.138)$$

This expression is analytic in the temperature, and therefore no phase transitions are present.

In conclusion, we have shown that the ground state changes its degeneracy at $h = 1$. Moreover, we have previously observed that by varying h in $[0, \infty)$ the ground state changes from an x -ferromagnet ((2.131) or (2.132)) to a quantum paramagnet (2.133)

and *vice versa*. These facts might suggest the occurrence of a phase transition, but in reality such a thermal transition does not take place. To deepen our understanding of the model, we must therefore examine in more detail what happens at zero temperature, and hence the *quantum phase transitions* [22]. The only points in the parameter space where such a radical change of the ground state can occur are those for which the minimum of the spectrum (2.112) vanishes, thereby allowing the ground state to reorganize itself and modify its macroscopic behavior. We therefore look for the values of (h, γ) such that, in the thermodynamic limit, there always exists at least one $q \in [-\pi, \pi)$ with $\epsilon(q) = 0$. Imposing (from (2.112))

$$\begin{cases} h - \cos q = 0 \\ \gamma \sin q = 0, \end{cases} \quad (2.139)$$

we find that, for $h, \gamma \geq 0$, the conditions are satisfied at

$$h = 1 \quad (2.140)$$

with $q = 0$, and at

$$\gamma = 0 \quad (2.141)$$

with $q = \pm \arccos h$. More precisely, $h = 1$ corresponds to the critical value of the magnetic field at which, at $T = 0$, the system changes from being magnetically ordered to disordered, while $\gamma = 0$ with $h < 1$ defines the critical line along which the system changes from an x -ferromagnet to a y -ferromagnet. We therefore expect that at (2.140) and (2.141) quantum phase transitions occur. To verify that these transitions are indeed present, one must study the derivatives of the ground state energy (2.137) in the thermodynamic limit. It has been shown [94] that along these gapless lines the second derivative (but not the first derivative) of the ground state energy exhibits discontinuities. Consequently, we conclude that at (2.140) and (2.141) second order quantum phase transitions take place. Relevantly, along the critical lines (2.140) and (2.141) the dispersion relation becomes relativistic when $\gamma \neq 0$, as you can see from the plots in Figure 2.3 and 2.4.

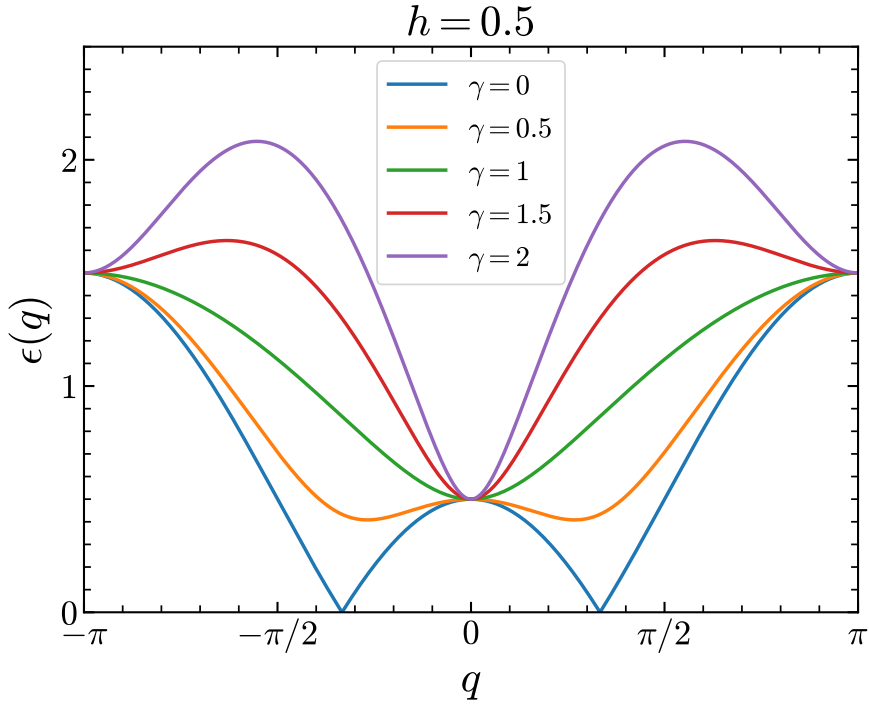


Figure 2.3.: Plot of the dispersion relation $\epsilon(q)$ as a function of $q \in [-\pi, \pi]$ for $h = 0.5$ and different values of the anisotropy parameter: $\gamma = 0$ (blue), $\gamma = 0.5$ (orange), $\gamma = 1$ (green), $\gamma = 1.5$ (red) and $\gamma = 2$ (purple).

More precisely, by performing a first-order Taylor expansion of $\epsilon(q)$ around $q = 0$ (for $h = 1$) and $q = \pm \arccos h$ (for $\gamma = 0$), one finds, respectively,

$$\epsilon(q) \sim \gamma|q| \quad (2.142)$$

and

$$\epsilon(q) \sim \sqrt{1-h^2}|q \mp \arccos h|. \quad (2.143)$$

Moreover, at $q = 0$ and $q = \pm \arccos h$ the energy gap closes, respectively, as

$$\Delta \sim \epsilon(0) = |h - 1| \quad (2.144)$$

and

$$\Delta \sim \epsilon(\pm \arccos h) = \sin(\arccos h)|\gamma| \sim |\gamma|. \quad (2.145)$$

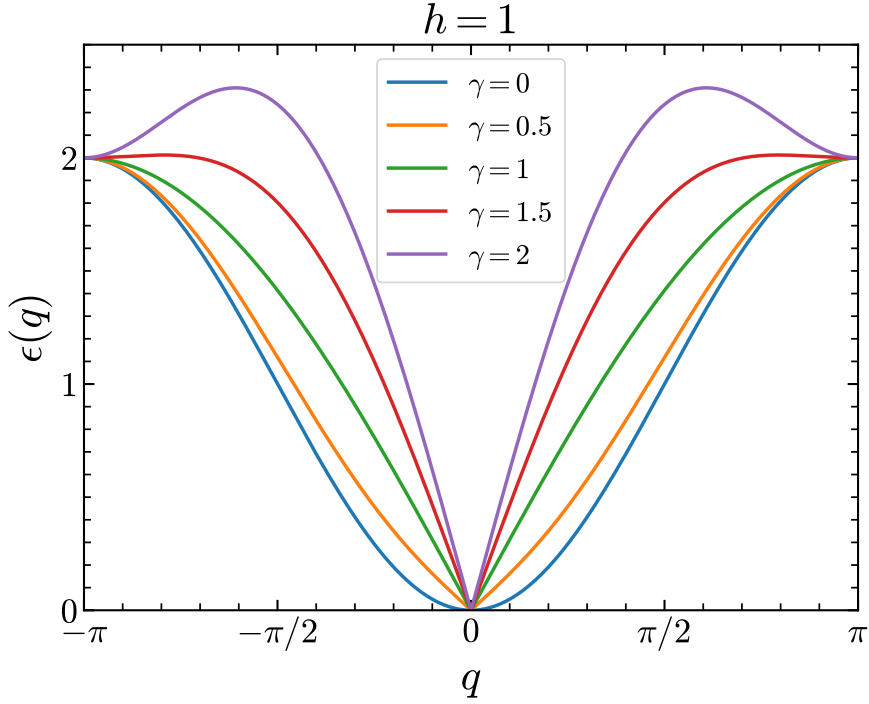


Figure 2.4.: Plot of the dispersion relation $\epsilon(q)$ as a function of $q \in [-\pi, \pi]$ for $h = 1$ and different values of the anisotropy parameter: $\gamma = 0$ (blue), $\gamma = 0.5$ (orange), $\gamma = 1$ (green), $\gamma = 1.5$ (red) and $\gamma = 2$ (purple).

Recalling that the critical exponents $\nu > 0$ and $z > 0$ [22] are defined through

$$\xi \sim \frac{1}{|\lambda - \lambda_c|^\nu}, \quad \Delta \sim |\lambda - \lambda_c|^{z\nu}, \quad \epsilon \sim |q - q_F|^z, \quad (2.146)$$

with ξ the correlation length, λ a control parameter with critical value λ_c , and q_F the Fermi momentum, we conclude that along the critical lines with $\gamma \neq 0$ one has

$$z = \nu = 1. \quad (2.147)$$

In $(1 + 1)$ dimensions, scale invariance together with Lorentz invariance, locality, and unitarity automatically imply conformal invariance [100, 101]. Accordingly, the critical lines of the XY chain are described by distinct conformal field theories. At $h = 1$ with $\gamma \neq 0$, the transition belongs to the Ising universality class with central charge $c = 1/2$, while along $\gamma = 0$ with $0 \leq h < 1$, where the model reduces to the XX chain, the continuum limit corresponds to a free massless Dirac fermion theory with $c = 1$. This conformal behavior manifests itself in universal finite-size scaling of the ground-state energy [102, 103], logarithmic scaling of entanglement entropy [104] and

algebraic decay of correlation functions [105]. The two critical lines discussed above meet at the bi-critical point $(h, \gamma) = (1, 0)$. Here, as you can also see from Figure 2.4, the dispersion relation is not relativistic but Galilean since its McLaurin expansion around $q = 0$ reads

$$\epsilon(q) \sim \frac{q^2}{2}, \quad (2.148)$$

meaning that $z = 2$. As a consequence, the bi-critical point, where the Ising and XX universality classes intersect, does not exhibit conformal invariance. To conclude, Figure 2.5 presents the phase diagram of the ferromagnetic XY chain.

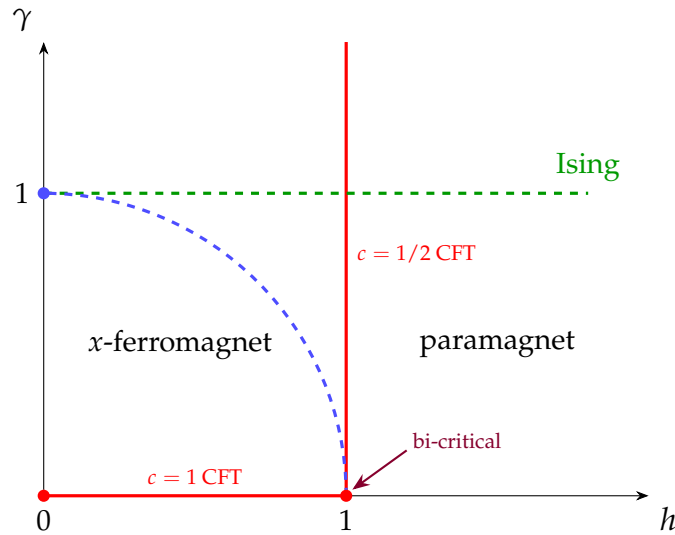


Figure 2.5.: Phase diagram of the ferromagnetic XY chain with PBC in the region $h, \gamma \geq 0$. Red lines indicate the quantum critical lines ($h = 1$ and $\gamma = 0$ for $0 \leq h \leq 1$), where the system undergoes second-order quantum phase transitions. The dashed green line corresponds to the transverse-field Ising chain ($\gamma = 1$), while the dashed blue curve denotes the circle $h^2 + \gamma^2 = 1$, along which the ground state is exactly doubly degenerate even at finite size.

2.3.4 Correlation functions and magnetization

In this Subsection we compute the two-spin correlation functions on the physical ground state at zero temperature, a calculation first carried out in [106]. Analyzing the behavior of correlation functions is useful, as it refines the physical interpretation of the different phases of the model. Before starting with the calculation, it is necessary to specify the physical ground states in terms of $|GS^+\rangle$ and $|GS^-\rangle$. To this end, it is

convenient to begin from the classical point $(h, \gamma) = (0, 1)$, where the physical ground state is either (2.131) or (2.132). We now express these two states in terms of $|GS^+\rangle$ and $|GS^-\rangle$. We observe that

$$\Pi^z \prod_{j=1}^N |\rightarrow_j\rangle = \Pi^z \prod_{j=1}^N \frac{1}{\sqrt{2}} (|\uparrow_j\rangle + |\downarrow_j\rangle) = \prod_{j=1}^N \frac{1}{\sqrt{2}} (|\uparrow_j\rangle - |\downarrow_j\rangle) = \prod_{j=1}^N |\leftarrow_j\rangle, \quad (2.149)$$

from which

$$\Pi^z \frac{1}{\sqrt{2}} \left(\prod_{j=1}^N |\rightarrow_j\rangle \pm \prod_{j=1}^N |\leftarrow_j\rangle \right) = \pm \frac{1}{\sqrt{2}} \left(\prod_{j=1}^N |\rightarrow_j\rangle \pm \prod_{j=1}^N |\leftarrow_j\rangle \right). \quad (2.150)$$

Thus, at the classical point

$$|GS^\pm\rangle = \frac{1}{\sqrt{2}} \left(\prod_{j=1}^N |\rightarrow_j\rangle \pm \prod_{j=1}^N |\leftarrow_j\rangle \right), \quad (2.151)$$

or, equivalently,

$$\prod_{j=1}^N |\rightarrow_j\rangle = \frac{1}{\sqrt{2}} (|GS^+\rangle + |GS^-\rangle) \quad (2.152)$$

$$\prod_{j=1}^N |\leftarrow_j\rangle = \frac{1}{\sqrt{2}} (|GS^+\rangle - |GS^-\rangle). \quad (2.153)$$

Thus, in the ordered phase, where the \mathbb{Z}_2 symmetry is spontaneously broken, the physical ground state of the system is one of (2.152) or (2.153). We would like to classify the phases of the model according to the behavior of the spontaneous magnetization, defined as

$$m_x(j) \equiv \langle GS | \sigma_j^x | GS \rangle = \pm \frac{1}{2} \left(\langle GS^+ | \sigma_j^x | GS^- \rangle + \langle GS^- | \sigma_j^x | GS^+ \rangle \right) = \pm \text{Re} \langle GS^+ | \sigma_j^x | GS^- \rangle, \quad (2.154)$$

where

$$|GS\rangle = \frac{1}{\sqrt{2}} (|GS^+\rangle \pm |GS^-\rangle). \quad (2.155)$$

However, so far, no method has been devised to compute (2.154), so the only information about the magnetization along the x axis must be inferred from the asymptotic

behavior of the correlation functions thanks to the cluster-decomposition principle [20]

$$\lim_{n \rightarrow \infty} \left(\langle \sigma_j^x \sigma_{j+n}^x \rangle - \langle \sigma_j^x \rangle \langle \sigma_{j+n}^x \rangle \right) = 0. \quad (2.156)$$

We therefore set ourselves, for obvious reasons, the goal of computing

$$\rho_{lm}^\alpha \equiv \langle GS | \sigma_l^\alpha \sigma_m^\alpha | GS \rangle \quad (2.157)$$

which represents the two-point spin correlation functions in the ground state. From translational invariance it follows that

$$\rho_{lm}^\alpha = \rho_{l-m,0}^\alpha \equiv \rho^\alpha(l-m). \quad (2.158)$$

The asymptotic behavior $n \equiv |l-m| \rightarrow \infty$ of the correlators of the ferromagnetic XY chain was computed in [106]. The fundamental aspects of this calculation are discussed in detail in Appendix C, and here we restrict ourselves to outlining only the procedure that must be followed. First, one has to rewrite the spin operator σ_l^α in terms of the spinless fermions ψ_j through (2.68). Subsequently, for future convenience, it is useful to express the Jordan–Wigner fermions in terms of two Majorana fermions

$$A_j \equiv \psi_j^\dagger + \psi_j \quad B_j \equiv i(\psi_j^\dagger - \psi_j). \quad (2.159)$$

At this point, the evaluation of (2.157) reduces to computing ground state expectation values of strings of Majorana operators. To this end, we employ Wick's theorem in many-body theory [107], which allows us to write n -point correlators in terms of products of two-point correlators only, namely $\langle A_i A_j \rangle$, $\langle B_i B_j \rangle$, and $\langle A_i B_j \rangle$ in our case. Since these expectation values are taken with respect to $|GS\rangle$, which is defined in terms of $|GS^\pm\rangle$, the calculation requires the evaluation of the two-point functions $\langle \chi_q \chi_k^\dagger \rangle$ and $\langle \chi_q \chi_k \rangle$. Now it remains to express the strings of Majorana operators in terms of χ_q and χ_q^\dagger by using (2.159), (2.86) and (2.103). Finally, using Wick's theorem, one finds the correlation functions (2.157). In particular, ρ_{lm}^x and ρ_{lm}^y are written in terms of determinants of $n \times n$ Toeplitz matrices, i.e. with constant descending diagonals from left to right. Since they appear in the Ising and XY chains and due to their fascinating mathematical structure, Toeplitz matrices have attracted the interest of many mathematicians and mathematical physicists [108, 109, 110, 111, 112, 113]. Their efforts have led to an impressive understanding of the properties of such matrices.

In particular, a vast mathematical literature has been devoted to the study of the asymptotic behavior of their determinants, known as *Toeplitz determinants* (for details see Appendix A of [49]). In the particular case of the XY chain, their behavior is determined by the parameters

$$\lambda_{\pm}(h, \gamma) \equiv \frac{h \pm \sqrt{\gamma^2 + h^2 - 1}}{1 + \gamma}, \quad (2.160)$$

whose values play a decisive role. This is not surprising: these parameters, which act as characteristic lengths, are the zeros of the dispersion relation in the complex plane once the identification $e^{iq} = z$ is made. Whenever a gap is present, the λ_{\pm} appear explicitly in the correlation expressions, while they do not appear in the gapless case. In particular, what matters is whether λ_{\pm} lie inside the unit circle in the complex plane and whether they possess an imaginary part. To obtain the asymptotic behavior of the correlation functions throughout the (h, γ) plane, it is sufficient to know λ_{\pm} and their inverses λ_{\pm}^{-1} in the region $h, \gamma \geq 0$. Here we restrict ourselves to briefly commenting on the behavior of $\rho^x(n)$ and we refer to Appendix C for a more detailed analysis. For $h > 1$ the system is in a disordered phase, since

$$\lim_{n \rightarrow \infty} \rho^x(n) = 0, \quad (2.161)$$

which implies the absence of net magnetization along the x -direction, *i.e.* $\langle \sigma_j^x \rangle = 0$. Conversely, for $|h| < 1$ the system is in an ordered phase, since

$$\lim_{n \rightarrow \infty} \rho^x(n) = [(1 - \lambda_-^2)(1 - \lambda_+^2)(1 - \lambda_+ \lambda_-)^2]^{1/4}, \quad (2.162)$$

implying a non-vanishing magnetization along the x -direction, given by

$$m_x \equiv \lim_{N \rightarrow \infty} |\langle \sigma_j^x \rangle| = [(1 - \lambda_-^2)(1 - \lambda_+^2)(1 - \lambda_+ \lambda_-)^2]^{1/8}, \quad (2.163)$$

which, on the Ising line $\gamma = 1$ reduces to

$$m_x = (1 - h^2)^{1/8}, \quad (2.164)$$

in accordance to the results of [23]. Finally, from the asymptotic behaviors of the correlators we observe that, in unit of the lattice spacing, the correlation length is given

by

$$\tilde{\zeta} = \frac{1}{|\log \lambda_+|}, \quad (2.165)$$

which diverges at the critical line $h = 1$.

Chapter 3.

Topologically Frustrated XY Chain

The aim of this Chapter, which is based on [1, 2], is to introduce *topological frustration* (TF) and investigate how it modifies the zero-temperature phase diagram of the XY quantum spin chain in a transverse magnetic field. In Section 3.1, we introduce a recently studied class of boundary conditions capable of modifying the physics of antiferromagnetic quantum spin chains, known as *frustrated boundary conditions* (FBC) [50]. Topologically frustrated quantum spin chains have attracted considerable interest due to their counterintuitive behavior: their properties differ strikingly from those of the same spin models without frustration, even in the thermodynamic limit [51]. In this context, the quantum phases exhibit an explicit dependence on the boundary conditions. These models offer a particularly strong example of how, at the quantum level, microscopic modifications—such as the choice of boundary conditions—can dramatically affect the excitation spectrum and the emergent low-energy physics, further enriching the landscape of exotic phases of matter. Subsequently, in Section 3.2, we present the topologically frustrated XY chain and derive its exact solution, comparing the frustrated and unfrustrated regimes. In Section 3.3 we discuss the general features of its ground state, focusing on the novelties induced by FBC. After a detailed analysis of the drastic changes in the ground state (GS) properties caused by the imposition of frustrated boundary conditions, we analytically prove that TF induces new *boundary quantum phase transitions* (b-QPTs) in the XY chain: an additional first-order b-QPT appears along the conformal lines of the unfrustrated case; a first-order b-QPT with Galilean dispersion emerges at zero field; and, finally, a second-order b-QPT with a quartic dispersion relation arises in a region of the phase diagram that would otherwise be ordered and gapped in the absence of frustration. To the best of our knowledge, this latter transition—separating two gapless regions of the parameter space with strikingly different GS behavior—constitutes the first example of a second-order QPT

characterized by a dispersion relation that is neither relativistic nor Galilean, but quartic. We also report numerical calculations supporting the validity of our analytical results. Sections 3.4 and 3.5 contain our detailed analysis of the b-QPTs induced by FBC. Finally, in Section 3.6 we summarize our findings.

3.1 Topologically frustrated quantum spin chains

According to Landau theory [98], one of the milestones of classical statistical mechanics, phases separated by a phase transition can be distinguished by a change in the behavior of a local order parameter, enabling to assess the macroscopic order in a system's phase. In particular, a non-zero local order parameter is a manifestation of spontaneous symmetry breaking [20, 21, 26] and the establishment of a macroscopic order that explicitly violates one of the specific symmetries of the theory. Symmetry breaking happens when crossing a critical point, where the system can reorganize itself modifying its macroscopic behavior [8]. Because of its success, Landau theory has firstly been borrowed without changes when dealing with quantum phases of matter [22]. However, it soon became clear that the complexity of quantum many-body systems was not fully captured by this theory. For example, it cannot explain nematic phases [114, 115] (where the breaking of a symmetry is not univocally associated to a single order parameter) and topological phases [38, 116] (described by non-local order parameters). This motivated calls for an extension of the Landau theory to include the description of those quantum phenomena which do not have any classical counterpart. Also a second assumption of the Landau theory could probably be challenged: its implicit assumption that microscopic changes in the system are negligible in determining its thermodynamic properties, hence the prescription to take the thermodynamic limit before doing any calculation. As a consequence, any change in the boundary conditions is considered to be irrelevant when dealing with the bulk, macroscopic behavior. Recently, however, it has been proven that at a quantum level this assumption misses part of the physics, precisely in the case of antiferromagnetic quantum spin chains with discrete symmetries and *frustrated boundary conditions* (FBC) [50], namely periodic boundary conditions with an odd number of sites. Such a peculiar choice of boundary conditions implies that the simultaneous minimization of all local interactions in the Hamiltonian is not compatible with the system's geometry, giving rise to geometrical frustration [117, 118]. Intuitively, one could still be led to think that the contributions of the boundary terms become irrelevant for sufficiently large systems. However, such an expectation has already been challenged several

times [51, 52, 119, 120, 121, 122, 123, 124]. For instance, it has been showed in [122] that by tuning the strength of a single bond defect in an odd length ferromagnetic quantum Ising ring in a transverse magnetic field the system can be driven across a quantum phase transition which separates a gapped magnetic phase from a gapless (but non relativistic) kink phase. Relevantly, at the transition point this model can be exactly mapped to the quantum Ising chain with FBC [50], which will be discussed soon. In the last few years important progresses have been made along this research line, particularly studying topologically frustrated quantum spin chains [53, 56, 57, 58, 59, 125, 126, 127, 128, 129], and the results indicate that FBC can completely change the zero temperature phase diagram and the low-energy properties. Over the years, extensively frustrated systems have been studied at large and it has been shown that they exhibit peculiar and exotic physical behaviors [118] which are very different with respect to those of their non-frustrated counterparts, both at a classical and at a quantum level. One of the main features of classical frustrated systems is the presence of highly degenerate ground state manifolds in the limit of a large number of sites [130]. This property can also be found in the simple case of a classical Ising chain with N sites and FBC, whose Hamiltonian is

$$H = \sum_{j=1}^N \sigma_j^x \sigma_{j+1}^x \quad (3.1)$$

and which can be thought as a single building block of an extensively frustrated system [50]. The GS space in the frustrated case is $2N$ times degenerate and spanned by kink states, with a single pair of nearest neighbor spins ferromagnetically aligned while the other $N - 1$ pairs are antiferromagnetically aligned (see Figure 1.1b). In contrast, without frustration the GS space would have degeneracy 2 and would be spanned the two Néel states, *i.e.* perfectly staggered antiferromagnetic states (see Figure (1.1a)). We denote by $|j\rangle$ with $j = 1, \dots, N$ the kink state such that $\sigma_j^x = \sigma_{j+1}^x = 1$. The other N kink states are obtained as $\Pi^z |j\rangle$, for which $\sigma_j^x = \sigma_{j+1}^x = -1$.

At the quantum level, turning on, for instance, a positive magnetic field h in the z -direction, *i.e.*

$$H = \sum_{j=1}^N \sigma_j^x \sigma_{j+1}^x + h \sum_{j=1}^N \sigma_j^z, \quad (3.2)$$

the extensive degeneracy introduced by FBC is lifted, and the ground state becomes unique and part of a Galilean band of gapless excitations, in a phase that would have

been gapped without frustration. This behavior can be understood straightforwardly if we study the Hamiltonian (3.2) at the lowest perturbative order in h [51, 131]. For $h \ll 1$ the $2N$ kink states split in energy into the states

$$|q, \pm\rangle = \frac{1 \pm \Pi^z}{\sqrt{2N}} \sum_{j=1}^N e^{iqj} |j\rangle \quad q \in \Gamma^-, \quad (3.3)$$

which have parity $\Pi^z = \pm 1$ and energy

$$E_{q,\pm} = -(N-2) \pm 2h \cos q. \quad (3.4)$$

Thus the ground state, given by

$$|GS\rangle = |0, -\rangle = \frac{1 - \Pi^z}{\sqrt{2N}} \sum_{j=1}^N |j\rangle, \quad (3.5)$$

is non-degenerate and separated from the first excited state by an energy gap closing algebraically as $1/N^2$. This behavior contrasts with its unfrustrated counterpart, where the gap between the two lowest-energy states closes exponentially with N , giving rise to a doubly degenerate ground state that remains separated from its first excited state by a gap which does not close in the thermodynamic limit. In a quasiparticle picture, the effect of FBC is to create, in the ground state, a quantum-dressed version of a single domain wall excitation that is delocalized over the entire chain [53]. The entanglement properties of this state were analyzed in [56], confirming the topological nature of the phase $h < 1$ and thereby providing a rigorous justification for the name *topological frustration* (TF). From a technological perspective, the ground state energy of the frustrated Ising chain is experimentally accessible in quantum simulators based on a few superconducting qubits [6], demonstrating that signatures of TF are already observable on current quantum computing platforms. Relevantly, TF has more recently been implemented on a programmable Rydberg atom array of 11 qubits composed of Rubidium atoms [132].

Notice that, since the ground state (3.5) is unique, the magnetization along the x direction vanishes, in contrast to the unfrustrated phase, where $|\langle \sigma_j^x \rangle| \simeq (1 - h^2)^{1/8}$ for small h . Moreover, the two-point correlation function on the ground state $|GS\rangle$ (3.5) given by

$$\rho^x(n) = (-1)^n \left(1 - \frac{2n}{N}\right). \quad (3.6)$$

Notice that

$$\rho^x\left(\frac{N-1}{2}\right) = (-1)^{\frac{N-1}{2}} \frac{1}{N}, \quad (3.7)$$

i.e. the correlator involving the two most distant spins on the ring vanishes in the thermodynamic limit, in accordance with the previously discussed zero value of the net magnetization along the x direction. The physical results obtained from this perturbative analysis are in agreement with the exact ones [50, 51]. In the opposite regime, namely for $h \gg 1$, the system enters a paramagnetic phase which, as expected, is not affected by the boundary conditions. Finally, in [1] it was analytically demonstrated that a first-order *boundary quantum phase transition* [54]—*i.e.* a discontinuity in the derivative of the ground-state energy that does not scale with N (in contrast to the two second-order quantum phase transitions discussed in Section (2.3))—occurs at $h = 0$ as a function of the applied field when the chain contains an odd number of spins:

$$\lim_{N \rightarrow \infty} \left(\left. \frac{\partial E_{GS}}{\partial h} \right|_{h \rightarrow 0^+} - \left. \frac{\partial E_{GS}}{\partial h} \right|_{h \rightarrow 0^-} \right) = -4, \quad (3.8)$$

whereas no such transition is present for even N .

Relevantly, the XY quantum spin chain (2.54) with FBC in the absence of an external magnetic field has also been studied in detail [53, 57, 58]. Notice that $h = 0$ implies

$$[H, \Pi^\alpha] = 0, \quad (3.9)$$

where

$$\Pi^\alpha \equiv \prod_{j=1}^N \sigma_j^\alpha, \quad (3.10)$$

with $\alpha = x, y, z$, is the α -parity operator. Moreover observe that, since N is odd, the parity operators satisfy the non-commuting algebra

$$\{\Pi^\alpha, \Pi^\beta\} = 2\delta_{\alpha,\beta}. \quad (3.11)$$

As a consequence, for a state $|\psi\rangle$ with definite energy and z -parity, $\Pi^x |\psi\rangle$ has the same energy but opposite z -parity. Hence, for $h = 0$ and odd N , even at finite size each energy level is always degenerate an even number of times (Kramers degeneracy [133]), and spontaneous symmetry breaking occurs even without taking the thermodynamic

limit. Taking advantage of this additional symmetry, the ground state magnetization (*i.e.* the expectation value of σ_j^α) and the two-spin correlation functions have been computed analytically [53, 57]. For $\gamma > 1$, where the ground state manifold is gapless and twofold degenerate, the average magnetization is constant but is suppressed by the total system size as $1/N$, a phenomenon called *mesoscopic ferromagnetic magnetization* [57]. On the other hand, for $\gamma < 1$ the ground state is still gapless but is fourfold degenerate. Here, since the operators H , Π^z , and the translation operator T , defined as

$$T^\dagger \sigma_j^\alpha T \equiv \sigma_{j+1}^\alpha, \quad (3.12)$$

form a complete set of compatible operators, two possibilities arise: choosing a translationally invariant state, thereby obtaining the mesoscopic ferromagnetic magnetization or break the translational invariance, producing a state whose magnetization looks like the staggered one but varies incommensurably over the chain [53]. Contrary to the former, the latter incommensurate configuration has been proven to be resilient even in the presence of antiferromagnetic-type defects breaking the translational symmetry of the model [126], paving the way for experimental observations. Moreover, the system undergoes a first order boundary quantum phase transition at the point $\gamma = 1$ [53]. Such a quantum phase transition is a consequence of the FBC and would be absent for other boundary conditions.

The results about the frustrated XY chain at $h = 0$ have been generalized [58] to the wider class of translationally invariant weakly-frustrated spin-1/2 Hamiltonians with a dominant antiferromagnetic Ising-type interaction in one direction and commuting with all three parity operators (3.10), *i.e.*

$$H = \sum_{j=1}^N \sigma_j^x \sigma_{j+1}^x + \lambda \sum_{j=1}^N H_j, \quad (3.13)$$

with N odd and

$$[H_j, \Pi^\alpha] = 0. \quad (3.14)$$

In this case, the expectation values of all local operators (with support on a finite, fixed number of sites) have been shown to decay to zero at least algebraically with the system size unless the ground state manifold contains at least two states whose momenta differ by π in the thermodynamic limit. Due to the previously discussed symmetries, this can be possible only for GS manifolds which are at least fourfold

degenerate. Finally, the same authors [59] provided an example of a quantum spin chain with FBC showing a complete destruction of the local order at both sides of a quantum phase transition, proving that TF can modify the nature of a critical point.

3.2 The model and its solution

The model we study is the XY chain in a transverse magnetic field [49, 89], which is defined by the Hamiltonian (2.54), that we analyzed in detail in Sections 2.2 and 2.3, focusing on its ferromagnetic version, *i.e.* $J < 0$. In this Chapter we will focus on the case in which the largest coupling between two spins is antiferromagnetic, and thus choose $J > 0$. In particular, here and in the rest of the Chapter we will set $J = 1$, so that the Hamiltonian reads

$$H = \frac{1}{2} \sum_{j=1}^N \left[\left(\frac{1+\gamma}{2} \right) \sigma_j^x \sigma_{j+1}^x + \left(\frac{1-\gamma}{2} \right) \sigma_j^y \sigma_{j+1}^y + h \sigma_j^z \right]. \quad (3.15)$$

Moreover, we impose FBC enforcing periodic boundary conditions

$$\sigma_{j+N}^\alpha \equiv \sigma_j^\alpha \quad \alpha = x, y, z \quad (3.16)$$

with an *odd* number of lattice sites. Analogously to the ferromagnetic case, we will again restrict our analysis, without loss of generality, to $h, \gamma \geq 0$ owing to the symmetries of the XY chain. Notice that, when $\gamma = 1$, the above model reduces to the frustrated quantum Ising chain, which has been studied in [1, 51, 125].

By following exactly the same steps discussed in detail in Section 2.2, we arrive at

$$H = \frac{1 + \Pi^z}{2} H^+ \frac{1 + \Pi^z}{2} + \frac{1 - \Pi^z}{2} H^- \frac{1 - \Pi^z}{2}, \quad (3.17)$$

with Π^z the z-parity symmetry (2.77) and

$$H^\pm = \frac{1}{2} \sum_{q \in \Gamma^\pm} \begin{pmatrix} \chi_q^\dagger & \chi_{-q} \end{pmatrix} \tilde{H}_q \begin{pmatrix} \chi_q \\ \chi_{-q}^\dagger \end{pmatrix}, \quad (3.18)$$

where \tilde{H}_q is given by (2.109), Γ^\pm are the two sets of quantized momenta (2.87), and

$$\{\chi_{q'}, \chi_{q'}^\dagger\} = \delta_{q,q'} \quad \{\chi_{q'}, \chi_{q'}\} = 0. \quad (3.19)$$

To diagonalize the Hamiltonian, here we choose the Bogoliubov angle θ_q such that

$$e^{i2\theta_q} = \frac{-h + \cos q - i\gamma \sin q}{\sqrt{(h - \cos q)^2 + \gamma^2 \sin^2 q}} \quad q \neq 0, \pi, \quad (3.20)$$

which, once inserted into (2.109), yields

$$\tilde{H}_{q \neq 0, \pi} = \begin{pmatrix} \epsilon(q) & 0 \\ 0 & -\epsilon(q) \end{pmatrix}, \quad (3.21)$$

where

$$\epsilon(q) = \sqrt{(h - \cos q)^2 + \gamma^2 \sin^2 q}. \quad (3.22)$$

Differently from the ferromagnetic case, now one needs to distinguish between the even N case and the odd one.

For even N one has

$$H^+ = \sum_{q \in \Gamma^+} \epsilon(q) \left(\chi_q^\dagger \chi_q - \frac{1}{2} \right) \quad (3.23)$$

$$H^- = \begin{cases} \sum_{q \in \Gamma^- \setminus \{\pi\}} \epsilon(q) \left(\chi_q^\dagger \chi_q - \frac{1}{2} \right) - \epsilon(\pi) \left(\chi_\pi^\dagger \chi_\pi - \frac{1}{2} \right) & \text{if } 0 \leq h < 1 \\ \sum_{q \in \Gamma^- \setminus \{0, \pi\}} \epsilon(q) \left(\chi_q^\dagger \chi_q - \frac{1}{2} \right) - \epsilon(\pi) \left(\chi_\pi^\dagger \chi_\pi - \frac{1}{2} \right) - \epsilon(0) \left(\chi_0^\dagger \chi_0 - \frac{1}{2} \right) & \text{if } h \geq 1. \end{cases} \quad (3.24)$$

For odd N , which is the frustrated case and represents the main focus of this Chapter, one has

$$H^+ = \sum_{q \in \Gamma^+ \setminus \{\pi\}} \epsilon(q) \left(\chi_q^\dagger \chi_q - \frac{1}{2} \right) - \epsilon(\pi) \left(\chi_\pi^\dagger \chi_\pi - \frac{1}{2} \right) \quad (3.25)$$

$$H^- = \begin{cases} \sum_{q \in \Gamma^-} \epsilon(q) \left(\chi_q^\dagger \chi_q - \frac{1}{2} \right) & \text{if } 0 \leq h < 1 \\ \sum_{q \in \Gamma^- \setminus \{0\}} \epsilon(q) \left(\chi_q^\dagger \chi_q - \frac{1}{2} \right) - \epsilon(0) \left(\chi_0^\dagger \chi_0 - \frac{1}{2} \right) & \text{if } h \geq 1. \end{cases} \quad (3.26)$$

3.3 Signatures of topological frustration on the GS

We now comment the general features of the frustrated XY chain, starting from its GS. We call $|GS'^{\pm}\rangle$, $|GS^{\pm}\rangle$ and $|GS\rangle$ the most general elements of the GS of H^{\pm} , $\frac{1 \pm \Pi^z}{2} H^{\pm}$

and H respectively. An analogous notation for the corresponding energies will also be employed. Furthermore, $|0^\pm\rangle$ denotes the vacuum of χ_q . We remember that the strategy to obtain the GS is the following: after having identified $|GS'^\pm\rangle$, the states $|GS^\pm\rangle$ can be found applying $(1 \pm \Pi^z)/2$. This in turn allows to find the GS energy $E = \min\{E^+, E^-\}$ and the corresponding set of $|GS\rangle$. In the thermodynamic limit $N \rightarrow \infty$ this procedure is fully analytical, while at finite N one has to resort to numerical methods.

3.3.1 In the absence of frustration

As it is evident from (3.23) and (3.24), in the absence of FBC, *i.e.* when N is even, the system is completely equivalent to its ferromagnetic counterpart (studied in Section 2.3), then $|GS^+\rangle = |GS'^+\rangle = |0^+\rangle$ and $|GS^-\rangle = |GS'^-\rangle = \chi_\pi^\dagger |0^-\rangle$ alternate as ground states and with corresponding energies

$$E^+ = -\frac{1}{2} \sum_{q \in \Gamma^+} \epsilon(q), \quad (3.27)$$

$$E^- = \begin{cases} -\frac{1}{2} \sum_{q \in \Gamma^-} \epsilon(q) + \epsilon(0) & \text{if } h \geq 1 \\ -\frac{1}{2} \sum_{q \in \Gamma^-} \epsilon(q) & \text{if } 0 \leq h < 1. \end{cases} \quad (3.28)$$

Furthermore one can observe that there are $N/2$ level crossings in the first quarter of the parameter space and that $h^2 + \gamma^2 = 1$ is an exact doubly degeneracy line for all sizes [94]. To determine precisely the GS at fixed (h, γ) one has to compare the energies (3.27) and (3.28). It can be shown that at large N the energy gap between these two states closes exponentially [99, 120], giving rise to a doubly degenerate manifold which spontaneously breaks \mathbb{Z}_2 symmetry [49]. To summarize, the unfrustrated antiferromagnetic case is exactly equivalent to the ferromagnetic one with even N , discussed in Section 2.3. Therefore, from now on we will focus exclusively on the odd N antiferromagnetic case.

3.3.2 The frustrated case

The presence of TF modifies significantly the scenario, particularly for $|h| < 1$, where one cannot choose $|GS'^+\rangle$ and $|GS'^-\rangle$ as ground states, with their z -parity being equal to -1 and $+1$ respectively. In other words, the lowest energy states of H^+ and H^-

are not compatible with the z -parity constraint (3.17). As a consequence, the GS with FBC can be interpreted as a single excitation in the system with respect to a fermionic vacuum state. This fact can be seen from Eqs. (3.25), (3.26), (3.22) imposing the parity constraint (3.17). From the shape of $\epsilon(q)$ when $0 < h < 1$ – see Figure 3.1 – we

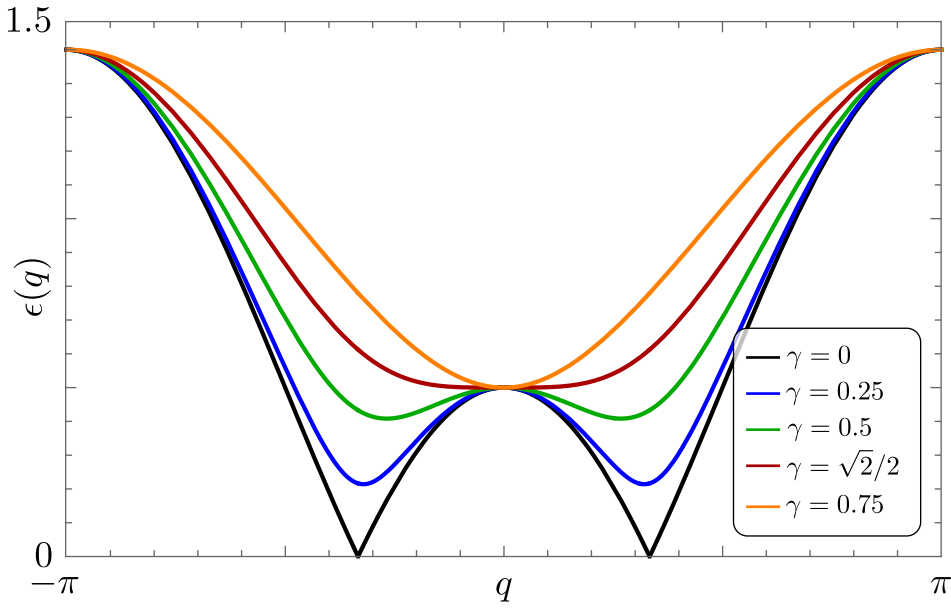


Figure 3.1.: Plot of the dispersion relation $\epsilon(q)$ as a function of $q \in [-\pi, \pi]$ for $h = 0.5$ and different values of γ : $\gamma = 0$ (black), $\gamma = 0.25$ (blue), $\gamma = 0.5$ (green), $\gamma = \gamma^*(0.5) = \sqrt{2}/2$ (red) and $\gamma = 0.75$ (orange).

can divide this region of the parameter space in two subregions, separated by a line $\gamma^*(N, h)$: one occurring when $0 < \gamma < \gamma^*(N, h)$ in which the set $\{\epsilon(q)\}_{q \in \Gamma^\pm}$ has two symmetric absolute minima and one for $\gamma > \gamma^*(N, h)$ where it has the only one minimum $\epsilon(0)$. It can be shown that [52]

$$\lim_{N \rightarrow \infty} \gamma^*(N, h) \equiv \gamma^*(h) = \sqrt{1-h}. \quad (3.29)$$

In the subregion $0 < h < 1$ when $\gamma > \gamma^*(h)$ the dispersion relation $\epsilon(q)$ always has the absolute minimum at $q = 0$ (as in Figure 3.1), hence the GS in the thermodynamic limit is not degenerate and given by $\chi_0^\dagger |0^-\rangle$ with energy

$$E \simeq E_0 + 1 - h, \quad (3.30)$$

where

$$E_0 \equiv -\frac{N}{4\pi} \int_0^{2\pi} \epsilon(q) dq \quad (3.31)$$

is the GS energy (2.137) in the absence of frustration. Moreover, the GS is now part of a band of states and the system is gapless, with the energy gap closing as $1/N^2$.

In the subregion $0 < h < 1$ when $0 \leq \gamma < \gamma^*(h)$ the dispersion relation has always two symmetric absolute minima (as shown in Figure 3.1) at $q = \pm p(h, \gamma)$ with [52]

$$p(h, \gamma) = \arccos\left(\frac{h}{1 - \gamma^2}\right), \quad (3.32)$$

hence the GS space depends on the exact position in the parameter space (h, γ) and is given by

$$GS^+ = \text{span}\left\{\chi_{p_+(h,\gamma)}^+ \chi_\pi^+ |0^+\rangle, \chi_{-p_+(h,\gamma)}^+ \chi_\pi^+ |0^+\rangle\right\}, \quad (3.33)$$

or

$$GS^- = \text{span}\left\{\chi_{p_-(h,\gamma)}^+ |0^-\rangle, \chi_{-p_-(h,\gamma)}^+ |0^-\rangle\right\} \quad (3.34)$$

where we denoted with $p_+(h, \gamma)$ and $p_-(h, \gamma)$ respectively the closest elements to $p(h, \gamma)$ in Γ^+ and Γ^- . It is interesting that, as already pointed out in [128], in the thermodynamic limit the GS fidelity does not vanish only if we move along one of the parabolas $h = c(1 - \gamma^2)$ with $c \in [0, 1]$, where the minima of $\epsilon(q)$ remain fixed. Hence the frustrated system exhibits a behavior similar to a model with a continuous symmetry (e.g. the XXZ chain in its paramagnetic phase [49, 134]).

In the thermodynamic limit, the energy of the GS in this particular region of the parameter space is

$$E \simeq E_0 + \gamma \sqrt{\frac{h^2 + \gamma^2 - 1}{\gamma^2 - 1}}. \quad (3.35)$$

Moreover, the energy gap separating the finite size two-fold degenerate ground state manifold with the first excited one closes exponentially with N in the thermodynamic limit [128], giving rise to a gapless GS with degeneracy 4, spanned by states with oppo-

site z -parity. Note that the cardinality of the two sets Γ^+ and Γ^- scales proportionally to the number of sites. As a consequence, increasing N the number of level crossings between twice degenerate manifolds with opposite z -parity and non-vanishing momenta [128] increases. In particular, observe that the mirror symmetry of our theory, *i.e.* the invariance of the Hamiltonian in Eq. (3.15) under the transformation mapping the spin operator σ_j^α into σ_{2k-j}^α where k is a generic site of the chain, implies that if the GS momentum is not zero, then the ground state manifold is a two-fold degenerate manifold spanned by single particle excitations with equal and opposite momenta, as proven in [53].

3.4 First order b-QPTs

In this Section we study the possible presence of curves in the (h, γ) plane at which the system undergoes first order b-QPTs, which are non-extensive discontinuities in the first derivative of the GS energy [54]. In the previous Section we computed the GS energy in the large N limit to be of the form $E = E_0 + \Delta E$ with E_0 defined in Eq. (3.31) and

$$\Delta E(h, \gamma) = \begin{cases} 0 & \text{if } |h| \geq 1 \\ |\gamma| \sqrt{\frac{h^2 + \gamma^2 - 1}{\gamma^2 - 1}} & \text{if } |h| < 1, |\gamma| < \gamma^*(|h|) \\ 1 - |h| & \text{if } |h| < 1, |\gamma| \geq \gamma^*(|h|) \end{cases} \quad (3.36)$$

This last quantity represents the energy difference induced by TF. Note that the correction ΔE , which is a distinguishing feature of FBC, does not scale with the number of sites. As a consequence, any possible new discontinuity of E cannot be extensive.

From Eq. (3.36) we observe that the system undergoes a first order b-QPT at $h = 1$ with $\gamma > 0$ and at $h = 0$ with $\gamma \geq 1$. Moreover, when $0 \leq h \leq 1$

$$\lim_{\gamma \rightarrow 0^+} \frac{\partial E}{\partial \gamma} - \lim_{\gamma \rightarrow 0^-} \frac{\partial E}{\partial \gamma} = 2\sqrt{1 - h^2}, \quad (3.37)$$

so there is another first order b-QPT at $\gamma = 0$ with $0 \leq h < 1$. Note that this discontinuity of the first derivative of the GS energy vanishes at the bi-critical point $(h, \gamma) = (1, 0)$.

To conclude, observe that the second order QPTs of the non-frustrated case [49] survive when FBC are applied, see Eqs. (3.31) and (3.36). This is because they are bulk (*i.e.*

extensive) QPTs [22] and, as a consequence, they are not sensitive to the choice of boundary conditions. At these critical lines the dispersion relation (3.22) vanishes for some values of q and is relativistic (except the bi-critical point), differently from what happens at $h = 0$, where $\epsilon(q)$ is Galilean around its minimum

$$\epsilon(q)|_{h=0} \approx 1 + \frac{\gamma^2 - 1}{2} q^2, \quad (3.38)$$

meaning that the energy gap between the ground state and the lightest excitation goes like $\delta\epsilon(q) \simeq \frac{\gamma^2 - 1}{2} q^2$.

3.5 Second order b-QPTs

In Section 3.3 it has been shown that the critical line $\gamma^*(N, h)$ divides the region $0 \leq h < 1$ of the first quarter of the parameter space into two subregions with completely different properties. Crossing this line the GS changes from a gapless non degenerate one, with negative z -parity and vanishing momentum, to a doubly degenerate one with two states with the same z -parity but opposite, non vanishing, momenta. Because of the quantization of momenta – see Eq. (2.87) – and the fact that the minima of $\epsilon(q)$ continuously change when moving γ for $\gamma < \gamma^*(h)$, increasing N the number of level crossings between two-fold degenerate manifolds with opposite z -parities and different non vanishing momenta increases. The gap between these alternating manifolds closes exponentially as N increases, giving rise to a four times degenerate gapless region. Relevantly, in the thermodynamic limit the crossover between ground states with opposite parities becomes continuous, giving rise to an extreme case of orthogonality catastrophe [135, 136] which is a typical feature of one-dimensional models with continuous symmetries [128], such as the XXZ chain [49]. The peculiar behaviour of the system in this region can be traced back to the fact that both the interactions along x and y become antiferromagnetic and, hence, sources of geometrical frustration. Thus, a natural question is whether crossing $\gamma^*(h)$ induces a b-QPT. In the following Subsection we will analytically prove that this is the case, and in Section 3.5.2 we will provide further numerical evidences that corroborate the correctness of our proof. It is here worth to remark that a counter-intuitive behavior takes place: a b-QPT, and not a usual, extensive, quantum phase transition, separates regions with strikingly different properties.

3.5.1 Analytical approach

By using the same notation introduced in Section 3.4, we have that

$$\frac{\partial \Delta E}{\partial \gamma} = \begin{cases} \frac{(1-\gamma^2)^2 - h^2}{(1-\gamma^2)^{3/2} \sqrt{1-h^2-\gamma^2}} & \text{if } 0 < \gamma < \gamma^*(h) \\ 0 & \text{if } \gamma \geq \gamma^*(h). \end{cases} \quad (3.39)$$

Figure 3.2 shows a plot of Eq. (3.39) as a function of γ . The *first* derivative of $\frac{\partial \Delta E}{\partial \gamma}$ has

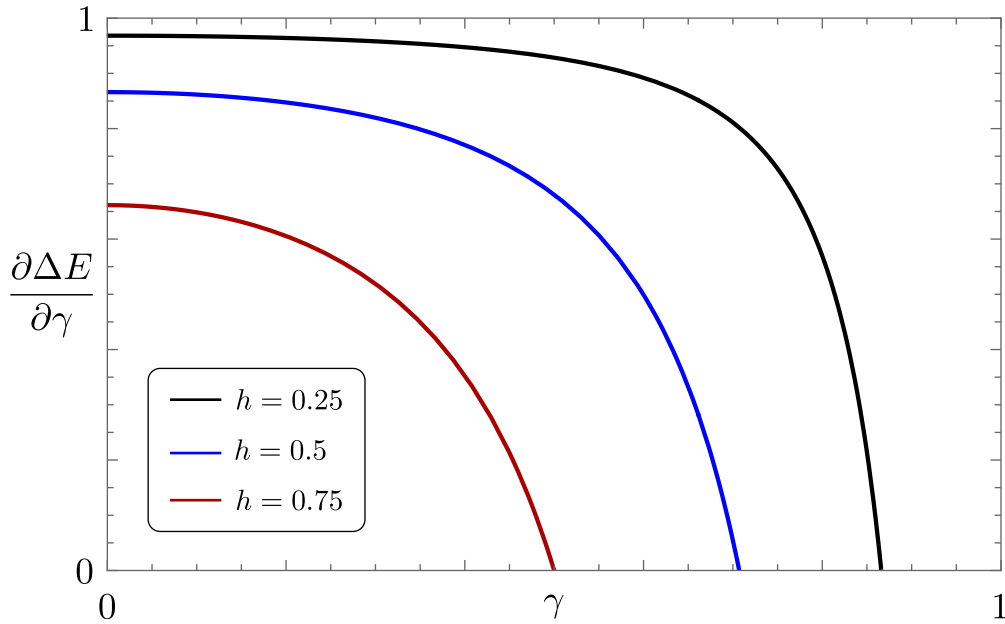


Figure 3.2.: Plot of $\frac{\partial \Delta E}{\partial \gamma}$ as a function of γ for different values of h : $h = 0.25$ (black), $h = 0.5$ (blue) and $h = 0.75$ (red).

a discontinuity at $\gamma = \gamma^*(h)$ and therefore the *second* derivative of E must have a jump discontinuity for $\gamma = \gamma^*(h)$. In particular, we observe that

$$\lim_{\gamma \rightarrow (\gamma^*)^+} \frac{\partial^2 E}{\partial \gamma^2} - \lim_{\gamma \rightarrow (\gamma^*)^-} \frac{\partial^2 E}{\partial \gamma^2} = \frac{4}{h'} \quad (3.40)$$

from which we arrive at the key result that the system undergoes a *second order b-QPT* at $\gamma^*(h)$. Note that the divergence of the discontinuity for $h \rightarrow 0$ seems compatible with the emergence of the first order b-QPT discussed previously.

It should be noted that this discontinuity was not found in [128], where the same model was analyzed. While here we took the thermodynamic limit first and studied

the energy discontinuity across the point $\gamma = \gamma^*$, in [128] the authors calculated the finite-size energy jump and performed a finite-size scaling analysis. In the latter way, for any finite N it is always possible to select a neighbor of the transition line where the momentum of ground state does not change with γ and N because of momentum quantization (see Eq. (2.87)). Calculated in this way, the energy jump vanishes faster with large N , but it is not clear if the thermodynamic limit can be safely taken, since in this limit the constant momentum neighbor shrinks to zero. Thus we will support our claim that the procedure employed in this work is correct through numerical analysis in the next Section. Before doing so, it is important to stress here that in sharp contrast from all the other critical points studied in Section 3.4, the dispersion relation for the lightest excitation at the critical parabola $\gamma^*(h)$ has the following McLaurin expansion around its minimum

$$\epsilon(q)|_{\gamma^*} \approx 1 - h + \frac{h}{8(1-h)} q^4, \quad (3.41)$$

indicating an energy gap of $\delta\epsilon(q)|_{\gamma^*} \simeq \frac{h}{8(1-h)} q^4$ which is thus neither Galilean nor relativistic, but *quartic*. To the best of our knowledge, this is the first case of second order QPT characterized by such a dispersion relation. In the scaling limit, quartic dispersion relations would be generated by high derivative or long-range field theories, but these terms are typically irrelevant and their contributions are usually unobservable corrections to the leading terms. In this case, this dispersion relation indicate a highly non-linear behavior of the single topological excitation injected in the GS by frustration [56], which is likely a quantum analog to the quartic solitons [137, 138, 139, 140].

3.5.2 Numerical analysis

In this Subsection we support our previous theoretical results with a numerical approach that confirms the existence of a second order b-QPT along the critical parabola $\gamma^*(h)$.

The second partial derivative of the GS energy $E(h, \gamma; N)$ with respect to γ for finite odd N has been evaluated employing a fourth-order "stencil" [141, 142]

$$\frac{\partial^2 E(h, \gamma; N)}{\partial \gamma^2} \simeq \frac{-E(\gamma + 2\delta\gamma) + 16E(\gamma + \delta\gamma) - 30E(\gamma) + 16E(\gamma - \delta\gamma) - E(\gamma - 2\delta\gamma)}{12\delta\gamma^2}, \quad (3.42)$$

where, for brevity, we have denoted $E(\gamma) = E(h, \gamma; N)$ at the right hand side of the above equation. The truncation error of Eq. (3.42) is $\mathcal{O}((\delta\gamma)^4)$. Concerning the stability of the fourth order stencil of Eq. (3.42), a sufficiently small value for $\delta\gamma$ has to be employed. A sensible order of magnitude for $\delta\gamma$ is given by the smallest typical energy scale of the system, i.e. $\delta k \equiv 2\pi/N$. Figure 3.3 shows a plot of $\frac{\partial^2 E(h, \gamma; N)}{\partial \gamma^2}$ as

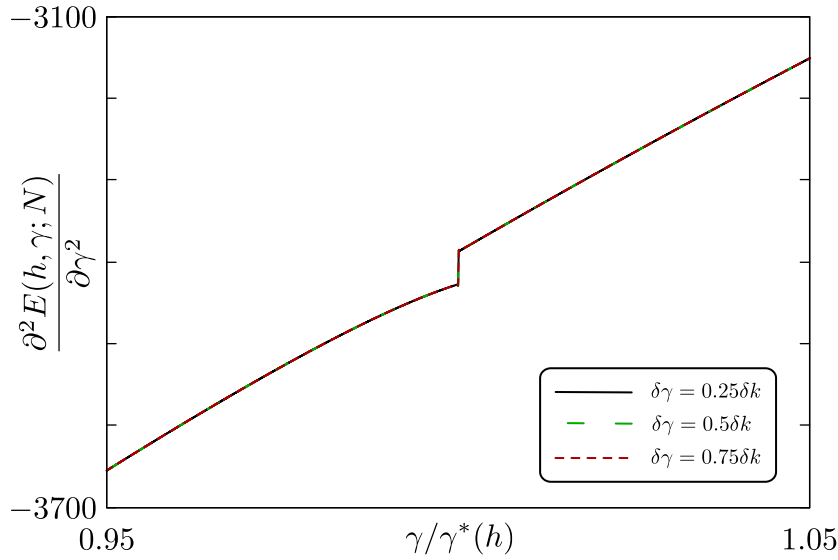


Figure 3.3.: Plot of $\frac{\partial^2 E(h, \gamma; N)}{\partial \gamma^2}$ as a function of $\gamma/\gamma^*(h)$ for three different values of $\delta\gamma$: $\delta\gamma = 0.25\delta k$ (black), $\delta\gamma = 0.5\delta k$ (green dashed), $\delta\gamma = 0.75\delta k$ (red dotted). Here, $h = 0.1$ and $N = 50001$.

a function of γ/γ^* for three different choices of $\delta\gamma < \delta k$. As can be seen, all curves collapse ontop of each other, signalling that the derivative is stable with respect to the choice of $\delta\gamma < \delta k$. All the subsequent numerical analyses have been performed employing $\delta\gamma = 0.25\delta k$ since the estimate of $\frac{\partial^2 E(h, \gamma; N)}{\partial \gamma^2}$ is numerically stable as long as $\delta\gamma < \frac{2\pi}{N}$.

Figure 3.4 shows the behaviour of $\frac{\partial^2 E(h, \gamma; N)}{\partial \gamma^2}$ as a function of $\gamma/\gamma^*(h)$ at finite odd N for three different values of h . As is clear, a sudden jump is found around $\gamma = \gamma^*(h)$. Crucially, this jump increases as h decreases. The inset of Figure 3.4 shows a zoom in a narrow window of γ around $\gamma^*(h)$: clearly, the curves exhibit a local minimum for $\gamma = \bar{\gamma}_- \lesssim \gamma^*(h)$ followed by a sudden jump and a local maximum for $\gamma = \bar{\gamma}_+ \gtrsim \gamma^*(h)$, a behaviour closely reminiscent of the Gibbs phenomenon [143, 144]. Via careful numerical analysis, we have found that the distance $\Delta\gamma \equiv \bar{\gamma}_+ - \bar{\gamma}_-$ scales

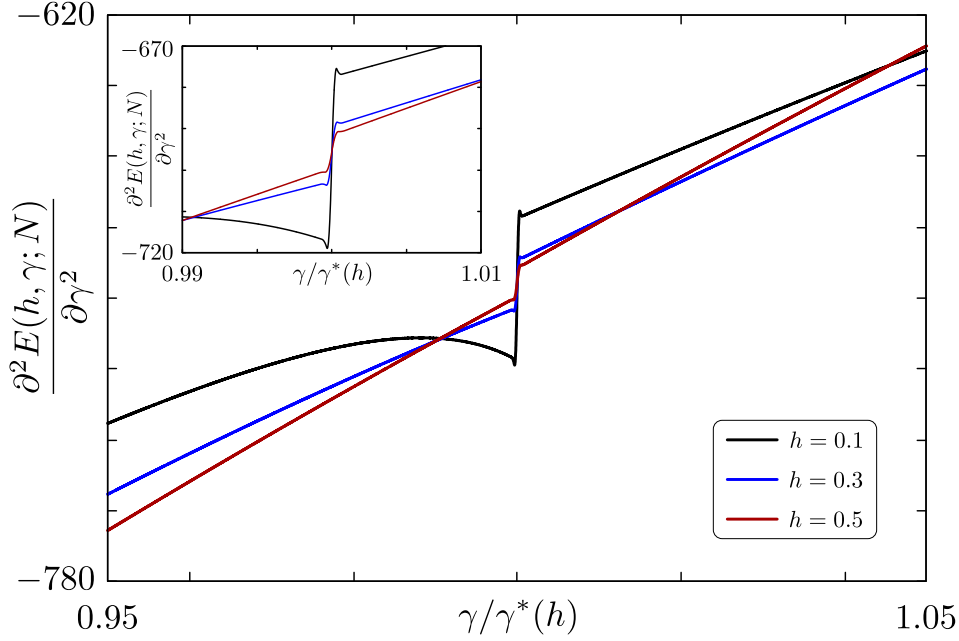


Figure 3.4.: Plot of $\frac{\partial^2 E(h, \gamma; N)}{\partial \gamma^2}$ as a function of $\gamma/\gamma^*(h)$ for different values of h : $h = 0.1$ (black), $h = 0.3$ (blue), $h = 0.5$ (red). The top left inset shows a zoom centered about the abrupt jump. Here $N = 10001$ and note that the curves have been offset in order to vertically align the center of the jump region.

with N as

$$\Delta\gamma = \frac{2\pi}{N} \sqrt{1-h}. \quad (3.43)$$

An example of this behaviour is shown in Figure 3.5 (a) for $h = 0.1$, where the green dots represent numerical data obtained for different large values of odd N and the red curve represents the scaling law of Eq. (3.43). The agreement is excellent and the same level of accuracy of the above scaling law has been observed for all values of h . To resume, as N is increased, the distance $\Delta\gamma$ is found to scale as $1/N$. This, together with the fact that the height of the jump is stable increasing N (as we will see below) strongly suggests that in the thermodynamic limit $\frac{\partial^2 E(h, \gamma; N)}{\partial \gamma^2}$ indeed develops a discontinuity. To obtain the value of this discontinuity without ambiguity, we extrapolate the jump of $\frac{\partial^2 E(h, \gamma; N)}{\partial \gamma^2}$ around $\gamma^*(h)$ at finite N introducing two third-order polynomial approximations $\varphi_-(\gamma)$ and $\varphi_+(\gamma)$, obtained fitting the numerical data for

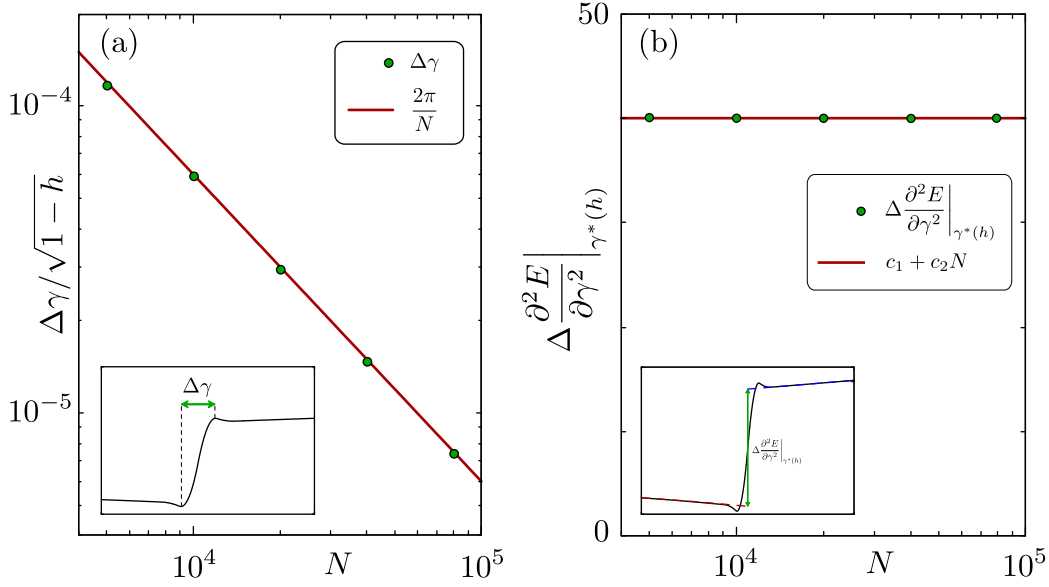


Figure 3.5.: Panel (a): Plot of $\Delta\gamma/\sqrt{1-h}$ (green dots) and of the function $2\pi/N$ (red line) as a function of N . Panel (b): plot of $\Delta\left.\frac{\partial^2 E}{\partial\gamma^2}\right|_{\gamma^*(h)}$ (green dots) and of the fitting function $c_1 + c_2N$ as a function of N . Here, $h = 0.1$ and the fitting parameters have been found to be $c_1 \approx 39.97$ and $c_2 \approx 6.79 \cdot 10^{-11}$.

$\gamma < \gamma_-$ and $\gamma > \gamma_+$. We then define the jump of the second derivative at finite N as

$$\Delta\left.\frac{\partial^2 E}{\partial\gamma^2}\right|_{\gamma^*(h)} \equiv \varphi_+(\gamma^*(h)) - \varphi_-(\gamma^*(h)). \quad (3.44)$$

The procedure is illustrated in Figure 3.6, which shows the second derivative of the GS energy and the approximating functions $\varphi_-(\gamma)$ and $\varphi_+(\gamma)$ (red and blue dashed curves respectively) as a function of $\gamma/\gamma^*(h)$. The quantity (3.44) shows an excellent stability with respect to N . As an example, Figure 3.5 (b) shows it plotted as a function of large N (green dots): the observed numerical independence of N strongly supports the presence of a finite jump in the thermodynamic limit. To quantitatively assess the stability of this result we have fitted the numerical data of Figure 3.5 (b) to a linear function of the form $c_1 + c_2N$. For the case of $h = 0.1$ shown in the Figure, the fitting parameters are found to be $c_1 \approx 39.97$ – in excellent agreement with the theoretically found law $4/h$ – and $c_2 < 10^{-11}$, which is a solid evidence of the insensitivity of the numerical results with respect to large N . Similar levels of robustness have been found for all values of h . This allows to conclude that our numerical results are thermodynamically robust. In other words, for large N , the quantity (3.44) shows

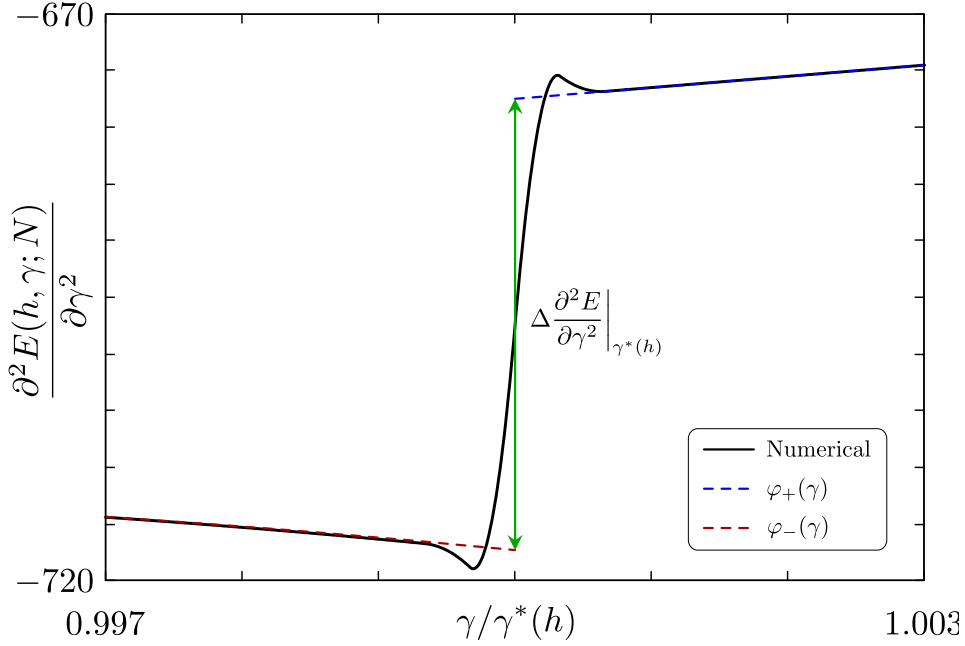


Figure 3.6.: Plots of $\frac{\partial^2 E(h, \gamma; N)}{\partial \gamma^2}$ as a function of $\gamma/\gamma^*(h)$ (black solid line) and of the extrapolating functions $\varphi_-(\gamma)$ (red dashed line) and $\varphi_+(\gamma)$ (blue dashed line). Here, $h = 0.1$ and $N = 10001$.

to be independent of N providing evidence to the fact that the jump is stable in the thermodynamic limit. At last, we show in Figure 3.7 the value of the jump of the second derivative of the GS energy obtained numerically as green dots, compared with the analytical result $4/h$ obtained in Eq. (3.40). The agreement is excellent, which confirms the robustness of the analytical calculations performed in Subsection 3.5.1.

3.6 Conclusions

We have shown that TF can deeply modify the zero temperature phase diagram of a one-dimensional quantum spin-1/2 system with discrete symmetries by inducing new b-QPTs, both of the first and of the second order. In particular, we focused on the example of the XY chain in an external magnetic field, possibly the simplest non-trivial integrable model. Without frustration, this model is characterized by two QPTs: one at $\gamma = 0, h \leq 1$ (belonging to the universality class with conformal charge $c = 1$) which separates two ordered phases and the other one at $h = 1$ ($c = 1/2$ conformal field theory) that divides the ordered phase from the disordered (*i.e.* paramagnetic) one. These two lines meet at the bi-critical point $(h, \gamma) = (1, 0)$, which is non-conformal.

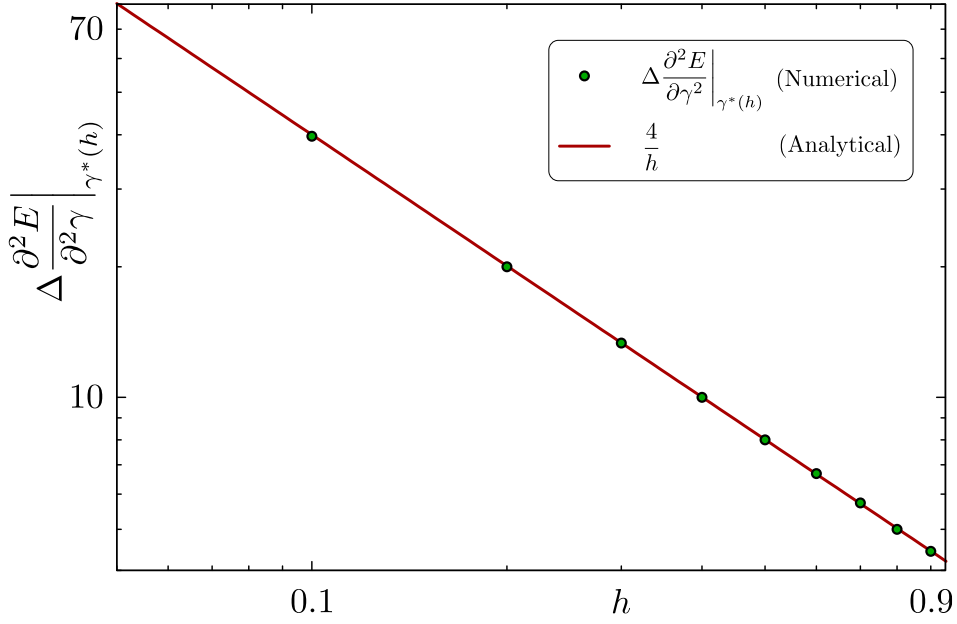


Figure 3.7.: Plots of the numerically evaluated gap $\Delta \frac{\partial^2 E}{\partial^2 \gamma} \Big|_{\gamma^*(h)}$ (defined by Eq. (3.44)) as a function of h (green dots) and of the analytical result $4/h$. Here, $N = 100001$.

When FBC are imposed, first order b-QPTs are induced at the conformal lines and at $h = 0, \gamma \geq 1$, where the dispersion relation is Galilean. Furthermore, TF generates a second order b-QPT in correspondence of the parabola $\gamma = \sqrt{1-h}$ which separates a non-degenerate gapless region with definite z-parity and zero momentum from a four times degenerate gapless region with non-vanishing momenta and characterized by an extreme case of orthogonality catastrophe (which is a typical feature of models with continuous symmetries).

Notably, the phase diagram does not show any feature at $h^2 + \gamma^2 = 1$ which, in the unfrustrated counterpart, marks a line of exact double degeneracy even at finite size and crossing through which the external magnetic field (h) and the anisotropy parameter (γ) exchange the role of being the dominant interaction.

Interestingly, to the best of our knowledge we also came across the first example of second order b-QPT characterized by a dispersion relation which is neither relativistic nor Galilean but quartic. The correctness of our analytical calculations is supported by a numerical analysis.

Figure 3.8 and Table 3.1 resume all the QPTs induced by FBC in the XY spin-1/2 chain.

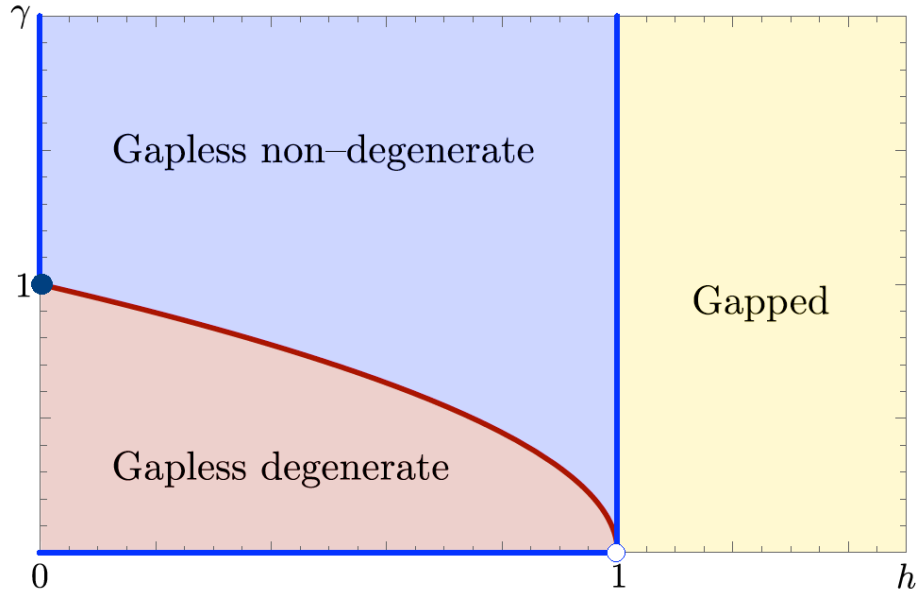


Figure 3.8.: Zero temperature phase diagram of the frustrated XY chain in the thermodynamic limit. The blue (red) bold lines represent the first (second) order boundary QPT induced by the imposition of FBC. The empty circle at $(1,0)$ stands for the absence of boundary quantum phase transitions and the filled circle at $(0,1)$ indicates the presence of a first order boundary quantum phase transition.

b-QPT	Order	Dispersion relation
$h = 0, \gamma \geq 1$	first	quadratic
$\gamma = 0, 0 \leq h < 1$	first	linear
$h = 1 (\gamma \neq 0)$	first	linear
$\gamma^2 + h = 1 (\gamma \neq 0, 1)$	second	quartic

Table 3.1.: Classification of b-QPT by order and dispersion relation in the XY quantum spin chain with FBC.

Chapter 4.

Fractons

From the middle of last century, Quantum Field Theory (QFT) has allowed us to enrich our modern comprehension of strongly correlated systems [38], characterized by a macroscopic number of interacting degrees of freedom whose collective behavior gives rise to emergent phenomena which are not expected by studying the single microscopic components only [9]. For instance, many quantum phases of matter [22], such as quantum Hall fluids [145] and quantum spin liquids [38], can be described in terms of vector gauge theories. As an example, Chern-Simons [34] and BF theories [75, 146] have been shown to be the natural theoretical frameworks to describe, respectively, the quantum Hall effect [40] and the topological insulators [147, 148]. On the other hand, many discoveries and ideas first developed in condensed matter and statistical physics had a later impact in the investigation of new fundamental problems of QFT [38]. This is exactly the case of *fractons*, exotic emergent excitations of certain quantum phases of matter which are completely immobile in isolation [62, 63, 66, 77]. Fractons represent an extreme case of subdimensional particles, *i.e.* which are restricted to move only in lower dimensional subspaces. In particular, as you can see in Figure 1.2, particles which can only move on zero-, one- and two-dimensional subspaces are known, respectively, as fractons, *lineons* and *planons* [62]. The first realization of this subdimensional behavior has been made in exactly solvable quantum spin models with discrete symmetries as quantum error-correcting codes [65, 67, 68]. The prototypical examples of fracton spin models in three spatial dimensions are the X-cube [67] and the Haah's Code [68] which belong, respectively, to "type I" and "type II" classes, the former being characterized by all three types of subdimensional excitations while the latter has fractons only. Subsequently it was realized that the restricted mobility of subdimensional particles can be also understood in the context of QFT in terms of higher moment conservation laws which can be derived from gapless

higher-rank symmetric tensor gauge theories [62, 149]. In the simplest models, the limited mobility property is achieved through a rank-2 generalization of the Gauss constraint, from which it follows immediately that both the total charge and the total dipole momentum are conserved up to boundary contributions, hence isolated single particles cannot move, which is the defining property of fractons. Since then, fractons have attracted more and more attention in many different areas of theoretical physics, such as QFT [150, 151, 152], elasticity [153, 154], hydrodynamics [155, 156, 157, 158], and gravity [70, 159, 160]. Relevantly, gapped spin fracton models and gapless higher-rank symmetric lattice gauge theories were related through a mechanism called Higgsing [161, 162], which gives a mass to the excitations by lowering the continuous gauge symmetry to a discrete one. More recently, there has been growing interest in developing relativistic and covariant formulations of fracton field theories [70, 74, 71, 163]. These formulations enable the adoption of theoretical high-energy tools in such a way that fracton properties can be derived from first principles of QFT: fields and symmetries.

The Chapter is organized as follows. In Section 4.1 we briefly review how sub-dimensional excitations emerge in exactly solvable quantum spin models, focusing in particular on the X-cube model, where the term “fracton” was introduced for the first time. The analysis of this model will be especially important, as it will also provide our first example of lineons, which will play a crucial role throughout the Thesis. In Section 4.2 we present how gapless subdimensional quasiparticles appear in the particle spectrum of higher-rank tensor gauge theories arising as the low-energy description of higher-rank $U(1)$ quantum spin liquids. In Section 4.3 we study the generalized electromagnetism that characterizes the Scalar Charge Theory, the most prominent rank-2 tensor gauge theory of fractons. In Section 4.4 we introduce the covariant approach to fracton gauge theories in 4D. We conclude the Chapter with Section 4.5, which discusses the motivations for studying fractons in 3D, whose covariant formulation will be the topic of Chapter 5.

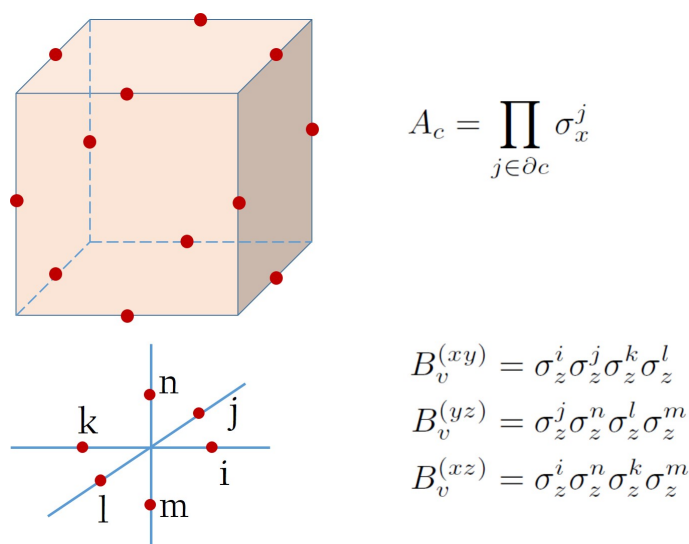
4.1 X-cube

The prototypical example for the fracton topological order is provided by the X-cube [66, 67], which is an exactly solvable quantum spin model defined on a cubic lattice with N qubit degrees of freedom living on each edge. This model is a milestone of fractonic literature since it exhibits the main features of these exotic topological phases

of matter. Its Hamiltonian reads

$$H = - \sum_c A_c - \sum_{v,i} B_v^i, \quad (4.1)$$

where A_c is the product of the twelve Pauli x -operators on the edges forming the boundary of the cube c , while B_v^i with $i = x, y, z$ is the product of the four Pauli z -operators adjacent to the vertex v and lying in the plane orthogonal to the i -th direction (see Figure 4.1). Furthermore, periodic boundary conditions are assumed on the



$$A_c = \prod_{j \in \partial c} \sigma_x^j$$

$$B_v^{(xy)} = \sigma_z^i \sigma_z^j \sigma_z^k \sigma_z^l$$

$$B_v^{(yz)} = \sigma_z^j \sigma_z^n \sigma_z^l \sigma_z^m$$

$$B_v^{(xz)} = \sigma_z^i \sigma_z^n \sigma_z^k \sigma_z^m$$

Figure 4.1.: Operators appearing in the X-cube Hamiltonian (4.1). Figure taken from [164].

$L_x \times L_y \times L_z$ lattice. We observe that $A_c^2 = (B_v^i)^2 = 1$, hence the operators A_c and B_v^i have eigenvalues ± 1 . Moreover, since

$$[A_c, B_v^i] = 0, \quad (4.2)$$

the Hamiltonian (4.1) is a sum of two mutually commuting terms, a property which guarantees the exact solvability of the model. A generic ground-state vector $|GS\rangle$ must satisfy

$$A_c |GS\rangle = B_v^i |GS\rangle = |GS\rangle \quad (4.3)$$

for all i, v and c . These conditions are precisely $N_c + 3N_v = 4L_x L_y L_z$ constraints, where $N_c = L_x L_y L_z$ and $N_v = L_x L_y L_z$ denote the numbers of cubes and vertices, respectively. However, these constraints are not all independent: the product of all cube operators

A_c lying in a given plane is equal to the identity, and similarly the product of all B_v^i operators on any plane orthogonal to the i -direction also yields the identity. In fact, one can show that there are

$$R = L_x L_y L_z + 2(L_x + L_y + L_z) - 3 \quad (4.4)$$

independent relations [66, 67]. Thus, the the total number of independent stabilizer constraints is

$$N_{ind} = N_c + 3N_v - R = 3L_x L_y L_z - 2(L_x + L_y + L_z) + 3, \quad (4.5)$$

which implies that the total number of independent qubits in the ground space (*logical qubits*) is

$$k = N - N_{ind} = 2(L_x + L_y + L_z) - 3. \quad (4.6)$$

Hence one concludes that the ground state degeneracy (*GSD*) is

$$GSD = 2^{2(L_x + L_y + L_z) - 3}, \quad (4.7)$$

from which we observe that the *GSD* scales exponentially with the linear system size, which is a hallmark of gapped fracton phases [68, 165]. The model is topologically ordered, since its ground states are indistinguishable under any local measurement [61]. This property is shared with conventional topological phases, such as fractional quantum Hall liquids, which however exhibit a constant *GSD* in the thermodynamic limit [10, 38, 45, 47], in contrast to the subextensive scaling of the X-cube model.

Let us now focus on the low-energy excitations. We would like to begin by considering the excitation that would arise from flipping the eigenvalue of a single cube operator, *i.e.* by imposing $A_c = -1$ on a cube c . However, such an isolated excitation cannot be created since a single spin flip necessarily changes the eigenvalues of the *four* cube operators that share the flipped link l . This follows from the fact that these four cube operators anticommute with σ_l^z , which is the Pauli operator acting on the link l . To summarize, we can only create four gapped cube excitations at a time, and they reside on the four cubes to which the flipped link belongs. More generally, one may act with a rectangular membrane operator consisting of a product of Pauli z-operators over a two-dimensional surface (see Figure 4.2 for clarity). Such an operator produces the same pattern of cube excitations as $\sigma_l^z |GS\rangle$, which now appear on the four cubes

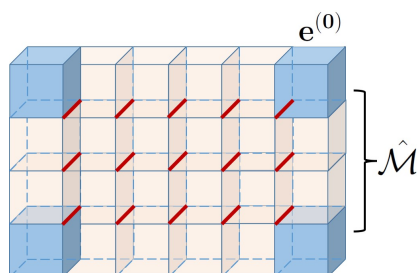


Figure 4.2.: When a membrane operator $\hat{\mathcal{M}}$, built as a product of σ_l^z operators (red lines), acts on the ground state, it creates four fractons (blue cubes). The notation $e^{(0)}$ indicates that each excitation is a 0-dimensional object. Figure taken from [164].

that intersect the membrane only along a single link. If we now focus on one of these cube excitations, it is immediate to see that there is no way to move it without paying a finite energy cost to create additional excitations (see Figure 4.3). Since they behave as

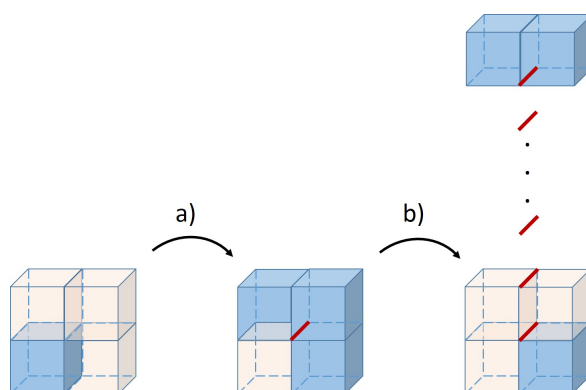


Figure 4.3.: A fracton (blue cube) can be moved, but doing so necessarily creates two additional excitations, each carrying a finite energy cost. The red line represents a z-Pauli operator. Figure taken from [164].

fractions of mobile quasiparticles, these new elementary topological excitations which are immobile under generic local perturbations were named *fractons* [66]. Relevantly, a pair of adjacent fractons becomes mobile within the plane containing the intersection of the two cube excitations (see Figure 4.4). Subdimensional quasiparticles of this type, whose motion is restricted to planes, are known as *planons*.

We now turn to the study of vertex excitations, beginning with the observation that a Pauli x -operator σ_l^x acting on a link l anticommutes with the four vertex operators associated with that link. This implies that the state $\sigma_l^x |GS\rangle$ corresponds to two gapped vertex excitations located at the endpoints of the link l . More generally, a product of Pauli x -operators along a straight line acting on the ground state creates

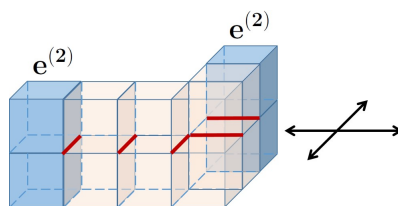


Figure 4.4.: A pair of adjacent fractons (blue cubes) can be moved freely by applying strings of z -Pauli operators (red lines) whose links lie in the plane containing the intersection of the two cube excitations. The notation $e^{(2)}$ reminds us that such an object is able to move only within a 2-dimensional manifold (a plane) without creating additional excitations. Figure taken from [164].

two gapped quasiparticle excitations at its endpoints. We observe that if we apply a Pauli x -operator on a link whose vertex is one of the two endpoints and which lies in a plane orthogonal to the straight string, we can turn the direction of one of the two quasiparticle excitations. However, this comes at the cost of creating an additional gapped one-dimensional excitation propagating along the original straight string. Thus, when we apply a straight string of Pauli x -operators on the ground state, we create two gapped quasiparticles at the endpoints which, at low energies, can move only along the line on which the Pauli string lies. Subdimensional quasiparticles whose motion is restricted to straight lines are called *lineons*. Let us finally consider a membrane operator defined as the product of Pauli- x operators over the links forming a rectangle. Acting on the ground state with such an operator creates four lineons, located at the four vertices of the rectangle. By changing the length of one of the two sides of the rectangle, we can move a dipole of lineons while keeping the other two fixed. More generally, we can construct an extended membrane operator as a product of such rectangular operators, arranged so that adjacent rectangles always share a side. In this way, the lineon dipole can be displaced within the plane spanned by these rectangles, *i.e.*, in the plane orthogonal to the segment connecting the two lineons we wish to move. Thus, a dipole of lineons behaves as a planon, living in the plane perpendicular to the line joining the two quasiparticles.

4.2 Higher-rank $U(1)$ gauge theories

Quantum spin liquids (QSLs) are zero-temperature disordered phases of quantum magnets characterized by strong quantum fluctuations, long-range quantum entanglement and exotic fractionalized excitations. Relevantly, they represent one of the most striking examples of emergent gauge theory in condensed matter physics. Indeed, in

their infrared limit, the microscopic spins disappear from the low-energy description and the relevant degrees of freedom are instead *emergent* gauge fields. In particular, the low-energy theory of a rank-1 $U(1)$ QSL shares the essential properties of ordinary Maxwell theory, being a deconfined compact $U(1)$ gauge theory. The prototypical realization is quantum spin ice, where the spin-ice rule (*i.e.* a geometrically frustrated spin interaction) generates an emergent $U(1)$ gauge symmetry. The fundamental degrees of freedom are a compact gauge field $A_\ell(x)$ and its canonically conjugate electric field $E_\ell(x)$, both defined on the oriented links ℓ of the lattice. On a cubic lattice in $(3 + 1)$ dimensions, it is convenient to assemble the link variables into spatial vector fields $\mathbf{A}(x)$ and $\mathbf{E}(x)$, whose i -th components correspond to the fields living on the link pointing in the i -direction from the vertex at position \mathbf{x} . These variables satisfy the equal-time canonical commutation relations

$$[A_j(\mathbf{x}), E_k(\mathbf{y})] = i\delta_{jk}\delta^{(3)}(\mathbf{x} - \mathbf{y}). \quad (4.8)$$

where, for the sake of convenience, we placed in the continuum limit. More precisely, in the lowest-energy sector, the spin ice rule translates into a source-free local Gauss constraint

$$\nabla \cdot \mathbf{E} = 0, \quad (4.9)$$

which generates the gauge transformations¹

$$\mathbf{A} \rightarrow \mathbf{A} + \nabla\alpha, \quad (4.10)$$

with $\alpha(\mathbf{x})$ a local scalar function. The low-energy effective rank-1 compact $U(1)$ Hamiltonian density reads

$$\mathcal{H} = \frac{1}{2}(g\mathbf{E}^2 + \mathbf{B}^2) + U(\nabla \cdot \mathbf{E})^2, \quad (4.11)$$

where g and U are numerical coefficient, and the emergent magnetic field is defined as

$$\mathbf{B} \equiv \nabla \times \mathbf{A}. \quad (4.12)$$

¹In Lattice Gauge Theory, the Gauss law $G(x) = 0$ is the generator of unitary operator $U(\alpha) = \exp\{-i \int d^3x \alpha(x)G(x)\}$ implementing a gauge transformation. Physical states satisfy $G(x)|\psi\rangle = 0$ or, equivalently, gauge invariance $U(\alpha)|\psi\rangle = |\psi\rangle$.

In the pure gauge sector (in the absence of dynamical charges), the Gauss-law term with large U energetically enforces (4.9) on physical states, and the Hamiltonian reduces to the emergent Maxwell characterized by a gapless photon excitation, with velocity $c \sim 1/\sqrt{g}$. In 3D, the compact $U(1)$ lattice gauge theory is not stable because of instanton effect, *i.e.* the proliferation of magnetic monopoles in Euclidean spacetime opens the photon gap [166]. This fact does not happen in 4D, where, in the infrared, monopole tunneling events are irrelevant and the Hamiltonian is self-dual under the electric-magnetic duality, a property which protect the stability of the deconfined Coulomb photon phase. At lowest energies, the source-free Gauss law (4.9) is obeyed, whereas higher energy states may violate it, *i.e.*

$$\nabla \cdot \mathbf{E} = \rho \neq 0, \quad (4.13)$$

where such violations of the low-energy constraint correspond to the charges of the emergent $U(1)$ gauge theory. In rank-1 $U(1)$ gauge theory, the emergent charge is a conserved quantity.

Historically, the study of QSLs has focused primarily on rank-1 gauge theories. However, it was subsequently shown in [69] that symmetric² $U(1)$ tensor gauge theories constitute an interesting new class of gapless QSLs, whose low-energy Hilbert space preserves all microscopic symmetries and whose gaplessness is protected against small arbitrary perturbations by a combination of emergent gauge invariance (enforced by a local Gauss constraint on the low-energy Hilbert space) and a generalized electromagnetic duality. Now we will focus in particular on rank-2 theories, which are characterized by a compact $U(1)$ symmetric tensor gauge field $A_{ij}(x)$, whose canonically conjugated variable is $E_{ij}(x)$, representing a generalized electric field and quantized to take integer values. In the lattice perspective, the off-diagonal components (such as $E_{12}(x)$) live on the faces of the lattice, whereas the diagonal components (such as $E_{11}(x)$) reside on the vertices. Since the precise choice of lattice is not important for the following discussion, we will work directly in the continuum limit. At rank-2, there are three different Gauss constraints that one may impose, and each choice corresponds to a different stable phase [69]. The procedure adopted in [69] is the following: one first imposes the Gauss constraint, which in general takes the form

$$G(x) = 0, \quad (4.14)$$

²Antisymmetric tensor gauge theories do not describe stable phases of matter and were therefore not taken into consideration.

where $G(x)$ may be either a scalar or a vector, and derives the corresponding gauge transformation that it generates. One then constructs the simplest possible gauge-invariant Hamiltonian whose terms commute with $G(x)$, which in turn requires defining a gauge-invariant rank-2 emergent magnetic field $B_{ij}(x)$. The resulting low-energy effective Hamiltonian density is

$$\mathcal{H} = \frac{1}{2}(E^{ij}E_{ij} + B^{ij}B_{ij}) + U G^2, \quad (4.15)$$

where U is a dimensionless parameter, and the explicit form of $B_{ij}(x)$ depends on the particular theory under consideration, *i.e.* on the choice of Gauss constraint (4.14). Other possible terms in the effective Hamiltonian contain a larger number of derivatives and are therefore irrelevant for the low-energy physics. At slightly higher energies there exist states that do not obey the Gauss constraint, and, exactly as in the rank-1 $U(1)$ gauge theory, such violations correspond to charged quasiparticles. Relevantly, in [60] it was demonstrated that the quasiparticle structures of these rank-2 emergent gauge theories are dramatically different from those of their rank-1 counterparts, due to the presence of several mobility restrictions analogous to those previously discussed for the X-cube model. In this sense, higher-rank theories can be viewed as gapless generalizations of the original gapped fracton models, which were characterized by discrete symmetries. Relevantly, the relation between gapped fracton models and gapless higher-rank gauge theories was investigated in [161, 162]. The restricted mobility of fractons was subsequently explored as a phenomenon that can be understood independently of the specific underlying microscopic model or physical mechanism enforcing it [149]. In particular, it can be realised as a consequence of higher-moment conservation laws and this development opened a new and exciting direction of research involving both condensed-matter and high-energy theorists. In the following, we review the quasiparticle structure of the four possible rank-2 emergent gauge theories, with particular emphasis on the associated mobility restrictions.

4.2.1 Vector Charge Theory

For a general state, the Gauss law is given by

$$\partial_i E^{ij} = \rho^j, \quad (4.16)$$

where ρ^j is a vector charge density. The corresponding source-free Gauss constraint generates the following gauge transformation [69]

$$\delta A_{ij} = \partial_i \Lambda_j + \partial_j \Lambda_i, \quad (4.17)$$

with $\Lambda_i(x)$ an arbitrary vector function. From (4.16) we observe immediately that, on an infinite volume V or up to boundary terms,

$$\int dV \rho^i = 0 \quad (4.18)$$

$$\int dV \epsilon_{0ijk} x^j \rho^k = 0, \quad (4.19)$$

which encode the conservation of, respectively, the total charge and the angular charge moment. In order to satisfy these conservation laws, vector charges are constrained to move only along the direction of their charge vector. To see this explicitly, consider a single vector charge \mathbf{q} located at position $\mathbf{x}(t)$ at time t , so that

$$\rho^i(\mathbf{x}, t) = q^i \delta^{(3)}(\mathbf{x} - \mathbf{x}(t)). \quad (4.20)$$

Then, from (4.19) one obtains $\epsilon_{0ijk} x^j(t) q^k = 0$, which implies that $\mathbf{x}(t)$ must remain parallel to \mathbf{q} at all times, *i.e.* it is a lineon. Finally, the magnetic field is defined as [69]

$$B_{ij} \equiv \epsilon_{0iab} \epsilon_{0jcd} \partial^a \partial^c A^{bd}, \quad (4.21)$$

and the resulting low-energy dispersion relation is quadratic, *i.e.* $\omega \sim k^2$.

4.2.2 Traceless Vector Charge Theory

The Gauss law for this theory is that of the Vector Charge Theory (4.16), supplemented by the additional requirement that $E_{ij}(x)$ be traceless throughout the entire Hilbert space, *i.e.*

$$E^i_i = 0. \quad (4.22)$$

From (4.16) and (4.22) we obtain

$$\int dV \rho_i x^i = 0 \quad (4.23)$$

$$\int dV \left(x_i \rho^i x^j - \frac{1}{2} x_i x^i \rho^j \right) = 0 \quad (4.24)$$

on an infinite volume V or up to boundary terms, and both the two conservation laws (4.18) and (4.19) of the Vector Charge Theory. These conservation laws imply that isolated vector charges cannot move at all, thus the tracelessness condition (4.22) converts them from lineons into fractons. Finally, in this theory the generalized magnetic field is defined as [149]

$$B_{ij} \equiv \frac{1}{2} \left[\epsilon_{0iab} (\partial_a \partial_k \partial_j A_{bk} - \partial_a \partial^c \partial_c A_{bj}) + \epsilon_{0jab} (\partial_a \partial_k \partial_i A_{bk} - \partial_a \partial^c \partial_c A_{bi}) \right], \quad (4.25)$$

and the resulting low-energy dispersion relation is cubic, *i.e.* $\omega \sim k^3$.

4.2.3 Scalar Charge Theory

The Gauss law on a general state is

$$\partial_i \partial_j E^{ij} = \rho, \quad (4.26)$$

where ρ is a scalar charge density. The source-free Gauss constraint generates the following gauge transformation [69]

$$\delta A_{ij} = \partial_i \partial_j \Lambda, \quad (4.27)$$

where $\Lambda(x)$ is an arbitrary scalar function. The Scalar Charge Theory (SCT) is the simplest of the four rank-2 theories, it is the only one that is not self-dual, yet it remains stable against confinement like the others. From the Gauss constraint (4.26) follow two mobility restrictions,

$$\int dV \rho = 0, \quad (4.28)$$

$$\int dV x^i \rho = 0, \quad (4.29)$$

on an infinite volume V or up to boundary terms. These imply that the fundamental quasiparticles must conserve their dipole moment and are therefore fractons, while

dipolar bound states are free to move. Furthermore, in this theory the magnetic field tensor is defined as [149]

$$B_{ij} \equiv \epsilon_{0iab} \partial^a A_j^b, \quad (4.30)$$

which is non-symmetric, traceless, and contains only a single spatial derivative. This structure leads to a linear dispersion relation, $\omega \sim k$. As a consequence, the low-energy physics can be described by a relativistic quantum field theory.

4.2.4 Traceless Scalar Charge Theory

The Gauss law is the same as in the SCT (4.26), supplemented by the additional tracelessness constraint (4.22). Together, these imply the mobility restrictions (4.28), (4.29), and

$$\int dV x_i x^i \rho = 0, \quad (4.31)$$

on an infinite volume V or up to boundary terms. As a consequence, the fundamental quasiparticles are fractons, unable to move without creating additional charges. Dipolar bound states, on the other hand, retain mobility but only within the plane orthogonal to their dipole moment, *i.e.* they behave as planons. To see this explicitly, consider an isolated physical dipole $\mathbf{p} = q \mathbf{d}$, with charge density

$$\rho(\mathbf{x}, t) = q [\delta^{(3)}(\mathbf{x} - \mathbf{x}(t) - \mathbf{d}) - \delta^{(3)}(\mathbf{x} - \mathbf{x}(t))], \quad (4.32)$$

where d^i denotes the vector from the negative to the positive charge, which must remain constant in order for the dipole moment to be conserved, as required by (4.29). Substituting (4.32) into (4.31) yields the condition $\Delta \mathbf{x}(t) \cdot \mathbf{p} = 0$, which implies that the dipole may move freely only within the plane orthogonal to its dipole moment \mathbf{p} . To conclude, the magnetic tensor field in this theory is defined as [149]

$$B_{ij} \equiv \frac{1}{2} \left(\epsilon_{0iab} \partial^a A_j^b + \epsilon_{0jab} \partial^a A_i^b \right), \quad (4.33)$$

which is symmetric, traceless, and contains only a single spatial derivative. As a result, the low-energy dispersion relation is linear, $\omega \sim k$.

4.3 Scalar Charge Theory: generalized electromagnetism

From the constrained Hamiltonian structure introduced in the previous Section (Eqs. (4.15) and (4.26)), it is useful to pass to a Lagrangian formulation. Following [167], we begin by writing down the partition function of the SCT

$$\begin{aligned}
Z &\propto \int \mathcal{D}A_{ij} \mathcal{D}E_{ij} \delta(\partial_i \partial_j E^{ij}) \exp \left\{ i \int d^3x dt \left(E^{ij} \partial_t A_{ij} - \frac{1}{2} E^{ij} E_{ij} - \frac{1}{2} B^{ij} B_{ij} \right) \right\} \\
&\propto \int \mathcal{D}A_{ij} \mathcal{D}E_{ij} \mathcal{D}\phi \exp \left\{ i \int d^3x dt \left(-\phi \partial_i \partial_j E^{ij} + E^{ij} \partial_t A_{ij} - \frac{1}{2} E^{ij} E_{ij} - \frac{1}{2} B^{ij} B_{ij} \right) \right\} \\
&\propto \int \mathcal{D}A_{ij} \mathcal{D}\phi \exp \left\{ i \int d^3x dt \left[\frac{1}{2} (\partial_t A_{ij} - \partial_i \partial_j \phi)^2 - \frac{1}{2} B^{ij} B_{ij} \right] \right\}, \tag{4.34}
\end{aligned}$$

where in the first step we introduced a scalar Lagrange multiplier $\phi(\mathbf{x}, t)$ to enforce the source-free Gauss constraint. From (4.34), we can read off the action of SCT

$$S_{inv} = \int d^3x dt \left[\frac{1}{2} (\partial_t A_{ij} - \partial_i \partial_j \phi)^2 - \frac{1}{2} B^{ij} B_{ij} \right], \tag{4.35}$$

which is invariant under the gauge transformation

$$\delta A_{ij} = \partial_i \partial_j \Lambda \quad \delta \phi = \partial_t \Lambda, \tag{4.36}$$

with $\Lambda(\mathbf{x}, t)$ an arbitrary scalar function.

In the Lagrangian formulation, the electric tensor field is, by definition, the conjugate momentum associated with the gauge field $A_{ij}(\mathbf{x}, t)$, *i.e.*

$$E^{ij} \equiv \frac{\delta \mathcal{L}_{inv}}{\delta \partial_t A_{ij}} = \partial_t A^{ij} - \partial^i \partial^j \phi, \tag{4.37}$$

where $\mathcal{L}_{inv}(A_{ij}, \phi)$ is the Lagrangian density. When matter is introduced, the total action becomes

$$S_{tot} = \int d^3x dt \left[\frac{1}{2} (\partial_t A_{ij} - \partial_i \partial_j \phi)^2 - \frac{1}{2} B^{ij} B_{ij} - \rho \phi - J^{ij} A_{ij} \right], \tag{4.38}$$

where J^{ij} is a symmetric tensor current, while ρ is the scalar charge density. The latter is fractonic, since the equation of motion for $\phi(\mathbf{x}, t)$ reproduces the generalized Gauss

law (4.26). From the equation of motion for $A_{ij}(\mathbf{x}, t)$, we obtain

$$-\partial_t E^{ij} + \frac{1}{2} \left(\epsilon^{0iab} \partial_a B_b^j + \epsilon^{0jab} \partial_a B_b^i \right) = J^{ij}, \quad (4.39)$$

which is a rank-2 generalization of the Ampère law

$$-\partial_t \mathbf{E} + \nabla \times \mathbf{B} = \mathbf{J}. \quad (4.40)$$

Relevantly, the symmetric tensor current $J_{ij}(\mathbf{x}, t)$ represents the current density of i -oriented dipoles moving in the j -th direction. This interpretation follows from the fact that dipolar bound states are the only mobile excitations in the theory, whereas isolated fractons remain immobile. By applying a double divergence $\partial_i \partial_j$ to the rank-2 Ampère law (4.39) and using the generalized Gauss law (4.26), we obtain

$$\partial_t \rho + \partial_i \partial_j J^{ij} = 0, \quad (4.41)$$

which is the rank-2 analogue of the ordinary continuity equation

$$\partial_t \rho + \nabla \cdot \mathbf{J} = 0. \quad (4.42)$$

Equation (4.41) will play a crucial role throughout this Thesis, as it encodes the fractonic nature of the theory. In particular, it implies the conservation of both the total charge and the total dipole moment

$$\frac{d}{dt} \int dV \rho = 0, \quad \frac{d}{dt} \int dV x^i \rho = 0 \quad (4.43)$$

on an infinite volume V or up to boundary terms.

From the definition of the magnetic tensor field (4.30), its divergence immediately yields

$$\partial_i B^{ij} = 0, \quad (4.44)$$

which is the rank-2 generalization of the familiar equation

$$\nabla \cdot \mathbf{B} = 0. \quad (4.45)$$

Furthermore, taking the time derivative of the magnetic tensor field (4.30) and using (4.37), we obtain

$$\partial_t B^{ij} + \epsilon^{0iab} \partial_a E_b^j = 0, \quad (4.46)$$

which generalizes Faraday's law

$$\partial_t \mathbf{B} + \nabla \times \mathbf{E} = 0 \quad (4.47)$$

to this rank-2 framework.

4.3.1 Electrostatics and Magnetostatics

Following [149], let us now consider a static isolated charge q (a fracton), which satisfies

$$\partial_i \partial_j E^{ij} = q \delta^{(3)}(\mathbf{x}), \quad (4.48)$$

and derive its generalized electrostatic Coulomb field. Dimensional analysis already suggests that $E^{ij}(\mathbf{x})$ must scale as $q/|\mathbf{x}|$, which is the first major difference with respect to the ordinary 4D case. Moreover, rotational invariance implies the general form

$$E^{ij}(\mathbf{x}) = q \left(\alpha \frac{\eta^{ij}}{|\mathbf{x}|} + \beta \frac{x^i x^j}{|\mathbf{x}|^3} \right), \quad (4.49)$$

where α and β are dimensionless coefficients to be determined. Substituting the ansatz (4.49) into (4.48), we find that the Gauss law is satisfied only if

$$\beta - \alpha = \frac{1}{4\pi}. \quad (4.50)$$

We observe that we still need to determine the coefficient α . This is another major difference from ordinary 4D electromagnetism, where the electric field of a static point charge is completely fixed by Gauss law together with rotational symmetry. To determine the value of α , we substitute the ansatz (4.49) into the generalized Faraday law (4.46) in the static limit. We find that this equation is satisfied only if

$$\alpha + \beta = 0. \quad (4.51)$$

Comparing (4.50) and (4.51), we can solve for α and β , thus concluding that the electric field generated by a fracton is

$$E^{ij}(\mathbf{x}) = \frac{q}{8\pi} \left(\frac{x^i x^j}{|\mathbf{x}|^3} - \frac{\eta^{ij}}{|\mathbf{x}|} \right). \quad (4.52)$$

One can also show that the rank-2 electric field generated by a dipole \mathbf{p} is [149]

$$E^{ij}(\mathbf{x}) = -\frac{1}{8\pi} \left[\frac{\eta^{ij}(\mathbf{p} \cdot \mathbf{x})}{|\mathbf{x}|^3} + \frac{p^i x^j + p^j x^i}{|\mathbf{x}|^3} - 3 \frac{x^i x^j (\mathbf{p} \cdot \mathbf{x})}{|\mathbf{x}|^5} \right], \quad (4.53)$$

which decays as $1/|\mathbf{x}|^2$, in contrast with the standard 4D electromagnetic dipole field. Moreover, from Eq. (4.37) we see that the electric potential generated by a fracton and by a dipole scales respectively as $|\mathbf{x}|$ and as $(\mathbf{p} \cdot \mathbf{x})/|\mathbf{x}|$ at large distances. This, in turn, implies that separating two fractons requires an amount of energy that grows linearly with their separation.

Let us now study a stationary current. From the generalized Ampère law (4.39), one finds that the magnetic tensor field generated by a steady current $J_{ij}(\mathbf{x})$ is [149]

$$B_{ij}(\mathbf{x}) = -\frac{1}{6\pi} \int d^3x' J_j^k(\mathbf{x}') \epsilon_{0ikl} \frac{x^l - x'^l}{|\mathbf{x} - \mathbf{x}'|^3}, \quad (4.54)$$

which serves as the generalized Biot–Savart law for the SCT. Moreover, we observe that, just as in ordinary 4D electromagnetism, the magnetic field decays as $1/|\mathbf{x}|$ at large distances.

4.3.2 Lorentz force

As we have learned so far, fundamental quasiparticles—being fractons—do not respond to electromagnetic fields, in contrast to dipolar bound states of a positive and a negative charge, which do not experience immobility restrictions. A dipole does respond to electromagnetic fields, although its orientation must remain fixed in order to preserve the total dipole moment. The generalized Lorentz force proposed in [149] and experienced by a dipole p^i moving with velocity v^i in an electromagnetic field is

$$F_j = -p^i \left(E_{ij} + \epsilon_{0jlk} v^l B^k_i \right). \quad (4.55)$$

As a physical check, let us study the electric force experienced by a dipole p^i located at x^i due to the presence of an identical dipole placed at the origin. The expression for this force is [149]

$$F^j = \frac{1}{8\pi} \left[2 \frac{p^j (\mathbf{p} \cdot \mathbf{x})}{|\mathbf{x}|^3} + p^2 \frac{x^j}{|\mathbf{x}|^3} - 3 \frac{(\mathbf{p} \cdot \mathbf{x})^2 x^j}{|\mathbf{x}|^5} \right], \quad (4.56)$$

whose radial component is [149]

$$F^j \hat{x}_j = \frac{p^2 \sin^2 \theta}{8\pi |\mathbf{x}|^2}, \quad (4.57)$$

where θ is the angle between p^i and x^i . From (4.57), we immediately observe that the radial component of the force is always non-negative, meaning that the interaction between two identical dipoles is repulsive. Conversely, if we consider the same configuration but with the dipoles oriented oppositely, the expression acquires an overall negative sign, implying an attractive force. This is physically intuitive, since oppositely oriented dipoles tend to recombine into the vacuum. Interestingly, the Lorentz force between two collinear dipoles, *i.e.* when $\theta = 0$ or $\theta = \pi$, vanishes. These configurations correspond respectively to a minimum and a maximum of the interaction potential for parallel and antiparallel dipoles [149]. In summary, identical dipoles tend to arrange themselves end to end, whereas antiparallel dipoles prefer to lie side by side.

4.4 Covariant approach

So far, the fractonic theories we have discussed are formulated in a non-covariant language. However, it was not long before high-energy theorists became interested in exploring the phenomenon of restricted mobility within the framework of relativistic quantum field theories. In particular, in [70] the authors introduced the first Lorentz-covariant 4D extension of the gauge transformation (4.27) that characterizes the SCT, and subsequently analyzed the resulting covariant tensor gauge theory using standard QFT techniques. They considered a symmetric tensor gauge field³

$$a_{\mu\nu} = a_{\nu\mu}, \quad (4.58)$$

³From now on, greek letters will denote spacetime indices.

with mass dimension

$$[a_{\mu\nu}] = 1 \quad (4.59)$$

transforming according to longitudinal diffeomorphisms [72]

$$\delta a_{\mu\nu} = \partial_\mu \partial_\nu \Lambda, \quad (4.60)$$

where $\Lambda(x)$ is a local scalar gauge parameter. Notice that (4.59) together with (4.60) implies that the mass dimension of $\Lambda(x)$ is negative,

$$[\Lambda] = -1. \quad (4.61)$$

In order for the gauge parameter to have vanishing mass dimension, as is often desirable, the tensor gauge field must itself have mass dimension two. This occurs in six spacetime dimensions (6D) for theories whose quadratic action contains two spacetime derivatives (such as Maxwell theory or Linearized Gravity), or in five dimensions for theories with only one derivative in the action, *i.e.* Chern-Simons-like theories. In lower dimensions, the gauge parameter unavoidably acquires a negative mass dimension. In 6D, the dimensionless nature of the gauge parameter is reflected in the structure of the energy-momentum tensor, which becomes traceless only in this spacetime dimension, thereby signaling scale invariance.

The most general 4D power-counting compatible action invariant under (4.60) is

$$S_{inv} = g_1 S_{LG} + g_2 S_M \quad (4.62)$$

where

$$S_{LG} = \int d^4x (\partial_\mu a \partial^\mu a - \partial_\rho a_{\mu\nu} \partial^\rho a^{\mu\nu} - 2\partial_\mu a \partial_\nu a^{\mu\nu} + 2\partial_\rho a_{\mu\nu} \partial^\mu a^{\nu\rho}) \quad (4.63)$$

$$S_M \equiv \int d^4x (\partial_\rho a_{\mu\nu} \partial^\mu a^{\nu\rho} - \partial_\rho a_{\mu\nu} \partial^\rho a^{\mu\nu}) \quad (4.64)$$

with g_1 and g_2 dimensionless constants,

$$a \equiv \eta^{\mu\nu} a_{\mu\nu} \quad (4.65)$$

and $\eta = \text{diag}(-1, +1, +1, +1)$ the 4D Minkowski metric. The invariant action (4.62) turns out to be a linear combination of the Linearized Gravity (LG) [73] action (4.63) to-

gether with an additional contribution (4.64). The former is the most general quadratic action invariant under infinitesimal diffeomorphisms,

$$\delta_{diff} a_{\mu\nu} = \partial_\mu \xi_\nu + \partial_\nu \xi_\mu, \quad (4.66)$$

where $\xi_\mu(x)$ is a vector gauge parameter. Observe that the covariant gauge symmetry (4.60) is less restrictive than longitudinal diffeomorphisms, since it can be obtained from (4.66) in the particular case

$$\xi_\mu = \frac{1}{2} \partial_\mu \Lambda. \quad (4.67)$$

Hence, one naturally expects the most general action to contain the LG action together with an additional term, representing the genuine novelty of the theory, which is not invariant under infinitesimal diffeomorphisms (4.66)

$$\delta_{diff} S_M \propto \int d^4x \partial^\mu \xi^\nu (\partial^\rho \partial_\mu a_{\nu\rho} + \partial^\rho \partial_\nu a_{\rho\mu} - 2\Box a_{\mu\nu}) \neq 0, \quad (4.68)$$

where

$$\Box \equiv \partial^\mu \partial_\mu \quad (4.69)$$

denotes the d'Alembertian operator. We will refer to S_M (4.64) as the “fractonic” term, since, as we will show in Section 4.4.3, it constitutes a covariant generalization of the Scalar Charge Theory previously studied.

Since the gauge field can be rescaled by an overall constant without affecting the physical content of the theory, the action (4.62) effectively depends on a single dimensionless parameter, which, however, cannot be absorbed by any field redefinition. This is a rather peculiar feature for a free quadratic theory. The only closely analogous situation occurs in the 3D Maxwell–Chern–Simons theory [168, 169], where the corresponding parameter plays the role of a topological mass. However, in order to keep track of the separate contributions of the gravitational ($g_2 = 0$) and fractonic ($g_1 = 0$) terms, we will retain both g_1 and g_2 in the following analysis.

4.4.1 Gauge fixing

In gauge field theory [170], in order to compute the physical degrees of freedom (DoF) and the propagators of a model, it is necessary to impose a suitable covariant

gauge fixing condition. This procedure eliminates the redundant and unphysical DoF associated with gauge invariance, which would otherwise render divergent the Green functions' generating functional

$$Z[J] = \int \mathcal{D}a_{\mu\nu} \exp \left\{ i \left(S_{inv} + \int d^4x J^{\mu\nu} a_{\mu\nu} \right) \right\}. \quad (4.70)$$

Looking at the right hand side of (4.60), since the gauge parameter is a scalar, the standard Faddeev–Popov procedure leads naturally to a scalar gauge-fixing condition

$$\partial^\mu \partial^\nu a_{\mu\nu} + \kappa \square a = 0, \quad (4.71)$$

where κ is a dimensionless gauge parameter. The scalar constraint (4.71), adopted in [70], is the rank-2 analogue of the covariant Lorentz gauge

$$\partial^\mu A_\mu = 0. \quad (4.72)$$

The scalar gauge condition (4.71) is implemented by adding to the invariant action S_{inv} (4.62) the gauge fixing term

$$S_{gf} = \int d^4x b \left(\partial^\mu \partial^\nu a_{\mu\nu} + \kappa \partial^2 a + \frac{\xi}{2} b \right), \quad (4.73)$$

where $b(x)$ is a scalar *Nakanishi–Lautrup multiplier* [171, 172] enforcing the gauge condition (4.71), with mass dimension $[b] = 1$. The parameter ξ is a gauge parameter with non-vanishing mass dimension $[\xi] = 2$. As a consequence, the choice of the Landau gauge $\xi = 0$ is required in order to avoid infrared divergences [173]. Moreover, as shown in [70], when adopting a scalar gauge condition the limit $g_2 \rightarrow 0$, corresponding to pure LG, cannot be smoothly reached, since it is affected by singularities both in the propagators and in the counting of DoF. This is a consequence of the fact that, since LG is invariant under the more restrictive infinitesimal diffeomorphism symmetry (4.66), the limit $g_2 \rightarrow 0$ is accompanied by a change in the gauge symmetry, switching from the weaker (4.60) to the stronger (4.66). Accordingly, when $g_2 \rightarrow 0$ the gauge parameter changes character: it ceases to be a scalar and becomes a vector field and, as a consequence, a vector gauge-fixing condition is required, whose general form is

$$\partial^\nu a_{\mu\nu} + \kappa \partial_\mu a = 0, \quad (4.74)$$

with κ a dimensionless gauge parameter which, for instance, reduces to the harmonic gauge when $\kappa = -1/2$. Interestingly, in [71] the vectorial condition (4.74) is employed to gauge fix the entire invariant action (4.62). This can be achieved by adding to S_{inv} the gauge fixing term

$$S_{gf} = \int d^4x b^\mu \left(\partial^\nu a_{\mu\nu} + \kappa \partial_\mu a + \frac{\xi}{2} b_\mu \right), \quad (4.75)$$

where $b^\mu(x)$ is a vector Nakanishi–Lautrup multiplier enforcing the gauge condition (4.74). Since its mass dimension is $[b_\mu] = 2$, the primary gauge parameter ξ is therefore dimensionless, and the Landau gauge is no longer mandatory. In [71] it has been shown that the vector gauge condition (4.74) leads to well defined propagators, exhibiting a pole for $2g_1 - g_2 = 0$ (corresponds to the traceless theory) in agreement with the results of [70], and yielding well defined gravitational and fractonic limits. Moreover, the counting of DoF coincides with that of [70], with the important difference that, by adopting a vectorial gauge fixing, one is no longer forced to work in the Landau gauge.

4.4.2 Higher-rank field strength

As anticipated above, the new term (4.64) generated by the less restrictive gauge symmetry (4.60) constitutes a covariant extension of the Scalar Charge Theory discussed in detail in Section 4.3. In that Section, we showed that SCT describes a rank-2 generalization of ordinary electromagnetism. Since ordinary electromagnetism admits a covariant formulation through the action

$$S_M^{(ord)} = -\frac{1}{4} \int d^4x F^{\mu\nu} F_{\mu\nu}, \quad (4.76)$$

with $F_{\mu\nu}(x)$ the usual field strength

$$F_{\mu\nu} = \partial_\mu A_\nu - \partial_\nu A_\mu, \quad (4.77)$$

it is now natural to ask whether there exists a rank-3 generalization of (4.77) in terms of which the fractonic action S_M (4.64) can be rewritten in a form reminiscent of (4.76). The most general expression for a rank-3 tensor built from first derivatives of the tensor gauge field $a_{\mu\nu}(x)$ is [74]

$$F_{\mu\nu\rho} \equiv c_1 \partial_\mu a_{\nu\rho} + c_2 \partial_\rho a_{\mu\nu} + c_3 \partial_\nu a_{\mu\rho}, \quad (4.78)$$

where c_1 , c_2 and c_3 are dimensionless constants to be determined. In complete analogy with the ordinary field strength $F_{\mu\nu}$ (4.77), which is invariant under the gauge transformation $\delta A_\mu(x) = \partial_\mu \Lambda(x)$, we require the higher-rank field strength to be invariant under longitudinal diffeomorphisms (4.60)

$$\delta F_{\mu\nu\rho} = 0, \quad (4.79)$$

which leads to the condition

$$c_3 = -(c_1 + c_2). \quad (4.80)$$

Upon substituting (4.80) into (4.78), we observe that the cyclic property

$$F_{\mu\nu\rho} + F_{\rho\mu\nu} + F_{\nu\rho\mu} = 0 \quad (4.81)$$

is automatically satisfied, further strengthening the analogy with the ordinary case, where

$$F_{\mu\nu} + F_{\nu\mu} = 0. \quad (4.82)$$

Since the tensor gauge field is symmetric, and with the goal of writing the action solely in terms of the higher-rank field strength we are constructing—built as a linear combination of first derivatives of $a_{\mu\nu}(x)$ —we require $F_{\mu\nu\rho}(x)$ to inherit a symmetry under the exchange of two indices [74]. In particular, we impose

$$F_{\mu\nu\rho} = F_{\nu\mu\rho}, \quad (4.83)$$

which implies $c_2 = -c_1$. Thus, absorbing c_1 into a redefinition of the gauge field, we arrive at the following expression for the higher-rank field strength:

$$F_{\mu\nu\rho} = \partial_\mu a_{\nu\rho} + \partial_\nu a_{\mu\rho} - 2\partial_\rho a_{\mu\nu}, \quad (4.84)$$

which also satisfies a Bianchi-like identity,

$$\epsilon_{\alpha\mu\nu\rho} \partial^\mu F^{\beta\nu\rho} = 0 \quad (4D) \quad (4.85)$$

$$\epsilon_{\mu\nu\rho} \partial^\mu F^{\alpha\nu\rho} = 0 \quad (3D), \quad (4.86)$$

which closely mirrors the ordinary Bianchi identity

$$\epsilon_{\alpha\mu\nu\rho} \partial^\mu F^{\nu\rho} = 0 \quad (4D) \quad (4.87)$$

$$\epsilon_{\mu\nu\rho} \partial^\mu F^{\nu\rho} = 0 \quad (3D), \quad (4.88)$$

and whose physical interpretation will play an important role in what follows.

In terms of the higher-rank field strength (4.84), we can rewrite both invariant actions (4.63) and (4.64) as, respectively,

$$S_{LG} = \int d^4x \left(\frac{1}{4} F^\mu{}_{\nu\lambda} F^\rho{}_{\sigma\mu} - \frac{1}{6} F^{\mu\nu\rho} F_{\mu\nu\rho} \right) \quad (4.89)$$

and

$$S_M = -\frac{1}{6} \int d^4x F^{\mu\nu\rho} F_{\mu\nu\rho}. \quad (4.90)$$

Relevantly, we observe that the latter expression (4.90) is a rank-2 analogue of the covariant Maxwell action (4.76). In terms of the new higher-rank field strength, we can write the equations of motion (EoM) as

$$\frac{\delta S_{inv}}{\delta a^{\alpha\beta}} = g_1 \left[\eta_{\alpha\beta} \partial_\mu F_\nu{}^{\nu\mu} - \frac{1}{2} \left(\partial_\alpha F^\mu{}_{\mu\beta} + \partial_\beta F^\mu{}_{\mu\alpha} \right) - \partial^\mu F_{\alpha\beta\mu} \right] - g_2 \partial^\mu F_{\alpha\beta\mu} = 0. \quad (4.91)$$

From this expression we see that the contribution of S_M ,

$$\partial^\mu F_{\alpha\beta\mu} = 0, \quad (4.92)$$

obtained by setting $g_1 = 0$, closely resembles the usual Maxwell equations in their covariant form. The EoM (4.92) will be analyzed in detail in the next Subsection.

Another important quantity in our analysis is the covariant momentum canonically conjugated to $a_{\mu\nu}(x)$, defined as

$$\Pi^{\alpha\beta} \equiv \frac{\partial \mathcal{L}_{inv}}{\partial \partial_t a_{\alpha\beta}} = -g_1 \left[\eta^{\alpha\beta} F_\lambda{}^{\lambda 0} - \frac{1}{2} \left(\eta^{0\alpha} F_\lambda{}^{\lambda\beta} + \eta^{0\beta} F_\lambda{}^{\lambda\alpha} \right) - F^{\alpha\beta 0} \right] + g_2 F^{\alpha\beta 0}, \quad (4.93)$$

whose components are

$$\Pi^{00} = 0, \quad (4.94)$$

$$\Pi^{i0} = -\frac{1}{2}g_1 F_j^{ji} + g_2 F^{i00}, \quad (4.95)$$

$$\Pi^{ij} = g_1 \left(F^{ij0} - \eta^{ij} F_k^{k0} \right) + g_2 F^{ij0}. \quad (4.96)$$

From these expressions we immediately see that $a_{00}(x)$ is not a dynamical field. Moreover,

$$\eta_{\alpha\beta} \Pi^{\alpha\beta} = \Pi^i_i = (g_2 - 2g_1) F_i^{i0}, \quad (4.97)$$

so that, in agreement with the results of [70], if $g_2 - 2g_1 = 0$ then the trace $a(x)$ does not correspond to a dynamical DoF. Indeed, for this specific relation between g_1 and g_2 , the invariant action S_{inv} (4.62) becomes traceless.

4.4.3 Higher-rank Maxwell theory of fractons

We now proceed to analyze in detail the properties of the action S_M (4.90), and we will show that it contains, as a particular sector, the Scalar Charge Theory of fractons studied in [149]. From this point on, we will focus our attention exclusively on S_M .

Generalized electromagnetic fields

As recalled in Section 4.3, the electric tensor field (4.37) was defined in [149] as the conjugate momentum associated with the spatial gauge field $a_{ij}(x)$. In the theory defined by S_M , using (4.96) we find that the spatial components of the covariant momentum canonically conjugated to $a_{\mu\nu}(x)$ are

$$\Pi_M^{ij} \equiv \frac{\delta S_M}{\delta \partial_t a_{ij}} = F^{ij0} = 2 \partial_0 a^{ij} + \partial^i a^{j0} + \partial^j a^{i0}, \quad (4.98)$$

which differs from the expression (4.37) in the SCT. Here we observe that a particular solution of the 00-component of the EoM (4.92),

$$\partial^i F_{00i} = 2 \partial^i (\partial_0 a_{0i} - \partial_i a_{00}) = 0, \quad (4.99)$$

is given by

$$a_{\mu 0} = \partial_{\mu} \psi, \quad (4.100)$$

where $\psi(x)$ is a local scalar function. On the solution (4.100), we observe that $\Pi^{ij}(x)$ coincides (up to an irrelevant constant prefactor) with the rank-2 electric tensor field of the Scalar Charge Theory (4.37). Thus we define our generalized electric field as

$$\mathcal{E}^{ij} \equiv F^{ij0} \Big|_{(4.100)} = 2 \left(\partial_0 a^{ij} - \partial^i \partial^j \psi \right), \quad (4.101)$$

which strongly resembles the situation in ordinary Maxwell theory, where the electric field is defined in terms of the electromagnetic field strength (4.77) as

$$E^i \equiv F^{i0}. \quad (4.102)$$

Moreover, on the particular solution (4.100), which will be assumed from now on even when matter is introduced, the following additional properties hold:

$$F^{i00} = 0, \quad (4.103)$$

$$F^{i0j} = -\frac{1}{2} F^{ij0}, \quad (4.104)$$

the former of which implies, once inserted into (4.95), that $\Pi_M^{i0} = 0$. Consequently, recalling also that $\Pi_M^{00}(x) = 0$, the dynamical DoF of the fracton theory reside solely in the spatial components $a_{ij}(x)$ of the tensor gauge field.

Let us now return to the analysis of the EoM (4.92). Taking $\alpha = 0$ and $\beta = i$ in the EoM and using (4.103) and (4.101), we find

$$\partial_j \mathcal{E}^{ij} = 0, \quad (4.105)$$

which immediately implies

$$\partial_i \partial_j \mathcal{E}^{ij} = 0, \quad (4.106)$$

namely the source-free Gauss law characteristic of the SCT [60].

Finally, taking $\alpha = i$ and $\beta = j$ in the EoM (4.92) and using (4.101), we arrive at

$$\partial_0 \mathcal{E}^{ij} + \partial_k F^{ijk} = 0, \quad (4.107)$$

which, once compared with the generalized source-free version of Ampère's law (4.39) in the SCT, suggests defining

$$F^{ijk} \equiv -\frac{1}{2} \left(\epsilon^{0ikl} \mathcal{B}_l^j + \epsilon^{0jkl} \mathcal{B}_l^i \right), \quad (4.108)$$

or, equivalently,

$$\mathcal{B}_i^j \equiv \frac{2}{3} \epsilon_{0ikl} F^{jkl} = 2 \epsilon_{0ikl} \partial^k a^{lj}, \quad (4.109)$$

which, up to an irrelevant constant prefactor, coincides with the rank-2 magnetic tensor field (4.30) of the SCT. As already noted in the previous Section, this tensor is traceless

$$\mathcal{B}^i_i = 0 \quad (4.110)$$

and satisfies

$$\partial_i \mathcal{B}^{ij} = 0, \quad (4.111)$$

moreover, importantly, the definition (4.108) strongly reminds that of ordinary electromagnetism

$$B_i(x) \equiv \frac{1}{2} \epsilon_{0ijk} F^{jk} = \epsilon_{0ijk} \partial^j A^k. \quad (4.112)$$

It is also important to emphasize that the generalized electromagnetic fields $\mathcal{E}^{ij}(x)$ (4.101) and $\mathcal{B}^{ij}(x)$ (4.109) are defined in terms of the higher-rank gauge invariant field strength $F_{\mu\nu\rho}(x)$ (4.84). This mirrors precisely the situation in ordinary 4D Maxwell theory, where the electromagnetic fields $E_i(x)$ (4.102) and $B_i(x)$ (4.112) are defined in terms of the usual rank-2 field strength $F_{\mu\nu}(x)$ (4.77). Thanks to the definition (4.109), we can rewrite the EoM (4.107) as

$$-\partial_0 \mathcal{E}^{ij} + \frac{1}{2} \left(\epsilon^{0ikl} \partial_k \mathcal{B}_l^j + \epsilon^{0jkl} \partial_k \mathcal{B}_l^i \right) = 0, \quad (4.113)$$

which coincides exactly with the rank-2 Ampère law (4.39).

Let us now analyze the components of the Bianchi-like identity (4.85) and translate them into the language of the rank-2 electromagnetic fields just defined. Taking $\alpha = 0$ and $\beta = i$, we recover the source-free magnetic tensor Gauss law (4.111). When instead

$\alpha = i$ and $\beta = j$, we find

$$\partial_0 \mathcal{B}^{ij} + \epsilon^{0ilk} \partial_l \mathcal{E}_k^j = 0, \quad (4.114)$$

which is precisely the rank-2 Faraday law (4.46) characterizing the SCT.

To summarize, we have seen that the covariant gauge field theory defined by S_M (4.64) embeds the fractonic SCT [60], which constitutes a rank-2 generalization of ordinary four-dimensional Maxwell electromagnetism. This fact becomes even more transparent when the action S_M is rewritten in terms of the generalized electromagnetic fields $\mathcal{E}^{ij}(x)$ and $\mathcal{B}^{ij}(x)$. By using (4.101), (4.109), (4.103), (4.104) and (4.110), one finds [74]

$$S_M = \frac{1}{4} \int d^4x \left(\mathcal{E}^{ij} \mathcal{E}_{ij} - \mathcal{B}^{ij} \mathcal{B}_{ij} \right), \quad (4.115)$$

which is the action of the SCT (4.35) and represents a higher-rank generalization of the ordinary Maxwell action, whose Lagrangian density is proportional to $E^2(x) - B^2(x)$.

Stress-energy tensor

The stress–energy tensor of the fracton theory (4.64) is [74]

$$T_{\alpha\beta} \equiv - \frac{2}{\sqrt{-g}} \frac{\delta S_M}{\delta g^{\alpha\beta}} \Big|_{g=\eta} = - \frac{1}{6} \eta_{\alpha\beta} F^{\mu\nu\rho} F_{\mu\nu\rho} + \frac{1}{3} \eta_{\alpha\gamma} \eta_{\beta\lambda} \left(2F^{\lambda\nu\rho} F_{\nu\rho}^{\gamma} + F^{\mu\nu\lambda} F_{\mu\nu}^{\gamma} \right), \quad (4.116)$$

and this expression remains valid even in a Minkowski spacetime of arbitrary spacetime dimension n . As a consequence, its trace in n dimensions is

$$\eta^{\alpha\beta} T_{\alpha\beta} = \frac{6-n}{6} F^{\mu\nu\rho} F_{\mu\nu\rho}, \quad (4.117)$$

which vanishes only when $n = 6$. This stands in contrast to ordinary Maxwell theory, where the trace of the stress–energy tensor vanishes in four dimensions, signalling the invariance of the theory under conformal transformations [174]. This observation suggests that $n = 6$, although not physically realized, is the natural spacetime dimension in which to study the covariant fracton theory (4.64).

Let us now focus our attention on the components of the stress–energy tensor (4.116) and on their physical interpretation. One finds (we refer to [74] for the details of the

computation)

$$T^{00} = \frac{1}{4} \left(\mathcal{E}^{ij} \mathcal{E}_{ij} + \mathcal{B}^{ij} \mathcal{B}_{ij} \right) \quad (4.118)$$

$$T^{0i} = \frac{1}{2} \epsilon^{0ilp} \mathcal{E}_{kl} \mathcal{B}_p{}^k \quad (4.119)$$

$$T^{ij} = \frac{1}{4} \eta^{ij} \left(\mathcal{E}^{ab} \mathcal{E}_{ab} + \mathcal{B}^{ab} \mathcal{B}_{ab} \right) - \eta_{ab} \mathcal{E}^{ia} \mathcal{E}^{jb} - \frac{1}{2} \eta_{ab} \left(\mathcal{B}^{ia} \mathcal{B}^{jb} - \mathcal{B}^{aj} \mathcal{B}^{ib} \right), \quad (4.120)$$

which generalize, respectively, the energy density

$$u = \frac{1}{2} \left(E^2 + B^2 \right), \quad (4.121)$$

the Poynting vector

$$\mathbf{S} = \mathbf{E} \times \mathbf{B}, \quad (4.122)$$

and the stress tensor

$$\sigma^{ij} = \frac{1}{2} \eta^{ij} \left(E^2 + B^2 \right) - E^i E^j - B^i B^j, \quad (4.123)$$

which characterize ordinary Maxwell theory.

Let us now discuss the on-shell conservation of the stress–energy tensor (4.116) by explicitly computing the on-shell components of $\partial_\nu T^{\mu\nu}(x)$. One can verify that the time component $\mu = 0$ is conserved [74]:

$$\partial_\nu T^{\nu 0} = \partial_0 T^{00} + \partial_i T^{i0} = 0, \quad (4.124)$$

which generalizes the Maxwell continuity equation

$$\partial_t u + \nabla \cdot \mathbf{S} = 0. \quad (4.125)$$

In contrast, the spatial component $\mu = i$ is not conserved on-shell [74]:

$$\partial_\nu T^{\nu i} = \frac{1}{4} \left[3 \mathcal{B}^{ni} \partial_m \mathcal{B}_n{}^m + 2 \mathcal{B}_n{}^m \partial_m \mathcal{B}^n{}_i - 2 \mathcal{E}_{ab} \partial^b \mathcal{E}^{ai} \right] \neq 0, \quad (4.126)$$

unlike what happens in standard electromagnetism. This non-conservation is a consequence of the fact that the curved space extension of the fracton action S_M (4.64) is not diffeomorphism invariant, unlike ordinary Maxwell theory. The resulting partial on-shell conservation of $T^{\mu\nu}(x)$ follows from the structure of the gauge symmetry

(4.60), which—although not a generic infinitesimal diffeomorphism (4.66)—constitutes a particular subclass of them (4.67).

Fractonic matter

Matter can be introduced into the theory by adding a matter action to (4.64), so that the total action becomes

$$S_{tot} \equiv S_M + S_J, \quad (4.127)$$

where

$$S_J \equiv - \int d^4x J^{\mu\nu} a_{\mu\nu}, \quad (4.128)$$

with $J^{\mu\nu}(x)$ a symmetric rank-2 tensor current coupled to the gauge field. The equations of motion now take the form

$$\partial_\mu F^{\alpha\beta\mu} = -J^{\alpha\beta}, \quad (4.129)$$

from which, using the cyclic property (4.81), one obtains the covariant higher-rank continuity equation

$$\partial_\alpha \partial_\beta J^{\alpha\beta} = 0, \quad (4.130)$$

a relation that plays a central role in the covariant formulation of fractonic theories. Let us now study the components of the EoM (4.129). Taking $\alpha = \beta = 0$ one finds

$$J^{00} = 0, \quad (4.131)$$

since we are assuming that the particular solution (4.100) continues to hold also in the presence of matter.

Taking $\alpha = 0$ and $\beta = i$, one arrives at

$$\partial_j \mathcal{E}^{ij} = 2J^{i0}, \quad (4.132)$$

whose divergence gives

$$\partial_i \partial_j \mathcal{E}^{ij} = \rho, \quad (4.133)$$

where $\rho(x)$ is a scalar charge density defined as

$$\rho \equiv 2 \partial_i J^{i0}. \quad (4.134)$$

Relevantly, (4.133) coincides with the higher-rank Gauss law (4.26) that defines the SCT [149]. Moreover, as already discussed in Section (4.2), the charge density $\rho(x)$ is fractonic, since (4.26) implies the conservation of both the total charge and the total dipole moment (4.43).

Finally, for $\alpha = i$ and $\beta = j$ in (4.129), one recovers the generalized Ampère law (4.39) of SCT

$$-\partial_0 \mathcal{E}^{ij} + \frac{1}{2} \left(\epsilon^{0ikl} \partial_k \mathcal{B}_l^j + \epsilon^{0jkl} \partial_k \mathcal{B}_l^i \right) = J^{ij}, \quad (4.135)$$

whose double divergence $\partial_i \partial_j$ yields

$$\partial_0 \rho + \partial_i \partial_j J^{ij} = 0, \quad (4.136)$$

the usual fractonic continuity equation (4.41) relating the fracton charge density $\rho(x)$ to the dipole current density $J^{ij}(x)$. Notice that (4.136) can also be derived directly from (4.130):

$$0 = \partial_\alpha \partial_\beta J^{\alpha\beta} = 2 \partial_0 \partial_i J^{i0} + \partial_i \partial_j J^{ij} = \partial_0 \rho + \partial_i \partial_j J^{ij}, \quad (4.137)$$

where (4.131) and (4.134) have been used.

We now study how the presence of matter modifies the quantity $\partial_\nu T^{\mu\nu}(x)$. In [74] it has been computed that

$$\partial_\mu T^{\mu 0} = -\frac{1}{2} \mathcal{E}_{ab} J^{ab} \quad (4.138)$$

$$\partial_\mu T^{\mu i} = \frac{1}{4} \left[3 \mathcal{B}^{ni} \partial_m \mathcal{B}_n^m + 2 \mathcal{B}_n^m \partial_m \mathcal{B}_i^n - 2 \mathcal{E}_{ab} \partial^b \mathcal{E}^{ai} \right] - \frac{1}{2} \epsilon^{0ikl} J_{jk} \mathcal{B}_l^i + 2 J_{j0} \mathcal{E}^{ij}. \quad (4.139)$$

In analogy with ordinary Maxwell theory, where the covariant Lorentz force $f^\mu(x)$ satisfies

$$\partial_\nu T^{\mu\nu} + f^\mu = 0, \quad (4.140)$$

here, by comparing (4.138) and (4.139) with (4.140), the authors of [74] identify

$$f^0 = \frac{1}{2} \mathcal{E}_{ab} J^{ab}, \quad (4.141)$$

$$f^i = -2 J_{j0} \mathcal{E}^{ij} + \frac{1}{2} \epsilon^{0ikl} J_{jk} \mathcal{B}_l^j, \quad (4.142)$$

representing, respectively, a generalization of the Maxwell power and Lorentz force density. Let us now focus our attention on $f^i(x)$ (4.142). We observe that, since the total dipole moment is

$$D^i \equiv \int dV x^i \rho = 2 \int dV x^i \partial_k J^{k0} = \int dV (-2J^{i0}), \quad (4.143)$$

we can identify the dipole moment density as

$$d^i \equiv -2J^{i0}. \quad (4.144)$$

Moreover, following the physical interpretation of $J_{ij}(x)$ given in [149], we may write

$$J_{ij} \equiv d_i v_j + d_j v_i, \quad (4.145)$$

with $v^i(x)$ the dipole velocity field. In this case, the generalized Lorentz force density (4.142) becomes

$$f^i = -d_j \mathcal{E}^{ij} + \frac{1}{2} \epsilon^{0ikl} (d_j v_k + d_k v_j) \mathcal{B}_l^j, \quad (4.146)$$

which closely resembles the Lorentz force on dipoles (4.55) conjectured in [149] for Scalar Charge Theory.

4.5 3D fractons

So far we have focused on fracton literature in 4D, but it is natural to ask: what about fractons living on a plane? The motivations for studying fracton phases of matter in 3D are numerous, ranging from their duality with elasticity theory [153] to the possibility of constructing massive fracton models [161], and including the higher-rank generalizations of topological quantum field theories [76].

In the previous Sections, we dealt with fractons in complicated spin models and in gauge theories, but there exists a more down-to-earth realization of subdimensional

particles as topological lattice defects of ordinary crystals in two spatial dimensions, based on the so-called “fracton–elasticity duality” [153]. In particular, this mapping shows that disclinations and dislocation defects of a two-dimensional crystal exhibit the restricted mobility properties of, respectively, fractons and lineonic dipoles. Moreover, the phonons of the solid map onto the gapless gauge modes of the spatial symmetric tensor gauge field $A_{ij}(x)$ transforming under (4.27). These properties become especially transparent through an exact duality between two-dimensional crystals and the 3D Scalar Charge Theory. The main features of fracton–elasticity duality are summarized in Figure 4.5.

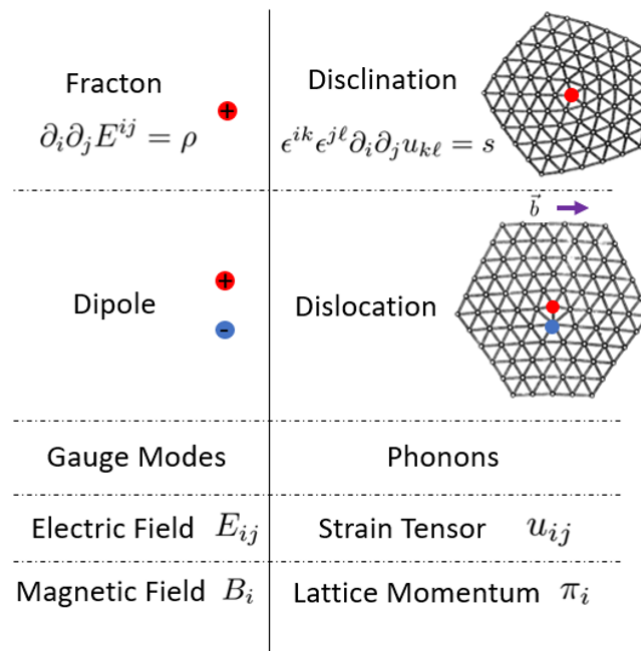


Figure 4.5.: Dictionary of the fracton-elasticity duality. Figure taken from [153].

Two of the main breakthroughs in condensed matter physics of the last century are the Quantum Hall Effect [40, 145] and Topological Insulators [147, 148], which, in field-theoretical language, are described by 3D Chern–Simons [34] and BF [75, 146] theories. This naturally raises the question: does there exist a dipolar analogue of the Quantum Hall Effect or of Topological Insulators? In a field-theoretical framework, the question can be reformulated as follows: given the power of 3D Topological Quantum Field Theories [75] to describe topological orders in two spatial dimensions, is there a higher-rank class of Chern–Simons or BF theories capable of capturing fractonic behaviour? The answer is yes: non-covariant theories describing the dipolar

Quantum Hall effect and topological dipole insulators have already been proposed [76, 77, 78, 79, 80]. In the next Section, we present two *covariant* formulations of higher-rank Chern–Simons and BF theories, which together constitute an important step toward the understanding and formal theoretical description of 3D gauge theories for dipolar Hall fluids.

Most existing models focus on *massless* fractons, describing gapless phases with long-range correlations; however, many physical systems exhibit *gapped* excitations and finite correlation lengths, motivating the study of massive fracton phases. Massive theories can capture softened mobility constraints or bound-state formation, and typically allow a clearer identification of the propagating degrees of freedom. In the context of higher-rank lattice gauge theories of gapless fractons, it has been shown that in most cases, breaking the $U(1)$ gauge symmetry down to \mathbb{Z}_n through a Higgs-like mechanism [161, 162] generates a mass gap but simultaneously destroys the fractonic behavior. The only known exception is the X-cube model [67, 175], which is defined in three spatial dimensions but is non-covariant and does not rely on a continuum field-theoretic setup. On the other hand, non-covariant rank-2 Maxwell–Chern–Simons models with fractonic features have been proposed [176, 177], and another example appears in [77, 167], where a Witten-like effect for fractons is considered. Finally, the introduction of a mass scale in fracton models has been argued to play a role in emergent gravitational-like phenomena [62]. In particular, massive fracton quasiparticles can experience an effective attractive interaction, derived from locality together with conservation of the center of mass [159], suggesting a potential link between massive fracton dynamics and emergent gravitational responses. In Section 5.3 we will construct a *covariant* gauge theory describing massive fractons in 3D, based on a symmetric rank-2 tensor field $a_{\mu\nu}(x)$ transforming under longitudinal diffeomorphisms (4.60). The model includes a covariant Chern–Simons-like term which generates a topological mass for the tensor gauge field, in direct analogy with the Maxwell–Chern–Simons mechanism of Deser–Jackiw–Templeton [168, 169].

Chapter 5.

Covariant Field Theories for 3D Fractons

In this Chapter we shall study 3D covariant theories for fractons starting from a pure field theoretical perspective. Thus, as done in the 4D case [70, 71, 74], the longitudinal diffeomorphisms [72] (4.60) will be the starting point to build the most general gauge invariant and power-counting compatible actions. The main goal is to investigate whether fractonic features are naturally embedded in such covariant field theoretical frameworks and eventually establish a link with preexisting condensed matter theory literature. In 3D there are two possible choices for the mass dimension of the gauge field, as it happens with the standard $U(1)$ vector gauge theory. In that case one can set the dimension of the field to be 1 and recover the topological Chern-Simons theory [34], while by setting the dimension to $1/2$ one has the topologically massive Maxwell-Chern-Simons theory, where a parity-odd Chern-Simons term gives mass to the vector gauge field while preserving gauge invariance and unitarity [168, 169]. We will consider both situations referred to fractons, thus studying covariant theories of a rank-2 symmetric tensor field with mass dimension 1 and $1/2$, and transforming under longitudinal diffeomorphisms (4.60). Thinking about topological theories and their relations to condensed matter physics, the higher-rank covariant generalization of the Chern-Simons case, which will be the subject of Section 5.1 (based on [3]), represents a first promising step towards the study of 3D covariant fracton models. Inspired by that successful example, in Section 5.2 (which is based on [4]) we build and study the covariant rank-2 generalization of another important 3D topological field theory: the BF model [75]. Once matter is introduced in this theory, a subdimensional behaviour naturally emerges, with both fractons and lineons, together with interesting links with

condensed matter literature. Finally, since in the context of covariant fracton theories both Maxwell [74] and Chern-Simons-like terms has been shown to exist as rank-2 generalizations of the ordinary ones, a question naturally raises: can a topological mass generation mechanism be implemented for higher-rank tensor gauge theories describing fractons? The answer to this question will be the main subject of Section 5.3, which is based on [5].

5.1 Higher-rank Chern-Simons theory of fractons

5.1.1 The model

The action

We start by considering the 3D theory of a symmetric rank-2 tensor field $a_{\mu\nu}(x)$ with mass dimension 1 transforming under longitudinal diffeomorphisms [72] (4.60), which, as seen in Section 4.4, characterize the 4D covariant theory of fractons [74], and is affected by a kind of original sin. In fact, in 3D, due to $[a_{\mu\nu}(x)] = 1$, the local gauge parameter $\Lambda(x)$ must have mass dimension -1 . This leads to singularities which manifest themselves only when treating the theory as a *gauge field theory*, as indeed it is, forcing to adopt the Landau gauge, as we shall see. The most general 3D action invariant under (4.60) and respecting power counting is

$$S_{\text{CS}} = \int d^3x \epsilon^{\mu\nu\rho} a_{\mu}^{\lambda} \partial_{\nu} a_{\rho\lambda} = \int d^3x \epsilon^{\mu\nu\rho} \tilde{a}_{\mu}^{\lambda} \partial_{\nu} \tilde{a}_{\rho\lambda}, \quad (5.1)$$

which depends only on the traceless part of $a_{\mu\nu}(x)$ ¹

$$\tilde{a}_{\mu\nu} \equiv a_{\mu\nu} - \frac{1}{3} \eta_{\mu\nu} a \quad (5.2)$$

where $a(x) \equiv \eta^{\mu\nu} a_{\mu\nu}(x)$ is the trace of the gauge field. The action S_{CS} (5.1) for the rank-2 symmetric tensor field $a_{\mu\nu}(x)$ reminds the 3D Chern-Simons action (5.3) for the ordinary vector gauge field $A_{\mu}(x)$

$$S_{\text{CS}}^{(\text{ord})}[A] = \int d^3x \epsilon^{\mu\nu\rho} A_{\mu} \partial_{\nu} A_{\rho}, \quad (5.3)$$

but, differently from (5.3), it depends on the metric and, hence, is not topological. Nonetheless, the generalized Chern-Simons action (5.1) shares with the ordinary

¹From now on, we shall denote traceless tensors with a tilde.

one (5.3) some peculiar properties, such as the level quantization (see Appendix D). Moreover, like the ordinary Chern-Simons theory, the action (5.1) can be written using a gauge-invariant bulk theta-like term, as commented in [74]. The equations of motion (EoM) derived from the topological action (5.3) are

$$\epsilon^{\mu\rho\sigma} F_{\rho\sigma} = 0, \quad (5.4)$$

where $F_{\rho\sigma}(x)$ is the usual electromagnetic field strength (4.77). From the action (5.1) the following EoM for the traceless tensor field $\tilde{a}_{\alpha\beta}(x)$ are derived

$$\frac{\delta S_{\text{CS}}}{\delta \tilde{a}_{\alpha\beta}} = \epsilon^{\alpha\mu\nu} \partial_\mu \tilde{a}_\nu^\beta + \epsilon^{\beta\mu\nu} \partial_\mu \tilde{a}_\nu^\alpha = 0, \quad (5.5)$$

which also can be written in terms of the higher rank field strength (4.84), as we shall see shortly.

Generalized electric and magnetic fields

If we wanted to follow in 3D the same approach adopted by Pretko in 4D [149] (and explained in Section 4.3), we would run into a problem since the conjugate momentum of $a_{ij}(x)$

$$p^{ij} = \frac{1}{2} \left(\epsilon^{0ik} a_k^j + \epsilon^{0jk} a_k^i \right) \quad (5.6)$$

is not gauge invariant

$$\delta p^{ij} = \frac{1}{2} (\epsilon^{0ik} \partial^j \partial_k \Lambda + \epsilon^{0jk} \partial^i \partial_k \Lambda) \neq 0. \quad (5.7)$$

and, hence, cannot represent a physical quantity. This problem can be solved thanks to the higher rank field strength (4.84), in terms of which a coherent covariant formulation of the 4D fracton Scalar Charge Theory has been given [74]. It is convenient to define a traceless field strength, reflecting the fact that the action S_{CS} (5.1) does not depend on the trace $a(x)$

$$\tilde{F}_{\mu\nu\rho} \equiv F_{\mu\nu\rho} - \frac{1}{4} \left(2\eta_{\mu\nu} F_{\lambda\rho}^\lambda - \eta_{\mu\rho} F_{\lambda\nu}^\lambda - \eta_{\nu\rho} F_{\lambda\mu}^\lambda \right), \quad (5.8)$$

which is fully traceless, in the sense that

$$\eta_{\mu\nu}\tilde{F}^{\mu\nu\rho} = \eta_{\mu\rho}\tilde{F}^{\mu\nu\rho} = \eta_{\nu\rho}\tilde{F}^{\mu\nu\rho} = 0 \quad (5.9)$$

and shares with the full tensor $F_{\mu\nu\rho}(x)$ the properties (4.79), (4.83) and (4.81). In close analogy with the Chern-Simons theory, the EoM (5.5) can be written as

$$\frac{\delta S_{CS}}{\delta \tilde{a}_{\alpha\beta}} = \frac{1}{3} \left(\epsilon^{\alpha\mu\nu} \tilde{F}_{\mu\nu}^{\beta} + \epsilon^{\beta\mu\nu} \tilde{F}_{\mu\nu}^{\alpha} \right) = 0, \quad (5.10)$$

whose time and space components are

- $\alpha = \beta = 0$

$$\frac{\delta S_{CS}}{\delta \tilde{a}_{00}} = \frac{2}{3} \epsilon^{0ij} \tilde{F}_{ij}^0 = 0 \quad (5.11)$$

- $\alpha = i, \beta = 0$

$$\frac{\delta S_{CS}}{\delta \tilde{a}_{0i}} = \frac{1}{3} \left(\epsilon^{0kl} \tilde{F}_{kl}^i - \frac{3}{2} \epsilon^{ik0} \tilde{F}_{0k}^0 \right) = 0 \quad (5.12)$$

- $\alpha = i, \beta = j$

$$\frac{\delta S_{CS}}{\delta \tilde{a}_{ij}} = \frac{1}{3} \epsilon^{0ik} \left(\tilde{F}_{k0}^j - \tilde{F}_{0k}^j \right) + \frac{1}{3} \epsilon^{0jk} \left(\tilde{F}_{k0}^i - \tilde{F}_{0k}^i \right) = 0, \quad (5.13)$$

where in (5.12) the cyclicity property (4.81) has been used. Notice that (5.11) implies that, on-shell, the traceless generalized field strength has the following additional symmetry

$$\tilde{F}_{0ij} = \tilde{F}_{0ji}. \quad (5.14)$$

Equivalently, the EoM (5.11) of \tilde{a}_{00} can be written in terms of the gauge field as

$$\epsilon^{0ij} \partial_i a_{0j} = 0, \quad (5.15)$$

which is solved by

$$a_{0i} = \partial_i \psi, \quad (5.16)$$

where $\psi(x)$ is a generic scalar field. Using (5.14) and the cyclicity property (4.81), the EoM (5.13) reads

$$\left. \frac{\delta S_{\text{CS}}}{\delta \tilde{a}_{ij}} \right|_{(5.14)} = \frac{1}{2} \left(\epsilon^{0ik} \tilde{F}_{k0}^j + \epsilon^{0jk} \tilde{F}_{k0}^i \right) = 0, \quad (5.17)$$

which will be useful in what follows. As anticipated, the higher rank field strength $F_{\mu\nu\rho}(x)$ allows to define invariant higher rank generalizations of the electric field (4.102) and of the magnetic field. In order to do so, we proceed, again, in analogy to what happens in Chern-Simons theory where [34, 40]

$$\frac{\delta S_{\text{CS}}^{(\text{ord})}[A]}{\delta A_a} \propto \epsilon^{0ab} E_b \quad (5.18)$$

$$\frac{\delta S_{\text{CS}}^{(\text{ord})}[A]}{\delta A_0} \propto B, \quad (5.19)$$

where

$$E^i \equiv F^{i0} \quad (5.20)$$

$$B \equiv -\frac{1}{2} \epsilon_{0ij} F^{ij} = -\epsilon_{0ij} \partial^i A^j \quad (5.21)$$

are, respectively, the ordinary electric and magnetic field in 3D. We are therefore led to identify the higher rank generalizations of the standard definitions (5.18) and (5.19) as

$$\left. \frac{\delta S_{\text{CS}}}{\delta \tilde{a}_{ij}} \right|_{(5.14)} \equiv \frac{1}{2} \left(\epsilon^{0ki} \tilde{\mathcal{E}}_k^j + \epsilon^{0kj} \tilde{\mathcal{E}}_k^i \right) \quad (5.22)$$

$$\frac{\delta S_{\text{CS}}}{\delta \tilde{a}_{0i}} \equiv \mathcal{B}^i. \quad (5.23)$$

It is easy to see that, as a consequence of the definition (5.22), the tensorial electric field is spatially traceless, *i.e.* $\eta_{ab} \tilde{\mathcal{E}}^{ab} = 0$. Comparing with (5.17) and (5.12), respectively, and using (5.14), we get

$$\tilde{\mathcal{E}}^{ij} = \tilde{F}^{ij0} \quad (5.24)$$

$$\mathcal{B}^i = \frac{2}{3} \epsilon^{0jk} \tilde{F}_{jk}^i = \epsilon^{0ij} \tilde{F}_{kj}^k, \quad (5.25)$$

which gives

$$\tilde{F}^{ijk} = \frac{1}{2} \left(\epsilon^{0ik} \mathcal{B}^j + \epsilon^{0jk} \mathcal{B}^i \right) . \quad (5.26)$$

The derivation of (5.25) requires some care. In particular, the tracelessness (5.9) and cyclicity (4.81) properties of $\tilde{F}_{\mu\nu\rho}(x)$ must be used. Because of the invariance of $\tilde{F}_{\mu\nu\rho}(x)$, both $\tilde{\mathcal{E}}^{ij}(x)$ and $\mathcal{B}^i(x)$ have the required property of being gauge invariants. Moreover, the tensorial traceless electric field (5.24) turns out to be symmetric, as it should be in fractonic theories [60, 61, 62, 74, 149].

5.1.2 Currents and fractons

Following [34, 40], matter current is introduced in Chern-Simons theory by adding a term in the action

$$S_{tot}^{(ord)} = S_{CS}^{(ord)} - \int d^3x A_\mu J^\mu , \quad (5.27)$$

so that

$$J^\mu = \frac{\delta S_{CS}^{(ord)}}{\delta A_\mu} , \quad (5.28)$$

which encodes the matter response to electric and magnetic fields, through (5.18) and (5.19). The higher rank generalization of (5.27) is

$$S_{tot} = S_{CS} - \int d^3x \tilde{J}^{\mu\nu} \tilde{a}_{\mu\nu} , \quad (5.29)$$

where S_{CS} is given by (5.1), and (5.28) translates into

$$\tilde{J}^{\alpha\beta} = \frac{\delta S_{CS}}{\delta \tilde{a}_{\alpha\beta}} . \quad (5.30)$$

Recalling that we are working on the solution (5.14) of the EoM of $\tilde{a}_{00}(x)$ (5.11)² (since the generalised electromagnetic fields are defined there), we have that

$$\tilde{j}^{00} = 0 . \quad (5.31)$$

Taking this into account, and using (5.22) and (5.23), equation (5.30) implies the following identifications

$$\tilde{j}^{0i} = \mathcal{B}^i \quad (5.32)$$

$$\tilde{j}^{ij} = \frac{1}{2} \left(\epsilon^{0ki} \tilde{\mathcal{E}}^j_k + \epsilon^{0kj} \tilde{\mathcal{E}}^i_k \right) . \quad (5.33)$$

Moreover, by writing explicitly (5.30)

$$\tilde{j}^{\alpha\beta} = \epsilon^{\alpha\mu\nu} \partial_\mu \tilde{a}_\nu^\beta + \epsilon^{\beta\mu\nu} \partial_\mu \tilde{a}_\nu^\alpha , \quad (5.34)$$

one can see that

$$\partial_\alpha \partial_\beta \tilde{j}^{\alpha\beta} = 0 , \quad (5.35)$$

which is the rank-two extension of what happens in Chern-Simons theory [34, 40], where (5.28)

$$J^\mu \propto \epsilon^{\mu\nu\rho} \partial_\nu A_\rho \quad (5.36)$$

implies the continuity equation

$$\partial_\mu J^\mu = 0 . \quad (5.37)$$

Indeed, given (5.31) and defining

$$\rho \equiv 2\partial_i \tilde{j}^{0i} , \quad (5.38)$$

²Notice that, since $a_{0i}(x)$ is a vector field, it can be decomposed as $a_{0i} = u_i + \partial_i \psi$, where $u_i(x)$ is transverse, *i.e.* $u_i = \epsilon_{0ij} \partial^j u$, with $u(x)$ a scalar function. Since the local gauge parameter $\Lambda(x)$ is a scalar, we have to apply a scalar gauge fixing and, in particular, we can choose the longitudinal gauge $u = 0$, thus recovering (5.16), which coincides with the solution (5.14) of the vacuum EoM of $\tilde{a}_{00}(x)$ (5.11). Thus, working partially on-shell on the solution (5.16), which is crucial in order to observe a fractonic behavior, is equivalent to fix the longitudinal gauge.

the conservation law (5.35) represents a continuity equation

$$\partial_0 \rho + \partial_i \partial_j \tilde{f}^{ij} = 0, \quad (5.39)$$

which is relevant in fractonic theories, since it implies dipole moment

$$D^i = \int d\Sigma x^i \rho = -2 \int d\Sigma \tilde{f}^{0i} \quad (5.40)$$

(with $d\Sigma \equiv dx_1 dx_2$) conservation [60, 61, 62, 154]

$$\frac{dD^i}{dt} = \int d\Sigma x^i \frac{d\rho}{dt} = - \int d\Sigma x^i \partial_a \partial_b \tilde{f}^{ab} = \int d\Sigma \partial_b \tilde{f}^{ib} = 0, \quad (5.41)$$

defining the fracton quasiparticle as an immobile object [60, 61, 62]. Moreover, from the continuity equations (5.39), the trace of the quadrupole moment³

$$D^{ij} \equiv \int d\Sigma x^i x^j \rho \quad (5.42)$$

is conserved

$$\partial_0 D^i_i = \partial_0 \int d\Sigma \eta^{ij} x_i x_j \rho = - \int d\Sigma \eta^{ij} x_i x_j \partial_k \partial_l \tilde{f}^{kl} \propto \int d\Sigma \eta_{kl} \tilde{f}^{kl} = \int d\Sigma \tilde{f}^{00} = 0 \quad (5.43)$$

where the last step follows from (5.31). Hence isolated dipoles are constrained to move in straight lines which are perpendicular to their dipole momenta [156], *i.e.* they behave as lineons. Thus, relevantly, our theory has exactly the same conservation laws which characterize Pretko's Traceless Scalar charge Theory of fractons [149].

To resume, it is possible to identify $\rho(x)$ as the charge density, $\tilde{f}^{0i}(x)$ as the local dipole moment and $\tilde{f}^{ij}(x)$ as the dipole current, in agreement with [74, 154]. Notice that in (5.33) the current $\tilde{f}^{ij}(x)$ coincides with the generalized Hall response described in [77, 154, 167], while (5.32) relates the magnetic vector field to the dipole charge. It is also interesting to notice that from (5.32) the presence of a nonvanishing divergence of the magnetic field implies a nonzero charge density

$$\rho = 2\partial_i \mathcal{B}^i, \quad (5.44)$$

³We adopt the traceful definition of quadrupole moment, instead of the traceless one, as in [149, 178] and in [179].

which could be associated to the presence of a 3D fracton vortex defect. In the ordinary Chern-Simons model [34], vorticity is related to the charge Q of the model, and hence to the magnetic flux Φ , through

$$Q = \int d^2x J^0 = \int d^2x B = \Phi \quad (5.45)$$

as a consequence of the so called “magnetic flux attachment”

$$J^0 = B \quad (5.46)$$

coming from the 0-component of the Chern-Simons EoM (5.28). Indeed the effect of the Chern-Simons coupling is to attach the magnetic flux of $B(x)$ to the matter charge density $J^0(x)$ in such a way that the flux follows the charge density wherever it goes [34]. Equation (5.32), which involves the generalized magnetic field $\mathcal{B}^i(x)$, is the fractonic equivalent of the flux attachment relation (5.46). In particular, the equivalent of the charge is a vector, represented by the the dipole density

$$d^i \equiv -2\tilde{j}^{0i}, \quad (5.47)$$

being the total dipole moment D^i given by (5.40), for which (5.32) can be written as

$$d^i = -2\mathcal{B}^i. \quad (5.48)$$

Thus in our case flux attachment is related to dipoles. This is not surprising, if we think about the fundamental properties of fractons, for which the relation (5.48) could not involve the fractonic charge $\rho(x)$ (5.38) since, by definition, it is an immobile object. Additionally, it is interesting to see that the Hall analogy can be extended also by noting that the current $\tilde{j}^{ij}(x)$ (5.33) can be interpreted as a generalized Hall current, if we define a generalized conductivity $\tilde{\sigma}^{ijkl}$ as

$$\tilde{j}^{ij} = \tilde{\sigma}^{ijkl} \tilde{\mathcal{E}}_{kl}, \quad (5.49)$$

where

$$\tilde{\sigma}^{ijkl} = \tilde{\sigma}^{jikl} = \tilde{\sigma}^{ijlk} \equiv \frac{1}{4} \left(\epsilon^{0ki} \eta^{jl} + \epsilon^{0kj} \eta^{il} + \epsilon^{0li} \eta^{jk} + \epsilon^{0lj} \eta^{ik} \right), \quad (5.50)$$

which is the kl -symmetrization of the one found in [77, 167]. This mimics the standard Hall current

$$J^i = \sigma^{ij} E_j \quad \text{with} \quad \sigma^{ij} \propto \epsilon^{0ij}, \quad (5.51)$$

also in its orthogonality condition with the (generalized) electric field (5.24)

$$\tilde{J}^{ij} \tilde{\mathcal{E}}_{ij} = -\epsilon^{0ij} \tilde{\mathcal{E}}_{ik} \tilde{\mathcal{E}}_j^k = 0. \quad (5.52)$$

We thus have from the EoM with matter coupling (5.30) the ‘‘dipole-flux attachment’’ (5.48) and the generalized Hall current (5.49), which represent the two main ingredients for the fracton generalization mentioned above. A comment is in order concerning the existing Literature. The invariant action (5.1) reduces to that studied in [77] when (5.16) holds, which plays a crucial role in the definition of both the generalized electromagnetic fields and it implies (5.31), hence leading us to the relevant fractonic continuity equation (5.39). Going back to the connections with the work [77], we observe that we recover their generalized Hall response in symmetrized form. Remarkably, differently from [77], which starts directly by writing a non-covariant Chern-Simons like action, we derive ours as the most general 3D action invariant under the covariant fractonic gauge transformation (4.60) with $[a_{\mu\nu}(x)] = 1$.

5.1.3 Gauge-fixing and propagators

The most general gauge fixing for the transformation (4.60), which depends on the scalar local parameter $\Lambda(x)$, is

$$\partial^\mu \partial^\nu a_{\mu\nu} + \kappa \square a = 0, \quad (5.53)$$

where \square is the 3D D’Alembertian operator. The scalar constraint (5.53) is realized by adding to the action S_{CS} (5.1) the gauge fixing term

$$S_{gf} = -\frac{1}{2\tilde{\zeta}} \int d^3x (\partial^\mu \partial^\nu a_{\mu\nu} + \kappa \square a)^2, \quad (5.54)$$

which depends on two gauge parameters $\tilde{\zeta}$ and κ . The former, $\tilde{\zeta}$, identifies the type of gauge fixing. For instance, $\tilde{\zeta} = 0$ and $\tilde{\zeta} = 1$ represent the Landau and Feynman gauges, respectively. The direct consequence of the fact that the local gauge parameter $\Lambda(x)$ in (4.60) has negative dimensions, is that the constant gauge parameter $\tilde{\zeta}$ in the

gauge fixing term S_{gf} (5.54) is massive [ξ] = 3, which leads to infrared divergences exactly like in ordinary Chern-Simons theory, which, for the same reason, is defined in the Landau gauge $\xi = 0$ only [173, 180, 181]. In momentum space⁴ and in the Landau gauge, the propagator of the gauge fixed action

$$S \equiv S_{CS} + S_{gf}, \quad (5.55)$$

is

$$\begin{aligned} \langle \hat{a}_{\alpha\beta}(p) \hat{a}_{\rho\sigma}(-p) \rangle = \frac{ip^\lambda}{16p^2} & \left[\epsilon_{\alpha\lambda\rho} \left(\eta_{\beta\sigma} + 3 \frac{p_\beta p_\sigma}{p^2} \right) + \epsilon_{\alpha\lambda\sigma} \left(\eta_{\beta\rho} + 3 \frac{p_\beta p_\rho}{p^2} \right) + \right. \\ & \left. + \epsilon_{\beta\lambda\rho} \left(\eta_{\alpha\sigma} + 3 \frac{p_\alpha p_\sigma}{p^2} \right) + \epsilon_{\beta\lambda\sigma} \left(\eta_{\alpha\rho} + 3 \frac{p_\alpha p_\rho}{p^2} \right) \right] \end{aligned} \quad (5.56)$$

where $p^2 \equiv p^\mu p_\mu$ and $\hat{a}_{\mu\nu}(p)$ is the Fourier transform of $a_{\mu\nu}(x)$ (the details of the calculation can be found in Appendix E.1). Notice that (5.56) implies

$$\langle \hat{a}(p) \hat{a}_{\rho\sigma}(-p) \rangle = \langle \hat{a}(p) \hat{a}(-p) \rangle = 0, \quad (5.57)$$

as it should, being the theory traceless. The propagator (5.56) does not display any pole and does not depend on the gauge parameter κ , coupled in the gauge fixing term S_{gf} (5.54) to the trace field $a(x)$, which is expected, being the theory defined by S_{CS} (5.1) traceless. The gauge fixing term (5.54) can alternatively be written as

$$S_{gf}^{(\xi)} = \int d^3x \left[b (\partial^\mu \partial^\nu a_{\mu\nu} + \kappa \square a) + \frac{\xi}{2} b^2 \right] \quad (5.58)$$

where the scalar field $b(x)$ is the Nakanishi - Lautrup Lagrange multiplier [171, 172] implementing the gauge condition (5.53). This form of the gauge fixing term will be useful in Appendix F.1, where we prove that the degrees of freedom (DoF) of the theory are two.

5.1.4 Energy momentum tensor

Chern-Simons and BF theories are topological QFTs of the Schwarz type [75], characterized by an invariant action which does not depend on the metric $g_{\mu\nu}(x)$. The energy

⁴The Fourier transform is defined as $\Phi(x) \equiv \int \frac{d^3p}{(2\pi)^3} e^{ip \cdot x} \hat{\Phi}(p)$.

momentum tensor of topological QFTs vanishes

$$T_{\mu\nu} \equiv -\frac{2}{\sqrt{-g}} \frac{\delta S_{\text{CS}}}{\delta g^{\mu\nu}} = 0. \quad (5.59)$$

This renders the energy momentum tensor unphysical, in the sense that the only contribution to it comes from the gauge fixing term, which depends on the metric. One of the most striking consequences of this fact is that topological QFTs have vanishing energy density $T_{00}(x)$ and hence vanishing energy. The model presented in this Section is a higher rank generalization of the standard Chern-Simons theory, and it is not topological. In fact, S_{CS} (5.1) displays a metric dependence

$$S_{\text{CS}} = \int d^3x \epsilon^{\mu\nu\rho} g^{\alpha\beta} a_{\alpha\mu} \partial_\nu a_{\beta\rho}, \quad (5.60)$$

which is mild, being only linear. To make a comparison, Maxwell theory has a cubic dependence on the metric

$$S_{\text{M}}^{(\text{ord})} = -\frac{1}{4} \int d^4x \sqrt{-g} g^{\mu\nu} g^{\rho\sigma} F_{\mu\rho} F_{\nu\sigma}. \quad (5.61)$$

We might say that the theory described by the action S_{CS} (5.60) is “almost” topological. There is indeed at least one property which our theory shares with a topological QFT: it has, on-shell, vanishing energy. In fact, the energy momentum is

$$T_{\mu\nu} = -\epsilon^{\alpha\beta\gamma} (a_{\alpha\mu} \partial_\beta a_{\gamma\nu} + a_{\alpha\nu} \partial_\beta a_{\gamma\mu}), \quad (5.62)$$

whose 00-component, namely the energy density, is

$$T_{00} = -2\epsilon^{\mu\nu\rho} a_{\mu 0} \partial_\nu a_{\rho 0} = -2\epsilon^{0mn} (a_{00} \partial_m a_{n0} - a_{m0} \partial_0 a_{n0} + a_{m0} \partial_n a_{00}). \quad (5.63)$$

It is immediate to see that on the solution (5.16), the total energy, given by the volume integral of the energy density, vanishes

$$\int d\Sigma T_{00} = 0, \quad (5.64)$$

which is a weaker statement of the corresponding one concerning topological QFTs. One can also verify that the energy momentum tensor is conserved on-shell⁵

$$\partial^\alpha T_{\alpha\beta} = 0. \quad (5.65)$$

5.2 Higher-rank BF theory of fractons

5.2.1 The model

Symmetries and equations of motion

The field content of the theory consists of two rank-2 tensor fields: $a_{\mu\nu}(x)$, which is symmetric, and $B_{\mu\nu}(x)$, which has no symmetry. Restricting to functionals with one derivative only, the most general 3D actions depending on these two tensor fields and invariant under the following field transformations

$$\delta_1 a_{\mu\nu} = \partial_\mu \partial_\nu \Lambda \quad ; \quad \delta_1 B_{\mu\nu} = 0 \quad (5.66)$$

$$\delta_2 a_{\mu\nu} = 0 \quad ; \quad \delta_2 B_{\mu\nu} = \partial_\mu \xi_\nu, \quad (5.67)$$

are

$$S_{\text{CS}} = \int d^3x \epsilon^{\mu\nu\rho} a_\mu^\lambda \partial_\nu a_{\rho\lambda} \quad (5.68)$$

$$S_{\text{CS}}^{(B)} = \int d^3x \epsilon^{\mu\nu\rho} B_\mu^\lambda \partial_\nu B_{\rho\lambda} \quad (5.69)$$

$$S_{\text{BF}} = \int d^3x \epsilon^{\mu\nu\rho} B_\mu^\sigma \partial_\nu a_{\rho\sigma}, \quad (5.70)$$

where the tensor fields have mass dimensions $[a_{\mu\nu}] = [B_{\mu\nu}] = 1$. The δ_1 -transformation acting on the symmetric tensor field $a_{\mu\nu}(x)$ represents the longitudinal diffeomorphisms characterizing the covariant formulation of fracton theories both in 4D [71, 74, 163] and 3D [3]. On the other hand, the δ_2 -transformation is the lowest order

⁵To prove this, it is convenient to work in momentum space, where, using the EoM (F.4),

$$\begin{aligned} p^\alpha \hat{T}_{\alpha\beta} &= i\epsilon^{\mu\nu\rho} p_\nu [p^\alpha \hat{a}_{\mu\alpha}(-p) \hat{a}_{\rho\beta}(p) + \hat{a}_{\mu\beta}(-p) p^\alpha \hat{a}_{\rho\alpha}(p)] \\ &= i\epsilon^{\mu\nu\rho} p_\nu \left[-p_\mu \frac{p^\alpha p^\lambda}{p^2} \hat{a}_{\lambda\alpha}(-p) \hat{a}_{\rho\beta}(p) + \hat{a}_{\mu\beta}(-p) p_\rho \frac{p^\alpha p^\lambda}{p^2} \hat{a}_{\lambda\alpha}(p) \right] \\ &= -i\epsilon^{\mu\nu\rho} p_\nu p_\mu \frac{p^\alpha p^\lambda}{p^2} \hat{a}_{\lambda\alpha}(-p) \hat{a}_{\rho\beta}(p) + i\epsilon^{\mu\nu\rho} p_\nu p_\rho \hat{a}_{\mu\beta}(-p) \frac{p^\alpha p^\lambda}{p^2} \hat{a}_{\lambda\alpha}(p) = 0. \end{aligned}$$

most general one acting on the generic tensor field $B_{\mu\nu}(x)$. It reduces to infinitesimal diffeomorphisms (4.66) (which contain their longitudinal component) in the particular case of symmetric $B_{\mu\nu}(x)$, and, for antisymmetric tensor field, $\delta_2 B_{\mu\nu} = \frac{1}{2}(\partial_\mu \xi_\nu - \partial_\nu \xi_\mu)$ is the standard transformation of the 2-form appearing in ordinary BF models [75]. This transformation has been shown to display fractonic behaviours as well [182]. The first two actions, (5.68) and (5.69), are the higher-rank extension of the ordinary Chern-Simons action (5.3) for the vector gauge field $A_\mu(x)$. In particular, the higher-rank Chern-Simons action (5.68) has been studied in Section 5.1, where it has been shown that it describes fracton quasiparticles exhibiting a Hall-like behaviour. The last action functional (5.70) is the generalization of the 3D BF action [38, 75]

$$S_{\text{BF}}^{(\text{ord})} = \int d^3x \epsilon^{\mu\nu\rho} B_\mu \partial_\nu A_\rho, \quad (5.71)$$

which couples the vector gauge field $A_\mu(x)$ to an additional gauge field $B_\mu(x)$. In this Section we focus on the action S_{BF} (5.70), which can be isolated by means of a discrete symmetry which assigns opposite charges to the fields $a_{\mu\nu}(x)$ and $B_{\mu\nu}(x)$. For instance, defining

$$\mathcal{P}a_{\mu\nu} = +a_{\mu\nu} \quad (5.72)$$

$$\mathcal{P}B_{\mu\nu} = -B_{\mu\nu}, \quad (5.73)$$

the charges of the actions (5.68), (5.69) and (5.70) are

$$\mathcal{P}S_{\text{CS}} = +2S_{\text{CS}} \quad (5.74)$$

$$\mathcal{P}S_{\text{CS}}^{(B)} = -2S_{\text{CS}}^{(B)} \quad (5.75)$$

$$\mathcal{P}S_{\text{BF}} = 0. \quad (5.76)$$

Requiring that the action has vanishing \mathcal{P} -charge uniquely identifies S_{BF} (5.70), which can be written in a form that is even more reminiscent to the standard BF action

$$S_{\text{BF}} = \frac{1}{3} \int d^3x \epsilon^{\mu\nu\rho} B_\mu{}^\sigma F_{\sigma\nu\rho}, \quad (5.77)$$

where we used the higher-rank field strength (4.84) which is invariant under the field transformations (5.66) and (5.67). It is useful to decompose the generic tensor $B_{\mu\nu}(x)$

in its symmetric and antisymmetric parts

$$B_{\mu\nu} \equiv b_{\mu\nu} + \epsilon_{\mu\nu\rho} b^\rho, \quad (5.78)$$

where

$$b_{\mu\nu} = b_{\nu\mu} = \frac{1}{2} (B_{\mu\nu} + B_{\nu\mu}) \quad (5.79)$$

$$\epsilon_{\mu\nu\rho} b^\rho = \frac{1}{2} (B_{\mu\nu} - B_{\nu\mu}) \rightarrow b^\rho = -\frac{1}{2} \epsilon^{\rho\alpha\beta} B_{\alpha\beta}, \quad (5.80)$$

which, from (5.67), transform as

$$\delta_2 b_{\mu\nu} = \frac{1}{2} (\partial_\mu \zeta_\nu + \partial_\nu \zeta_\mu) \quad (5.81)$$

$$\delta_2 b^\rho = -\frac{1}{2} \epsilon^{\rho\alpha\beta} \partial_\alpha \zeta_\beta. \quad (5.82)$$

The invariant action (5.70), written in terms of $a_{\mu\nu}(x)$, $b_{\mu\nu}(x)$ and $b_\mu(x)$, reads

$$S_{\text{BF}} = \int d^3x \left(\epsilon^{\mu\nu\rho} b_\mu^\sigma \partial_\nu a_{\rho\sigma} - b^\mu \partial^\nu a_{\mu\nu} + b^\mu \partial_\mu a \right), \quad (5.83)$$

where $a(x) \equiv \eta^{\mu\nu} a_{\mu\nu}(x)$ is the trace of the gauge field. The gauge transformations δ_1 (5.66) and δ_2 (5.67) depend on the scalar gauge parameter $\Lambda(x)$ and on the vector $\xi_\mu(x)$, respectively, and, correspondingly, require a scalar and a vector gauge condition

$$k_0 \partial^\mu \partial^\nu a_{\mu\nu} + k_1 \square a = 0 \quad (5.84)$$

$$\kappa_0 \partial^\nu b_{\mu\nu} + \kappa_1 \partial_\mu b + \kappa_2 \epsilon_{\mu\nu\rho} \partial^\nu b^\rho = 0, \quad (5.85)$$

where $b(x) \equiv \eta^{\mu\nu} b_{\mu\nu}(x)$ and $k_0, k_1, \kappa_0, \kappa_1$ and κ_2 are constant parameters. The above gauge conditions can be implemented by adding to the invariant action S_{BF} (5.70) the gauge fixing term

$$S_{gf} = \int d^3x \left[d \left(k_0 \partial^\mu \partial^\nu a_{\mu\nu} + k_1 \square a + \frac{k}{2} d \right) + d^\mu \left(\kappa_0 \partial^\nu b_{\mu\nu} + \kappa_1 \partial_\mu b + \kappa_2 \epsilon_{\mu\nu\rho} \partial^\nu b^\rho + \frac{\kappa}{2} d_\mu \right) \right], \quad (5.86)$$

where $d(x)$ and $d^\mu(x)$ are Nakanishi-Lautrup multipliers [171, 172], with mass dimensions $[d] = 0$ and $[d_\mu] = 1$, which imply that the gauge parameters k and κ have non-vanishing mass dimensions $[k] = 3$ and $[\kappa] = 1$, which renders the Landau gauge $k = \kappa = 0$ mandatory, in order to avoid infrared divergences [75, 173]. The EoM of the

gauge fixed action

$$S \equiv S_{\text{BF}} + S_{\text{gf}} , \quad (5.87)$$

are

$$\frac{\delta S}{\delta a_{\alpha\beta}} = \frac{1}{2} \left(\epsilon^{\alpha\mu\nu} \partial_\mu b_\nu^\beta + \epsilon^{\beta\mu\nu} \partial_\mu b_\nu^\alpha + \partial^\alpha b^\beta + \partial^\beta b^\alpha \right) - \eta^{\alpha\beta} \partial_\mu b^\mu + k_0 \partial^\alpha \partial^\beta d + k_1 \eta^{\alpha\beta} \square d \quad (5.88)$$

$$\frac{\delta S}{\delta b_{\alpha\beta}} = \frac{1}{2} \left(\epsilon^{\alpha\mu\nu} \partial_\mu a_\nu^\beta + \epsilon^{\beta\mu\nu} \partial_\mu a_\nu^\alpha \right) - \frac{\kappa_0}{2} \left(\partial^\alpha d^\beta + \partial^\beta d^\alpha \right) - \kappa_1 \eta^{\alpha\beta} \partial_\mu d^\mu \quad (5.89)$$

$$\frac{\delta S}{\delta b^\alpha} = -\partial^\mu a_{\mu\alpha} + \partial_\alpha a + \kappa_2 \epsilon_{\alpha\mu\nu} \partial^\mu d^\nu \quad (5.90)$$

$$\frac{\delta S}{\delta d} = k_0 \partial^\mu \partial^\nu a_{\mu\nu} + k_1 \square a \quad (5.91)$$

$$\frac{\delta S}{\delta d^\alpha} = \kappa_0 \partial^\mu b_{\mu\alpha} + \kappa_1 \partial_\alpha b + \kappa_2 \epsilon_{\alpha\mu\nu} \partial^\mu b^\nu . \quad (5.92)$$

From (5.88) and (5.89) we get

$$\eta_{\alpha\beta} \frac{\delta S}{\delta a_{\alpha\beta}} = -2\partial_\mu b^\mu + (k_0 + 3k_1) \square d \quad (5.93)$$

$$\eta_{\alpha\beta} \frac{\delta S}{\delta b_{\alpha\beta}} = -(\kappa_0 + 3\kappa_1) \partial_\mu d^\mu , \quad (5.94)$$

so we see that, if

$$k_0 + 3k_1 = 0 \quad (5.95)$$

the trace $a(x)$ plays the role of a multiplier for the condition

$$\partial^\mu b_\mu = 0 , \quad (5.96)$$

and S does not depend on the trace $b(x)$ anymore. In Appendix E.2 we find that the propagators are defined only when (5.95) is satisfied, *i.e.* when the gauge fixed action (5.87) depends only on the traceless part of $B_{\mu\nu}(x)$

$$\tilde{B}_{\mu\nu} \equiv B_{\mu\nu} - \frac{1}{3} \eta_{\mu\nu} b . \quad (5.97)$$

We choose not to impose this constraint, although reasonable, to leave the tracelessness property as a check of the correctness of our approach. The propagators (see Appendix

E.2) display poles for

$$\kappa_0 = 0 \quad ; \quad \kappa_1 = \kappa_2 \quad ; \quad k_1 = -k_0, \quad (5.98)$$

which identify values of the gauge fixing parameters for which the propagators of the theory, hence the theory itself, are not defined. Finally, using the on-shell EoM (5.88)-(5.92) and the tracelessness condition (5.95) we computed the number of DoF. In particular (see Appendix F.2 for explicit calculations), we have three DoF from $a_{\mu\nu}(x)$, two from $b_{\mu\nu}(x)$ and one from $b^\mu(x)$, for a total of six DoF for the whole theory described by the gauge fixed action S (5.87).

Energy-momentum tensor

Making explicit the dependence of the invariant action S_{BF} (5.70) on the metric in a curved spacetime

$$S_{\text{BF}} = \int d^3x \epsilon^{\mu\nu\rho} g^{\sigma\lambda} B_{\mu\lambda} \partial_\nu a_{\rho\sigma}, \quad (5.99)$$

we can compute the energy-momentum tensor

$$T_{\alpha\beta} \equiv -\frac{2}{\sqrt{-g}} \frac{\delta S_{\text{BF}}}{\delta g^{\alpha\beta}} \Big|_{g=\eta} = -B_{\mu\alpha} \epsilon^{\mu\nu\rho} \partial_\nu a_{\rho\beta} - B_{\mu\beta} \epsilon^{\mu\nu\rho} \partial_\nu a_{\rho\alpha}. \quad (5.100)$$

Using the EoM, written in terms of $B_{\mu\nu}(x)$ and $a_{\mu\nu}(x)$

$$\frac{\delta S_{\text{BF}}}{\delta B_{\alpha\beta}} = \epsilon^{\alpha\nu\rho} \partial_\nu a_\rho^\beta \quad (5.101)$$

$$\frac{\delta S_{\text{BF}}}{\delta a_{\alpha\beta}} = \frac{1}{2} \left(\epsilon^{\alpha\mu\nu} \partial_\mu B_\nu^\beta + \epsilon^{\beta\mu\nu} \partial_\mu B_\nu^\alpha \right), \quad (5.102)$$

it is readily seen that on-shell the energy-momentum tensor vanishes:

$$T_{\alpha\beta} \Big|_{\text{on-shell}} = 0. \quad (5.103)$$

This is analogous to topological quantum field theories [75], where the only contribution to the energy-momentum tensor comes from the gauge fixing term. The difference is that in topological quantum field theories the contribution to $T_{\mu\nu}(x)$ from S_{BF} (5.70) vanishes off-shell, which is a stronger property than the on-shell vanishing we are observing in this case. This latter is quite a peculiar feature of this theory, which is

not topological, because on a curved manifold the action S_{BF} does depend on the generic spacetime metric $g_{\mu\nu}(x)$, although the dependence is mild, as it is apparent if we compare the action (5.99) with, for instance, 3D Maxwell theory (5.61),

5.2.2 Currents and fractons

Since our theory depends on two fields, $a_{\mu\nu}(x)$ and $\tilde{B}_{\mu\nu}(x)$, we have two currents $J^{\mu\nu}(x)$ and $\tilde{K}^{\mu\nu}(x)$. This is in complete analogy with the BF description of 3D topological insulators (see for instance Eq. (14) of [148]). Finally, $\tilde{K}^{\mu\nu}(x)$ is traceless because it couples to $\tilde{B}_{\mu\nu}(x)$ (5.97), which is traceless. Hence, the total action of our theory which includes matter is

$$S_{\text{tot}} \equiv S_{\text{BF}} + S_J + S_K, \quad (5.104)$$

where S_{BF} is given by (5.70) and

$$S_J \equiv - \int d^3x J^{\mu\nu} a_{\mu\nu} \quad (5.105)$$

$$S_K \equiv - \int d^3x \tilde{K}^{\mu\nu} \tilde{B}_{\mu\nu}, \quad (5.106)$$

with $J^{\mu\nu}(x)$ a rank-2 symmetric tensor current, $\tilde{K}^{\mu\nu}(x)$ a rank-2 traceless tensor current and $\tilde{B}_{\mu\nu}(x)$ is the traceless part of $B_{\mu\nu}(x)$ (5.97). The on-shell EoM of the total action S_{tot} (5.104) are

$$J^{\alpha\beta} = \frac{\delta S_{\text{BF}}}{\delta a_{\alpha\beta}} = \frac{1}{2} \left(\epsilon^{\mu\nu\alpha} \partial_\mu \tilde{B}_\nu^\beta + \epsilon^{\mu\nu\beta} \partial_\mu \tilde{B}_\nu^\alpha \right) \quad (5.107)$$

$$\tilde{K}^{\alpha\beta} = \frac{\delta S_{\text{BF}}}{\delta \tilde{B}_{\alpha\beta}} = \epsilon^{\mu\nu\alpha} \partial_\mu a_\nu^\beta. \quad (5.108)$$

In vacuum, the 00-component of the on-shell EoM (5.107) of the symmetric field $a_{\mu\nu}(x)$ reads

$$\frac{\delta S_{\text{BF}}}{\delta a_{00}} = \epsilon^{0mn} \partial_m \tilde{B}_n^0 = 0, \quad (5.109)$$

which is solved by

$$\tilde{B}_{j0} \equiv \partial_j \phi, \quad (5.110)$$

where $\phi(x)$ is a local scalar function. This scalar field $\phi(x)$ plays the role of the one (typically called $A_0(x)$) introduced by hand in fracton theories [60, 149], and recovered as a vacuum solution in the covariant theories [3, 74]. Thus it is at the heart of the fractonic interpretation. From now on, we will assume the solution (5.110) to hold also when matter is introduced, in order to preserve the fractonic field content. As we shall see below, this is crucial in order to have a fractonic physical interpretation of our theory. This assumption on the on-shell EoM (5.107) implies

$$J^{00} = 0. \quad (5.111)$$

From the on-shell EoM (5.107) we also get

$$\partial_\alpha \partial_\beta J^{\alpha\beta} = 0, \quad (5.112)$$

which, as a consequence of (5.111), can be rewritten as

$$\partial_0 \rho + \partial_i \partial_j J^{ij} = 0, \quad (5.113)$$

where we defined the charge density

$$\rho \equiv 2\partial_i J^{0i}. \quad (5.114)$$

We observe that (5.113) is a continuity equation for a scalar fractonic charge $\rho(x)$ since it implies both the conservation of the total charge and of the total dipole moment, which encodes immobility, which is the fundamental property of fracton quasiparticles [62]. Therefore we have a fully constrained fractonic charge and a fully mobile dipole excitation. Analogously to (5.107), in vacuum the on-shell 00-component of the EoM (5.108) is

$$\frac{\delta S_{\text{BF}}}{\delta \vec{B}_{00}} = \epsilon^{0ij} \partial_i a_j^0 = 0, \quad (5.115)$$

which we already encountered in the previous Section (see (5.15)) and whose solution is

$$a_{j0} = \partial_j \psi, \quad (5.116)$$

with $\psi(x)$ a local scalar function. This will be important for the fractonic interpretation of the theory because it will allow us to define, in analogy with the standard abelian BF

[38, 148, 183], higher-rank electromagnetic fields, which are typical of fracton models [3, 74, 149]. In analogy to (5.110), from now on we will assume that the solution (5.116) continues to be true when matter is introduced. Thus, when using the solution (5.116) in the 00-component of the on-shell EoM (5.108), it implies

$$\tilde{K}^{00} = 0, \quad (5.117)$$

which, again, will play an important role in the physical interpretation of the theory. Moreover, from the on-shell EoM (5.108) we also get

$$\partial_\alpha \tilde{K}^{\alpha\beta} = 0, \quad (5.118)$$

whose components are explicitly given by

- $\beta = 0$

$$\partial_i \tilde{K}^{i0} = 0, \quad (5.119)$$

where (5.117) has been used, and from which we observe that the vector quantity $\tilde{K}^{i0}(x)$ is solenoidal.

- $\beta = i$

$$\partial_0 \rho^i + \partial_j \tilde{K}^{ji} = 0, \quad (5.120)$$

which is a continuity equation for a vector charge density

$$\rho^i \equiv \tilde{K}^{0i}, \quad (5.121)$$

with traceless current density $\tilde{K}^{ij}(x)$.

From the continuity equation (5.120) we get

$$\partial_0 \int d\Sigma \rho^i = - \int d\Sigma \partial_j \tilde{K}^{ji} = 0, \quad (5.122)$$

which encodes the conservation of the vector charge. Using (5.117), we also get

$$\partial_0 \int d\Sigma x_i \rho^i = - \int d\Sigma x_i \partial_j \tilde{K}^{ji} = \int d\Sigma \eta_{ij} \tilde{K}^{ji} = \int d\Sigma \tilde{K}^{00} = 0, \quad (5.123)$$

which constrains the motion of the vector dipole-like charge to be transverse only [60, 149]. It is worth to note that from the continuity equation (5.120) we get

$$\partial_0 \int d\Sigma \epsilon_{0ij} x^i \rho^j = \int d\Sigma \epsilon_{0ij} \tilde{K}^{ij} = \int d\Sigma k_0, \quad (5.124)$$

where we decomposed the current $\tilde{K}^{\alpha\beta}(x)$ into its symmetric and antisymmetric parts

$$\tilde{K}^{\mu\nu} \equiv \tilde{k}^{\mu\nu} - \frac{1}{2} \epsilon^{\mu\nu\rho} k_\rho. \quad (5.125)$$

Therefore, from (5.124) we observe that if $k_0(x) = 0$ the theory displays an additional angular momentum-like conservation relation, and the dipole-like lineon becomes fractonic. From (5.125) we see that the condition $k_0(x) = 0$ implies $\tilde{K}^{ij}(x) = \tilde{k}^{ij}(x)$, which is the symmetric component which intervenes in the fractonic continuity equation (5.113). The spatially antisymmetric components of $\tilde{B}_{\mu\nu}(x)$, which are coupled to $\tilde{K}^{\mu\nu}(x)$ through S_K (5.106), are not physically relevant, and we may say that the condition $k_0 = 0$ implies a pure fractonic behaviour: both conserved charges of the theory, $\rho(x)$ (5.114) and $\rho^i(x)$ (5.121), are associated to fractonic quasiparticles, and only dipolar bound states of $\rho(x)$ can move. On the other hand, when $k_0 \neq 0$ the angular momentum-like quantity (5.124) is not conserved, which allows the vector charge $\rho^i(x)$ (5.121) to have a lineon-like behaviour.

Now, taking into account the solutions (5.110) and (5.116), the non-trivial components of the on-shell EoM (5.108) read

- $\alpha = 0, \beta = i$

$$\rho^i = \frac{\delta S_{\text{BF}}}{\delta \tilde{B}_{0i}} = \epsilon^{0jk} \partial_j a_k^i. \quad (5.126)$$

- $\alpha = i, \beta = j$

$$\tilde{K}^{ij} = \frac{\delta S_{\text{BF}}}{\delta \tilde{B}_{ij}} = \epsilon^{0ki} \partial_0 a_k^j + \epsilon^{0ik} \partial_k a_0^j. \quad (5.127)$$

We recall that in ordinary 3D BF theory (5.71), one has

$$\frac{\delta S_{\text{BF}}^{(\text{ord})}}{\delta B_i} \propto \epsilon^{0ij} \mathcal{E}_j \quad (5.128)$$

$$\frac{\delta S_{\text{BF}}^{(\text{ord})}}{\delta B_0} \propto \mathcal{B}, \quad (5.129)$$

with $\mathcal{E}_i(x)$ and $\mathcal{B}(x)$ being the planar electric and magnetic fields [38, 148, 183]. Analogously, here we define

$$\left. \frac{\delta S_{\text{BF}}}{\delta \tilde{B}_{ij}} \right|_{(5.116)} \equiv \frac{1}{2} \epsilon^{0ki} \mathcal{E}_k^j \quad (5.130)$$

$$\frac{\delta S_{\text{BF}}}{\delta \tilde{B}_{0i}} \equiv \frac{1}{2} \mathcal{B}^i, \quad (5.131)$$

where $\mathcal{E}_{ij}(x)$ and $\mathcal{B}_i(x)$ are generalized electric and magnetic fields. These, by comparing with (5.107) and (5.108) in vacuum, can be written in terms of the fracton field strength (4.84) as

$$\mathcal{E}^{ij} \equiv F^{ij0} \Big|_{(5.116)} = 2(\partial_0 a^{ij} - \partial^i \partial^j \psi) \quad (5.132)$$

$$\mathcal{B}^i \equiv -\frac{2}{3} \epsilon_{0jk} F^{ijk} = -2\epsilon_{0jk} \partial^j a^{ik}. \quad (5.133)$$

Notice that, due to (5.132) and to the solution (5.116), the generalized electric field $\mathcal{E}_{ij}(x)$ is symmetric as in fractonic theories [74, 77, 167]. Furthermore, using the definitions (5.130) and (5.131), the EoM (5.126) and (5.127) can be rewritten, respectively, as

$$\rho^i = \frac{1}{2} \mathcal{B}^i \quad (5.134)$$

and

$$\tilde{K}^{ij} = \tilde{\sigma}^{ijkl} \mathcal{E}_{kl}, \quad (5.135)$$

with

$$\tilde{\sigma}^{ijkl} = \tilde{\sigma}^{ijlk} \equiv \frac{1}{4} \left(\epsilon^{0ki} \eta^{jl} + \epsilon^{0li} \eta^{jk} \right), \quad (5.136)$$

which is traceless on the first two indices. Notice also that (5.134) and (5.135) are, respectively, a generalization of the magnetic flux attachment relation (5.46) which

characterize both the ordinary Chern-Simons (5.3) and BF (5.71) actions when coupled to matter [38, 148, 183]. Notice that the 0-component of the EoM of the antisymmetric part, represented by the vector $b^\mu(x)$, coupled to its current k_μ (5.125) reads

$$k_0 = \frac{\delta S_{\text{BF}}}{\delta b^0} = -\partial^\mu a_{\mu 0} + \partial_0 a = -\frac{1}{2} F^i{}_{i0} = \frac{1}{2} \mathcal{E}^i{}_i, \quad (5.137)$$

where we used the definition of the electric tensor field (5.132). A physical interpretation of the lineon-to-fracton transformation thus emerges and is the following: the general theory (5.104) features a scalar fracton and a vectorial lineon whose motion is associated to electromagnetic-like fields $\mathcal{E}_{ij}(x)$ (5.132) and $\mathcal{B}^i(x)$ (5.133) through the Hall-like relations (5.135) and (5.134) respectively. A transition happens when the trace of the electric tensor $\mathcal{E}_{ij}(x)$ is turned off (*i.e.* $k_0 = 0$ on-shell in (5.137)), for which the system acquires an angular-momentum-like conservation and the lineon becomes a fracton. In other words the trace of the electric tensor $\mathcal{E}^i{}_i$ is related to the breaking of angular momentum. This transition can be seen as stepping from the so called Vector Charge Theory of fractons to the Traceless Vector Charge Theory of fractons" [149]. To conclude, a comment on the connection between this theory and the existing literature is in order. Using the vacuum solutions of the on-shell EoM (5.107) and (5.108) for $a_{00}(x)$ and $\tilde{B}_{\alpha 0}(x)$, thus implying $\tilde{K}_{i0}(x) = 0$ in addition to (5.111) and (5.117), these fields can be integrated out from the partition function associated to the total action S_{tot} (5.104), which leads to the effective action

$$S_{\text{eff}} = \int d^3x (\psi \epsilon^{0ij} \partial_j \partial_k \tilde{B}_i^k + \tilde{B}_0^k \epsilon^{0ij} \partial_i a_{jk} - a_{ik} \epsilon^{0ij} \partial_0 \tilde{B}_j^k - \tilde{B}_{0i} \rho^i - \tilde{B}_{ij} \tilde{K}^{ij} + \psi \rho - a_{ij} J^{ij}), \quad (5.138)$$

which can be mapped into Eq. (3.32) of [184]. Thus in this case our theory describes the low-energy limit of the *Rank-2 Toric Code* (R2TC) in two spatial dimensions [185, 186], which is an exactly solvable quantum lattice model whose quasiparticle excitations have restricted mobility and exhibit unusual braiding statistics [185, 187, 188]. The R2TC can be obtained from the rank-2 $U(1)$ lattice gauge theory (whose excitations are subdimensional) through the Higgsing procedure [161], which lowers the $U(1)$

continuous gauge symmetry to \mathbb{Z}_N . Explicitly, the mapping is the following

$$\begin{array}{cc} \mathbf{R2TC} & \mathbf{Covariant BF-like} \\ (E_t^x, E_t^y) & \equiv (-\tilde{B}_{02}, \tilde{B}_{01}) \end{array} \quad (5.139)$$

$$(E_{xx}, E_{yy}, E_{xy}) \equiv (-\tilde{B}_{12}, \tilde{B}_{21}, \tilde{B}_{11} - \tilde{B}_{22}) \quad (5.140)$$

$$(A_t, A_{xx}, A_{yy}, A_{xy}) \equiv (\psi, a_{22}, a_{11}, -a_{12}) \quad (5.141)$$

$$(\tilde{J}_t, J_{xx}, J_{xy}, J_{yy}) \equiv -(\rho, J_{11}, 2J_{12}, J_{22}) \quad (5.142)$$

$$(K_{xx}, K_{xy}, K_{yy}) \equiv (-\tilde{K}_{12}, \tilde{K}_{11}, \tilde{K}_{21}) \quad (5.143)$$

$$(\rho^x, \rho^y) \equiv (-\rho_2, \rho_1), \quad (5.144)$$

from which we observe that the components of the vector charge density $\rho_i(x)$ correspond to the two magnetic excitations which characterize the R2TC. Moreover, we stress that this relation between the covariant BF-like theory and the R2TC is a higher-rank generalization of what is proved in [175], where an equivalence between the ordinary 3D BF theory and the Kitaev's Toric Code [45] has been demonstrated. Finally, since the R2TC action is equivalent to the dipolar BF action studied in [189], then our theory is also equivalent to the foliated BF theory with global and dipole symmetry of [189] (see in particular Eq. (3.7)).

5.2.3 Symmetric tensor fields

As a particular case, we now consider the theory where also the tensor field $B_{\mu\nu}(x)$ appearing in the action S_{BF} (5.70) is symmetric. To avoid confusion with the generic case, we call this latter field $\Phi_{\mu\nu}(x)$. Therefore, both the tensor fields $a_{\mu\nu}(x)$ and $\Phi_{\mu\nu}(x)$ are symmetric and whose transformations δ'_1 and δ'_2 are longitudinal diffeomorphisms (4.60) with two different local scalar gauge parameters. As done for the action (5.70), requiring vanishing \mathcal{P} -charge (5.76), we get the most general invariant action

$$S_{\text{BF}}^{(s)} = \int d^3x \epsilon^{\mu\nu\rho} \Phi_{\mu\sigma} \partial_\nu a_\rho^\sigma, \quad (5.145)$$

which satisfies $\delta'_1 S_{\text{BF}}^{(s)} = \delta'_2 S_{\text{BF}}^{(s)} = \mathcal{P} S_{\text{BF}}^{(s)} = 0$. The two longitudinal diffeomorphisms transformations require two scalar gauge fixing conditions of the type (5.84), and the gauge fixing procedure straightforwardly follows what we have already done in Section 5.2.1. It is worth to remark that, as in the standard abelian case [75], the BF-like action (5.145) can be cast into the sum of two Chern-Simons-like actions (5.1), which is a rank-2 generalization of what happens in the ordinary abelian 3D BF theory, where

the action (5.71) results from the combination of two Chern–Simons actions (5.3) with opposite chiralities [75]. In fact, by means of the linear transformation

$$a_{\mu\nu}^{\pm} \equiv a_{\mu\nu} \pm \Phi_{\mu\nu}, \quad (5.146)$$

the action (5.145) becomes

$$S_{\text{BF}}^{(s)} = \frac{1}{4} (S_{\text{CS}}^+ - S_{\text{CS}}^-), \quad (5.147)$$

where

$$S_{\text{CS}}^{\pm} \equiv \int d^3x \epsilon^{\mu\nu\rho} a_{\mu}^{\pm\sigma} \partial_{\nu} a_{\rho\sigma}^{\pm}. \quad (5.148)$$

The single Chern-Simons-like action was studied in Subsection 5.1. Therefore, due to the relation (5.147), the Hall-like interpretation of the fractonic Chern-Simons-like action (5.148), discussed in [3], holds for the action (5.145) as well. Once matter is introduced (see Appendix G for details), the completely symmetric case studied in this Subsection corresponds to two fractonic traceless scalar charge theories and it is a rank-2 generalization of the action proposed in [148], where it has been proved that ordinary 3D BF theory is a good effective field theory for the description of quantum spin Hall insulators in two spatial dimensions. Recently in [80], in a related context of dipole conserving theories, a bulk description of topological dipole insulators has been proposed starting from an effective edge theory and by means of so-called coupled wire construction [190]. In this approach, they made the assumption that the dipole moment is conserved *only* in one direction, say the x_1 direction. Related to this, is the fact that the gauge fields of the resulting bulk theory appearing in [80] do not transform under the covariant fracton gauge transformations δ'_1 and δ'_2 . Our theory generalizes the one studied in [80] since (see Appendix G for details), we have conservation of both the x_1 and x_2 components of the total dipole moment. This is a consequence of the covariance of our fracton gauge theory. In terms of subdimensional quasiparticles, there are no fractons in [80] but only scalar lineons, defined by the conservation of the dipolar momentum component transverse to their propagation direction. Unlike [80], as we showed in Appendix G, our theory is characterized by two types of fractons and lineons. Importantly, the latter are a consequence of the tracelessness of our theory and are given by the dipoles, which are constrained to move in the direction orthogonal to their dipole momenta. A detailed study of the resulting edge theory in our case is an interesting direction to be inspected.

5.3 Covariant field theory of 3D massive fractons

5.3.1 The general model

The action

We consider a 3D symmetric rank-2 tensor field $a_{\mu\nu}(x)$ transforming under longitudinal diffeomorphisms (4.60) [3, 70, 71, 74, 163]. The most general 3D local integrated functionals invariant under (4.60) are

$$S_{\text{LG}} = \int d^3x (\partial_\mu a \partial^\mu a - \partial_\rho a_{\mu\nu} \partial^\rho a^{\mu\nu} - 2\partial_\mu a \partial_\nu a^{\mu\nu} + 2\partial_\rho a_{\mu\nu} \partial^\mu a^{\nu\rho}) \quad (5.149)$$

$$S_{\text{M}} = \int d^3x (\partial_\rho a_{\mu\nu} \partial^\mu a^{\nu\rho} - \partial_\rho a_{\mu\nu} \partial^\rho a^{\mu\nu}) \quad (5.150)$$

$$S_{\text{CS}} = \int d^3x \epsilon^{\mu\nu\rho} a_\mu^\lambda \partial_\nu a_{\rho\lambda}, \quad (5.151)$$

where $a(x) \equiv \eta^{\mu\nu} a_{\mu\nu}(x)$ is the trace of the tensor field $a_{\mu\nu}(x)$. Assigning canonical mass dimension $[a_{\mu\nu}] = 1/2$, we see that S_{CS} (5.151) is a lower dimensional term with respect to S_{LG} (5.149) and S_{M} (5.150). Each of the above terms has an important physical meaning. S_{LG} (5.149) is the action of Linearized Gravity, which is invariant under the more restrictive infinitesimal diffeomorphism transformation (4.66). The second term S_{M} (5.150), once matter is introduced, describes the dynamics of the fracton quasi-particles [149], in its covariant extension described in Section 4.4 (based on [74]). We will refer to (5.150) as the ‘‘fractonic’’ term of the invariant action S_{inv} . Finally, S_{CS} (5.151) is peculiar to 3D spacetime only, due to the presence of the Levi-Civita tensor $\epsilon^{\mu\nu\rho}$. It encodes a higher rank Chern-Simons theory of fractons, whose Hall-like behaviour has been described in Section 5.1. In [191] it has been shown that S_{CS} (5.151) induces a mechanism of ‘‘quasi topological’’ mass generation for 3D Linearized Gravity. The aim of this Section is to study whether a similar mechanism of mass generation holds for the pure fracton theory, and the action we consider is⁶

$$S_{\text{inv}} = S_{\text{M}} + m S_{\text{CS}}, \quad (5.152)$$

where m is a massive parameter $[m] = 1$.

⁶The invariant action (5.152) reminds the action discussed in [176, 177] in the context of the study of ground state degeneracies of certain fracton models. In that case the theory is however noncovariant and the massive term has a matrix coefficient which determines the model and its properties.

Gauge-fixing term

In order to identify the parameter m appearing in the action S_{inv} (5.152) as a mass of the tensor field $a_{\mu\nu}(x)$, we have to show that it is a pole of the propagator $\langle a_{\mu\nu}(x)a_{\rho\sigma}(x') \rangle$. Being the local gauge parameter $\Lambda(x)$ a scalar field, the most general gauge condition is

$$\kappa_0 \partial^\mu \partial^\nu a_{\mu\nu} + \kappa_1 \square a = 0, \quad (5.153)$$

where κ_0 and κ_1 are dimensionless gauge parameters. The gauge-fixing condition (5.153) is implemented by the gauge-fixing term

$$S_{gf} = \int d^3x b \left(\kappa_0 \partial^\mu \partial^\nu a_{\mu\nu} + \kappa_1 \square a + \frac{k}{2} b \right), \quad (5.154)$$

where k is the usual gauge parameter, which is massive $[k] = 2$ and $b(x)$ is the Nakanishi-Lautrup Lagrange multiplier [171, 172] for the gauge condition (5.153), with $[b] = 1/2$. A massive gauge parameter induces infrared divergences, hence the Landau gauge choice $k = 0$ is mandatory [173] therefore, the total gauge-fixed action is

$$S = S_{inv} + S_{gf}|_{k=0}. \quad (5.155)$$

Requiring that both $a_{\mu\nu}(x)$ and the transformed field $a'_{\mu\nu}(x) = a_{\mu\nu}(x) + \partial_\mu \partial_\nu \Lambda(x)$ satisfy the gauge condition (5.153), yields

$$(\kappa_0 + \kappa_1) \square^2 \Lambda = 0. \quad (5.156)$$

Hence, in order to satisfy equation (5.156), one must either have

$$\kappa_0 + \kappa_1 = 0 \quad (5.157)$$

or

$$\square^2 \Lambda = 0. \quad (5.158)$$

A particular solution of the polyharmonic gauge condition (5.158) is the harmonic one $\square \Lambda = 0$, which is the usual residual gauge condition of abelian gauge theories [192].

The choice (5.158) turns out to be the only possibility in order to have the propagators, since, as we will see, (5.157) corresponds to a pole of the propagators.

5.3.2 Propagator

Among the propagators of the theory, computed in Appendix E.3, the tensor field propagator in momentum space is

$$\begin{aligned} \langle \hat{a}_{\alpha\beta}(p)\hat{a}_{\rho\sigma}(-p) \rangle = & \frac{1}{2(p^2 + m^2)} \left[-2A^{(0)} - \frac{1}{p^2}A^{(1)} - \frac{1}{p^2}A^{(2)} + A^{(3)} + \frac{7}{p^4}A^{(4)} + \right. \\ & \left. + \frac{m}{2p^2} \left(A^{(5)} + \frac{3}{p^2}A^{(6)} \right) \right]_{\alpha\beta,\rho\sigma} + \frac{1}{2p^2} \left[\frac{\kappa_0+3\kappa_1}{(\kappa_0+\kappa_1)p^2}A^{(2)} - A^{(3)} + \right. \\ & \left. - \frac{(\kappa_0+3\kappa_1)^2}{(\kappa_0+\kappa_1)^2p^4}A^{(4)} \right]_{\alpha\beta,\rho\sigma}, \end{aligned} \quad (5.159)$$

where the $\{A_{\alpha\beta,\rho\sigma}^{(i)}(p)\}$ is the basis of tensors (E.5)-(E.11). The propagator (5.159) displays a massive pole

$$p^2 = -m^2, \quad (5.160)$$

and has a good massless limit, which agrees with [70]. As anticipated, we notice a pole at

$$\kappa_0 + \kappa_1 = 0, \quad (5.161)$$

which we take care of by keeping away from it in the gauge-fixing condition (5.153). Having a well defined massless limit, the action (5.152) describes a massive theory for the higher rank tensor field $a_{\mu\nu}(x)$, where the mass is introduced by means of a mechanism which closely reminds the one which characterizes the Maxwell-Chern-Simons theory [168, 169]. The analogy is even more evident if we introduce the fracton field strength (4.84) [74]. The action S_{inv} (5.152) can be written in terms of the fracton field strength (4.84) as follows

$$S_{inv} = \int d^3x \left(-\frac{1}{6}F_{\mu\nu\rho}F^{\mu\nu\rho} + m\epsilon^{\mu\nu\rho}a_\mu^\lambda\partial_\nu a_{\rho\lambda} \right), \quad (5.162)$$

which closely reminds the Maxwell-Chern-Simons theory

$$S_{\text{MCS}}^{(\text{ord})} = \int d^3x \left(-\frac{1}{4} F_{\mu\nu} F^{\mu\nu} + \frac{M}{2} \epsilon^{\mu\nu\rho} A_\mu \partial_\nu A_\rho \right). \quad (5.163)$$

5.3.3 Degrees of freedom

In order to analyze the number and nature of the DoF in the theory defined by the action S_{inv} (5.152), it may be useful to begin by considering the Maxwell-Chern-Simons case (see Appendix F.3.1), which serves both as a warm-up for the method we will adopt and as a physically relevant model in its own right. To count the DoF of the theory (5.152), and in order to make contact with a well-established procedure adopted in similar cases, we follow the approach of Deser, Jackiw, and Templeton for 3D Linearized Gravity, based on the decomposition of the rank-2 symmetric tensor field $a_{\mu\nu}(x)$. This approach can be found in [168, 169], and, for 4D Linearized Gravity, in [193]. The EoM of the action S_{inv} (5.152) are

$$\frac{\delta S_{\text{inv}}}{\delta a_{\alpha\beta}} = -\partial_\mu F^{\alpha\beta\mu} + m(\epsilon^{\alpha\mu\nu} \partial_\mu a_\nu^\beta + \epsilon^{\beta\mu\nu} \partial_\mu a_\nu^\alpha). \quad (5.164)$$

Following [168, 169], we decompose the spacetime components of the symmetric tensor field $a_{\mu\nu}(x)$ into scalar, transverse, longitudinal and, for $a_{ij}(x)$, solenoidal parts

$$a_{00} = \lambda \quad (5.165)$$

$$a_{0i} = u_i + \partial_i \psi \quad (5.166)$$

$$a_{ij} = (\eta_{ij} - \hat{\partial}_i \hat{\partial}_j) \varphi + \hat{\partial}_i \hat{\partial}_j \chi + \partial_i \phi_j + \partial_j \phi_i, \quad (5.167)$$

where $\hat{\partial}_i \equiv \partial_i / \sqrt{\nabla^2}$, and $u_i(x)$ and $\phi_i(x)$ are transverse planar vectors

$$\partial^i u_i = \partial^i \phi_i = 0, \quad (5.168)$$

hence

$$u_i = \epsilon_{0ij} \partial^j u \quad ; \quad \phi_i = \epsilon_{0ij} \partial^j \xi, \quad (5.169)$$

so that the six components of $a_{\mu\nu}(x)$ are parametrized by λ , u , ψ , φ , χ and ξ . By using the decompositions (5.165), (5.166) and (5.167), the EoM (5.164) reduce to (see

Appendix F.3.2 for details)

$$\lambda - \partial_0 \psi - mu = 0 \quad (5.170)$$

$$\partial_0 \chi + \nabla^2(m\zeta - \psi) = 0 \quad (5.171)$$

$$(\square - m^2)u + \nabla^2(u - \partial_0 \zeta) - m\varphi = 0 \quad (5.172)$$

$$\square\varphi + m\nabla^2(\partial_0 \zeta - u) = 0 \quad (5.173)$$

$$m\partial_0 \varphi - (\square - m^2)\nabla^2 \zeta - \nabla^2 \partial_0(u - \partial_0 \zeta) = 0. \quad (5.174)$$

The number and the nature of the DoF – massive or massless, propagating or not – are gauge independent. However, particular gauge choices can help make these aspects manifest. Due to the symmetry (4.60), which involves the scalar gauge parameter $\Lambda(x)$, a scalar gauge-fixing condition is required. A convenient gauge choice to exhibit the structure of the theory is

$$u = 0, \quad (5.175)$$

implying, from (5.166) and (5.169), that $a_{0i}(x)$ is a longitudinal planar vector

$$a_{0i} = \partial_i \psi, \quad (5.176)$$

and simplifies the identification of the propagating modes. Moreover, as we will see, this choice, which will be adopted in this Subsection from now on, has the physical significance of allowing the fractonic sector of the theory to be identified.

Massless case $\mathbf{m} = 0$: the pure fractonic action S_M (5.150), which corresponds to a rank-2 Maxwell action, features two DoF: $\varphi(x)$, associated to the transverse component of $a_{ij}(x)$ through (5.167) and satisfying a wave equation (from (5.173)), and $\chi(x)$, associated with the longitudinal sector. The fields $\psi(x)$ and $\lambda(x)$ are determined by $\chi(x)$ through (5.171) and (5.170), while $\zeta(x)$, associated to the solenoidal part of $a_{ij}(x)$, due to (5.172) and (5.174) vanishes.

Massive case $\mathbf{m} \neq 0$: from (5.172) and (5.173) we immediately find that $\varphi(x)$ satisfies the Klein-Gordon equation

$$(\square - m^2)\varphi = 0. \quad (5.177)$$

Alternatively, using (5.172) in (5.174) we find that $\nabla^2\zeta(x)$ satisfies the same Klein-Gordon equation

$$(\square - m^2)\nabla^2\zeta = 0, \quad (5.178)$$

but $\nabla^2\zeta(x)$ and $\varphi(x)$ are non independent one from each other because they are related by (5.172). Hence, $\varphi(x)$ – or, equivalently, $\nabla^2\zeta(x)$ – is a propagating massive DoF. The field $\chi(x)$ remains dynamical and continues to determine $\psi(x)$ and $\lambda(x)$, as in the massless case.

Summarizing, the symmetric rank-2 tensor field $a_{\mu\nu}(x)$ contains six scalar components. In the massless theory defined by the action S_M (5.150), two of these – $\varphi(x)$ and $\chi(x)$ – correspond to independent DoF. The presence of the lower dimensional Chern-Simons-like term S_{CS} (5.151) does not change the number of propagating DoF, as in Maxwell-Chern-Simons theory. In fact, the number of DoF, either in the massless or in the massive case is thus two (see Appendix F.3.1 for a detailed discussion). The difference is that, in the massive case, one of the DoF satisfies a Klein-Gordon equation, hence it is a propagating massive one. It is interesting to notice that the Chern-Simons-like term (5.151), although not topological because metric dependent, behaves as the topological Chern-Simons term in Maxwell-Chern-Simons, namely gives mass without changing the number of DoF, as expected for a topological term. This confirms the “quasi” topological nature of the Chern-Simons-like term (5.151), already remarked in [182]

5.3.4 Physical interpretation

In analogy to the ordinary Maxwell-Chern-Simons theory [34, 168, 169], we define the generalized electromagnetic fields in terms of the invariant fracton field strength (4.84) as (5.132) and (5.133). We can combine (5.165), (5.166) and (5.170) in

$$a_{\mu 0} = \partial_\mu \psi + \epsilon_{0\mu\nu} \partial^\nu u - m\eta_{\mu 0} u, \quad (5.179)$$

which, in the longitudinal gauge (5.175), becomes (4.100), that coincides with the solution in [74]. In this sense, as anticipated, that gauge choice enhances the fractonic interpretation of the theory. In this case, due to the cyclic property (4.81), the field strength (4.84) satisfies also (4.103) and (4.104), and we recover the same expression of the fractonic electric tensor field (5.132) given in [74, 149] which is a symmetric rank-2

generalization of the expression of the electric field of the ordinary $U(1)$ vector gauge theory. In terms of the generalized electric (5.132) and magnetic (5.133) fields, the EoM of $a_{0i}(x)$ can be written as

$$\partial_j \mathcal{E}^{ij} = -m \mathcal{B}^i \equiv -\rho_{\text{CS}}^i, \quad (5.180)$$

from which it also follows that

$$\partial_i \partial_j \mathcal{E}^{ij} = -m \partial_i \mathcal{B}^i \equiv \rho_{\text{CS}}, \quad (5.181)$$

which are fractonic Gauss constraints [60, 149] where the magnetic field $\mathcal{B}^i(x)$ (5.133) plays the role of an internal “electric” charge related to the Chern-Simons-like term (5.151) in the action S_{inv} (5.152). In particular, $\rho_{\text{CS}}^i(x)$ can be seen as a dipole density by writing the total dipole moment

$$D_{\text{CS}}^i \equiv \int d\Sigma x^i \rho_{\text{CS}} = -m \int d\Sigma x^i \partial_j \mathcal{B}^j = \int d\Sigma \rho_{\text{CS}}^i \quad (5.182)$$

$$= \int d\Sigma x^i \partial_a \partial_b \mathcal{E}^{ab} = - \int d\Sigma \partial_a \mathcal{E}^{ai} = 0. \quad (5.183)$$

From (5.183) we have that the total dipole moment vanishes on the 2D surface. Hence, single charges cannot move, since otherwise their motion would change the total dipole moment. Moreover, using the definitions in (5.180) and (5.181) and the constraint (following directly from (5.133))

$$\int d\Sigma x_i \mathcal{B}^i = 0, \quad (5.184)$$

we have that the trace of the total quadrupole moment vanishes

$$D_{\text{CS}}^i{}_i = \eta_{ij} \int d\Sigma x^i x^j \rho_{\text{CS}} = \int d\Sigma x^2 \rho_{\text{CS}} = 2 \int d\Sigma x_i \rho_{\text{CS}}^i = 0, \quad (5.185)$$

which constrains the motion of the internal dipole-like charge $\rho_{\text{CS}}^i(x)$ in the direction perpendicular to the vector $\rho_{\text{CS}}^i(x)$ itself [156]. Furthermore, from the Gauss law (5.180) and the transverse property (5.184) of the magnetic field, we get

$$\int d\Sigma \eta_{ij} \mathcal{E}^{ij} = \int d\Sigma \partial_i x_j \mathcal{E}^{ij} = - \int d\Sigma x_j \partial_i \mathcal{E}^{ij} = m \int d\Sigma x_j \mathcal{B}^j = 0, \quad (5.186)$$

i.e. the electric tensor field (5.132) is constrained to be globally traceless on-shell.

It is easy to check that the EoM of $a_{ij}(x)$, in terms of the generalized electric (5.132)

and magnetic (5.133) fields, becomes the Ampère-like equation

$$-\partial_0 \mathcal{E}^{ij} + \frac{1}{2} \left(\epsilon^{0ki} \partial_k \mathcal{B}^j + \epsilon^{0kj} \partial_k \mathcal{B}^i \right) = \tilde{J}_{\text{CS}}^{ij}, \quad (5.187)$$

where

$$\tilde{J}_{\text{CS}}^{ij} \equiv \frac{1}{2} m \left(\epsilon^{0ik} \tilde{\mathcal{E}}_k^j + \epsilon^{0jk} \tilde{\mathcal{E}}_k^i \right), \quad (5.188)$$

which is traceless. From (5.181) and (5.187) we observe that the Chern-Simons-like term (5.151) plays the role of “intrinsic” matter, in the following sense. In “standard” fracton theories, the fractonic charge and current densities $\rho(x)$ and $J^{ij}(x)$ depend on external matter fields while, in the present case, $\rho_{\text{CS}}(x)$ and $\tilde{J}_{\text{CS}}^{ij}(x)$ are expressed directly in terms of the tensor field $a_{\mu\nu}(x)$. We thus see that, due to the presence of the massive Chern-Simons-like term, the tensor gauge field plays a dual role: that of matter, through $\rho_{\text{CS}}(x)$ and $\tilde{J}_{\text{CS}}^{ij}(x)$, and that of generalized electromagnetic fields, as in (5.132) and (5.133). We refer to this matter as “intrinsic”⁷, in the sense that it originates from the tensor gauge field $a_{\mu\nu}(x)$ itself, rather than from external matter fields, as in QED, for example. It is interesting to observe that the theory described by the action S_{inv} (5.152) is the first case in which a fractonic behaviour is already present without introducing matter, as a consequence of the presence of the massive Chern-Simons-like term, which therefore, besides giving a mass to the tensor field $a_{\mu\nu}(x)$, plays also the role of an “intrinsic” matter contribution.

Fractonic behaviours may emerge in two possible ways: through Gauss-like constraints on the motion of the dipole coming from charge neutrality conditions, like (5.180) and (5.181), and/or through continuity equations for the matter contribution [149]. Indeed to further confirm the fractonic nature of the theory and the role of “intrinsic matter” played by the Chern-Simons-like term, we observe that taking the double divergence $\partial_i \partial_j$ of the Ampère-like equation (5.187) and using the Gauss constraint (5.181), we obtain a fractonic continuity equation [149] relating the fractonic charge $\rho_{\text{CS}}(x)$ to its

⁷Intrinsic matter is not peculiar to our theory since it also appears in various frameworks of ordinary, non-fractonic, theories, such as those involving axions and θ -terms. In particular, see [194, 195] (standard axions), [196] (Witten effect in topological insulators), and [197] (axions and θ -terms in Linearized Gravity). Regarding fractons, in [74, 163, 167] the same phenomenon has been observed in the context of the Witten effect for higher-spin fracton theories. In that case, a quasitopological θ -term is added to the pure fracton action. This suggests that the emergence of intrinsic matter is generally tied to the presence of topological or quasitopological terms.

dipole current $\tilde{J}_{CS}^{ij}(x)$ (5.188)

$$\partial_0 \rho_{CS} + \partial_i \partial_j \tilde{J}_{CS}^{ij} = 0. \quad (5.189)$$

From (5.189) we recover the conservation of both the total dipole moment

$$\partial_0 D_{CS}^i = \int d\Sigma x^i \partial_0 \rho_{CS} = \int d\Sigma \partial_j \tilde{J}_{CS}^{ij} = 0 \quad (5.190)$$

and of the trace of the quadrupole moment

$$\partial_0 \int d\Sigma x^2 \rho_{CS} = \int d\Sigma x_k \partial_j \tilde{J}_{CS}^{kj} = - \int d\Sigma \tilde{J}_{CS}^i{}_i = 0, \quad (5.191)$$

where the last step is a consequence of the tracelessness of the intrinsic current $\tilde{J}_{CS}^{ij}(x)$ (5.188). Both conservations (5.190) and (5.191) reflect the constraints implied by (5.183) and (5.185), *i.e.* immobile fractonic charges and dipoles constrained on a line.

From the Bianchi-like identity (4.86) we have

$$\epsilon_{k0j} \partial^k F^{i0j} + \epsilon_{kj0} \partial^k F^{ij0} + \epsilon_{0jk} \partial^0 F^{ijk} = 0, \quad (5.192)$$

which, using the definitions (5.132) and (5.133), can be written as

$$\partial_0 \mathcal{B}^i + \epsilon_{0jk} \partial^j \mathcal{E}^{ik} = 0, \quad (5.193)$$

which strongly reminds the Faraday law of ordinary electromagnetism, and coincides with the fractonic higher-rank Faraday law introduced in [153].

Finally, the Chern-Simons-like term (5.151) can be seen as a fractonic matter contribution [149, 167], since, on the fracton solution (4.100), we can write

$$mS_{CS} = -\frac{1}{2} \int d^3x \tilde{a}_{\mu\nu} \tilde{J}_{CS}^{\mu\nu}, \quad (5.194)$$

where we defined the “intrinsic” matter current

$$\tilde{J}_{CS}^{\mu\nu} \equiv -\frac{m}{3} \left(\epsilon^{\mu\alpha\beta} \tilde{F}_{\alpha\beta}^\nu + \epsilon^{\nu\alpha\beta} \tilde{F}_{\alpha\beta}^\mu \right), \quad (5.195)$$

whose spatial components are given by (5.188) and, considering the definitions of fractonic charges $\rho_{\text{CS}}(x)$ (5.181) and $\rho_{\text{CS}}^i(x)$ (5.180),

$$\tilde{j}_{\text{CS}}^{00} = 0 \quad ; \quad \tilde{j}_{\text{CS}}^{0i} = -\frac{1}{2}m\mathcal{B}^i = -\frac{1}{2}\rho_{\text{CS}}^i \quad ; \quad \partial_i \tilde{j}_{\text{CS}}^{0i} = \frac{1}{2}\rho_{\text{CS}}, \quad (5.196)$$

so that the Chern-Simons-like term (5.151) reads

$$mS_{\text{CS}} = \frac{1}{2} \int d^3x \left(\psi \rho_{\text{CS}} - \tilde{a}_{ij} \tilde{j}_{\text{CS}}^{ij} \right), \quad (5.197)$$

which can be seen as a fractonic matter coupling [149, 167]. The continuity equation (5.189), in this picture, naturally emerges as a consequence of gauge invariance, since, asking that the action S_{CS} (5.194) is invariant under the gauge transformation (4.60), and taking into account that $\delta\psi = \partial_0\phi$, gives

$$\delta S_{\text{CS}} = - \int d^3x \phi \left(\partial_0 \rho_{\text{CS}} + \partial_i \partial_j \tilde{j}_{\text{CS}}^{ij} \right) = 0, \quad (5.198)$$

which implies (5.189).

We conclude this Subsection with a further interpretation of the nontrivial role of the Chern-Simons-like term (5.151). The fractonic charge density $\rho_{\text{CS}}(x)$ represents one of the two propagating massive DoF of the theory found in Subsection 5.3.3, in fact, using its definition (5.181) and (5.133), it can be associated to the solenoidal sector of $a_{ij}(x)$ (5.167)

$$\rho_{\text{CS}} = 2m\epsilon_{0jk} \partial^j \partial_i a^{ik} = -2m\nabla^2 \xi, \quad (5.199)$$

that satisfies the Klein-Gordon equation (5.178), which therefore can be equivalently written as

$$(\square - m^2)\rho_{\text{CS}} = 0. \quad (5.200)$$

Our theory therefore provides two key insights:

1. the Klein-Gordon equation (5.200) describing a massive, propagating DoF;
2. the Gauss (5.181) and continuity (5.189) equations, which constrain this DoF to be fractonic, ensuring that its motion remains compatible with the conservation of the total dipole moment.

The fact that a fracton quasiparticle can propagate, *i.e.* it possesses a nonvanishing propagator is not contradictory, regardless of whether the fracton is massless or massive. In [70, 74], the covariant extension of fracton Scalar Charge Theory [60, 149] was formulated and the propagators were explicitly computed, turning out to be nonvanishing. Fractonic features can be obtained within the Scalar Charge Theory [60, 149] through the generalized Gauss law (4.26) or, equivalently, through the rank-2 continuity equation (4.41), enforcing both charge and dipole-moment conservation. However, in a dipolar system, pairs of fractons can move (and thus propagate), provided the total dipole moment is preserved. In fact, the very term “fracton” originates from the idea of “being a fraction of a mobile quasiparticle” [66].

5.3.5 Coupling to matter

When external matter is introduced, the picture becomes even richer and we refer to Appendix H for a detailed analysis. The EoM acquire additional source terms, and the total energy-momentum tensor receives contributions both from the intrinsic (Chern-Simons-like) and extrinsic sectors. In Appendix I, we study in detail the energy-momentum tensor and the structure of conserved currents. While the intrinsic sector continues to exhibit fully fractonic behaviours – including restricted motion and conservation of both dipole and trace of the quadrupole moment – the external sector allows for dipoles with complete mobility since the quadrupole trace is no longer conserved. Moreover, the intrinsic dipole-like current $\tilde{J}_{CS}^{ij}(x)$ is such that the corresponding power vanishes while, in contrast, the extrinsic dipole-like current $J^{ij}(x)$ contributes non-trivially to the power (see Appendix I for details). To summarize, when external matter is present, the theory realizes two superimposed fractonic subsystems:

- an *intrinsic* one with a massive fractonic charge density $\rho_{CS}(x)$ and a lineonic dipole density $\rho_{CS}^i(x)$;
- an *external* one with fractonic charges and free dipoles.

5.4 Summary

In this Chapter, following the QFT approach of [70, 71, 74], we investigated 3D invariant actions involving a rank-2 symmetric tensor gauge field $a_{\mu\nu}(x)$ transforming under the covariant fracton transformation (4.60). First of all, in Section 5.1 we studied

the most general 3D action of $a_{\mu\nu}(x)$ with mass dimension 1 and the theory appears as a traceless non-topological higher-rank generalization of the ordinary Chern-Simons model [34]. Once matter is introduced, a fractonic behavior emerges and our model shows a Hall-like dipole current together with a vectorial “flux-attachment” relation for dipoles. In particular, the single isolated charges are fractons while the dipoles are constrained to move in straight lines which are perpendicular to their dipole momenta, *i.e.* they behave as lineons. Subsequently, in 5.2 we investigated the possibility of covariant 3D fractonic BF models. We thus started by considering the 3D field theory of two tensor gauge fields with mass dimension 1: $a_{\mu\nu}(x)$, transforming under the covariant fracton symmetry (5.66), and $B_{\mu\nu}(x)$, with no symmetry on its indices and obeying the more general electromagnetic-like transformation with a vector gauge parameter (5.67). The corresponding invariant action is a higher-rank BF-like model but which is not topological, due to a linear dependence on the metric. This is similar to what happens in the covariant higher-rank Chern-Simons-like model, from which, however, it differs by having an on-shell vanishing energy-momentum tensor, making the BF-like model “quasi-topological”. Once matter is introduced, a subdimensional behavior emerges, with both fractons and lineons. Moreover our theory can be mapped to the low-energy effective field theory describing the Rank-2 Toric Code (R2TC) in two spatial dimensions [185, 186], an exactly solvable quantum lattice model with subdimensional excitations and which is a higher-rank generalization of the Kitaev’s Toric Code [45]. Finally we analyzed the case in which $B_{\mu\nu}(x)$ is a symmetric tensor too, where it turns out that the action can be cast into the sum of two rank-2 Chern-Simons actions (5.1), thus generalizing the ordinary abelian case, which well describes the low-energy physics of quantum spin Hall insulators in two spatial dimensions [148]. Finally, in Section 5.3 we constructed a covariant and gauge-invariant theory for a fractonic gauge field $a_{\mu\nu}(x)$ with mass dimension 1/2. The cornerstone of the model is the presence of the Chern-Simons-like term (which was the main subject of Section 5.1) playing a dual role: it generates a topological mass for the gauge field and simultaneously acts as a source of intrinsic fractonic matter. This dual mechanism is novel and leads to a propagating fractonic degree of freedom described by a massive Klein-Gordon equation. The theory propagates two DoF – one massive, one massless – whose number is preserved in the massless limit, in analogy with the Maxwell-Chern-Simons mechanism of Deser-Jackiw-Templeton [168, 169]. This is a crucial consistency check since it supports the interpretation of the Chern-Simons-like term as a quasi-topological contribution: although it is metric-dependent and hence not fully topological in the strict sense, it retains the key property of a genuine topo-

logical term, *i.e.* it modifies the nature of the dynamics (introducing a mass) without increasing the number of physical DoF.

Chapter 6.

Conclusions and follow-ups

In this Thesis, we investigated two distinct classes of quasiparticles that emerge in different physical contexts. The first class arises in one-dimensional quantum systems, with particular emphasis on the quasiparticles appearing in topologically frustrated quantum spin chains, where the competition between global (geometric) and local (Hamiltonian) orders gives rise to exotic excitations above the ground state. The second class consists of subdimensional quasiparticles, which emerge in fracton phases of matter. In this part of the Thesis, we focused on developing covariant gauge field theory formulations for fractons in $2 + 1$ dimensions (3D), with the aim of embedding the features observed in condensed matter systems into a more formal field theoretical framework. To set the stage for the results presented in this Thesis, we now summarize the two research areas that constitute its core, outline the main contributions of my work, and discuss several possible directions for future investigation.

Understanding the nature of collective quasiparticle excitations is a central theme in the study of quantum phases of matter, as they often provide an accurate description of low-energy physics and reveal properties that are not immediately apparent from a microscopic perspective. In Chapter 2, we examined two of the most celebrated spin models whose low-energy physics is well captured by a quasiparticle picture. In Section 2.1, we studied the Heisenberg model [81] in generic spatial dimension d , which is integrable only in $d = 1$. By means of the Holstein–Primakoff transformation, we mapped it to a free bosonic system and, in order to investigate its low-energy properties, we adopted the semiclassical large-spin description. The resulting gapless emergent bosonic quasiparticles, known as magnons, are relativistic only in the anti-ferromagnetic case, while in the ferromagnetic case the dispersion relation is Galilean. Magnons constitute one of the most famous examples of quasiparticles and are rele-

vant also from a technological point of view. The analysis of the Heisenberg model in different spatial dimensions highlights the special nature of quantum models in $d = 1$, where quantum fluctuations are so strong that they overwhelm semiclassical intuition, giving rise to phenomena with no analogue in higher dimensions.

We then focused on the XY quantum spin chain, the most famous non-trivial one-dimensional integrable quantum system. Similarly to the Heisenberg model, the XY Hamiltonian can be mapped to a free spinless fermionic system via the Jordan–Wigner transformation. The exact diagonalization procedure, performed in Section 2.2, is crucial, as it forms the basis for the striking physical behaviors that emerge in the frustrated case. In Section 2.3, we then concentrated on the ferromagnetic regime, studying in detail the ground state, the zero-temperature phase diagram, the quantum phase transitions, and the correlation functions.

Subsequently, in Section 3.1, we introduced the striking phenomenon of topological frustration. Historically, Landau theory [98] provided the first systematic framework for classifying phases of matter, based on the behavior of a local order parameter that captures macroscopic order [8]. A non-zero order parameter signals spontaneous symmetry breaking and the emergence of a macroscopic order that explicitly violates one of the symmetries of the theory. Symmetry breaking occurs upon crossing a critical point, where the system reorganizes itself and modifies its macroscopic behavior. Because of its success, Landau theory was initially adopted without substantial modifications in the study of quantum phases of matter. However, it soon became clear that the complexity of quantum many-body systems is not fully captured by this framework. A second implicit assumption of Landau theory must also be reconsidered: the idea that microscopic details are irrelevant for determining thermodynamic properties, which justifies taking the thermodynamic limit before performing any calculation. As a consequence, boundary conditions are traditionally assumed to have no influence on bulk behavior. Recently, however, it has been shown that this assumption fails at the quantum level in antiferromagnetic quantum spin chains with discrete symmetries and *frustrated boundary conditions* (FBC) [50], namely periodic boundary conditions with an odd number of sites [51]. This choice of boundary conditions makes it impossible to simultaneously minimize all local interactions in the Hamiltonian, giving rise to a form of geometrical frustration. In this context, the phenomenon is known as *topological frustration*. In terms of quasiparticles, the frustrated boundary condition effectively injects a single delocalized topological excitation into the ground state [56]. Remarkably, this excitation influences the low-energy sector of the entire system, even in the thermodynamic limit, giving rise to exotic phases that are completely absent

in the unfrustrated counterparts. In particular, it can induce new quantum phase transitions [53], suppress local order on both sides of a quantum phase transition [57, 58], and more generally modify the nature of the associated quantum critical point [59].

Topologically frustrated spin chains have attracted considerable interest in the scientific community, since in such systems quantum phases exhibit a genuine dependence on boundary conditions. In Chapter 3, based on [1, 2], we showed that topological frustration modifies the zero-temperature phase diagram of the Ising [1] and XY [2] chains in a transverse magnetic field by inducing new boundary quantum phase transitions, both of first and second order. By boundary quantum phase transitions we mean non-analyticities in the ground-state energy that are non-extensive in the number of particles [54]. Moreover, we identified the first example of a second-order boundary quantum phase transition characterized by a quartic dispersion relation. These analytical results, supported by both exact calculations and numerical investigations, lay the foundation for understanding the phase diagram of the frustrated version of one of the most celebrated integrable models.

The possible follow-ups are numerous. From a fundamental point of view, since quantum spin chains with frustrated boundary conditions constitute a new family of topological models characterized by a non-relativistic gapless spectrum and deconfined fractionalized excitations, it would be interesting to identify topological indices capable of capturing their properties and thus enabling a classification of these new exotic phases of matter. The novel features of such systems are also relevant from a technological perspective, particularly in the realization of quantum devices, as recently explored in [132, 198].

Fracton phases of matter constitute an intriguing point of contact between Condensed Matter and High Energy Physics. Fractons represent an extreme case of subdimensional quasiparticles, namely excitations whose mobility is restricted to lower-dimensional subspaces [60]. More precisely, quasiparticles constrained to move only within zero-, one-, or two-dimensional subspaces are known respectively as fractons, lineons, and planons. The first realizations of such subdimensional behavior appeared in exactly solvable quantum spin models with discrete symmetries, originally developed in the context of Quantum Information Theory [65, 66, 67]. In Section 4.1, we studied the X-cube model [66, 67], the prototypical example of a gapped fracton phase.

Subsequently, it was understood that quasiparticle excitations with restricted mobility also emerge in the low-energy sector of higher-rank $U(1)$ quantum spin liquids [60, 69]. As seen in Section 4.2, these systems are effectively described by higher-rank $U(1)$ tensor gauge theories, whose Gauss constraints encode generalized spin-ice rules that characterize their low-energy sectors. Moreover, the Gauss law determines the gauge transformations of the emergent gauge field, defined as the canonical conjugate of the emergent electric field. Crucially, high-energy states host gapless emergent quasiparticle excitations that violate the lowest-energy constraint. Such emergent matter obeys higher-moment conservation laws [60], which in turn impose severe mobility restrictions, analogous to those previously discussed for the X-cube model. In addition, higher-rank gauge theories give rise to generalized forms of 4D electromagnetism [149]. In Section 4.3, we analyzed the generalized electromagnetism emerging in the fracton Scalar Charge Theory.

Up to that point, these fractonic theories had been formulated in a non-covariant language. However, it was not long before high-energy theorists became interested in exploring restricted mobility within the framework of relativistic quantum field theories. In [70], the authors introduced the first Lorentz-covariant 4D extension of the gauge transformation that characterizes the Scalar Charge Theory, and subsequently analyzed the resulting covariant tensor gauge theory using standard QFT techniques, as reviewed in Section 4.4. Relevantly, the most general 4D power-counting-compatible action involving a rank-2 symmetric tensor gauge field $a_{\mu\nu}(x)$, transforming under longitudinal diffeomorphisms [72], is a combination of Linearized Gravity and an additional term representing the genuine novelty of the theory. The latter constitutes a covariant embedding of the Scalar Charge Theory and thus defines a higher-rank covariant Maxwell theory for fractons [74].

Importantly, since longitudinal diffeomorphisms form a particular subset of infinitesimal diffeomorphisms, the 4D covariant theory necessarily contains both fractonic and gravitational degrees of freedom. This is a crucial point: up to now, no symmetry has been identified that allows one to fully decouple fracton dynamics from linearized gravity. The connection between fracton gauge theories and gravitational modes, previously inferred in the condensed matter literature [159], becomes immediate and transparent in a field-theoretical framework. Identifying a symmetry principle that isolates the fracton gauge sector alone would represent an outstanding direction for future research.

At this stage, a natural question arises: what about fractons living on a plane? The motivations for studying fracton phases of matter in three spacetime dimensions (3D) are numerous, and some of these are discussed in Section 4.5. Given the power of 3D Topological Quantum Field Theories [75] in describing topological orders in two spatial dimensions, one may ask whether there exists a higher-rank class of Chern–Simons or BF theories capable of capturing fractonic behavior. From a more physical perspective, one may also wonder whether dipolar analogues of the Quantum Hall Effect or of Topological Insulators can exist. Several theories describing the dipolar Quantum Hall effect and topological dipole insulators have already been proposed [76, 77, 78, 79, 80], but all within a non-covariant framework.

In Chapter 5, we presented two *covariant* formulations of higher-rank Chern–Simons and BF theories, which together constitute an important step toward the understanding and formal theoretical description of 3D gauge theories for dipolar Hall fluids.

In Section 5.1, based on [3], we studied the most general 3D action for a tensor gauge field $a_{\mu\nu}(x)$ with mass dimension 1, which takes the form of a traceless, non-topological, higher-rank generalisation of the ordinary Chern–Simons model. Upon coupling to matter, the theory exhibits fractonic behavior: a Hall-like dipole current emerges together with a vectorial “flux-attachment” relation for dipoles.

Subsequently, in Section 5.2, based on [4], we analysed a 3D field theory involving two tensor gauge fields with mass dimension 1: $a_{\mu\nu}(x)$, transforming under longitudinal diffeomorphisms, and $B_{\mu\nu}(x)$, with no symmetry imposed on its indices. The corresponding invariant action is a non-topological higher-rank BF-like model, constructed from a purely field-theoretical perspective using standard gauge-theory techniques. When matter is introduced, the theory exhibits subdimensional excitations, including both fractons and lineons. Moreover, our model can be mapped to the low-energy effective field theory of the Rank-2 Toric Code (R2TC) in two spatial dimensions [185], an exactly solvable quantum lattice model that generalises Kitaev’s Toric Code [45] to higher rank. The R2TC displays restricted mobility, unconventional braiding statistics, and can be obtained from the rank-2 $U(1)$ lattice gauge theory—whose excitations are subdimensional—via a Higgsing procedure [161] that reduces the continuous $U(1)$ gauge symmetry to \mathbb{Z}_N .

We also analysed the case in which $B_{\mu\nu}(x)$ is taken to be symmetric. In this situation, the action can be written as the sum of two rank-2 Chern–Simons terms [3], thus providing a higher-rank generalisation of the ordinary abelian BF theory [38, 148, 183],

which famously describes the low-energy physics of quantum spin Hall insulators in two spatial dimensions.

Topological Chern–Simons and BF models have a long history of important physical results when boundaries are introduced [43, 148, 199, 200, 201, 202, 203]. The higher-rank similarities shared by the BF-like models studied in this Thesis thus suggest promising perspectives for an analysis of boundary phenomena. In particular, the completely symmetric case (see Appendix G) generalizes the recently proposed bulk description of topological dipole insulators [80], where a non-covariant BF-like model is recovered from an effective edge theory via a coupled-wire construction [190]. A study of the corresponding boundary action of the covariant $S_{BF}^{(s)}$ (5.145) is therefore worthwhile. Moreover, it would be interesting to investigate boundary effects also for S_{BF} (5.77), where non-symmetric contributions might lead to non-trivial physics.

In the context of higher-rank lattice gauge theories of gapless fractons, it has been shown that in most cases, breaking the $U(1)$ gauge symmetry to \mathbb{Z}_n through a Higgs-like mechanism [161, 162] gives mass to the excitations but destroys fractonic behaviour. This motivated us to look for a 3D higher-rank gauge theory describing massive fractons. In Section 5.3, based on [5], we constructed a covariant and gauge-invariant theory for a fractonic gauge field $a_{\mu\nu}(x)$ with mass dimension $1/2$. The model includes a rank-2 Chern–Simons term [3] that plays a dual role: it generates a topological mass for the gauge field and simultaneously acts as a source of intrinsic fractonic matter. This dual mechanism is novel and leads to a propagating fractonic degree of freedom described by a massive Klein–Gordon equation. The theory propagates two degrees of freedom—one massive and one massless—whose number remains unchanged in the massless limit, in close analogy with the Maxwell–Chern–Simons mechanism of Deser–Jackiw–Templeton [168, 169]. Our model thus provides a unified framework for describing massive fractons with internal structure and offers a covariant setting for exploring their interactions and possible extensions.

Finally, another interesting follow-up of these works would be the formulation of a non-abelian gauge field theory for fractons.

To conclude, this Thesis explored two distinct exotic phases of matter, both of which admit a natural and powerful description in terms of quasiparticles. Although the methods employed—integrability and gauge theory techniques—are profoundly different, they share a common spirit: phases of matter provide a unifying bridge

between disparate areas of Theoretical Physics, allowing ideas to flow across fields that would otherwise remain disconnected.

Appendix A.

Proof of some equations

A.1 Proofs of (2.73)-(2.76)

$$\begin{aligned}\sigma_j^+ \sigma_{j+1}^- &= \prod_{l=1}^{j-1} (1 - 2\psi_l^\dagger \psi_l) \psi_j \prod_{m=1}^j (1 - 2\psi_m^\dagger \psi_m) \psi_{j+1}^\dagger = \psi_j \prod_{l=1}^{j-1} \sigma_l^z \prod_{m=1}^j \sigma_m^z \psi_{j+1}^\dagger = \\ &= \psi_j (1 - 2\psi_j^\dagger \psi_j) \psi_{j+1}^\dagger = \psi_{j+1}^\dagger \psi_j\end{aligned}\quad (\text{A.1})$$

$$\begin{aligned}\sigma_j^+ \sigma_{j+1}^+ &= \prod_{l=1}^{j-1} (1 - 2\psi_l^\dagger \psi_l) \psi_j \prod_{m=1}^j (1 - 2\psi_m^\dagger \psi_m) \psi_{j+1} = \psi_j \prod_{l=1}^{j-1} \sigma_l^z \prod_{m=1}^j \sigma_m^z \psi_{j+1} = \\ &= \psi_j (1 - 2\psi_j^\dagger \psi_j) \psi_{j+1} = \psi_{j+1} \psi_j\end{aligned}\quad (\text{A.2})$$

$$\sigma_N^+ \sigma_1^- = \prod_{l=1}^{N-1} (1 - 2\psi_l^\dagger \psi_l) \psi_N \psi_1^\dagger = \Pi^z (1 - 2\psi_N^\dagger \psi_N) \psi_N \psi_1^\dagger = -\Pi^z \psi_1^\dagger \psi_N \quad (\text{A.3})$$

$$\sigma_N^+ \sigma_1^+ = \prod_{l=1}^{N-1} (1 - 2\psi_l^\dagger \psi_l) \psi_N \psi_1 = \Pi^z (1 - 2\psi_N^\dagger \psi_N) \psi_N \psi_1 = -\Pi^z \psi_1 \psi_N. \quad (\text{A.4})$$

A.2 Proofs of (2.93)-(2.95)

$$\sum_{j=1}^N \psi_{j+1}^{(\pm)\dagger} \psi_j^{(\pm)} = \sum_{q,q' \in \Gamma^\pm} e^{-iq} \tilde{\psi}_q^\dagger \tilde{\psi}_{q'} \frac{1}{N} \sum_{j=1}^N e^{-i(q-q')j} = \sum_{q \in \Gamma^\pm} e^{-iq} \tilde{\psi}_q^\dagger \tilde{\psi}_q \quad (\text{A.5})$$

$$\sum_{j=1}^N \psi_j^{(\pm)\dagger} \psi_j^{(\pm)} = \sum_{q,q' \in \Gamma^\pm} \tilde{\psi}_q^\dagger \tilde{\psi}_{q'} \frac{1}{N} \sum_{j=1}^N e^{-i(q-q')j} = \sum_{q \in \Gamma^\pm} \tilde{\psi}_q^\dagger \tilde{\psi}_q \quad (\text{A.6})$$

$$\sum_{j=1}^N \psi_{j+1}^{(\pm)} \psi_j^{(\pm)} = i \sum_{q,q' \in \Gamma^\pm} e^{iq} \tilde{\psi}_q \tilde{\psi}_{q'} \frac{1}{N} \sum_{j=1}^N e^{i(q+q')j} = i \sum_{q \in \Gamma^\pm} e^{iq} \tilde{\psi}_q \tilde{\psi}_{2\pi-q} = i \sum_{q \in \Gamma^\pm} e^{iq} \tilde{\psi}_q \tilde{\psi}_{-q}. \quad (\text{A.7})$$

Appendix B.

Partition function of the XY chain

In this Appendix, we compute the partition function of the XY chain and derive the corresponding free energy, from which all thermodynamic quantities follow. Its explicit expression makes it clear that the model does not exhibit any thermal phase transitions.

The partition function for $h < 1$ is

$$\begin{aligned} Z &= \sum_i e^{-\beta E_i} = e^{-\beta E_0^+} + e^{-\beta E_1^+} + e^{-\beta E_2^+} + \dots + e^{-\beta E_0^-} + e^{-\beta E_1^-} + e^{-\beta E_2^-} + \dots \\ &= e^{-\beta E_0^+} \left[1 + e^{-\beta(E_1^+ - E_0^+)} + e^{-\beta(E_2^+ - E_0^+)} + \dots \right] + e^{-\beta E_0^-} \left[1 + e^{-\beta(E_1^- - E_0^-)} + e^{-\beta(E_2^- - E_0^-)} + \dots \right], \end{aligned} \quad (\text{B.1})$$

where the energy difference $(E_j^\pm - E_0^\pm)$ with $j \geq 1$ between the j -th excited state and the ground state of the corresponding parity sector is given by the sum of an even number of excitations (each of which contributes an amount $-J\epsilon(q)$). This observation allows us to write

$$\begin{aligned} Z &= \frac{1}{2} e^{-\beta E_0^+} \left[\prod_{q \in \Gamma^+} (1 + e^{\beta J \epsilon(q)}) + \prod_{q \in \Gamma^+} (1 - e^{\beta J \epsilon(q)}) \right] + \\ &+ \frac{1}{2} e^{-\beta E_0^-} \left[\prod_{q \in \Gamma^-} (1 + e^{\beta J \epsilon(q)}) + \prod_{q \in \Gamma^-} (1 - e^{\beta J \epsilon(q)}) \right]. \end{aligned} \quad (\text{B.2})$$

Here we observe that

$$\begin{aligned} \frac{1}{2}e^{-\beta E_0^\pm} \prod_{q \in \Gamma^\pm} \left(1 + e^{\beta J \epsilon(q)}\right) &= \frac{1}{2}e^{-\beta E_0^\pm} \prod_{q \in \Gamma^\pm} \cosh \left[\frac{\beta}{2} J \epsilon(q) \right] \prod_{q \in \Gamma^\pm} e^{\beta \frac{1}{2} \epsilon(q)} \cdot 2^N \\ &= 2^{N-1} \prod_{q \in \Gamma^\pm} \cosh \left[\frac{\beta}{2} J \epsilon(q) \right] \end{aligned} \quad (\text{B.3})$$

$$\frac{1}{2}e^{-\beta E_0^\pm} \prod_{q \in \Gamma^\pm} \left(1 - e^{\beta J \epsilon(q)}\right) = 2^{N-1} \prod_{q \in \Gamma^\pm} \sinh \left[\frac{\beta}{2} J \epsilon(q) \right], \quad (\text{B.4})$$

where the mathematical identities

$$\cosh x = \frac{1 + e^{-2x}}{2e^{-x}} \quad \sinh x = \frac{1 - e^{-2x}}{2e^{-x}} \quad (\text{B.5})$$

have been used. Thus we obtain

$$\begin{aligned} Z &= 2^{N-1} \left\{ \prod_{q \in \Gamma^+} \cosh \left[\frac{\beta}{2} J \epsilon(q) \right] + \prod_{q \in \Gamma^+} \sinh \left[\frac{\beta}{2} J \epsilon(q) \right] \right\} + \\ &+ 2^{N-1} \left\{ \prod_{q \in \Gamma^-} \cosh \left[\frac{\beta}{2} J \epsilon(q) \right] + \prod_{q \in \Gamma^-} \sinh \left[\frac{\beta}{2} J \epsilon(q) \right] \right\}, \end{aligned} \quad (\text{B.6})$$

which, in the large- N limit, becomes

$$Z = 2^N \prod_{q \in \Gamma^-} \cosh \left[\frac{\beta}{2} J \epsilon(q) \right] \left\{ 1 + \prod_{q \in \Gamma^-} \tanh \left[\frac{\beta}{2} J \epsilon(q) \right] \right\}. \quad (\text{B.7})$$

Now that we have the partition function, we can compute the free energy. However, since we are interested in the thermodynamic limit, we focus on the free energy per site

$$\begin{aligned} f \equiv -\frac{1}{\beta N} \log Z &= -\frac{1}{\beta} \log 2 - \frac{1}{\beta N} \log \prod_{q \in \Gamma^-} \cosh \left[\frac{\beta}{2} J \epsilon(q) \right] + \\ &- \frac{1}{\beta N} \log \left\{ 1 + \prod_{q \in \Gamma^-} \tanh \left[\frac{\beta}{2} J \epsilon(q) \right] \right\}, \end{aligned} \quad (\text{B.8})$$

where

$$\frac{1}{N} \log \prod_{q \in \Gamma^-} \cosh \left[\frac{\beta}{2} J \epsilon(q) \right] = \frac{1}{N} \sum_{q \in \Gamma^-} \log \cosh \left[\frac{\beta}{2} J \epsilon(q) \right] \xrightarrow{N \rightarrow \infty} \frac{1}{2\pi} \int_0^{2\pi} \log \cosh \left[\frac{\beta}{2} J \epsilon(q) \right] dq.$$

In conclusion, the free energy per site in the thermodynamic limit in the region $h < 1$ of the parameter space is given by

$$f = -\frac{1}{\beta} \log 2 - \frac{1}{\pi\beta} \int_0^\pi \log \cosh \left[\frac{\beta}{2} J \epsilon(q) \right] dq. \quad (\text{B.9})$$

We now turn to the region $h > 1$. Since, unlike E_0^+ (2.126), the ground state energy in the negative z -parity sector $|GS^-\rangle$ differs by $-J\epsilon(0)$ with respect to the region $h < 1$ (see Eq. (2.128)), the partition function will differ from the one just computed only through the second term in (B.1), given by

$$\begin{aligned} e^{-\beta E_0^-} \left[1 + e^{-\beta(E_1^- - E_0^-)} + \dots \right] &= e^{-\beta \frac{J}{2} \sum_{q \in \Gamma^-} \epsilon(q)} \left[1 + e^{-\beta(E_1^- - E_0^-)} + e^{-\beta(E_2^- - E_0^-)} + \dots \right] e^{\beta J \epsilon(0)} \\ &= \frac{1}{2} e^{-\beta \frac{J}{2} \sum_{q \in \Gamma^-} \epsilon(q)} \left[\prod_{q \in \Gamma^-} (1 + e^{\beta J \epsilon(q)}) - \prod_{q \in \Gamma^-} (1 - e^{\beta J \epsilon(q)}) \right] \\ &= 2^{N-1} \left\{ \prod_{q \in \Gamma^-} \cosh \left[\frac{\beta}{2} J \epsilon(q) \right] - \prod_{q \in \Gamma^-} \sinh \left[\frac{\beta}{2} J \epsilon(q) \right] \right\}, \end{aligned}$$

where we have followed the same procedure as in the $h < 1$ case. Therefore, the partition function of the XY chain for $h > 1$ is

$$\begin{aligned} Z &= 2^{N-1} \left\{ \prod_{q \in \Gamma^+} \cosh \left[\frac{\beta}{2} J \epsilon(q) \right] + \prod_{q \in \Gamma^+} \sinh \left[\frac{\beta}{2} J \epsilon(q) \right] \right\} + \\ &+ 2^{N-1} \left\{ \prod_{q \in \Gamma^-} \cosh \left[\frac{\beta}{2} J \epsilon(q) \right] - \prod_{q \in \Gamma^-} \sinh \left[\frac{\beta}{2} J \epsilon(q) \right] \right\}, \quad (\text{B.10}) \end{aligned}$$

which, in the large- N limit, reads

$$Z = 2^N \prod_{q \in \Gamma^-} \cosh \left[\frac{\beta}{2} J \epsilon(q) \right]. \quad (\text{B.11})$$

From this expression, one recovers the same expression for free energy per site in the region $h < 1$, given by (B.9). As a consequence, we can conclude that, at finite temperature, no phase transitions occur.

Appendix C.

Calculation of the two–spin correlators in the ferromagnetic XY chain

In this Appendix we review the calculations leading from (2.157) to the expressions for the asymptotic values of the correlators. The starting point is the evaluation of

$$\langle GS | \sigma_l^\alpha \sigma_m^\alpha | GS \rangle = \frac{1}{2} (\langle GS^+ | \sigma_l^\alpha \sigma_m^\alpha | GS^+ \rangle + \langle GS^- | \sigma_l^\alpha \sigma_m^\alpha | GS^- \rangle), \quad (\text{C.1})$$

where we have used the fact that the operator $\sigma_l^\alpha \sigma_m^\alpha$ preserves the z-parity, since it can be written as

$$\sigma_l^x \sigma_m^x = (\sigma_l^+ + \sigma_l^-)(\sigma_m^+ + \sigma_m^-), \quad (\text{C.2})$$

$$\sigma_l^y \sigma_m^y = -(\sigma_l^+ + \sigma_l^-)(\sigma_m^+ + \sigma_m^-), \quad (\text{C.3})$$

with the σ_j^\pm defined in (2.60).

Since one can show that

$$\langle GS | \sigma_l^\alpha \sigma_m^\alpha | GS \rangle = \langle GS^+ | \sigma_l^\alpha \sigma_m^\alpha | GS^+ \rangle, \quad (\text{C.4})$$

we now compute, for instance, the two-spin correlator along the x direction:

$$\rho_{lm}^x = \langle GS^+ | (\sigma_l^+ + \sigma_l^-)(\sigma_m^+ + \sigma_m^-) | GS^+ \rangle, \quad (\text{C.5})$$

where, without loss of generality, we assume $m > l$.

Recalling the Wigner–Jordan transformation (2.68), we obtain

$$\begin{aligned}
\rho_{lm}^x &= \langle GS^+ | (\psi_l + \psi_l^\dagger) \bigotimes_{i=1}^{l-1} \sigma_i^z \bigotimes_{j=1}^{m-1} \sigma_j^z (\psi_m + \psi_m^\dagger) | GS^+ \rangle \\
&= \langle GS^+ | (\psi_l + \psi_l^\dagger) \bigotimes_{j=l}^{m-1} \sigma_j^z (\psi_m + \psi_m^\dagger) | GS^+ \rangle \\
&= \langle GS^+ | (\psi_l + \psi_l^\dagger) (1 - 2\psi_l^\dagger \psi_l) \bigotimes_{j=l+1}^{m-1} (1 - 2\psi_j^\dagger \psi_j) (\psi_m + \psi_m^\dagger) | GS^+ \rangle \\
&= \langle GS^+ | (\psi_l^\dagger - \psi_l) \bigotimes_{j=l+1}^{m-1} (\psi_j^\dagger + \psi_j) (\psi_j^\dagger - \psi_j) (\psi_m + \psi_m^\dagger) | GS^+ \rangle. \tag{C.6}
\end{aligned}$$

We now define

$$A_j \equiv \psi_j^\dagger + \psi_j, \tag{C.7}$$

$$B_j \equiv i(\psi_j^\dagger - \psi_j). \tag{C.8}$$

It is straightforward to verify that

$$A_j^2 = B_j^2 = 1, \tag{C.9}$$

$$A_j^\dagger = A_j, \quad B_j^\dagger = B_j, \tag{C.10}$$

$$\{A_i, A_j\} = \{B_i, B_j\} = \{A_i, B_j\} = 2\delta_{ij}, \tag{C.11}$$

meaning that A_j and B_j are Majorana fermions. In terms of the operators just defined, the correlation function can be written as

$$\rho_{lm}^x = (-i)^{m-l} \langle GS^+ | B_l A_{l+1} B_{l+1} \dots A_{m-1} B_{m-1} A_m | GS^+ \rangle. \tag{C.12}$$

Following an entirely analogous procedure, one finds [49]:

$$\rho_{lm}^y = (-1)^{m-1} (-i)^{m-l} \langle GS^+ | A_l B_{l+1} A_{l+1} \dots B_{m-1} A_{m-1} B_m | GS^+ \rangle, \tag{C.13}$$

$$\rho_{lm}^z = -\langle GS^+ | A_l B_l A_m B_m | GS^+ \rangle. \tag{C.14}$$

At this stage, we would like to compute these expectation values using Wick’s theorem [107]. To do so, it is first necessary to evaluate the following correlators:

$$\langle GS^+ | A_l A_m | GS^+ \rangle \quad \langle GS^+ | B_l B_m | GS^+ \rangle \quad \langle GS^+ | A_l B_m | GS^+ \rangle. \quad (\text{C.15})$$

From the definitions of the operators A_j and B_j , it is clear that computing these correlators requires the two-point correlators of the Wigner–Jordan fermionic operators:

$$\langle GS^+ | \psi_l \psi_m | GS^+ \rangle \quad \langle GS^+ | \psi_l \psi_m^\dagger | GS^+ \rangle \quad \langle GS^+ | \psi_l^\dagger \psi_m | GS^+ \rangle, \quad (\text{C.16})$$

whose evaluation is simplified once the correlators

$$\langle GS^+ | \tilde{\psi}_q^{(+)} \tilde{\psi}_k^{(+)} | GS^+ \rangle \quad \langle GS^+ | \tilde{\psi}_q^{(+)} \tilde{\psi}_k^{(+)\dagger} | GS^+ \rangle \quad \langle GS^+ | \tilde{\psi}_q^{(+)\dagger} \tilde{\psi}_k^{(+)} | GS^+ \rangle, \quad (\text{C.17})$$

are known. These, in turn, are computed from the two-fermion χ correlators, given by

$$\langle GS^+ | \chi_q^{(+)} \chi_k^{(+)\dagger} | GS^+ \rangle = \delta_{k,q}, \quad \langle GS^+ | \chi_q^{(+)} \chi_k^{(+)} | GS^+ \rangle = \langle GS^+ | \chi_q^{(+)\dagger} \chi_k^{(+)} | GS^+ \rangle = 0. \quad (\text{C.18})$$

Recalling (2.103), one easily finds that

$$\begin{aligned} \langle GS^+ | \tilde{\psi}_q^{(+)\dagger} \tilde{\psi}_k^{(+)} | GS^+ \rangle &= \frac{1 - \cos(2\theta_q)}{2} \delta_{k,q}, & \langle GS^+ | \tilde{\psi}_q^{(+)} \tilde{\psi}_k^{(+)\dagger} | GS^+ \rangle &= \frac{1 + \cos(2\theta_q)}{2} \delta_{k,q}, \\ \langle GS^+ | \tilde{\psi}_q^{(+)} \tilde{\psi}_k^{(+)} | GS^+ \rangle &= -\frac{\sin(2\theta_q)}{2} \delta_{2\pi-k,q}, \end{aligned} \quad (\text{C.19})$$

for which the following identities, derived from (2.110), are useful:

$$\sin \theta_{2\pi-k} = -\sin \theta_k, \quad \cos \theta_{2\pi-k} = -\cos \theta_k. \quad (\text{C.20})$$

From the correlators just obtained, one can easily compute (using (2.86)) the two-fermion Wigner–Jordan correlators:

$$\langle GS^+ | \psi_j \psi_l | GS^+ \rangle = -\langle GS^+ | \psi_j^\dagger \psi_l^\dagger | GS^+ \rangle = -\frac{i}{N} \sum_{q \in \Gamma^+} e^{iq(j-l)} \frac{\sin(2\theta_q)}{2}, \quad (\text{C.21})$$

$$\langle GS^+ | \psi_j \psi_l^\dagger | GS^+ \rangle = -\langle GS^+ | \psi_j^\dagger \psi_l | GS^+ \rangle = \frac{1}{N} \sum_{q \in \Gamma^+} e^{iq(j-l)} \frac{1 + \cos(2\theta_q)}{2}. \quad (\text{C.22})$$

Here, to show the first equality in both lines, it is useful to employ (C.20) together with the fact that $\Gamma^+ = 2\pi - \Gamma^+$. From the correlators just computed, it follows that

$$\langle GS^+ | A_l A_m | GS^+ \rangle = \langle GS^+ | B_l B_m | GS^+ \rangle = 0. \quad (\text{C.23})$$

The only remaining correlator to evaluate is

$$\begin{aligned} \langle GS^+ | A_m B_l | GS^+ \rangle &= i \langle GS^+ | (\psi_m^\dagger + \psi_m)(\psi_l^\dagger - \psi_l) | GS^+ \rangle \\ &= 2i (\langle GS^+ | \psi_m^\dagger \psi_l^\dagger | GS^+ \rangle + \langle GS^+ | \psi_m \psi_l | GS^+ \rangle) \\ &= -\frac{1}{N} \sum_{q \in \Gamma^+} e^{iq(m-l)} \sin(2\theta_q) + \underbrace{\frac{i}{N} \sum_{q \in \Gamma^+} e^{iq(m-l)} + \frac{i}{N} \sum_{q \in \Gamma^+} e^{iq(m-l)} \cos(2\theta_q)}_0 \\ &= \frac{i}{N} \sum_{q \in \Gamma^+} e^{iq(m-l)} e^{i2\theta_q}. \end{aligned} \quad (\text{C.24})$$

We will denote

$$G(m-l) \equiv -i \langle GS^+ | A_m B_l | GS^+ \rangle. \quad (\text{C.25})$$

We can now finally compute ρ_{lm}^α by making use of Wick's theorem. Let us start from the simplest correlation function, namely

$$\begin{aligned} \rho_{lm}^z &= - \langle GS^+ | A_l B_l A_m B_m | GS^+ \rangle \\ &= - \langle GS^+ | A_l B_l | GS^+ \rangle \langle GS^+ | A_m B_m | GS^+ \rangle + \langle GS^+ | A_l B_m | GS^+ \rangle \langle GS^+ | A_m B_l | GS^+ \rangle \\ &= G^2(0) - G(l-m)G(m-l). \end{aligned} \quad (\text{C.26})$$

Proceeding analogously, it is straightforward to verify that

$$\rho_{lm}^x = (-1)^n \det \begin{pmatrix} G(1) & G(0) & G(-1) & \dots & G(2-n) \\ G(2) & G(1) & G(0) & \dots & G(3-n) \\ G(3) & G(2) & G(1) & \dots & G(4-n) \\ \vdots & \vdots & \vdots & \ddots & \vdots \\ G(n) & G(n-1) & G(n-2) & \dots & G(1) \end{pmatrix} \quad (\text{C.27})$$

$$\rho_{lm}^y = (-1)^{m-1} \det \begin{pmatrix} G(-1) & G(0) & G(1) & \dots & G(n-2) \\ G(-2) & G(-1) & G(0) & \dots & G(n-3) \\ \vdots & \vdots & \vdots & \ddots & \vdots \\ G(-n) & G(1-n) & G(2-n) & \dots & G(-1) \end{pmatrix} \quad (\text{C.28})$$

where $n \equiv m - l$. We have therefore found that the two-spin correlation functions along the x and y directions are given by the determinant of $n \times n$ Toeplitz matrices, namely matrices whose entries are constant along each descending diagonal from left to right. Because of their appearance in the Ising and XY chains, as well as their rich mathematical structure, Toeplitz matrices have attracted the interest of many mathematicians and mathematical physicists, whose efforts have led to an impressive understanding of their properties. In particular, a vast mathematical literature has been devoted to the study of the asymptotic behaviour of their determinants, known as Toeplitz Determinants (for details, see Appendix A of [49]).

Appendix D.

Level quantization of rank-2 Chern-Simons theory

Following a procedure similar to the one adopted in [77, 79], the same approach of ordinary Chern-Simons theory [34, 40] can be followed to show that the generalized Chern-Simons action for fractons is not invariant under large gauge transformations, but it changes by

$$\delta S_{\text{CS}} = 8\pi^2 k, \quad (\text{D.1})$$

where k is the coupling constant of the generalized Chern-Simons action (which we reabsorbed by a redefinition of the field $a_{\mu\nu}(x)$). In order for the partition function

$$Z[a_{\mu\nu}] = e^{iS_{\text{CS}}[a_{\mu\nu}]} \quad (\text{D.2})$$

to be invariant, it must be

$$k = \frac{n}{4\pi}, \quad n \in \mathbb{Z}, \quad (\text{D.3})$$

which is the quantized level for dipolar Chern-Simons theory.

D.1 Flux quantization

The magnetic flux quantization is a crucial point. Indeed, on the solution (5.16) of the EoM of $a_{00}(x)$ (5.11), we have that the magnetic field $B^a(x)$ (5.25) writes as a curl :

$$\mathcal{B}^i = \epsilon^{0mn} \partial_m \left[a_n^i - \delta_n^i (a_0^0 + \partial_0 \psi) \right] . \quad (\text{D.4})$$

Notice that one could for instance make the gauge-fixing choice $a_0^0 = -\partial_0 \psi$, which extends (5.16) to the covariant form

$$a_{\mu 0} = \partial_\mu \psi , \quad (\text{D.5})$$

such that the magnetic field $\mathcal{B}^i(x)$ (D.4) simplifies to

$$\mathcal{B}^i = \epsilon^{0mn} \partial_m a_n^i , \quad (\text{D.6})$$

however that is not necessary. Therefore one can use Stokes' theorem for the flux on a surface Σ whose boundary is a closed curve γ

$$\int_\Sigma d^2x \mathcal{B}^j = \int_\gamma dx^i \left[a_i^j - \delta_i^j (a_0^0 + \partial_0 \psi) \right] . \quad (\text{D.7})$$

The minimum is reached when the integral is done on $\Sigma = S^2$, as done in [77, 79] or [40] for standard CS, for which the integral over the boundary γ only contributes as a 2π phase. Thus

$$\int_\Sigma d^2x \mathcal{B}^j = 2\pi \hat{x}^j , \quad (\text{D.8})$$

where \hat{x}^j is the unit vector of the direction of the dipole through (5.48). Notice that this reasoning works if we are considering surfaces with genus zero, and in the continuum, which is our case. However for manifolds of different genus or on the lattice (and their continuum limits) the curve γ is not necessarily contractible to give a phase contribution. In these cases singular or discontinuous field configurations must be taken into account, as done for instance in [78, 150, 152, 204].

D.2 Shift of the action and the large gauge transformation

In order to discuss the level quantization as done in [40, 77, 79] the flux of the magnetic field must be taken into account, whose quantization condition, as discussed above, is (D.8). The definition of the fractonic electric and magnetic fields (5.24) and (5.25), and the whole electromagnetic interpretation of Section 5.2.2 emerges on the solution of the EoM of $a_{00}(x)$ (5.14). This solution in terms of the field strength $\tilde{F}_{\mu\nu\rho}(x)$ (5.8) can be used interchangeably with the one in terms of the gauge field (5.16). Notice that this coincides with the construction done in [60, 77, 149], where the scalar field is introduced from the beginning, while here we motivate it from a covariant construction as a solution of an EoM. On the invariant action S_{CS} (5.1) this implies

$$S_{\text{CS}}|_{a_{0m}=\partial_m\psi} = \int d^3x \epsilon^{\mu\nu\rho} a_\mu^\lambda \partial_\nu a_{\rho\lambda} = \int d^3x \epsilon^{0mn} \left(2\partial^l \psi \partial_m a_{nl} - a_{ml} \partial_0 a_n^l \right). \quad (\text{D.9})$$

We can thus consider the thermal partition function in the euclidean periodic time $\tau \sim \tau + \beta$, where β is the inverse of the temperature, and define the large gauge transformation defined by the following finite gauge parameter

$$\phi'(\tau, \vec{x}) \equiv \frac{2\pi}{\beta} \tau \hat{x}_i x^i, \quad (\text{D.10})$$

such that under the fracton symmetry (4.60) the tensor field $a_{\mu\nu}(x)$ and its generalized field strength $F_{\mu\nu\rho}(x)$ transforms as

$$a_{00} \rightarrow a_{00} \quad ; \quad a_{0m} \rightarrow a_{0m} + \frac{2\pi}{\beta} \hat{r}_m \quad ; \quad a_{mn} \rightarrow a_{mn} \quad ; \quad F_{\mu\nu\rho} \rightarrow F_{\mu\nu\rho}. \quad (\text{D.11})$$

Notice that (D.10) is not single valued on the periodic time, *i.e.* $\phi'(\tau) \neq \phi'(\tau + \beta)$, however this does not reflect on the transformed fields (D.11), as happens in the standard case of CS theory [40]. Notice also that the transformation (D.10) is the of the same kind as the one considered in [77], and can be reconduced to the one in [79] by taking its gradient $-\partial^a \phi'$. Keeping in mind the definition of the magnetic field (5.25) and the definition of the traceless field strength $\tilde{F}_{\mu\nu\rho}(x)$ (5.8), we can rewrite the

invariant action (5.1), expliciting the coupling constant k , as follows :

$$\begin{aligned}
S_{\text{CS}} &= \frac{k}{3} \int d^3x \epsilon^{\mu\nu\rho} a_\mu^\lambda \tilde{F}_{\lambda\nu\rho} \\
&= \frac{k}{3} \int d^3x \epsilon^{0mn} \left(a_0^0 \tilde{F}_{0mn} + a_0^l \tilde{F}_{lmn} - a_n^0 \tilde{F}_{00n} - a_m^l \tilde{F}_{l0n} + a_m^0 \tilde{F}_{0n0} + a_m^l \tilde{F}_{ln0} \right) \\
&= \frac{k}{3} \int d^3x \left\{ \epsilon^{0mn} \left[a_0^0 \tilde{F}_{0mn} - a_m^l (\tilde{F}_{0ln} - \tilde{F}_{ln0}) \right] + 3a_{0l} \mathcal{B}^l \right\} \\
&= k \int d^3x \left[\epsilon^{0mn} \left(a_m^l \partial_0 a_{nl} + a_{0m} \partial_0 a_{0n} \right) + 2a_{0l} \mathcal{B}^l \right] \\
&= k \int d^3x \left(\epsilon^{0mn} a_m^l \partial_0 a_{nl} + 2a_{0l} \mathcal{B}^l \right) .
\end{aligned} \tag{D.12}$$

where we used the tracelessness and ciclicity properties of $\tilde{F}_{\mu\nu\rho}(x)$ (5.9), (4.81), the definition of $\mathcal{B}^l(x)$ (5.25) and, in the last line, the solution (5.16). Under the large gauge transformation (D.11) we have that the action transforms as

$$S_{\text{CS}} \rightarrow S_{\text{CS}} + 2k \int d^3x \frac{2\pi}{\beta} \hat{x}_l \mathcal{B}^l , \tag{D.13}$$

which, evaluated on the sphere S^2 using the quantization condition (D.8), finally yields

$$S_{\text{CS}} \rightarrow S_{\text{CS}} + 8\pi^2 k , \tag{D.14}$$

which implies that k must be quantized as

$$8\pi^2 k = 2\pi n \quad \Rightarrow \quad k = \frac{1}{4\pi} n , \quad n \in \mathbb{Z} , \tag{D.15}$$

which is analogous to what happens in ordinary 3D CS theory [37] with the remarkable difference that the theory we are considering here is not topological.

D.3 An example on the torus

We have seen that the invariant action $S_{\text{CS}}|_{a_{0m}=\partial_m\psi}$ can be written in two ways, either as

$$S_{\text{CS}}|_{a_{0m}=\partial_m\psi} = k \int d^3x \epsilon^{0mn} \left(2\partial^l \psi \partial_m a_{nl} - a_{ml} \partial_0 a_n^l \right) , \tag{D.16}$$

from (D.9), or

$$S_{\text{CS}}|_{a_{0m}=\partial_m\psi} = k \int d^3x \left(-\epsilon^{0mn} a_m^l \partial_0 a_{nl} + 2\partial_l \psi \mathcal{B}^l \right), \quad (\text{D.17})$$

from (D.12). On the large gauge transformation (D.11) the ∂_0 contribution has no role in changing the action, so that we can equivalently use

$$2k \int d^3x \partial^l \psi \epsilon^{0mn} \partial_m a_{nl} \quad \text{or} \quad 2k \int d^3x \partial_l \psi \mathcal{B}^l. \quad (\text{D.18})$$

Therefore the flux of the magnetic field is equivalent to the flux of the curl of the gauge field, as in standard electromagnetism. As a consequence of the magnetic-dipole relation (5.48) and the symmetry of the gauge field, we have that

$$a_{ij} = H \hat{x}_i \hat{x}_j. \quad (\text{D.19})$$

We can for instance consider a dipole oriented along the x_1 -axis, *i.e.* $\hat{x}_1 = 1$, $\hat{x}_2 = 0$, which implies that

$$a_{11} = H \quad ; \quad a_{12} = a_{21} = a_{22} = 0, \quad (\text{D.20})$$

as a consequence of (D.19). We want to consider an example of quantization on a surface of nonzero genus, such as the torus T^2 with periodicity $x_1 \sim x_1 + l_1$ and $x_2 \sim x_2 + l_2$, as done in [150, 152]. The only nontrivial component of the magnetic field is $\mathcal{B}^1(x)$, for which we have that the flux on the torus is

$$\int_{T^2} d^2x \mathcal{B}_1 = \int_{T^2} d^2x \partial_2 a_{11} \quad (\text{D.21})$$

as a consequence of the equivalence (D.18). We shall see that the magnetic field is quantized if we consider, for instance, the following transition function

$$g(x_1) = \pi \left[(x_1 - x_1^*) \theta(x_1 - x_1^*) - \frac{x_1}{l_1} (x_1 - x_1^*) + \frac{3}{2} \frac{(x_1)^2}{l_1} \right], \quad (\text{D.22})$$

which is similar to those used in [150, 152]. We thus have

$$a_{11}(x_1, l_2) - a_{11}(x_1, 0) = \partial_1 \partial_1 g, \quad (\text{D.23})$$

i.e. a_{11} is non-periodic only around the x_2 -coordinate. For instance

$$a_{11} = \pi \frac{x_2}{l_2} \left[\delta(x_1 - x_1^*) + \frac{1}{l_1} \right]. \quad (\text{D.24})$$

Therefore from (D.21) we get

$$\begin{aligned} \int_{T^2} d^2x \mathcal{B}_1 &= \int_{T^2} d^2x \partial_2 a_{11} \\ &= \int_0^{l_1} dx_1 \int_0^{l_2} dx_2 \left\{ \pi \frac{1}{l_2} \left[\delta(x_1 - x_1^*) + \frac{1}{l_1} \right] \right\} \\ &= \pi \int_0^{l_1} dx_1 \left[\delta(x_1 - x_1^*) + \frac{1}{l_1} \right] \\ &= 2\pi. \end{aligned} \quad (\text{D.25})$$

Therefore in this configuration (D.24), from (D.25) and taking the large gauge transformation (D.11), the action changes as follows

$$S_{\text{CS}} \rightarrow S_{\text{CS}} + 2k \int_0^\beta d\tau \frac{2\pi}{\beta} \int_{T^2} d^2x B^1 = S_{\text{CS}} + 8\pi^2 k \quad (\text{D.26})$$

which give the same quantization condition as (D.15).

Appendix E.

Propagators

E.1 Rank-2 Chern-Simons theory

In momentum space the invariant action S_{CS} (5.1) and the gauge fixing term S_{gf} (5.54) read

$$S_{CS} = \int d^3p \hat{a}_{\mu\nu}(p) \left[\frac{i}{4} \left(\epsilon^{\mu\lambda\alpha} \eta^{\nu\beta} + \epsilon^{\nu\lambda\alpha} \eta^{\mu\beta} + \epsilon^{\mu\lambda\beta} \eta^{\nu\alpha} + \epsilon^{\nu\lambda\beta} \eta^{\mu\alpha} \right) p_\lambda \right] \hat{a}_{\alpha\beta}(-p) \quad (\text{E.1})$$

$$S_{gf} = -\frac{1}{2\xi} \int d^3p \hat{a}_{\mu\nu}(p) \left(p^\mu p^\nu p^\alpha p^\beta + \kappa p^\mu p^\nu p^2 \eta^{\alpha\beta} + \kappa p^\alpha p^\beta p^2 \eta^{\mu\nu} + \kappa^2 \eta^{\mu\nu} \eta^{\alpha\beta} p^4 \right) \hat{a}_{\alpha\beta}(-p), \quad (\text{E.2})$$

where $p^4 \equiv (p^2)^2 = (p^\mu p_\mu)^2$. The momentum space gauge fixed action S_{tot} (5.55) is

$$S = -\frac{1}{4} \int d^3p \hat{a}_{\mu\nu}(p) \hat{G}^{\mu\nu,\alpha\beta}(p) \hat{a}_{\alpha\beta}(-p), \quad (\text{E.3})$$

where the tensor $\hat{G}^{\mu\nu,\alpha\beta}(p)$, defined by the sum of (E.1) and (E.2), has the following symmetries

$$\hat{G}^{\mu\nu,\alpha\beta}(p) = \hat{G}^{\nu\mu,\alpha\beta}(p) = \hat{G}^{\mu\nu,\beta\alpha}(p) = \hat{G}^{\alpha\beta,\mu\nu}(-p), \quad (\text{E.4})$$

and can be expanded on the following basis of tensors (displaying these same symmetries):

$$A_{\alpha\beta,\rho\sigma}^{(0)} = \frac{1}{2}(\eta_{\alpha\rho}\eta_{\beta\sigma} + \eta_{\alpha\sigma}\eta_{\beta\rho}) \quad (\text{E.5})$$

$$A_{\alpha\beta,\rho\sigma}^{(1)} = \eta_{\alpha\rho}p_\beta p_\sigma + \eta_{\alpha\sigma}p_\beta p_\rho + \eta_{\beta\rho}p_\alpha p_\sigma + \eta_{\beta\sigma}p_\alpha p_\rho \quad (\text{E.6})$$

$$A_{\alpha\beta,\rho\sigma}^{(2)} = \eta_{\alpha\beta}p_\rho p_\sigma + \eta_{\rho\sigma}p_\alpha p_\beta \quad (\text{E.7})$$

$$A_{\alpha\beta,\rho\sigma}^{(3)} = \eta_{\alpha\beta}\eta_{\rho\sigma} \quad (\text{E.8})$$

$$A_{\alpha\beta,\rho\sigma}^{(4)} = p_\alpha p_\beta p_\rho p_\sigma \quad (\text{E.9})$$

$$A_{\alpha\beta,\rho\sigma}^{(5)} = ip^\lambda(\epsilon_{\alpha\lambda\rho}\eta_{\sigma\beta} + \epsilon_{\beta\lambda\rho}\eta_{\sigma\alpha} + \epsilon_{\alpha\lambda\sigma}\eta_{\rho\beta} + \epsilon_{\beta\lambda\sigma}\eta_{\rho\alpha}) \quad (\text{E.10})$$

$$A_{\alpha\beta,\rho\sigma}^{(6)} = ip^\lambda(\epsilon_{\alpha\lambda\rho}p_\sigma p_\beta + \epsilon_{\alpha\lambda\sigma}p_\rho p_\beta + \epsilon_{\beta\lambda\rho}p_\sigma p_\alpha + \epsilon_{\beta\lambda\sigma}p_\rho p_\alpha) \quad (\text{E.11})$$

as follows

$$\hat{G}^{\mu\nu,\alpha\beta}(p) = \left[-A^{(5)} + \frac{2}{\xi} \left(\kappa p^2 A^{(2)} + \kappa^2 p^4 A^{(3)} + A^{(4)} \right) \right]^{\mu\nu,\alpha\beta}. \quad (\text{E.12})$$

The momentum space propagator in a generic ξ -gauge

$$\hat{\Delta}_{\alpha\beta,\rho\sigma}^{(\xi)}(p) \equiv \langle \hat{a}_{\alpha\beta}(p) \hat{a}_{\rho\sigma}(-p) \rangle^{(\xi)} \quad (\text{E.13})$$

is defined as

$$\hat{G}\hat{\Delta}^{(\xi)} = \mathcal{A}^{(0)}. \quad (\text{E.14})$$

In the basis $\{A^{(i)}\}$ the propagator $\hat{\Delta}^{(\xi)}$ reads

$$\hat{\Delta}^{(\xi)} = \sum_{i=0}^6 c_i A^{(i)}, \quad (\text{E.15})$$

where the p -dependent coefficients $c_i(p)$ are determined by (E.157). In order to solve the equation (E.157) the following tensorial relations are useful [200, 203]

$$A^{(0)}A^{(0)} = \mathcal{A}^{(0)} \quad (\text{E.16})$$

$$A^{(0)}A^{(1)} = \mathcal{A}^{(1)} \quad (\text{E.17})$$

$$A^{(0)}A^{(2)} = \mathcal{A}^{(2)} + \mathcal{B}^{(2)} \quad (\text{E.18})$$

$$A^{(0)}A^{(3)} = \mathcal{A}^{(3)} \quad (\text{E.19})$$

$$A^{(0)}A^{(4)} = \mathcal{A}^{(4)} \quad (\text{E.20})$$

$$A^{(0)}A^{(5)} = \mathcal{A}^{(5)} \quad (\text{E.21})$$

$$A^{(0)}A^{(6)} = \mathcal{A}^{(6)} \quad (\text{E.22})$$

$$A^{(1)}A^{(0)} = \mathcal{A}^{(1)} \quad (\text{E.23})$$

$$A^{(1)}A^{(1)} = 2p^2\mathcal{A}^{(1)} + 8\mathcal{A}^{(4)} \quad (\text{E.24})$$

$$A^{(1)}A^{(2)} = 4\mathcal{A}^{(4)} + 4p^2\mathcal{B}^{(2)} \quad (\text{E.25})$$

$$A^{(1)}A^{(3)} = 4\mathcal{B}^{(2)} \quad (\text{E.26})$$

$$A^{(1)}A^{(4)} = 4p^2\mathcal{A}^{(4)} \quad (\text{E.27})$$

$$A^{(1)}A^{(5)} = 2\mathcal{A}^{(6)} \quad (\text{E.28})$$

$$A^{(1)}A^{(6)} = 2p^2\mathcal{A}^{(6)} \quad (\text{E.29})$$

$$A^{(2)}A^{(0)} = \mathcal{A}^{(2)} + \mathcal{B}^{(2)} \quad (\text{E.30})$$

$$A^{(2)}A^{(1)} = 4p^2\mathcal{A}^{(2)} + 4\mathcal{A}^{(4)} \quad (\text{E.31})$$

$$A^{(2)}A^{(2)} = p^2(\mathcal{A}^{(2)} + \mathcal{B}^{(2)} + p^2\mathcal{A}^{(3)}) + 3\mathcal{A}^{(4)} \quad (\text{E.32})$$

$$A^{(2)}A^{(3)} = 3\mathcal{B}^{(2)} + p^2\mathcal{A}^{(3)} \quad (\text{E.33})$$

$$A^{(2)}A^{(4)} = p^4\mathcal{A}^{(2)} + p^2\mathcal{A}^{(4)} \quad (\text{E.34})$$

$$A^{(2)}A^{(5)} = A^{(2)}A^{(6)} = 0 \quad (\text{E.35})$$

$$A^{(3)}A^{(0)} = \mathcal{A}^{(3)} \quad (\text{E.36})$$

$$A^{(3)}A^{(1)} = 4\mathcal{A}^{(2)} \quad (\text{E.37})$$

$$A^{(3)}A^{(2)} = 3\mathcal{A}^{(2)} + p^2\mathcal{A}^{(3)} \quad (\text{E.38})$$

$$A^{(3)}A^{(3)} = 3\mathcal{A}^{(3)} \quad (\text{E.39})$$

$$A^{(3)}A^{(4)} = p^2\mathcal{A}^{(2)} \quad (\text{E.40})$$

$$A^{(3)}A^{(5)} = A^{(3)}A^{(6)} = 0 \quad (\text{E.41})$$

$$A^{(4)}A^{(0)} = \mathcal{A}^{(4)} \quad (\text{E.42})$$

$$A^{(4)}A^{(1)} = 4p^2\mathcal{A}^{(4)} \quad (\text{E.43})$$

$$A^{(4)}A^{(2)} = p^4\mathcal{B}^{(2)} + p^2\mathcal{A}^{(4)} \quad (\text{E.44})$$

$$A^{(4)}A^{(3)} = p^2\mathcal{B}^{(2)} \quad (\text{E.45})$$

$$A^{(4)}A^{(4)} = p^4\mathcal{A}^{(4)} \quad (\text{E.46})$$

$$A^{(4)}A^{(5)} = A^{(4)}A^{(6)} = 0 \quad (\text{E.47})$$

$$A^{(5)}A^{(0)} = \mathcal{A}^{(5)} \quad (\text{E.48})$$

$$A^{(5)}A^{(1)} = 2\mathcal{A}^{(6)} \quad (\text{E.49})$$

$$A^{(5)}A^{(2)} = A^{(5)}A^{(3)} = A^{(5)}A^{(4)} = 0 \quad (\text{E.50})$$

$$A^{(5)}A^{(5)} = -16p^2\mathcal{A}^{(0)} + 6\mathcal{A}^{(1)} - 8\mathcal{A}^{(2)} - 8\mathcal{B}^{(2)} + 8p^2\mathcal{A}^{(3)} \quad (\text{E.51})$$

$$A^{(5)}A^{(6)} = 8\mathcal{A}^{(4)} - 2p^2\mathcal{A}^{(1)} \quad (\text{E.52})$$

$$A^{(6)}A^{(0)} = \mathcal{A}^{(6)} \quad (\text{E.53})$$

$$A^{(6)}A^{(1)} = 2p^2\mathcal{A}^{(6)} \quad (\text{E.54})$$

$$A^{(6)}A^{(2)} = A^{(6)}A^{(3)} = A^{(6)}A^{(4)} = 0 \quad (\text{E.55})$$

$$A^{(6)}A^{(5)} = -2p^2\mathcal{A}^{(1)} + 8\mathcal{A}^{(4)} \quad (\text{E.56})$$

$$A^{(6)}A^{(6)} = 8p^2\mathcal{A}^{(4)} - 2p^4\mathcal{A}^{(1)}, \quad (\text{E.57})$$

where the contraction of indices, which has been omitted, is as follows

$$(XY = Z) \equiv (X^{\mu\nu,\alpha\beta} Y_{\alpha\beta,\rho\sigma} = Z_{\rho\sigma}^{\mu\nu}), \quad (\text{E.58})$$

and the operators appearing at the right hand side of (E.16)-(E.57) form a basis on the space of the tensors

$$Z_{\rho\sigma}^{\mu\nu} = Z_{\rho\sigma}^{\nu\mu} = Z_{\sigma\rho}^{\mu\nu}, \quad (\text{E.59})$$

which is larger than the one concerning the more symmetric tensors (E.4):

$$\mathcal{A}_{\rho\sigma}^{(0)\mu\nu} = \frac{1}{2}(\delta_{\rho}^{\mu}\delta_{\sigma}^{\nu} + \delta_{\sigma}^{\mu}\delta_{\rho}^{\nu}) \quad (\text{E.60})$$

$$\mathcal{A}_{\rho\sigma}^{(1)\mu\nu} = \delta_{\rho}^{\mu}p^{\nu}p_{\sigma} + \delta_{\sigma}^{\mu}p^{\nu}p_{\rho} + \delta_{\rho}^{\nu}p^{\mu}p_{\sigma} + \delta_{\sigma}^{\nu}p^{\mu}p_{\rho} \quad (\text{E.61})$$

$$\mathcal{A}_{\rho\sigma}^{(2)\mu\nu} = \eta^{\mu\nu}p_{\rho}p_{\sigma} \quad (\text{E.62})$$

$$\mathcal{B}_{\rho\sigma}^{(2)\mu\nu} = \eta_{\rho\sigma}p^{\mu}p^{\nu} \quad (\text{E.63})$$

$$\mathcal{A}_{\rho\sigma}^{(3)\mu\nu} = \eta^{\mu\nu}\eta_{\rho\sigma} \quad (\text{E.64})$$

$$\mathcal{A}_{\rho\sigma}^{(4)\mu\nu} = p^{\mu}p^{\nu}p_{\rho}p_{\sigma} \quad (\text{E.65})$$

$$\mathcal{A}_{\rho\sigma}^{(5)\mu\nu} = ip^{\lambda}(\epsilon_{\alpha\lambda\rho}\eta^{\mu\alpha}\delta_{\sigma}^{\nu} + \epsilon_{\alpha\lambda\sigma}\eta^{\mu\alpha}\delta_{\rho}^{\nu} + \epsilon_{\alpha\lambda\rho}\eta^{\nu\alpha}\delta_{\sigma}^{\mu} + \epsilon_{\alpha\lambda\sigma}\eta^{\nu\alpha}\delta_{\rho}^{\mu}) \quad (\text{E.66})$$

$$\mathcal{A}_{\rho\sigma}^{(6)\mu\nu} = ip^{\lambda}(\eta^{\mu\alpha}\epsilon_{\alpha\lambda\rho}p_{\sigma}p^{\nu} + \eta^{\mu\alpha}\epsilon_{\alpha\lambda\sigma}p_{\rho}p^{\nu} + \eta^{\nu\alpha}\epsilon_{\alpha\lambda\rho}p_{\sigma}p^{\mu} + \eta^{\nu\alpha}\epsilon_{\alpha\lambda\sigma}p_{\rho}p^{\mu}) \quad (\text{E.67})$$

The usual long but straightforward calculations lead then to

$$\begin{aligned} \hat{G}\hat{\Delta}^{(\xi)} &= 16c_5p^2\mathcal{A}^{(0)} + (-6c_5 + 2p^2c_6)\mathcal{A}^{(1)} \\ &+ \left\{ \frac{2\kappa p^4}{\xi} \left[\frac{c_0}{p^2} + 4(\kappa + 1)p^2c_1 + (3\kappa + 1)c_2 + (\kappa + 1)p^2c_4 \right] + 8c_5 \right\} \mathcal{A}^{(2)} \\ &+ \left\{ \frac{2p^2}{\xi} \left[\kappa c_0 + (\kappa + 1)p^2c_2 + (3\kappa + 1)c_3 \right] + 8c_5 \right\} \mathcal{B}^{(2)} \\ &+ \left\{ \frac{2\kappa p^2}{\xi} \left[\kappa c_0 + (\kappa + 1)p^2c_2 + (3\kappa + 1)c_3 \right] - 8c_5 \right\} p^2\mathcal{A}^{(3)} \\ &+ \left\{ \frac{2p^2}{\xi} \left[\frac{c_0}{p^2} + 4(\kappa + 1)c_1 + (3\kappa + 1)c_2 + (\kappa + 1)p^2c_4 \right] - 8c_6 \right\} \mathcal{A}^{(4)} - c_0\mathcal{A}^{(5)} - 2c_1\mathcal{A}^{(6)} \\ &= \mathcal{A}^{(0)}. \end{aligned} \quad (\text{E.68})$$

The solution of the above equation gives the coefficients $c_i(p)$ appearing in the propagator expansion (E.15)

$$\xi = c_0 = c_1 = 0 ; c_2 = \text{free} ; c_3 = -c_2 \frac{1 + \kappa}{1 + 3\kappa} p^2 ; c_4 = -c_2 \frac{1 + 3\kappa}{(1 + \kappa)p^2} ; c_5 = \frac{1}{16p^2} ; c_6 = \frac{3}{16p^4} . \quad (\text{E.69})$$

The propagator displays poles at $\kappa = \{-1, -\frac{1}{3}\}$, and κ is coupled to the trace $a(x)$ in the gauge fixing term (5.54), on which, on the other hand, the invariant action S_{inv} (5.1) does not depend. We notice that $c_2(p)$ is a free parameter, which means that it does not have a role in inverting the matrix (E.12), hence we can set it to zero. This also makes the singular coefficients vanish. Additionally, as one might hope and expect, the Landau gauge is a mandatory choice. Indeed, due to the fact that the gauge parameter is massive ($[\xi] = 3$), its presence would lead to infrared divergences in the correlation functions. Therefore, the only surviving coefficients are $c_5(p)$ and $c_6(p)$, and the propagator is

$$\begin{aligned} \langle \hat{a}_{\alpha\beta}(p) \hat{a}_{\rho\sigma}(-p) \rangle &= \hat{\Delta}_{\alpha\beta,\rho\sigma}(p) = \\ &= \frac{ip^\lambda}{16p^2} \left[\epsilon_{\alpha\lambda\rho} \left(\eta_{\beta\sigma} + 3 \frac{p_\beta p_\sigma}{p^2} \right) + \epsilon_{\alpha\lambda\sigma} \left(\eta_{\beta\rho} + 3 \frac{p_\beta p_\rho}{p^2} \right) + \epsilon_{\beta\lambda\rho} \left(\eta_{\alpha\sigma} + 3 \frac{p_\alpha p_\sigma}{p^2} \right) + \epsilon_{\beta\lambda\sigma} \left(\eta_{\alpha\rho} + 3 \frac{p_\alpha p_\rho}{p^2} \right) \right] . \end{aligned} \quad (\text{E.70})$$

E.2 Rank-2 BF theory

The gauge fixed action (5.87) in the Landau gauge and in momentum space¹, writes

$$\begin{aligned} S &= \int \frac{d^3p}{(2\pi)^3} \left\{ i\hat{a}_{\mu\nu}(-p) \left[\epsilon^{\mu\lambda\rho} p_\lambda \hat{b}_\rho^\nu(p) + p^\mu \hat{b}^\nu(p) - \eta^{\mu\nu} p_\lambda \hat{b}^\lambda(p) \right] - \hat{d}(-p) \left(k_0 p^\alpha p^\beta + k_1 p^2 \eta^{\alpha\beta} \right) \hat{a}_{\alpha\beta}(p) \right. \\ &\quad \left. + i\hat{d}^\mu(-p) \left[\kappa_0 p^\nu \hat{b}_{\mu\nu}(p) + \kappa_1 \eta^{\alpha\beta} p_\mu \hat{b}_{\alpha\beta}(p) + \kappa_2 \epsilon_{\mu\nu\rho} p^\nu \hat{b}^\rho(p) \right] \right\} \\ &\equiv \int \frac{d^3p}{(2\pi)^3} \left[\hat{a}_{\mu\nu}(-p) G^{\mu\nu,\alpha\beta} \hat{b}_{\alpha\beta}(p) + \hat{a}_{\mu\nu}(-p) G^{\mu\nu,\alpha} \hat{b}_\alpha(p) + \hat{d}(-p) G^{\alpha\beta} \hat{a}_{\alpha\beta}(p) + \right. \\ &\quad \left. + \hat{d}_\mu(-p) G_{(\kappa_0,\kappa_1)}^{\alpha\beta,\mu} \hat{b}_{\alpha\beta}(p) + \hat{d}_\mu(-p) G^{\mu,\alpha} \hat{b}_\alpha(p) \right] \\ &\equiv \int \frac{d^3p}{(2\pi)^3} \hat{\phi}_M(-p) G^{MA} \hat{\phi}_A(p) , \end{aligned} \quad (\text{E.71})$$

¹The Fourier transform is defined as $\Phi(x) \equiv \int \frac{d^3p}{(2\pi)^3} e^{ip \cdot x} \hat{\Phi}(p)$.

where we defined

$$\hat{\phi}_M \equiv \{\hat{a}_{\mu\nu}, \hat{b}_{\mu\nu}, \hat{b}_\mu, \hat{d}_\mu, \hat{d}\}, \quad (\text{E.72})$$

$$G^{MA} \equiv \frac{1}{2} \begin{bmatrix} 0 & G^{\mu\nu,\alpha\beta} & G^{\mu\nu,\alpha} & 0 & G^{\mu\nu} \\ G^{\mu\nu,\alpha\beta} & 0 & 0 & G_{(\kappa_0,\kappa_1)}^{*\mu\nu,\alpha} & 0 \\ G^{*\alpha\beta,\mu} & 0 & 0 & G^{\mu,\alpha} & 0 \\ 0 & G_{(\kappa_0,\kappa_1)}^{\alpha\beta,\mu} & G^{*\alpha,\mu} & 0 & 0 \\ G^{\alpha\beta} & 0 & 0 & 0 & 0 \end{bmatrix}, \quad (\text{E.73})$$

and

$$G^{\mu\nu,\alpha\beta}(p) \equiv \frac{i}{4} p_\lambda (\epsilon^{\mu\lambda\alpha} \eta^{\beta\nu} + \epsilon^{\nu\lambda\alpha} \eta^{\beta\mu} + \epsilon^{\mu\lambda\beta} \eta^{\alpha\nu} + \epsilon^{\nu\lambda\beta} \eta^{\alpha\mu}) \quad (\text{E.74})$$

$$G^{\mu\nu,\alpha}(p) \equiv \frac{i}{2} (\eta^{\mu\alpha} p^\beta + \eta^{\mu\beta} p^\alpha) - i p^\mu \eta^{\alpha\beta} \quad (\text{E.75})$$

$$G^{\mu\nu}(p) \equiv -k_0 p^\mu p^\nu - k_1 p^2 \eta^{\mu\nu} \quad (\text{E.76})$$

$$G_{(\kappa_0,\kappa_1)}^{\mu\nu,\alpha}(p) \equiv \frac{i}{2} \kappa_0 (\eta^{\mu\alpha} p^\nu + \eta^{\nu\alpha} p^\mu) + i \kappa_1 p^\alpha \eta^{\mu\nu} \quad (\text{E.77})$$

$$G^{\mu,\alpha}(p) \equiv i \kappa_2 \epsilon^{\mu\lambda\alpha} p_\lambda, \quad (\text{E.78})$$

which display the following symmetries

$$G^{\mu\nu,\alpha\beta} = G^{*\alpha\beta,\mu\nu} = G^{\nu\mu,\alpha\beta} = G^{\mu\nu,\beta\alpha} \quad (\text{E.79})$$

$$G^{\mu\nu} = G^{\nu\mu} = G^{*\mu\nu} \quad (\text{E.80})$$

$$G_{(\kappa_0,\kappa_1)}^{\mu\nu,\alpha} = G_{(\kappa_0,\kappa_1)}^{\nu\mu,\alpha} = -G_{(\kappa_0,\kappa_1)}^{*\mu\nu,\alpha} \quad (\text{E.81})$$

$$G^{\mu,\alpha} = -G^{*\mu,\alpha} = G^{*\alpha,\mu}. \quad (\text{E.82})$$

The propagators of the theory are encoded in the matrix

$$\Delta_{AP} \equiv \begin{bmatrix} \Delta_{\alpha\beta,\rho\sigma}^{(1)} & \Delta_{\alpha\beta,\rho\sigma}^{(2)} & \Delta_{\alpha\beta,\rho}^{(3)} & \Delta_{\alpha\beta,\rho}^{(4)} & \Delta_{\alpha\beta}^{(5)} \\ \Delta_{\rho\sigma,\alpha\beta}^{(2)*} & \Delta_{\alpha\beta,\rho\sigma}^{(6)} & \Delta_{\alpha\beta,\rho}^{(7)} & \Delta_{\alpha\beta,\rho}^{(8)} & \Delta_{\alpha\beta}^{(9)} \\ \Delta_{\rho\sigma,\alpha}^{(3)*} & \Delta_{\rho\sigma,\alpha}^{(7)*} & \Delta_{\alpha,\rho}^{(10)} & \Delta_{\alpha,\rho}^{(11)} & \Delta_{\alpha}^{(12)} \\ \Delta_{\rho\sigma,\alpha}^{(4)*} & \Delta_{\rho\sigma,\alpha}^{(8)*} & \Delta_{\rho,\alpha}^{(11)*} & \Delta_{\alpha,\rho}^{(13)} & \Delta_{\alpha}^{(14)} \\ \Delta_{\rho\sigma}^{(5)*} & \Delta_{\rho\sigma}^{(9)*} & \Delta_{\rho}^{(12)*} & \Delta_{\rho}^{(14)*} & \Delta^{(15)} \end{bmatrix}, \quad (\text{E.83})$$

with

$$\begin{aligned}\Delta_{\alpha\beta,\rho\sigma}^{(1)}(p) &\equiv \langle \hat{a}_{\alpha\beta}(-p) \hat{a}_{\rho\sigma}(p) \rangle & (E.84) \\ &= \left(c_0 A^{(0)} + c_1 A^{(1)} + c_2 A^{(2)} + c_3 A^{(3)} + c_4 A^{(4)} + c_5 A^{(5)} + c_6 A^{(6)} \right)_{\alpha\beta,\rho\sigma}\end{aligned}$$

$$\begin{aligned}\Delta_{\alpha\beta,\rho\sigma}^{(2)}(p) &\equiv \langle \hat{a}_{\alpha\beta}(-p) \hat{b}_{\rho\sigma}(p) \rangle & (E.85) \\ &= \left(c_7 A^{(0)} + c_8 A^{(1)} + c_9 A'^{(2)} + c_{10} B^{(2)} + c_{11} A^{(3)} + c_{12} A^{(4)} + c_{13} A^{(5)} + c_{14} A^{(6)} \right)_{\alpha\beta,\rho\sigma}\end{aligned}$$

$$\begin{aligned}\Delta_{\alpha\beta,\rho}^{(3)}(p) &\equiv \langle \hat{a}_{\alpha\beta}(-p) \hat{b}_{\rho}(p) \rangle & (E.86) \\ &= ic_{15} \eta_{\alpha\beta} p_{\rho} + ic_{16} p_{\alpha} p_{\beta} p_{\rho} + c_{17} p^{\lambda} (\epsilon_{\alpha\lambda\rho} p_{\beta} + \epsilon_{\beta\lambda\rho} p_{\alpha}) + ic_{18} (\eta_{\alpha\rho} p_{\beta} + \eta_{\beta\rho} p_{\alpha})\end{aligned}$$

$$\begin{aligned}\Delta_{\alpha\beta,\rho}^{(4)}(p) &\equiv \langle \hat{a}_{\alpha\beta}(-p) \hat{d}_{\rho}(p) \rangle & (E.87) \\ &= ic_{19} \eta_{\alpha\beta} p_{\rho} + ic_{20} p_{\alpha} p_{\beta} p_{\rho} + c_{21} p^{\lambda} (\epsilon_{\alpha\lambda\rho} p_{\beta} + \epsilon_{\beta\lambda\rho} p_{\alpha}) + ic_{22} (\eta_{\alpha\rho} p_{\beta} + \eta_{\beta\rho} p_{\alpha})\end{aligned}$$

$$\begin{aligned}\Delta_{\alpha\beta}^{(5)}(p) &\equiv \langle \hat{a}_{\alpha\beta}(-p) \hat{d}(p) \rangle & (E.88) \\ &= c_{23} \eta_{\alpha\beta} + c_{24} p_{\alpha} p_{\beta}\end{aligned}$$

$$\begin{aligned}\Delta_{\alpha\beta,\rho\sigma}^{(6)}(p) &\equiv \langle \hat{b}_{\alpha\beta}(-p) \hat{b}_{\rho\sigma}(p) \rangle & (E.89) \\ &= \left(c_{25} A^{(0)} + c_{26} A^{(1)} + c_{27} A^{(2)} + c_{28} A^{(3)} + c_{29} A^{(4)} + c_{30} A^{(5)} + c_{31} A^{(6)} \right)_{\alpha\beta,\rho\sigma}\end{aligned}$$

$$\begin{aligned}\Delta_{\alpha\beta,\rho}^{(7)}(p) &\equiv \langle \hat{b}_{\alpha\beta}(-p) \hat{b}_{\rho}(p) \rangle & (E.90) \\ &= ic_{32} \eta_{\alpha\beta} p_{\rho} + ic_{33} p_{\alpha} p_{\beta} p_{\rho} + c_{34} p^{\lambda} (\epsilon_{\alpha\lambda\rho} p_{\beta} + \epsilon_{\beta\lambda\rho} p_{\alpha}) + ic_{35} (\eta_{\alpha\rho} p_{\beta} + \eta_{\beta\rho} p_{\alpha})\end{aligned}$$

$$\begin{aligned}\Delta_{\alpha\beta,\rho}^{(8)}(p) &\equiv \langle \hat{b}_{\alpha\beta}(-p) \hat{d}_{\rho}(p) \rangle & (E.91) \\ &= ic_{36} \eta_{\alpha\beta} p_{\rho} + ic_{37} p_{\alpha} p_{\beta} p_{\rho} + c_{38} p^{\lambda} (\epsilon_{\alpha\lambda\rho} p_{\beta} + \epsilon_{\beta\lambda\rho} p_{\alpha}) + ic_{39} (\eta_{\alpha\rho} p_{\beta} + \eta_{\beta\rho} p_{\alpha})\end{aligned}$$

$$\begin{aligned}\Delta_{\alpha\beta}^{(9)}(p) &\equiv \langle \hat{b}_{\alpha\beta}(-p) \hat{d}(p) \rangle & (E.92) \\ &= c_{40} \eta_{\alpha\beta} + c_{41} p_{\alpha} p_{\beta}\end{aligned}$$

$$\begin{aligned}\Delta_{\alpha,\rho}^{(10)}(p) &\equiv \langle \hat{b}_{\alpha}(-p) \hat{b}_{\rho}(p) \rangle & (E.93) \\ &= c_{42} \eta_{\alpha\rho} + c_{43} p_{\alpha} p_{\rho} + ic_{44} p^{\lambda} \epsilon_{\alpha\lambda\rho}\end{aligned}$$

$$\begin{aligned}\Delta_{\alpha,\rho}^{(11)}(p) &\equiv \langle \hat{b}_{\alpha}(-p) \hat{d}_{\rho}(p) \rangle & (E.94) \\ &= c_{45} \eta_{\alpha\rho} + c_{46} p_{\alpha} p_{\rho} + ic_{47} p^{\lambda} \epsilon_{\alpha\lambda\rho}\end{aligned}$$

$$\begin{aligned}\Delta_{\alpha}^{(12)}(p) &\equiv \langle \hat{b}_{\alpha}(-p) \hat{d}(p) \rangle & (E.95) \\ &= ic_{48} p_{\alpha}\end{aligned}$$

$$\begin{aligned}\Delta_{\alpha,\rho}^{(13)}(p) &\equiv \langle \hat{d}_{\alpha}(-p) \hat{d}_{\rho}(p) \rangle & (E.96) \\ &= c_{49} \eta_{\alpha\rho} + c_{50} p_{\alpha} p_{\rho} + ic_{51} p^{\lambda} \epsilon_{\alpha\lambda\rho}\end{aligned}$$

$$\Delta_{\alpha}^{(14)}(p) \equiv \langle \hat{d}_{\alpha}(-p) \hat{d}(p) \rangle \quad (E.97)$$

$$\begin{aligned}
&= ic_{52} p_\alpha \\
\Delta^{(15)}(p) &\equiv \langle \hat{d}(-p) \hat{d}(p) \rangle, \tag{E.98}
\end{aligned}$$

expanded on the basis of tensors (E.5)-(E.11), where, since

$$\Delta_{AP} = \Delta_{PA}^\dagger, \tag{E.99}$$

the symmetries

$$\Delta_{M,P}^{(i)}(p) = \Delta_{P,M}^{(i)*}(p) = \Delta_{M,P}^{(i)*}(-p) \quad \text{for } i = \{1, 6, 10, 11, 13\} \tag{E.100}$$

i.e. when $M = \mu\nu$ and $P = \rho\sigma$ or $M = \mu$ and $P = \rho$, and

$$\Delta_{\alpha\beta,P}^{(i)}(p) = \Delta_{\beta\alpha,P}^{(i)}(p) = \Delta_{\alpha\beta,P}^{(i)*}(-p) \quad \text{for } i = \{1, \dots, 9\} \tag{E.101}$$

i.e. when $P = \{\rho\sigma, \sigma\rho, \rho, \dots\}$, have been taken into account. The propagator matrix $\Delta_{AP}(p)$ (E.83) is defined as the inverse of the quadratic operator $G^{AB}(p)$ (E.73)

$$G^{MA} \Delta_{AP} = I_P^M, \tag{E.102}$$

where

$$I_P^M \equiv \begin{bmatrix} \mathcal{I}_{\rho\sigma}^{\mu\nu}(0) & 0 & 0 & 0 & 0 \\ 0 & \mathcal{I}_{\rho\sigma}^{\mu\nu}(\lambda) & 0 & 0 & 0 \\ 0 & 0 & \delta_\rho^\mu & 0 & 0 \\ 0 & 0 & 0 & \delta_\rho^\mu & 0 \\ 0 & 0 & 0 & 0 & 1 \end{bmatrix} \tag{E.103}$$

is the identity matrix with

$$\mathcal{I}_{\rho\sigma}^{\mu\nu}(\lambda) \equiv \frac{1}{2} \left(\delta_\rho^\mu \delta_\sigma^\nu + \delta_\sigma^\mu \delta_\rho^\nu \right) + \lambda \eta^{\mu\nu} \eta_{\rho\sigma}. \tag{E.104}$$

A comment is in order concerning the presence of the constant λ in the matrix identity. The idempotency of the identity

$$\mathcal{I}_{\rho\sigma}^{\mu\nu} \mathcal{I}_{\alpha\beta}^{\rho\sigma} = \mathcal{I}_{\alpha\beta}^{\mu\nu}, \tag{E.105}$$

requires that either

$$\lambda = 0, \quad (\text{E.106})$$

or

$$\lambda = -\frac{1}{3}. \quad (\text{E.107})$$

The latter option (E.107) corresponds to a traceless identity

$$\eta_{\mu\nu} \mathcal{I}_{\rho\sigma}^{\mu\nu}(-\frac{1}{3}) = \eta^{\rho\sigma} \mathcal{I}_{\rho\sigma}^{\mu\nu}(-\frac{1}{3}) = 0, \quad (\text{E.108})$$

which is suitable for a traceless tensorial space such as that involving the field $b_{\mu\nu}(x)$.

From the invertibility condition (E.102) we get the following system of equations

$$\frac{1}{2} G^{\mu\nu, \alpha\beta} \Delta_{\rho\sigma, \alpha\beta}^{(2)*} + \frac{1}{2} G^{\mu\nu, \alpha} \Delta_{\rho\sigma, \alpha}^{(3)*} + \frac{1}{2} G^{\mu\nu} \Delta_{\rho\sigma}^{(5)*} = \mathcal{I}_{\rho\sigma}^{\mu\nu}(0) \quad (\text{E.109})$$

$$\frac{1}{2} G^{\mu\nu, \alpha\beta} \Delta_{\alpha\beta, \rho\sigma}^{(6)} + \frac{1}{2} G^{\mu\nu, \alpha} \Delta_{\rho\sigma, \alpha}^{(7)*} + \frac{1}{2} G^{\mu\nu} \Delta_{\rho\sigma}^{(9)*} = 0 \quad (\text{E.110})$$

$$\frac{1}{2} G^{\mu\nu, \alpha\beta} \Delta_{\alpha\beta, \rho}^{(7)} + \frac{1}{2} G^{\mu\nu, \alpha} \Delta_{\alpha, \rho}^{(10)} + \frac{1}{2} G^{\mu\nu} \Delta_{\rho}^{(12)*} = 0 \quad (\text{E.111})$$

$$\frac{1}{2} G^{\mu\nu, \alpha\beta} \Delta_{\alpha\beta, \rho}^{(8)} + \frac{1}{2} G^{\mu\nu, \alpha} \Delta_{\alpha, \rho}^{(11)} + \frac{1}{2} G^{\mu\nu} \Delta_{\rho}^{(14)*} = 0 \quad (\text{E.112})$$

$$\frac{1}{2} G^{\mu\nu, \alpha\beta} \Delta_{\alpha\beta}^{(9)} + \frac{1}{2} G^{\mu\nu, \alpha} \Delta_{\alpha}^{(12)} + \frac{1}{2} G^{\mu\nu} \Delta^{(15)} = 0 \quad (\text{E.113})$$

$$\frac{1}{2} G^{\mu\nu, \alpha\beta} \Delta_{\alpha\beta, \rho\sigma}^{(1)} + \frac{1}{2} G_{(\kappa_0, \kappa_1)}^{*\mu\nu, \alpha} \Delta_{\rho\sigma, \alpha}^{(4)*} = 0 \quad (\text{E.114})$$

$$\frac{1}{2} G^{\mu\nu, \alpha\beta} \Delta_{\alpha\beta, \rho\sigma}^{(2)} + \frac{1}{2} G_{(\kappa_0, \kappa_1)}^{*\mu\nu, \alpha} \Delta_{\rho\sigma, \alpha}^{(8)*} = \mathcal{I}_{\rho\sigma}^{\mu\nu}(\lambda) \quad (\text{E.115})$$

$$\frac{1}{2} G^{\mu\nu, \alpha\beta} \Delta_{\alpha\beta, \rho}^{(3)} + \frac{1}{2} G_{(\kappa_0, \kappa_1)}^{*\mu\nu, \alpha} \Delta_{\rho, \alpha}^{(11)*} = 0 \quad (\text{E.116})$$

$$\frac{1}{2} G^{\mu\nu, \alpha\beta} \Delta_{\alpha\beta, \rho}^{(4)} + \frac{1}{2} G_{(\kappa_0, \kappa_1)}^{*\mu\nu, \alpha} \Delta_{\alpha, \rho}^{(13)} = 0 \quad (\text{E.117})$$

$$\frac{1}{2} G^{\mu\nu, \alpha\beta} \Delta_{\alpha\beta}^{(5)} + \frac{1}{2} G_{(\kappa_0, \kappa_1)}^{*\mu\nu, \alpha} \Delta_{\alpha}^{(14)} = 0 \quad (\text{E.118})$$

$$\frac{1}{2} G^{*\alpha\beta, \mu} \Delta_{\alpha\beta, \rho\sigma}^{(1)} + \frac{1}{2} G^{\mu, \alpha} \Delta_{\rho\sigma, \alpha}^{(4)*} = 0 \quad (\text{E.119})$$

$$\frac{1}{2} G^{*\alpha\beta, \mu} \Delta_{\alpha\beta, \rho\sigma}^{(2)} + \frac{1}{2} G^{\mu, \alpha} \Delta_{\rho\sigma, \alpha}^{(8)*} = 0 \quad (\text{E.120})$$

$$\frac{1}{2} G^{*\alpha\beta, \mu} \Delta_{\alpha\beta, \rho}^{(3)} + \frac{1}{2} G^{\mu, \alpha} \Delta_{\rho, \alpha}^{(11)*} = \delta_{\rho}^{\mu} \quad (\text{E.121})$$

$$\frac{1}{2} G^{*\alpha\beta, \mu} \Delta_{\alpha\beta, \rho}^{(4)} + \frac{1}{2} G^{\mu, \alpha} \Delta_{\alpha, \rho}^{(13)} = 0 \quad (\text{E.122})$$

$$\frac{1}{2} G^{*\alpha\beta, \mu} \Delta_{\alpha\beta}^{(5)} + \frac{1}{2} G^{\mu, \alpha} \Delta_{\alpha}^{(14)} = 0 \quad (\text{E.123})$$

$$\frac{1}{2} G_{(\kappa_0, \kappa_1)}^{\alpha\beta, \mu} \Delta_{\rho\sigma, \alpha\beta}^{(2)*} + \frac{1}{2} G^{*\alpha, \mu} \Delta_{\rho\sigma, \alpha}^{(3)*} = 0 \quad (\text{E.124})$$

$$\frac{1}{2} G_{(\kappa_0, \kappa_1)}^{\alpha\beta, \mu} \Delta_{\alpha\beta, \rho\sigma}^{(6)} + \frac{1}{2} G^{*\alpha, \mu} \Delta_{\rho\sigma, \alpha}^{(7)*} = 0 \quad (\text{E.125})$$

$$\frac{1}{2}G_{(\kappa_0, \kappa_1)}^{\alpha\beta, \mu} \Delta_{\alpha\beta, \rho}^{(7)} + \frac{1}{2}G^{*\alpha, \mu} \Delta_{\alpha, \rho}^{(10)} = 0 \quad (\text{E.126})$$

$$\frac{1}{2}G_{(\kappa_0, \kappa_1)}^{\alpha\beta, \mu} \Delta_{\alpha\beta, \rho}^{(8)} + \frac{1}{2}G^{*\alpha, \mu} \Delta_{\alpha, \rho}^{(11)} = \delta_{\rho}^{\mu} \quad (\text{E.127})$$

$$\frac{1}{2}G_{(\kappa_0, \kappa_1)}^{\alpha\beta, \mu} \Delta_{\alpha\beta}^{(9)} + \frac{1}{2}G^{*\alpha, \mu} \Delta_{\alpha}^{(12)} = 0 \quad (\text{E.128})$$

$$\frac{1}{2}G^{\alpha\beta} \Delta_{\alpha\beta, \rho\sigma}^{(1)} = 0 \quad (\text{E.129})$$

$$\frac{1}{2}G^{\alpha\beta} \Delta_{\alpha\beta, \rho\sigma}^{(2)} = 0 \quad (\text{E.130})$$

$$\frac{1}{2}G^{\alpha\beta} \Delta_{\alpha\beta, \rho}^{(3)} = 0 \quad (\text{E.131})$$

$$\frac{1}{2}G^{\alpha\beta} \Delta_{\alpha\beta, \rho}^{(4)} = 0 \quad (\text{E.132})$$

$$\frac{1}{2}G^{\alpha\beta} \Delta_{\alpha\beta}^{(5)} = 1. \quad (\text{E.133})$$

Notice that saturating the $\rho\sigma$ indices in (E.115), and using the definitions (E.84)-(E.98), we have

$$\begin{aligned} (1 + 3\lambda)\eta^{\mu\nu} &= \frac{1}{2}G^{\mu\nu, \alpha\beta} \eta^{\rho\sigma} \Delta_{\alpha\beta, \rho\sigma}^{(2)} + \frac{1}{2}G^{*\mu\nu, \alpha} \eta^{\rho\sigma} \Delta_{\rho\sigma, \alpha}^{(8)*} \\ &= \frac{1}{2}G^{\mu\nu, \alpha\beta} \eta^{\rho\sigma} \langle \hat{a}_{\alpha\beta}(-p) \hat{b}_{\rho\sigma}(p) \rangle + \frac{1}{2}G^{*\mu\nu, \alpha} \eta^{\rho\sigma} \langle \hat{d}_{\alpha}(-p) \hat{b}_{\rho\sigma}(p) \rangle \quad (\text{E.134}) \\ &= \frac{1}{2}G^{\mu\nu, \alpha\beta} \langle \hat{a}_{\alpha\beta}(-p) \hat{b}(p) \rangle + \frac{1}{2}G^{*\mu\nu, \alpha} \langle \hat{d}_{\alpha}(-p) \hat{b}(p) \rangle, \end{aligned}$$

which must vanish if the theory does not depend on the trace $\hat{b}(p)$, which would imply $\lambda = -1/3$. This further justifies the introduction of the λ parameter in the identity. From (E.109)-(E.133) the following equations are recovered through the multiplication rules of the basis (E.5)-(E.11), which can be found in [3]

$$\begin{aligned} 2p^2 c_{13} + 1 &= 0 && \text{from (E.109)} \\ 3c_{13} - p^2 c_{14} + c_{18} &= 0 \\ -c_{13} - \frac{1}{2}p^2 c_{16} - c_{18} - \frac{1}{2}k_1 p^2 c_{24} &= 0 \\ -c_{13} + \frac{1}{2}c_{15} - \frac{1}{2}k_0 c_{23} &= 0 \\ c_{13} p^2 - \frac{1}{2}p^2 c_{15} - \frac{1}{2}k_1 p^2 c_{23} &= 0 \\ c_{14} + \frac{1}{2}c_{16} - \frac{1}{2}k_0 c_{24} &= 0 \\ c_7 &= 0 \\ c_7 - c_{17} &= 0 \\ c_{30} &= 0 && \text{from (E.110)} \\ 3c_{30} - p^2 c_{31} + c_{35} &= 0 \end{aligned}$$

$$c_{30} + \frac{1}{2}p^2c_{33} + c_{35} + \frac{1}{2}k_1p^2c_{41} = 0$$

$$-c_{30} + \frac{1}{2}c_{32} - \frac{1}{2}k_0c_{40} = 0$$

$$c_{30}p^2 - \frac{1}{2}p^2c_{32} - \frac{1}{2}k_1p^2c_{40} = 0$$

$$c_{31} + \frac{1}{2}c_{33} - \frac{1}{2}k_0c_{41} = 0$$

$$c_{25} = 0$$

$$c_{26} - c_{34} = 0$$

$$p^2c_{34} + c_{42} = 0 \quad \text{from (E.111)}$$

$$c_{34} - c_{43} - k_0c_{48} = 0$$

$$c_{35} + c_{44} = 0$$

$$-c_{42} - p^2c_{43} + k_1p^2c_{48} = 0$$

$$p^2c_{38} + c_{45} = 0 \quad \text{from (E.112)}$$

$$c_{38} - c_{46} - k_0c_{52} = 0$$

$$c_{39} + c_{47} = 0$$

$$-c_{45} - p^2c_{46} + k_1p^2c_{52} = 0$$

$$c_{48}p^2 - \Delta^{(15)}k_1p^2 = 0 \quad \text{from (E.113)}$$

$$c_{48} + \Delta^{(15)}k_0 = 0$$

$$c_5 = 0 \quad \text{from (E.114)}$$

$$-3c_5 + p^2c_6 + \kappa_0c_{22} = 0$$

$$2c_5 + \kappa_1(p^2c_{19} + 2c_{22}) = 0$$

$$2c_5 + \kappa_0c_{19} = 0$$

$$-2c_5 + \kappa_1p^2c_{19} = 0$$

$$-2c_6 + \kappa_0c_{20} = 0$$

$$c_0 = 0$$

$$c_1 + \kappa_0c_{21} = 0$$

$$2c_{13}p^2 + 1 = 0 \quad \text{from (E.115)}$$

$$-3c_{13} + p^2c_{14} + \kappa_0c_{39} = 0$$

$$c_{13} + \frac{1}{2}\kappa_1p^2c_{37} + \kappa_1c_{39} = 0$$

$$c_{13} + \frac{1}{2}\kappa_0c_{36} = 0$$

$$\begin{aligned}
p^2 c_{13} - \frac{1}{2} \kappa_1 p^2 c_{36} - \lambda &= 0 \\
-c_{14} + \frac{1}{2} \kappa_0 c_{37} &= 0 \\
c_7 &= 0 \\
c_8 + \kappa_0 c_{38} &= 0 \\
-p^2 c_{17} + \kappa_0 c_{45} &= 0 && \text{from (E.116)} \\
c_{17} + \kappa_0 c_{46} &= 0 \\
c_{18} - \kappa_0 c_{47} &= 0 \\
\kappa_1 (c_{45} + p^2 c_{46}) &= 0 \\
-p^2 c_{21} + \kappa_0 c_{49} &= 0 && \text{from (E.117)} \\
c_{21} + \kappa_0 c_{50} &= 0 \\
c_{22} - \kappa_0 c_{51} &= 0 \\
\kappa_1 (c_{49} + p^2 c_{50}) &= 0 \\
\kappa_0 c_{52} &= 0 && \text{from (E.118)} \\
\kappa_1 c_{52} &= 0 \\
c_0 + 2c_1 p^2 + 2\kappa_2 p^2 c_{21} &= 0 && \text{from (E.119)} \\
-c_1 - c_2 - \kappa_2 c_{21} &= 0 \\
c_3 - c_0 &= 0 \\
c_5 + p^2 c_6 + \kappa_2 c_{22} &= 0 \\
c_7 + 2c_8 p^2 + 2\kappa_2 p^2 c_{38} &= 0 && \text{from (E.120)} \\
-c_8 - c_9 - \kappa_2 c_{38} &= 0 \\
c_{11} - c_7 &= 0 \\
c_{13} + p^2 c_{14} + \kappa_2 c_{39} &= 0 \\
2 - p^2 c_{18} + \kappa_2 p^2 c_{47} &= 0 && \text{from (E.121)} \\
-2c_{15} - c_{18} + \kappa_2 c_{47} &= 0 \\
p^2 c_{17} - \kappa_2 c_{45} &= 0 \\
p^2 c_{22} - \kappa_2 p^2 c_{51} &= 0 && \text{from (E.122)} \\
-2c_{19} - c_{22} + \kappa_2 c_{51} &= 0 \\
c_{20} - \kappa_2 c_{49} &= 0
\end{aligned}$$

$$c_{23} = 0 \quad \text{from (E.123)}$$

$$\frac{1}{2}\kappa_0 c_7 + \kappa_0 p^2 c_8 - \kappa_2 p^2 c_{17} = 0 \quad \text{from (E.124)}$$

$$\kappa_0 c_{13} + \kappa_0 p^2 c_{14} - \kappa_2 c_{18} = 0$$

$$2(\kappa_0 + 2\kappa_1)c_8 + (\kappa_0 + 3\kappa_1)c_{10} + (\kappa_0 + \kappa_1)p^2 c_{12} + 2\kappa_2 c_{17} = 0$$

$$(\kappa_0 + \kappa_1)p^2 c_9 + (\kappa_0 + 3\kappa_1)c_{11} + \kappa_1 c_7 = 0$$

$$\frac{1}{2}\kappa_0 c_{25} + \kappa_0 p^2 c_{26} - \kappa_2 p^2 c_{34} = 0 \quad \text{from (E.125)}$$

$$\kappa_0 c_{30} + \kappa_0 p^2 c_{31} - \kappa_2 c_{35} = 0$$

$$2(\kappa_0 + 2\kappa_1)c_{26} + (\kappa_0 + 3\kappa_1)c_{27} + (\kappa_0 + \kappa_1)p^2 c_{29} + 2\kappa_2 c_{34} = 0$$

$$(\kappa_0 + \kappa_1)p^2 c_{27} + (\kappa_0 + 3\kappa_1)c_{28} + \kappa_1 c_{25} = 0$$

$$(\kappa_0 + 3\kappa_1)c_{32} + (\kappa_0 + \kappa_1)p^2 c_{33} + (\kappa_0 + 2\kappa_1)c_{35} - \kappa_2 c_{44} = 0 \quad \text{from (E.126)}$$

$$\kappa_0 p^2 c_{34} + \kappa_2 c_{42} = 0$$

$$\kappa_0 c_{35} + \kappa_2 c_{44} = 0$$

$$(\kappa_0 + 3\kappa_1)c_{36} + (\kappa_0 + \kappa_1)p^2 c_{37} + (\kappa_0 + 2\kappa_1)c_{39} - \kappa_2 c_{47} = 0 \quad \text{from (E.127)}$$

$$\kappa_0 p^2 c_{38} + \kappa_2 c_{45} = 0$$

$$\kappa_0 p^2 c_{39} + \kappa_2 p^2 c_{47} + 2 = 0$$

$$(\kappa_0 + 3\kappa_1)c_{40} + (\kappa_0 + \kappa_1)p^2 c_{41} = 0 \quad \text{from (E.128)}$$

$$k_0 c_0 + 4(k_0 + k_1)p^2 c_1 + (k_0 + 3k_1)p^2 c_2 + (k_1 + k_0)p^4 c_4 = 0 \quad \text{from (E.129)}$$

$$k_1 p^2 c_0 + (k_0 + k_1)p^4 c_2 + (k_0 + 3k_1)p^2 c_3 = 0$$

$$k_0 c_7 + 4(k_0 + k_1)p^2 c_8 + (k_0 + 3k_1)p^2 c_9 + (k_1 + k_0)p^4 c_{12} = 0 \quad \text{from (E.130)}$$

$$k_1 p^2 c_7 + (k_0 + k_1)p^4 c_{10} + (k_0 + 3k_1)p^2 c_{11} = 0$$

$$(k_0 + 3k_1)c_{15} + (k_0 + k_1)p^2 c_{16} + 2(k_0 + k_1)c_{18} = 0 \quad \text{from (E.131)}$$

$$(k_0 + 3k_1)c_{19} + (k_0 + k_1)p^2 c_{20} + 2(k_0 + k_1)c_{22} = 0 \quad \text{from (E.132)}$$

$$(k_0 + 3k_1)p^2 c_{23} + (k_0 + k_1)p^4 c_{24} + 2 = 0 \quad \text{from (E.133)}$$

Solutions to this system of equations are

$$\lambda = -\frac{1}{3} \quad \kappa_1 = -\frac{1}{3}\kappa_0 \quad (E.135)$$

$$c_{13} = -\frac{1}{2p^2} \quad c_{14} = \frac{\kappa_0 + 3\kappa_2}{\kappa_0 - \kappa_2} \frac{1}{2p^4} \quad c_{15} = -\frac{1}{p^2} \quad (E.136)$$

$$c_{16} = -\left(\frac{k_0 - k_1}{k_0 + k_1} + 2\frac{\kappa_0 + \kappa_2}{\kappa_0 - \kappa_2}\right) \frac{1}{p^4} \quad c_{18} = \frac{2\kappa_0}{\kappa_0 - \kappa_2} \frac{1}{p^2} \quad c_{24} = -\frac{2}{k_0 + k_1} \frac{1}{p^4} \quad (E.137)$$

$$c_{36} = \frac{1}{\kappa_0 p^2} \quad c_{37} = \frac{\kappa_0 + 3\kappa_2}{\kappa_0(\kappa_0 - \kappa_2)} \frac{1}{p^4} \quad c_{39} = -\frac{2}{\kappa_0 - \kappa_2} \frac{1}{p^2} \quad (E.138)$$

$$c_{47} = \frac{2}{\kappa_0 - \kappa_2} \frac{1}{p^2}, \quad (E.139)$$

and

$$c_i = \Delta^{(15)} = 0 \quad \text{for } i = \{0-12, 17, 19-23, 25-35, 38, 40-46, 48-52\}, \quad (E.140)$$

$$(E.141)$$

which signal poles at

$$\kappa_0 = 0 \quad ; \quad \kappa_0 = \kappa_2 \quad ; \quad k_1 = -k_0. \quad (E.142)$$

Non-trivial propagators are thus the following

$$\begin{aligned}\Delta_{\alpha\beta,\rho\sigma}^{(2)}(p) &\equiv \langle \hat{a}_{\alpha\beta}(-p) \hat{b}_{\rho\sigma}(p) \rangle & (E.143) \\ &= \frac{1}{2p^2} \left(-A_{\alpha\beta,\rho\sigma}^{(5)} + \frac{\kappa_0 + 3\kappa_2}{\kappa_0 - \kappa_2} \frac{1}{p^2} A_{\alpha\beta,\rho\sigma}^{(6)} \right) \\ &= -\frac{i}{2p^2} p^\lambda \left[(\epsilon_{\alpha\lambda\rho} t_{\sigma\beta} + \epsilon_{\beta\lambda\rho} t_{\sigma\alpha} + \epsilon_{\alpha\lambda\sigma} t_{\rho\beta} + \epsilon_{\beta\lambda\sigma} t_{\rho\alpha}) + \right. \\ &\quad \left. - \frac{4\kappa_2}{\kappa_0 - \kappa_2} \left(\epsilon_{\alpha\lambda\rho} \frac{p_\sigma p_\beta}{p^2} + \epsilon_{\alpha\lambda\sigma} \frac{p_\rho p_\beta}{p^2} + \epsilon_{\beta\lambda\rho} \frac{p_\sigma p_\alpha}{p^2} + \epsilon_{\beta\lambda\sigma} \frac{p_\rho p_\alpha}{p^2} \right) \right]\end{aligned}$$

$$\begin{aligned}\Delta_{\alpha\beta,\rho}^{(3)}(p) &\equiv \langle \hat{a}_{\alpha\beta}(-p) \hat{b}_\rho(p) \rangle & (E.144) \\ &= -\frac{i}{p^2} \left[\eta_{\alpha\beta} p_\rho + i \left(\frac{k_0 - k_1}{k_0 + k_1} + 2 \frac{\kappa_0 + \kappa_2}{\kappa_0 - \kappa_2} \right) \frac{p_\alpha p_\beta}{p^2} p_\rho - \frac{2\kappa_0}{\kappa_0 - \kappa_2} (\eta_{\alpha\rho} p_\beta + \eta_{\beta\rho} p_\alpha) \right] \\ &= \frac{i}{p^2} \left[\frac{2\kappa_0}{\kappa_0 - \kappa_2} (t_{\alpha\rho} p_\beta + t_{\beta\rho} p_\alpha) - \frac{1}{k_0 + k_1} (k_0 t_{\alpha\beta} p_\rho + k_1 \tilde{t}_{\alpha\beta} p_\rho) \right]\end{aligned}$$

$$\Delta_{\alpha\beta}^{(5)}(p) \equiv \langle \hat{a}_{\alpha\beta}(-p) \hat{d}(p) \rangle = -\frac{2}{k_0 + k_1} \frac{p_\alpha p_\beta}{p^4} \quad (E.145)$$

$$\begin{aligned}\Delta_{\alpha\beta,\rho}^{(8)}(p) &\equiv \langle \hat{b}_{\alpha\beta}(-p) \hat{d}_\rho(p) \rangle & (E.146) \\ &= \frac{i}{p^2} \left[\frac{1}{\kappa_0} \eta_{\alpha\beta} p_\rho + \frac{\kappa_0 + 3\kappa_2}{\kappa_0(\kappa_0 - \kappa_2)} \frac{p_\alpha p_\beta}{p^2} p_\rho - \frac{2}{\kappa_0 - \kappa_2} (\eta_{\alpha\rho} p_\beta + \eta_{\beta\rho} p_\alpha) \right] \\ &= \frac{i}{p^2} \left[\frac{1}{\kappa_0} \tilde{t}_{\alpha\beta} p_\rho - \frac{2}{\kappa_0 - \kappa_2} (t_{\alpha\rho} p_\beta + t_{\beta\rho} p_\alpha) \right]\end{aligned}$$

$$\Delta_{\alpha,\rho}^{(11)}(p) \equiv \langle \hat{b}_\alpha(-p) \hat{d}_\rho(p) \rangle = \frac{2i}{\kappa_0 - \kappa_2} \frac{\epsilon_{\alpha\lambda\rho} p^\lambda}{p^2}, \quad (E.147)$$

where

$$t_{\alpha\beta} \equiv \eta_{\alpha\beta} - \frac{p_\alpha p_\beta}{p^2} \quad ; \quad \tilde{t}_{\alpha\beta} \equiv \eta_{\alpha\beta} - 3 \frac{p_\alpha p_\beta}{p^2}, \quad (E.148)$$

such that

$$p^\alpha t_{\alpha\beta} = 0 \quad ; \quad \eta^{\alpha\beta} \tilde{t}_{\alpha\beta} = 0. \quad (E.149)$$

It is thus immediate to observe that

$$\eta^{\rho\sigma} \Delta_{\alpha\beta,\rho\sigma}^{(2)}(p) = \langle \hat{a}_{\alpha\beta}(-p) \hat{b}(p) \rangle = 0 = \eta^{\alpha\beta} \Delta_{\alpha\beta,\rho}^{(8)}(p) = \langle \hat{b}(-p) \hat{d}_\rho(p) \rangle, \quad (E.150)$$

which confirms that the trace $b(x)$ has no role in the theory.

E.3 Covariant massive fractons

In momentum space, the action S (5.155) reads:

$$\begin{aligned} S &= \int d^3p \left[\hat{a}_{\mu\nu}(p) \left(\eta^{\mu\alpha} p^\nu p^\beta - p^2 \eta^{\mu\alpha} \eta^{\nu\beta} - i m p_\lambda \epsilon^{\mu\lambda\alpha} \eta^{\beta\nu} \right) \hat{a}_{\alpha\beta}(-p) \right. \\ &\quad \left. + \hat{b}(p) \left(-\kappa_0 p^\alpha p^\beta - \kappa_1 p^2 \eta^{\alpha\beta} \right) \hat{a}_{\alpha\beta}(-p) \right] \\ &= \int d^3p \hat{\phi}_M(p) \hat{K}^{MA}(p) \hat{\phi}_A(-p), \end{aligned} \quad (\text{E.151})$$

with

$$\hat{K}^{MA}(p) \equiv \begin{bmatrix} \hat{K}^{\mu\nu,\alpha\beta}(p) & \hat{K}^{*\mu\nu}(p) \\ \hat{K}^{\alpha\beta}(p) & 0 \end{bmatrix}; \quad \hat{\phi}_M \equiv (\hat{a}_{\mu\nu}, \hat{b}), \quad (\text{E.152})$$

and

$$\hat{K}^{\mu\nu,\alpha\beta} = \left[p^2 \left(-A^{(0)} + \frac{1}{4p^2} A^{(1)} \right) - \frac{m}{4} A^{(5)} \right]^{\mu\nu,\alpha\beta} \quad (\text{E.153})$$

$$\hat{K}^{\alpha\beta} = -\frac{1}{2} \left(\kappa_0 p^\alpha p^\beta + \kappa_1 p^2 \eta^{\alpha\beta} \right), \quad (\text{E.154})$$

where we expanded the tensor $\hat{K}^{\mu\nu,\alpha\beta}(p)$ on the $A^{(i)}$ -basis (E.5)-(E.11) [202, 205], and the fact that $a_{\mu\nu}(x)$ is a symmetric tensor field has been taken into account, for which the following symmetries hold

$$\hat{K}^{\mu\nu,\alpha\beta}(p) = \hat{K}^{\nu\mu,\alpha\beta}(p) = \hat{K}^{\mu\nu,\beta\alpha}(p) = \hat{K}^{\alpha\beta,\mu\nu}(-p) = \hat{K}^{*\alpha\beta,\mu\nu}(p) \quad (\text{E.155})$$

$$\hat{K}^{\alpha\beta}(p) = \hat{K}^{\beta\alpha}(p) = \hat{K}^{\alpha\beta}(-p) = \hat{K}^{*\alpha\beta}(p). \quad (\text{E.156})$$

The matrix of the propagators in momentum space is

$$\hat{\Delta}_{AP}(p) \equiv \begin{bmatrix} \hat{\Delta}_{\alpha\beta,\rho\sigma}(p) & \hat{\Delta}_{\alpha\beta}^*(p) \\ \hat{\Delta}_{\rho\sigma}(p) & \hat{\Delta}(p) \end{bmatrix}, \quad (\text{E.157})$$

with

$$\hat{\Delta}_{\alpha\beta,\rho\sigma}(p) \equiv \langle \hat{a}_{\alpha\beta}(p) \hat{a}_{\rho\sigma}(-p) \rangle \quad (\text{E.158})$$

$$\hat{\Delta}_{\alpha\beta}(p) \equiv \langle \hat{a}_{\alpha\beta}(p) \hat{b}(-p) \rangle \quad (\text{E.159})$$

$$\hat{\Delta}(p) \equiv \langle \hat{b}(p) \hat{b}(-p) \rangle, \quad (\text{E.160})$$

and is defined such that

$$\hat{K}^{MA} \hat{\Delta}_{AP} = \begin{bmatrix} \mathcal{I}_{\rho\sigma}^{\mu\nu} & 0 \\ 0 & 1 \end{bmatrix}, \quad (\text{E.161})$$

with

$$\mathcal{I}_{\rho\sigma}^{\mu\nu} \equiv \frac{1}{2} \left(\delta_{\rho}^{\mu} \delta_{\sigma}^{\nu} + \delta_{\sigma}^{\mu} \delta_{\rho}^{\nu} \right). \quad (\text{E.162})$$

On the basis $\{A^{(i)}\}$ (E.5)-(E.11) the propagator $\hat{\Delta}_{\alpha\beta,\rho\sigma}(p)$ can be expanded as

$$\hat{\Delta}_{\alpha\beta,\rho\sigma}(p) = \sum_{i=0}^6 c_i(p) A_{\alpha\beta,\rho\sigma}^{(i)}(p), \quad (\text{E.163})$$

and

$$\hat{\Delta}_{\alpha\beta}(p) = a_1(p) \eta_{\alpha\beta} + a_2(p) \frac{p_{\alpha} p_{\beta}}{p^2}, \quad (\text{E.164})$$

where $c_i(p)$ and $a_1(p)$, $a_2(p)$ are real functions. Our aim is to evaluate $c_i(p)$, $a_1(p)$, $a_2(p)$ from (E.161), which explicitly reads

$$\hat{K}^{\mu\nu,\alpha\beta} \hat{\Delta}_{\alpha\beta,\rho\sigma} + \hat{K}^{*\mu\nu} \hat{\Delta}_{\rho\sigma} = \mathcal{I}_{\rho\sigma}^{\mu\nu} \quad (\text{E.165})$$

$$\hat{K}^{\mu\nu,\alpha\beta} \hat{\Delta}_{\alpha\beta}^* + \hat{K}^{\mu\nu} \hat{\Delta} = 0 \quad (\text{E.166})$$

$$\hat{K}^{\alpha\beta} \hat{\Delta}_{\alpha\beta,\rho\sigma} = 0 \quad (\text{E.167})$$

$$\hat{K}^{\alpha\beta} \hat{\Delta}_{\alpha\beta}^* = 1. \quad (\text{E.168})$$

We thus get

$$-c_0 + 4mc_5 = \frac{1}{p^2} \quad \text{from (E.165)} \quad (\text{E.169})$$

$$\frac{1}{2}c_0 - p^2c_1 - 3mc_5 + mp^2c_6 = 0 \quad (\text{E.170})$$

$$-p^2c_2 + 2mc_5 - \frac{1}{2}\kappa_1a_2 = 0 \quad (\text{E.171})$$

$$c_3 + 2mc_5 - \frac{1}{2}\kappa_0a_1 = 0 \quad (\text{E.172})$$

$$c_3 + 2mc_5 + \frac{1}{2}\kappa_1a_1 = 0 \quad (\text{E.173})$$

$$2p^2c_1 + p^2c_2 - 2mp^2c_6 - \frac{1}{2}\kappa_0a_2 = 0 \quad (\text{E.174})$$

$$p^2c_5 + \frac{m}{4}c_0 = 0 \quad (\text{E.175})$$

$$\frac{1}{2}p^2c_5 - \frac{1}{2}mp^2c_1 - \frac{1}{2}p^4c_6 = 0 \quad (\text{E.176})$$

$$\kappa_0c_0 + 4p^2c_1(\kappa_0 + \kappa_1) + p^2c_2(\kappa_0 + 3\kappa_1) + p^4c_4(\kappa_0 + \kappa_1) = 0 \quad \text{from (E.166)} \quad (\text{E.177})$$

$$\kappa_1c_0 + (\kappa_0 + \kappa_1)p^2c_2 + c_3(\kappa_0 + 3\kappa_1) = 0 \quad (\text{E.178})$$

$$a_1 + \frac{\kappa_1}{2}\hat{\Delta} = 0 \quad \text{from (E.167)} \quad (\text{E.179})$$

$$a_1 - \frac{\kappa_0}{2}\hat{\Delta} = 0 \quad (\text{E.180})$$

$$-\frac{1}{2}[(\kappa_0 + \kappa_1)a_2 + (\kappa_0 + 3\kappa_1)a_1] = \frac{1}{p^2} \quad \text{from (E.168)} \quad (\text{E.181})$$

The solutions to (E.161) are given by

$$c_0 = -\frac{1}{p^2 + m^2} \quad c_1 = -\frac{1}{2p^2(p^2 + m^2)} \quad (\text{E.182})$$

$$c_2 = \frac{1}{2p^2} \left[\frac{\kappa_0 + 3\kappa_1}{(\kappa_0 + \kappa_1)p^2} - \frac{1}{p^2 + m^2} \right] \quad c_3 = \frac{1}{2} \left(\frac{1}{p^2 + m^2} - \frac{1}{p^2} \right) \quad (\text{E.183})$$

$$c_4 = \frac{1}{2p^4} \left[\frac{7}{p^2 + m^2} - \frac{(\kappa_0 + 3\kappa_1)^2}{p^2(\kappa_0 + \kappa_1)^2} \right] \quad c_5 = \frac{m}{4p^2(p^2 + m^2)} \quad (\text{E.184})$$

$$c_6 = \frac{m}{4p^4} \frac{3}{p^2 + m^2}, \quad (\text{E.185})$$

$$a_1 = 0 \quad ; \quad a_2 = -\frac{2}{p^2(\kappa_0 + \kappa_1)}, \quad (\text{E.186})$$

and

$$\hat{\Delta}(p) = 0. \quad (\text{E.187})$$

The massless limit of the above solution gives the following nontrivial coefficients

$$c_0 = -\frac{1}{p^2} \quad ; \quad c_1 = -\frac{1}{2p^4} \quad ; \quad c_2 = \frac{1}{p^4} \frac{\kappa_1}{\kappa_0 + \kappa_1} \quad ; \quad c_4 = \frac{1}{2p^6} \left[7 - \frac{(\kappa_0 + 3\kappa_1)^2}{(\kappa_0 + \kappa_1)^2} \right] \quad (\text{E.188})$$

$$a_2 = -\frac{2}{p^2(\kappa_0 + \kappa_1)}. \quad (\text{E.189})$$

Explicitly, the nonvanishing propagators are

$$\begin{aligned} \hat{\Delta}_{\alpha\beta,\rho\sigma}(p) &= \langle \hat{a}_{\alpha\beta}(p) \hat{a}_{\rho\sigma}(-p) \rangle \quad (\text{E.190}) \\ &= \frac{1}{2(p^2 + m^2)} \left[-2A^{(0)} - \frac{1}{p^2}A^{(1)} - \frac{1}{p^2}A^{(2)} + A^{(3)} + \frac{7}{p^4}A^{(4)} + \right. \\ &\quad \left. + \frac{m}{2p^2} \left(A^{(5)} + \frac{3}{p^2}A^{(6)} \right) \right]_{\alpha\beta,\rho\sigma} + \frac{1}{2p^2} \left[\frac{\kappa_0 + 3\kappa_1}{(\kappa_0 + \kappa_1)p^2} A^{(2)} - A^{(3)} + \right. \\ &\quad \left. - \frac{(\kappa_0 + 3\kappa_1)^2}{(\kappa_0 + \kappa_1)^2 p^4} A^{(4)} \right]_{\alpha\beta,\rho\sigma}, \quad (\text{E.191}) \end{aligned}$$

where in (E.190) we isolated the poles contributions. The propagators have a massive pole

$$p^2 = -m^2 \quad (\text{E.192})$$

and a good massless limit

$$\tilde{\Delta}_{\alpha\beta,\rho\sigma}(p) = \frac{1}{2p^2} \left[-2A^{(0)} - \frac{1}{p^2}A^{(1)} + \frac{2\kappa_1}{(\kappa_0 + \kappa_1)p^2}A^{(2)} + 2\frac{3\kappa_0^2 + 4\kappa_1\kappa_0 - \kappa_1^2}{(\kappa_0 + \kappa_1)^2 p^4}A^{(4)} \right]_{\alpha\beta,\rho\sigma}, \quad (\text{E.193})$$

which agrees with [70].

Appendix F.

Degrees of Freedom

F.1 Rank-2 Chern-Simons

To count the degrees of freedom (DoF) of the theory, we look for the number of independent components of the tensor field $a_{\mu\nu}(x)$ which, as a symmetric rank-2 tensor field, has a total of six components. The usual way to proceed [201, 202, 206, 207, 208, 209] is to write the equations of motion of the gauge fixed action S (5.55) in momentum space, and it is convenient to write the gauge fixing term S_{gf} in the form (5.154), where the scalar gauge condition is implemented by the scalar Lagrange multiplier $b(x)$. As already said, the Landau gauge $\zeta = 0$ is mandatory, due to fact that the gauge parameter ζ is massive ($[\zeta] = 3$). Therefore, the gauge fixing term is

$$S_{gf}^{(\zeta=0)} = \int d^3x b (\partial^\mu \partial^\nu a_{\mu\nu} + \kappa \square a). \quad (\text{F.1})$$

In momentum space, the EoM of the theory are

$$\frac{\delta S}{\delta \hat{a}_{\mu\nu}} = i\epsilon^{\alpha\beta\mu} p_\beta \hat{a}_\alpha^\nu + i\epsilon^{\alpha\beta\nu} p_\beta \hat{a}_\alpha^\mu - p^\mu p^\nu \hat{b} - \kappa \eta^{\mu\nu} p^2 \hat{b} \quad (\text{F.2})$$

$$\frac{\delta S}{\delta \hat{b}} = -p^\mu p^\nu \hat{a}_{\mu\nu} - \kappa p^2 \hat{a} = -p^\mu p^\nu \hat{a}_{\mu\nu} - \left(\frac{1}{3} + \kappa\right) p^2 \hat{a}, \quad (\text{F.3})$$

where $\hat{a}_{\mu\nu}(x)$ is the Fourier transform of the traceless part $\tilde{a}_{\mu\nu}(x)$ of the tensor field $a_{\mu\nu}(x)$. From the EoM (F.2), on shell one gets

$$\left(\epsilon_{\mu\lambda\rho} \frac{p^\lambda p_\nu}{p^2}\right) \frac{\delta S}{\delta \hat{a}_{\mu\nu}} = -i \frac{p_\rho}{p^2} (p^\nu p^\lambda \hat{a}_{\nu\lambda}) + i p^\nu \hat{a}_{\nu\rho} = -i \frac{p_\rho}{p^2} (p^\nu p^\lambda \hat{a}_{\nu\lambda}) + i p^\nu \hat{a}_{\nu\rho} = 0. \quad (\text{F.4})$$

The theory defined by the covariant fracton symmetry (4.60) is described by the invariant action S_{CS} (5.1), which actually is traceless. The trace $a(x)$ is introduced only through the gauge fixing term S_{gf} (5.54), which is needed to well define the Green function's generating functional $Z[J]$. The role of the gauge fixing procedure is that of eliminating the redundant degrees of freedom, and certainly not that of introducing new ones. Therefore, the trace $a(x)$, which enters the theory only through the gauge fixing term, cannot count as a physical DoF. The outcome of this reasoning is that, in order to avoid to introduce the trace $a(x)$ as a spurious DoF, we may (we should, actually), set in S_{gf} (5.54) the gauge parameter κ to the value which corresponds to gauge fix only the traceless part $\tilde{a}_{\mu\nu}(x)$ of $a_{\mu\nu}(x)$, that is

$$\kappa = -\frac{1}{3}, \quad (\text{F.5})$$

so that

$$S_{gf}^{(\tilde{\xi}=0)} \Big|_{\kappa=-\frac{1}{3}} = \int d^3x b \partial^\mu \partial^\nu \tilde{a}_{\mu\nu}. \quad (\text{F.6})$$

Using the momentum space gauge condition

$$\frac{\delta S}{\delta \hat{b}} = -p^\mu p^\nu \hat{a}_{\mu\nu} = 0 \quad (\text{F.7})$$

in (F.4), gives

$$p^\nu \hat{a}_{\nu\rho} = 0 \quad (\text{F.8})$$

representing three conditions on the five components of the traceless rank-2 symmetric tensor field $\hat{a}_{\nu\alpha}(p)$, which therefore has two independent components. Hence, the degrees of freedom of the theory are two.

F.2 Rank-2 BF

The on-shell EoM (5.88)-(5.92) in momentum space read

$$\frac{\delta S}{\delta \hat{a}_{\alpha\beta}} = \frac{i}{2} \left(\epsilon^{\alpha\mu\nu} p_\mu \hat{b}_\nu^\beta + \epsilon^{\beta\mu\nu} p_\mu \hat{b}_\nu^\alpha + p^\alpha \hat{b}^\beta + p^\beta \hat{b}^\alpha \right) - i\eta^{\alpha\beta} p_\mu \hat{b}^\mu - k_0 p^\alpha p^\beta \hat{d} - k_1 \eta^{\alpha\beta} p^2 \hat{d} = 0 \quad (\text{F.9})$$

$$\frac{\delta S}{\delta \hat{b}_{\alpha\beta}} = \frac{1}{2} \left(\epsilon^{\alpha\mu\nu} p_\mu \hat{a}_\nu^\beta + \epsilon^{\beta\mu\nu} p_\mu \hat{a}_\nu^\alpha \right) - \frac{\kappa_0}{2} \left(p^\alpha \hat{d}^\beta + p^\beta \hat{d}^\alpha \right) + \frac{1}{3} \kappa_0 \eta^{\alpha\beta} p_\mu \hat{d}^\mu = 0 \quad (\text{F.10})$$

$$\frac{\delta S}{\delta \hat{b}^\alpha} = -p^\mu \hat{a}_{\mu\alpha} + p_\alpha \hat{a} + \kappa_2 \epsilon_{\alpha\mu\nu} p^\mu \hat{d}^\nu = 0 \quad (\text{F.11})$$

$$\frac{\delta S}{\delta \hat{d}} = k_0 p^\mu p^\nu \hat{a}_{\mu\nu} + k_1 p^2 \hat{a} = 0 \quad (\text{F.12})$$

$$\frac{\delta S}{\delta \hat{d}^\alpha} = \kappa_0 p^\mu \hat{b}_{\mu\alpha} - \frac{1}{3} \kappa_0 p_\alpha \hat{b} + \kappa_2 \epsilon_{\alpha\mu\nu} p^\mu \hat{b}^\nu = \kappa_0 p^\mu \hat{\tilde{b}}_{\alpha\mu} + \kappa_2 \epsilon_{\alpha\mu\nu} p^\mu \hat{b}^\nu = 0, \quad (\text{F.13})$$

where the tracelessness condition (5.95) on the gauge parameters κ_0 and κ_1 has been taken into account, and

$$\tilde{b}_{\mu\nu} \equiv b_{\mu\nu} - \frac{1}{3} \eta_{\mu\nu} b \quad (\text{F.14})$$

is the traceless part of the $b_{\mu\nu}(x)$ field. From the above on-shell EoM we derive

$$\eta_{\alpha\beta} \frac{\delta S}{\delta \hat{a}_{\alpha\beta}} = -2i p_\mu \hat{b}^\mu - (k_0 + 3k_1) p^2 \hat{d} = 0 \quad (\text{F.15})$$

$$\frac{p_\alpha p_\beta}{p^2} \frac{\delta S}{\delta \hat{a}_{\alpha\beta}} = (k_0 + k_1) p^2 \hat{d} = 0 \quad (\text{F.16})$$

$$\frac{p_\alpha p_\beta}{p^2} \frac{\delta S}{\delta \hat{b}_{\alpha\beta}} = \frac{2}{3} \kappa_0 p_\mu \hat{d}^\mu = 0 \quad (\text{F.17})$$

$$p^\alpha \frac{\delta S}{\delta \hat{b}^\alpha} = -p^\mu p^\nu \hat{a}_{\mu\nu} + p^2 \hat{a} = 0 \quad (\text{F.18})$$

$$p^\alpha \frac{\delta S}{\delta \hat{d}^\alpha} = \kappa_0 p^\mu p^\nu \hat{b}_{\mu\nu} - \frac{1}{3} \kappa_0 p^2 \hat{b} = \kappa_0 p^\mu p^\nu \hat{\tilde{b}}_{\mu\nu} = 0. \quad (\text{F.19})$$

Using the conditions from the poles (5.98), according to which it must be $\kappa_0 \neq 0$ and $k_0 \neq -k_1$, and the EoM (F.15), (F.16) and (F.17), we get

$$p^2 \hat{d} = 0 \quad (\text{F.20})$$

$$p_\mu \hat{d}^\mu = 0 \quad (\text{F.21})$$

$$p_\mu \hat{b}^\mu = 0. \quad (\text{F.22})$$

Moreover, from (F.12) and (F.18) we find

$$p^\mu p^\nu \hat{a}_{\mu\nu} = 0 \quad (\text{F.23})$$

$$p^2 \hat{a} = 0. \quad (\text{F.24})$$

Considering (F.9), we have

$$\epsilon_{\alpha\lambda\rho} \frac{p^\lambda p_\beta}{p^2} \frac{\delta S}{\delta \hat{a}_{\alpha\beta}} = -\frac{i}{2} \left(p^\mu \hat{b}_{\mu\rho} + \epsilon_{\rho\mu\nu} p^\mu \hat{b}^\nu \right) = 0, \quad (\text{F.25})$$

where we used (F.14) and the EoM (F.19) with $\kappa_0 \neq 0$. Comparing (F.25) with (F.13) and considering the pole condition $\kappa_0 \neq \kappa_2$, we get

$$p^\mu \hat{b}_{\mu\sigma} = 0 \quad (\text{F.26})$$

$$\epsilon_{\mu\nu\rho} p^\nu \hat{b}^\rho = 0. \quad (\text{F.27})$$

We observe that Eq. (F.26) represents three equations on a 5-components field, thus the DoF contained in the traceless symmetric tensor $b_{\mu\nu}(x)$ are $5 - 3 = 2$. Furthermore, (F.27) can be solved

$$\hat{b}^\rho = p^\rho \hat{\varphi}, \quad (\text{F.28})$$

where $\varphi(x)$, due to (F.22), is a scalar harmonic function, indicating that the vector field $\hat{b}^\mu(x)$ only contributes with one DoF. Finally, from (F.11) we have

$$p^2 \frac{\delta S}{\delta \hat{b}^\alpha} = -p^\mu p^2 \hat{a}_{\mu\alpha} + \kappa_2 \epsilon_{\alpha\mu\nu} p^2 p^\mu \hat{d}^\nu = 0, \quad (\text{F.29})$$

where we used (F.24), and

$$\epsilon_{\beta\rho\sigma} \frac{p_\alpha p^\rho}{p^2} \frac{\delta S}{\delta \hat{b}_{\alpha\beta}} = \epsilon_{\beta\rho\sigma} p^\rho \left(\epsilon^{\beta\mu\nu} \frac{p_\mu p^\alpha}{p^2} \hat{a}_{\nu\alpha} + \kappa_0 \hat{d}^\beta \right) = -p^\alpha \hat{a}_{\alpha\sigma} + \kappa_0 \epsilon_{\sigma\mu\nu} p^\mu \hat{d}^\nu. \quad (\text{F.30})$$

Comparing (F.29) and (F.30), using (F.21), (F.23) and the pole condition $\kappa_0 \neq \kappa_2$ (5.98), we have

$$p^\alpha \hat{a}_{\alpha\sigma} = 0 \quad (\text{F.31})$$

$$\epsilon_{\alpha\mu\nu} p^\mu \hat{d}^\nu = 0. \quad (\text{F.32})$$

Eq.(F.31) represents three constraints on the 6-components of the symmetric tensor field $a_{\mu\nu}(x)$, which thus contribute with three DoF. We thus have three DoF from $a_{\mu\nu}(x)$, two from $b_{\mu\nu}(x)$ and one from $b^\mu(x)$, for a total of six DoF for the whole theory described by the gauge fixed action S (5.87).

F.3 Massive gauge theories

F.3.1 Maxwell-Chern-Simons

The EoM of the MCS action $S_{\text{MCS}}^{(ord)}$ (5.163) are :

$$\frac{\delta S_{\text{MCS}}^{(ord)}}{\delta A_\alpha} = -\partial_\mu F^{\alpha\mu} + M\epsilon^{\alpha\mu\nu} \partial_\mu A_\nu. \quad (\text{F.33})$$

By separating time and space components, and working in the Coulomb gauge

$$\partial^a A_a = 0, \quad (\text{F.34})$$

we obtain the following on-shell equations :

$$\frac{\delta S_{\text{MCS}}^{(ord)}}{\delta A_0} = \nabla^2 A^0 + M\epsilon^{0ab} \partial_a A_b = 0 \quad (\text{F.35})$$

$$\frac{\delta S_{\text{MCS}}^{(ord)}}{\delta A_a} = \square A^a - \partial^a \partial_0 A^0 + M\epsilon^{0ab} (\partial_b A_0 - \partial_0 A_b) = 0, \quad (\text{F.36})$$

where $\nabla^2 \equiv \partial_a \partial^a$ is the Laplace operator. Let us first consider the massless case, *i.e.* the pure Maxwell theory in 3D :

Massless case $M = 0$: from (F.35) we obtain

$$\nabla^2 A_0 = 0, \quad (\text{F.37})$$

a Poisson equation whose solution is

$$A_0 = 0 \quad (\text{F.38})$$

for fields vanishing at spatial infinity. Substituting this result into (F.36), gives

$$\square A_a = 0. \quad (\text{F.39})$$

Together with the transversality condition (F.34), this describes a single massless propagating DoF corresponding to a planar transverse spin-1 mode, thus recovering the well known fact that in 3D the photon is equivalent to a massless scalar field, known as the “dual photon” [210].

Massive case $M \neq 0$: we decompose $A_a(x)$ into its transverse and longitudinal components

$$A_a = u_a + \partial_a \psi, \quad (\text{F.40})$$

with

$$\partial^a u_a = 0 \quad \Rightarrow \quad u_a = \epsilon_{0ab} \partial^b u, \quad (\text{F.41})$$

where $u(x)$ and $\psi(x)$ are two scalar fields. The Coulomb gauge (F.34) then implies

$$\nabla^2 \psi = 0 \quad \Rightarrow \quad \psi = 0. \quad (\text{F.42})$$

The on-shell EoM (F.35), on the gauge condition (F.42), yields the Poisson equation

$$\nabla^2 (A^0 + Mu) = 0, \quad (\text{F.43})$$

whose solution relates the time component $A_0(x)$ to the longitudinal component of $A_a(x)$

$$A_0 = Mu, \quad (\text{F.44})$$

which generalizes (F.38) to the massive case. Using (F.42) and (F.44) into the EoM (F.36), we get

$$(\square - M^2)A_a = 0, \quad (\text{F.45})$$

which generalizes the massless wave equation (F.39) to a Klein-Gordon equation for $A_a(x)$ which shows that the MCS theory propagates a single massive scalar mode, since $A_a(x)$ is a planar transverse vector.

We therefore recovered that both 3D Maxwell and MCS theories display one propagating DoF, as expected since the topological nature of the CS term cannot change the number of DoF.

F.3.2 Massive fractons

From (5.164) and going on-shell, we have

$$\frac{\delta S_{inv}}{\delta a_{00}} = 0 \quad \Rightarrow \quad \nabla^2(\lambda - \partial_0\psi - mu) = 0, \quad (\text{F.46})$$

which gives

$$\lambda = \partial_0\psi + mu. \quad (\text{F.47})$$

From

$$\frac{\delta S_{inv}}{\delta a_{0i}} = 0, \quad (\text{F.48})$$

and using (F.47), we get

$$\epsilon^{0ij}\partial_j[(\square - m^2 + \nabla^2)u - \partial_0\nabla^2\xi - m\varphi] + \partial^i(-\nabla^2\psi + \partial_0\chi + m\nabla^2\xi) = 0. \quad (\text{F.49})$$

Taking the divergence ∂_i (F.49), we find the Poisson equation

$$\nabla^2[\partial_0\chi + \nabla^2(m\xi - \psi)] = 0 \quad \Rightarrow \quad \partial_0\chi + \nabla^2(m\xi - \psi) = 0. \quad (\text{F.50})$$

Moreover, acting with $\epsilon_{0ki}\partial^k$ (F.49) we find, again, a Poisson equation which gives

$$(\square - m^2)u + \nabla^2(u - \partial_0\xi) - m\varphi = 0. \quad (\text{F.51})$$

Finally, from

$$\frac{\delta S_{inv}}{\delta a_{ij}} = 0, \quad (\text{F.52})$$

and using (F.50), we get

$$\begin{aligned}
& [2(\eta^{ij} - \hat{\partial}^i \hat{\partial}^j) \square + m(\epsilon^{0ik} \hat{\partial}^j + \epsilon^{0jk} \hat{\partial}^i) \partial_0 \hat{\partial}_k] \varphi + \\
& + [(\epsilon^{0ik} \partial^j + \epsilon^{0jk} \partial^i) \partial_k (2\partial_0^2 - \nabla^2 + m^2) + 2m(\eta^{ij} \nabla^2 - \partial^i \partial^j) \partial_0] \xi + \\
& - [(\epsilon^{0ik} \partial^j + \epsilon^{0jk} \partial^i) \partial_k \partial_0 + 2m(\eta^{ij} \nabla^2 - \partial^i \partial^j)] u = 0, \quad (\text{F.53})
\end{aligned}$$

whose trace gives

$$\square \varphi + m \nabla^2 (\partial_0 \xi - u) = 0, \quad (\text{F.54})$$

and by computing $\epsilon_{0il} \partial^l \partial_j$ (F.53) we find

$$m \partial_0 \varphi - (\square - m^2) \nabla^2 \xi - \nabla^2 \partial_0 (u - \partial_0 \xi) = 0. \quad (\text{F.55})$$

In order to have the relevant equations at hand, we summarize them altogether :

$$\lambda - \partial_0 \psi - mu = 0 \quad (\text{F.56})$$

$$\partial_0 \chi + \nabla^2 (m\xi - \psi) = 0 \quad (\text{F.57})$$

$$(\square - m^2)u + \nabla^2 (u - \partial_0 \xi) - m\varphi = 0 \quad (\text{F.58})$$

$$\square \varphi + m \nabla^2 (\partial_0 \xi - u) = 0 \quad (\text{F.59})$$

$$m \partial_0 \varphi - (\square - m^2) \nabla^2 \xi - \nabla^2 \partial_0 (u - \partial_0 \xi) = 0, \quad (\text{F.60})$$

which in the longitudinal gauge (5.175) read

$$\lambda - \partial_0 \psi = 0 \quad (\text{F.61})$$

$$\partial_0 \chi + \nabla^2 (m\xi - \psi) = 0 \quad (\text{F.62})$$

$$\nabla^2 \partial_0 \xi + m\varphi = 0 \quad (\text{F.63})$$

$$\square \varphi + m \nabla^2 \partial_0 \xi = 0 \quad (\text{F.64})$$

$$m \partial_0 \varphi - (\square - m^2) \nabla^2 \xi + \nabla^2 \partial_0^2 \xi = 0. \quad (\text{F.65})$$

Massless case $m = 0$: let us consider first the massless case, where the above equations become

$$\lambda - \partial_0 \psi = 0 \quad (\text{F.66})$$

$$\partial_0 \chi - \nabla^2 \psi = 0 \quad (\text{F.67})$$

$$\nabla^2 \partial_0 \xi = 0 \quad (\text{F.68})$$

$$\square \varphi = 0 \quad (\text{F.69})$$

$$\square \nabla^2 \xi - \nabla^2 \partial_0^2 \xi = 0, \quad (\text{F.70})$$

which imply that the massless theory described by the pure fractonic action S_M (5.150), which corresponds to the Maxwell action, features two DoF: $\varphi(x)$, associated to the transverse component of $a_{ij}(x)$ through (5.167) and satisfying the wave equation (F.69), and $\chi(x)$, associated with the longitudinal sector. The fields $\psi(x)$ and $\lambda(x)$ are determined by $\chi(x)$ through (F.67) and (F.66), while $\xi(x)$, associated to the solenoidal part of $a_{ij}(x)$, due to (F.68) is constant

$$\partial_0 \xi = 0, \quad (\text{F.71})$$

as a consequence of which (F.70) becomes $(\nabla^2)^2 \xi = 0$, which is solved by

$$\xi = 0. \quad (\text{F.72})$$

Massive case $m \neq 0$: in the longitudinal gauge (5.175), described by Eqs. (F.61)-(F.65), from (F.63) and (F.64) we immediately find that $\varphi(x)$ satisfies the Klein-Gordon equation

$$(\square - m^2)\varphi = 0. \quad (\text{F.73})$$

Alternatively, using (F.63) in (F.65) we find that $\nabla^2 \xi(x)$ satisfies the same Klein-Gordon equation

$$(\square - m^2)\nabla^2 \xi = 0, \quad (\text{F.74})$$

but $\nabla^2 \xi(x)$ and $\varphi(x)$ are non independent one from each other because they are related by (F.63). Hence, $\varphi(x)$ – or, equivalently, $\nabla^2 \xi(x)$ – is a propagating massive DoF. The field $\chi(x)$ remains dynamical and continues to determine $\psi(x)$ and $\lambda(x)$, as in the massless case.

It is also worth noting that the two DoF of the theory – $\nabla^2\zeta(x)$ and $\chi(x)$ – belong to the spatial component $a_{ij}(x)$ of the tensor field $a_{\mu\nu}(x)$, as it happens also in 4D Linearized Gravity [193, 211]. Hence, one might argue that, by adopting – as in 4D Linearized Gravity – a vector gauge fixing, in particular the condition

$$a_{0\mu} = 0 \Leftrightarrow \lambda = u = \psi = 0, \quad (\text{F.75})$$

instead of the scalar one (5.153), we would obtain the same physical content. This is despite the fact that a vector gauge condition like (F.75) corresponds to the infinitesimal diffeomorphism transformation (4.66), which is not a symmetry of the action S_M (5.150). Nonetheless, such a situation may arise in fractonic theories. Indeed, in [71], where fractons coupled to 4D Linearized Gravity were studied, it was shown that this property holds: over-gauging the longitudinal diffeomorphisms (4.60) with a vector gauge condition, instead of the more appropriate scalar one, leads to the same number of DoF. A closer inspection here, however, shows that this is not the case. In fact, considering the gauge fixing (F.75), Eq. (F.62) reduces to $\partial_0\chi + m\nabla^2\zeta = 0$

$$\partial_0\chi + m\nabla^2\zeta = 0, \quad (\text{F.76})$$

which relates the two DoF previously identified. Hence, a vectorial gauge fixing is not applicable in this context, since over-gauging the theory with a vector condition removes one DoF out of two. This is perfectly natural – if anything, the opposite would have been surprising.

Appendix G.

Rank 2 BF: symmetric case

When matter is introduced, the total action reads

$$S_{tot}^{(s)} \equiv S_{BF}^{(s)} + S_J^{(s)} + S_K^{(s)}, \quad (\text{G.1})$$

where $S_{BF}^{(s)}$ is given by (5.145) and

$$S_J^{(s)} \equiv - \int d^3x \tilde{j}^{\mu\nu} \tilde{a}_{\mu\nu} \quad (\text{G.2})$$

$$S_K^{(s)} \equiv - \int d^3x \tilde{k}^{\mu\nu} \tilde{\Phi}_{\mu\nu}, \quad (\text{G.3})$$

where $\tilde{a}_{\mu\nu}(x)$ and $\tilde{\Phi}_{\mu\nu}(x)$ are the traceless components of $a_{\mu\nu}(x)$ and $\Phi_{\mu\nu}(x)$ while $\tilde{j}^{\mu\nu}(x)$ and $\tilde{k}^{\mu\nu}(x)$ are rank-2 symmetric traceless tensor currents. The corresponding on-shell EoM are

$$\tilde{j}^{\alpha\beta} = \frac{\delta S_{BF}^{(s)}}{\delta \tilde{a}_{\alpha\beta}} = \frac{1}{2} \left(\epsilon^{\mu\nu\alpha} \partial_\mu \tilde{\Phi}_\nu^\beta + \epsilon^{\mu\nu\beta} \partial_\mu \tilde{\Phi}_\nu^\alpha \right) \quad (\text{G.4})$$

$$\tilde{k}^{\alpha\beta} = \frac{\delta S_{BF}^{(s)}}{\delta \tilde{\Phi}_{\alpha\beta}} = \frac{1}{2} \left(\epsilon^{\mu\nu\alpha} \partial_\mu \tilde{a}_\nu^\beta + \epsilon^{\mu\nu\beta} \partial_\mu \tilde{a}_\nu^\alpha \right), \quad (\text{G.5})$$

which we observe to be a rank-2 generalization of the ones derived for the description of topological insulators [148]. From (G.4) and (G.5) and assuming that the vacuum solutions of the EoM of $\tilde{a}_{00}(x)$ and $\tilde{\Phi}_{00}(x)$, given by

$$\tilde{a}_{0j} = \partial_j \psi \quad (\text{G.6})$$

$$\tilde{\Phi}_{0j} = \partial_j \phi, \quad (\text{G.7})$$

continue to be true also when matter is introduced, we can derive the two continuity equations

$$\partial_0 \rho_J + \partial_i \partial_j \tilde{J}^{ij} = 0 \quad (\text{G.8})$$

$$\partial_0 \rho_K + \partial_i \partial_j \tilde{K}^{ij} = 0, \quad (\text{G.9})$$

where we defined the two scalar charge densities

$$\rho_J = 2\partial_i \tilde{J}^{i0} \quad (\text{G.10})$$

$$\rho_K = 2\partial_i \tilde{K}^{i0}. \quad (\text{G.11})$$

These charge densities are fractonic since (G.8) and (G.9) imply both the conservation of total charges and of the total dipole momenta. Moreover, from the continuity equations (G.8) and (G.9), the traces of the quadrupole momenta are conserved

$$\partial_0 \int d\Sigma \eta^{ij} x_i x_j \rho_J = - \int d\Sigma \eta^{ij} x_i x_j \partial_k \partial_l \tilde{J}^{kl} \propto \int d\Sigma \eta_{kl} \tilde{J}^{kl} = \int d\Sigma \tilde{J}^{00} = 0 \quad (\text{G.12})$$

$$\partial_0 \int d\Sigma \eta^{ij} x_i x_j \rho_K = - \int d\Sigma \eta^{ij} x_i x_j \partial_k \partial_l \tilde{K}^{kl} \propto \int d\Sigma \eta_{kl} \tilde{K}^{kl} = \int d\Sigma \tilde{K}^{00} = 0, \quad (\text{G.13})$$

where the last steps follow from the solutions (G.6) and (G.7), which imply that the 00-components of the traceless tensor currents $\tilde{k}^{\alpha\beta}(x)$ and $\tilde{J}^{\alpha\beta}(x)$ vanish. Hence both dipoles are constrained to move in straight lines which are perpendicular to their dipole momenta [156], *i.e.* they behave as lineons. Working on-shell on the vacuum solution (G.6) of the EoM of $\tilde{\Phi}_{00}(x)$, in analogy with the standard abelian BF theory in 3D [38, 148, 183], we can rewrite the on-shell EoM (G.5) explicitly in terms of generalized electric and magnetic fields

$$\left. \frac{\delta S_{BF}^{(s)}}{\delta \tilde{\Phi}_{ij}} \right|_{(\text{G.6})} \equiv \frac{1}{4} \left(\epsilon^{0ki} \tilde{\mathcal{E}}_k^j + \epsilon^{0kj} \tilde{\mathcal{E}}_k^i \right) \quad (\text{G.14})$$

$$\frac{\delta S_{BF}^{(s)}}{\delta \tilde{\Phi}_{0i}} \equiv \frac{1}{2} \tilde{\mathcal{B}}^i \quad (\text{G.15})$$

as

$$\rho_K = \partial_i \tilde{\mathcal{B}}^i \quad (\text{G.16})$$

$$\tilde{K}^{ij} = \tilde{\sigma}_{(s)}^{ijkl} \tilde{\mathcal{E}}_{kl}, \quad (\text{G.17})$$

with

$$\tilde{\sigma}_{(s)}^{ijkl} = \tilde{\sigma}_{(s)}^{ijlk} = \tilde{\sigma}_{(s)}^{jikl} \equiv \frac{1}{8} \left(\epsilon^{0ki} \eta^{jl} + \epsilon^{0li} \eta^{jk} + \epsilon^{0kj} \eta^{il} + \epsilon^{0lj} \eta^{ik} \right). \quad (\text{G.18})$$

Notice that (G.16) and (G.17) represent, respectively, a magnetic Gauss law and a generalized Hall current for the type-K charges.

Appendix H.

Massive fractons: coupling to matter

In presence of external matter the action can be written as

$$S_{tot} \equiv S_{inv} + S_J , \quad (\text{H.1})$$

where S_{inv} is given by (5.152),

$$S_J \equiv - \int d^3x J^{\mu\nu} a_{\mu\nu} \quad (\text{H.2})$$

and $J^{\mu\nu}(x) = J^{\nu\mu}(x)$ is the matter current. The on-shell EoM

$$\frac{\delta S_{tot}}{\delta a_{\alpha\beta}} = 0 \quad (\text{H.3})$$

generalizes (5.164) to

$$-\partial_\mu F^{\alpha\beta\mu} = J_{CS}^{\alpha\beta} + J^{\alpha\beta} , \quad (\text{H.4})$$

where $J_{CS}^{\mu\nu}(x)$ is given by (5.195). Therefore, according to the discussion of the previous Sections, we can see that the MCS-like theory (H.1) is characterized by two types of matter: an intrinsic one $J_{CS}^{\mu\nu}(x)$ (5.195) and an external one $J^{\mu\nu}(x)$ (H.2). Using (4.100), the 00-component of the on-shell EoM (H.4), implies

$$J^{00} = 0 . \quad (\text{H.5})$$

Moreover, from the EoM (H.4), one has

$$\partial_\alpha \partial_\beta J^{\alpha\beta} = 0 , \quad (\text{H.6})$$

which is the typical sign of a fractonic behaviour. In fact, as a consequence of (H.5), this nonstandard conservation equation can be rewritten in the same way as (5.189)

$$\partial_0 \rho + \partial_i \partial_j J^{ij} = 0, \quad (\text{H.7})$$

where we defined the charge density

$$\rho \equiv 2\partial_i J^{0i}, \quad (\text{H.8})$$

as in (5.196). The fractonic behaviour emerges from (H.7), since it implies the conservations of both the total charge

$$\partial_0 \int d\Sigma \rho = - \int d\Sigma \partial_i \partial_j J^{ij} = 0 \quad (\text{H.9})$$

and, up to boundary terms, the total dipole moment $D^k(t)$:

$$\partial_0 D^k \equiv \partial_0 \int d\Sigma d^k = \partial_0 \int d\Sigma x^k \rho = - \int d\Sigma x^k \partial_i \partial_j J^{ij} = 0, \quad (\text{H.10})$$

where

$$d^i \equiv -2J^{i0} \quad (\text{H.11})$$

is the dipole density. Notice however that, differently from the intrinsic case (5.189), which implies the conservation of $D_{\text{CS}}^i(t)$ (5.191), the continuity equation (H.7) for the external matter does not imply the conservations of the trace of the quadrupole moment

$$D \equiv \int d\Sigma x^2 \rho, \quad (\text{H.12})$$

since in this case $J^\mu{}_\mu(x) \neq 0$. Therefore the external matter contribution describes quasiparticles with different mobility: fractonic immobile charges and free dipoles, related to the conservation of charge (H.9) and total dipole moment (H.10) only [60, 149]. Taking into account the definitions of the electric and magnetic-like fields $\mathcal{E}^{ij}(x)$ (5.132) and $\mathcal{B}^i(x)$ (5.133), the nontrivial components of the EoM (H.4) read

- $\alpha = 0, \beta = i$

$$\partial_j \mathcal{E}^{ij} = -\rho_{\text{CS}}^i - d^i, \quad (\text{H.13})$$

from which it follows that the Gauss constraint is

$$\partial_i \partial_j \mathcal{E}^{ij} = \rho_{\text{CS}} + \rho, \quad (\text{H.14})$$

where we used the definitions of intrinsic fractonic charge $\rho_{\text{CS}}(x)$ (5.181) and dipole $\rho_{\text{CS}}^i(x)$ (5.180) densities. Remembering that $\rho_{\text{CS}}(x) \propto \partial_i \mathcal{B}^i(x)$ through (5.181), the above equation implies that the fracton density $\rho(x)$ is a source for both generalized electric and magnetic fields, similarly to [167]. Moreover, from (H.13), we observe that

$$- \int d\Sigma \mathcal{B}^i = \frac{D^i}{m}, \quad (\text{H.15})$$

is a higher-rank generalization of the relation which characterizes the ordinary abelian MCS theory [168, 169]

$$- \int d\Sigma B = \frac{Q}{m}, \quad (\text{H.16})$$

where $B(x)$ and $Q(t)$ are the ordinary magnetic field and the total electric charge respectively. Notice that (H.15) can be seen as an integrated version of the dipole-flux attachment relation that is found in the higher-rank CS theory for fractons [3]. As a consequence of the introduction of external matter, we also observe that from (H.14) and (5.185) it follows that

$$\int d\Sigma x^2 \rho = 2 \int d\Sigma \mathcal{E}, \quad (\text{H.17})$$

which means that in this case, differently from the (vacuum) intrinsic CS-like matter case (5.186), the trace of the electric field $\mathcal{E}^{ij}(x)$ does not vanish globally. In other words, in presence of an external matter coupling, a longitudinal motion of the dipole $d^i(x)$ is allowed and associated to a change in the trace $E(x)$ [153].

- $\alpha = i, \beta = j$

$$\partial_0 \mathcal{E}^{ij} - \frac{1}{2} \left(\epsilon^{0ki} \partial_k \mathcal{B}^j + \epsilon^{0kj} \partial_k \mathcal{B}^i \right) + \frac{1}{2} m \left(\epsilon^{0ik} \mathcal{E}_k^j + \epsilon^{0jk} \mathcal{E}_k^i \right) + J^{ij} = 0, \quad (\text{H.18})$$

which, by recalling the definition (5.188), can also be written as

$$-\partial_0 \mathcal{E}^{ij} + \frac{1}{2} \left(\epsilon^{0ki} \partial_k \mathcal{B}^j + \epsilon^{0kj} \partial_k \mathcal{B}^i \right) = J_{\text{CS}}^{ij} + J^{ij}. \quad (\text{H.19})$$

When taking into account the external matter contribution (H.2), the changes in the on-shell conservation of the total energy-momentum tensor allow us to identify additional contributions to the power and force in (I.24) and (I.25):

$$\partial^\alpha T_{\alpha 0}^{(fr)} = -f_0^{(L)} \quad (\text{H.20})$$

$$\partial^\alpha T_{\alpha i}^{(fr)} = F_i - f_i^{\text{CS}} - f_i^{(L)}, \quad (\text{H.21})$$

where $F_i(x)$ is the diffeomorphism breaking term (I.26), $f_i^{\text{CS}}(x)$ is the intrinsic Lorentz force (I.27) and

$$f_0^{(L)} \equiv -\frac{1}{2} \mathcal{E}_{ij} J^{ij} \quad (\text{H.22})$$

$$f_i^{(L)} \equiv -d^j \mathcal{E}_{ij} + \frac{1}{2} \epsilon_{0ij} J^{jk} \mathcal{B}_k \quad (\text{H.23})$$

are respectively the fractonic power and Lorentz-like force associated to the external fractonic matter. Notice that, due to the external matter contribution, the power $f_0^{(L)}(x)$ (H.22) does not vanish, differently from the contribution (I.28) of the CS-like term.

Appendix I.

3D covariant massive fractons: energy momentum tensor

Making explicit the metric dependence of the invariant action (5.162)

$$S_{inv} = \int d^3x \left(-\frac{1}{6} \sqrt{-g} g^{\mu\alpha} g^{\nu\beta} g^{\rho\gamma} F_{\alpha\beta\gamma} F_{\mu\nu\rho} + m \epsilon^{\mu\nu\rho} g^{\lambda\sigma} a_{\mu\lambda} \partial_\nu a_{\rho\sigma} \right), \quad (\text{I.1})$$

we can compute the energy-momentum tensor

$$\begin{aligned} T_{\alpha\beta} &\equiv -\frac{2}{\sqrt{-g}} \frac{\delta S_{inv}}{\delta g^{\alpha\beta}} \Big|_{g=\eta} \\ &= -\frac{1}{6} \eta_{\alpha\beta} F^2 + \frac{1}{3} \eta_{\alpha\gamma} \eta_{\beta\lambda} \left(2F^{\lambda\nu\rho} F^\gamma_{\nu\rho} + F^{\mu\nu\lambda} F_{\mu\nu}{}^\gamma \right) - m \epsilon^{\mu\nu\rho} (a_{\mu\alpha} \partial_\nu a_{\rho\beta} + a_{\mu\beta} \partial_\nu a_{\rho\alpha}). \end{aligned} \quad (\text{I.2})$$

On the particular solution (4.100) the components of (I.2) read

$$T_{00} = \frac{1}{4} \left(\mathcal{E}^{ij} \mathcal{E}_{ij} + \mathcal{B}^i \mathcal{B}_i \right) \quad (\text{I.3})$$

$$T_{0i} = -\frac{1}{2} \left[\epsilon_{0ij} \mathcal{E}^{jk} \mathcal{B}_k + m \left(\partial_0 \psi \mathcal{B}_i - \epsilon^{0jk} \partial_j \psi \mathcal{E}_{ik} \right) \right] \quad (\text{I.4})$$

$$\begin{aligned} T_{ij} &= \frac{1}{4} \eta_{ij} (\mathcal{E}^{ab} \mathcal{E}_{ab} + \mathcal{B}^a \mathcal{B}_a) - \mathcal{E}_i{}^a \mathcal{E}_{ja} + \frac{1}{2} \mathcal{B}_i \mathcal{B}_j + \\ &\quad + \frac{m}{2} \left[\epsilon^{0mn} (a_{mi} \mathcal{E}_{nj} + a_{mj} \mathcal{E}_{ni}) - (\partial_i \psi \mathcal{B}_j + \partial_j \psi \mathcal{B}_i) \right]. \end{aligned} \quad (\text{I.5})$$

We observe that the energy density (I.3) is positive definite and formally identical to the 3D electromagnetic one

$$u = \frac{1}{2} \left(E^i E_i + B^2 \right) , \quad (\text{I.6})$$

of which it represents a higher rank extension. We however notice that the CS-like contribution in $T_{\alpha\beta}(x)$ (I.2) breaks gauge invariance by a term which is a total derivative

$$\delta T_{\alpha\beta} = -m\epsilon^{\mu\nu\rho} \partial_\mu \left(\partial_\alpha \phi \partial_\nu a_{\rho\beta} + \partial_\beta \phi \partial_\nu a_{\rho\alpha} \right) . \quad (\text{I.7})$$

Notice that on the fractonic solution (4.100) one has

$$\delta T_{00}|_{(4.100)} = 0 , \quad (\text{I.8})$$

while $\delta T_{\alpha i}|_{(4.100)} = \text{boundary terms}$. Hence in the fractonic embedding the energy density (I.3) is indeed invariant. The same issue of non-gauge invariance (I.7) affects Linearized Gravity [212, 213], and is related to the fact that the action of the model is invariant up to boundary terms. Therefore, in order to obtain a gauge-invariant physical energy-momentum tensor, an ‘‘average’’ over a length scale l is performed, as done in Linearized Gravity [212, 213]: a convolution with a well behaved weighting function is taken over a spacetime volume of size l , in such a way that boundary terms can be neglected $\langle X\partial Y \rangle \sim -\langle Y\partial X \rangle$. In this way, the resulting ‘‘averaged’’ energy moment tensor

$$\bar{T}_{\mu\nu} \equiv \langle T_{\mu\nu} \rangle \quad (\text{I.9})$$

is gauge invariant

$$\delta \bar{T}_{\mu\nu} = 0 . \quad (\text{I.10})$$

In particular the averaged component $\bar{T}_{0i}(x)$ (I.4) reads

$$\bar{T}_{0i} = -\frac{1}{2} \langle \epsilon_{0ij} \mathcal{E}^{jk} \mathcal{B}_k \rangle , \quad (\text{I.11})$$

where Faraday’s law (5.193) has been used, which strongly reminds the Poynting vector of 3D electromagnetism

$$S^i = \epsilon^{0ij} E_j B . \quad (\text{I.12})$$

One might see also an analogy between $T_{ij}(x)$ (I.5) (and its average $\bar{T}_{ij}(x)$) and the electromagnetic stress tensor

$$\sigma_{ij} = E_i E_j - \frac{1}{2} \eta_{ij} (E^i E_i + B^2), \quad (\text{I.13})$$

since both are quadratic forms diagonal in the (generalized) electric and magnetic fields. The differences reside in the fact that the CS-like term (5.151) contributes to the energy moment tensor. In the massless limit ($m \rightarrow 0$) the contribution to the total energy moment tensor comes from the fractonic Maxwell-like action only S_{fr} (5.150)

$$T_{\mu\nu}|_{m=0} = T_{\mu\nu}^{(\text{fr})}, \quad (\text{I.14})$$

which is gauge invariant without the need of the average prescription (I.9). The components of $T_{\mu\nu}^{(\text{fr})}(x)$, on the solution (4.100), read

$$T_{00}^{(\text{fr})} = \frac{1}{4} (\mathcal{E}^{ij} \mathcal{E}_{ij} + \mathcal{B}^i \mathcal{B}_i) \quad (\text{I.15})$$

$$T_{0i}^{(\text{fr})} = -\frac{1}{2} \epsilon_{0ij} \mathcal{E}^{jk} \mathcal{B}_k \quad (\text{I.16})$$

$$T_{ij}^{(\text{fr})} = \frac{1}{4} \eta_{ij} (\mathcal{E}^{ab} \mathcal{E}_{ab} + \mathcal{B}^a \mathcal{B}_a) - \mathcal{E}_i^a \mathcal{E}_{ja} + \frac{1}{2} \mathcal{B}_i \mathcal{B}_j. \quad (\text{I.17})$$

Using the Gauss (5.181), Ampère (5.187), and Faraday (5.193) laws at $m = 0$, we have

$$\partial^\alpha T_{\alpha 0}^{(\text{fr})} \Big|_{m=0} = \left(\partial^0 T_{00}^{(\text{fr})} + \partial^i T_{i0}^{(\text{fr})} \right) \Big|_{m=0} = 0, \quad (\text{I.18})$$

which is the continuity equation for the energy density $T_{00}^{(\text{fr})}(x)$ in the massless limit. On the other hand we have

$$\partial^\alpha T_{\alpha i}^{(\text{fr})} \Big|_{m=0} = \frac{3}{4} B_i \partial^j B_j + \frac{1}{2} B_j \partial^j B_i - \frac{1}{2} E^{jk} \partial_j E_{ik}, \quad (\text{I.19})$$

which therefore is not conserved, as in the 4D case [74]¹. Nonetheless this result is useful to identify a fractonic force, which can be done as follows. In ordinary electromagnetism matter is introduced by adding a source term to the Maxwell action

$$S_{\text{Max}} \rightarrow S_{\text{Max}} + \int d^3x A_\mu J^\mu, \quad (\text{I.20})$$

¹We remind that, as discussed in [74], the energy-momentum tensor defined as (I.2) is the conserved current associated to the diffeomorphism invariance, and it should not be conserved in a theory invariant under (4.60), which is a subclass of the diffeomorphism transformation (4.66).

which contributes to the total energy-momentum tensor by means of an additional term $T_{\mu\nu}^{(J)}(x)$

$$T_{\mu\nu}^{(tot)} = T_{\mu\nu}^{(Max)} + T_{\mu\nu}^{(J)}, \quad (\text{I.21})$$

where $T_{\mu\nu}^{(Max)}(x)$ is the energy-momentum tensor associated to the Maxwell action S_{Max} . The Lorentz force can be identified as the contribution from $T_{\mu\nu}^{(J)}(x)$, as [214, 215]

$$f_\nu \equiv \partial^\mu T_{\mu\nu}^{(J)}, \quad (\text{I.22})$$

so that, from the conservation of the total energy-momentum tensor, we have

$$f_\nu = -\partial^\mu T_{\mu\nu}^{(Max)}. \quad (\text{I.23})$$

In the massive fractonic theory we have seen that the CS-like term plays the role of “intrinsic matter” (5.194), and is thus analogous to S_J in (I.20), in the same way as S_{fr} (5.150) can be related to the invariant Maxwell action S_{Max} . We therefore expect the appearance of an “intrinsic force” in analogy with (I.23). From the fractonic energy-momentum tensor (I.15)-(I.17), using the Gauss (5.181), Ampère (5.187), and Faraday (5.193) laws, *i.e.* going on-shell, we have

$$\partial^\alpha T_{\alpha 0}^{(fr)} = \frac{1}{2} \mathcal{E}_{ij} J_{CS}^{ij} = 0 \quad (\text{I.24})$$

$$\partial^\alpha T_{\alpha i}^{(fr)} = F_i - f_i^{CS}, \quad (\text{I.25})$$

where (I.24) can be directly verified using (5.188), and

$$F_i \equiv \frac{3}{4} \mathcal{B}_i \partial^j \mathcal{B}_j + \frac{1}{2} \mathcal{B}_j \partial^j \mathcal{B}_i - \frac{1}{2} \mathcal{E}^{jk} \partial_j \mathcal{E}_{ik} \quad (\text{I.26})$$

$$f_i^{CS} \equiv -\rho_{CS}^j \mathcal{E}_{ij} + \frac{1}{2} \epsilon_{0ij} J_{CS}^{jk} \mathcal{B}_k. \quad (\text{I.27})$$

In analogy with (I.23), (I.24) leads to

$$f_0^{CS} = -\frac{1}{2} E_{ij} J_{CS}^{ij} = 0, \quad (\text{I.28})$$

which means that the generalized current $J_{CS}^{ij}(x)$ (5.188) and the electric tensor field $\mathcal{E}^{ij}(x)$ (5.132) are orthogonal to each other, which is typical of a Hall-like current [3, 77], and the fractonic power $f_0^{CS}(x)$ due to the CS-like term vanishes (I.28). Notice that

the fact that the power $f_0^{\text{CS}}(x)$ (I.28) vanishes is in agreement with the interpretation of the CS-like contribution as intrinsic matter. Indeed, since the power is referred to some kind of dispersion/energy transfer, we expect it to vanish in a process which is exclusively internal. On the other hand, we see that with respect to the massless case (I.19), the divergence of the energy-momentum tensor (I.25) has two contributions. The first $F_i(x)$ (I.26) is a consequence of the breaking of diffeomorphism invariance, and the second $f_i^{\text{CS}}(x)$ (I.27) is due to the presence of the CS-like term and can be recognized as a kind of Lorentz-like force related to the (intrinsic) matter contribution. Interestingly, this force can also be rewritten in terms of the electric and magnetic fields as

$$f_i^{\text{CS}} = -\frac{1}{4}m (2\mathcal{E}_{ia}\mathcal{B}^a + \mathcal{E}\mathcal{B}_i) , \quad (\text{I.29})$$

with $\mathcal{E}(x) \equiv \eta^{ij}\mathcal{E}_{ij}(x)$, which makes explicit its gauge invariance and reminds the Lorentz force contribution (Eq.(28) of [216] for instance) of axion electrodynamics [194, 195, 217].

Bibliography

- [1] D. Sacco Shaikh, M. Sassetti and N. Traverso Ziani, “Parity-Dependent Quantum Phase Transition in the Quantum Ising Chain in a Transverse Field,” *Symmetry* **14** (2022) no.5, 996 doi:10.3390/sym14050996
- [2] D. S. Shaikh, A. G. Catalano, F. Cavaliere, F. Franchini, M. Sassetti and N. T. Ziani, “Phase diagram of the topologically frustrated XY chain,” *Eur. Phys. J. Plus* **139** (2024) no.8, 743 doi:10.1140/epjp/s13360-024-05534-z
- [3] E. Bertolini, A. Blasi, N. Maggiore and D. S. Shaikh, “Hall-like behaviour of higher rank Chern-Simons theory of fractons,” *JHEP* **10** (2024), 232 doi:10.1007/JHEP10(2024)232.
- [4] E. Bertolini, A. Blasi, M. Carrega, N. Maggiore and D. S. Shaikh, “Fractons from covariant higher-rank three-dimensional BF theory,” *Phys. Rev. B* **111** (2025) no.8, 085126 doi:10.1103/PhysRevB.111.085126.
- [5] E. Bertolini, M. Carrega, N. Maggiore and D. Sacco Shaikh, “Covariant field theory of 3D massive fractons,” *Eur. Phys. J. C* **85** (2025) no.10, 1222 doi:10.1140/epjc/s10052-025-14978-1
- [6] F. R. De Filippi, A. F. Mello, D. S. Shaikh, M. Sassetti, N. T. Ziani and M. Grossi, “Few-Body Precursors of Topological Frustration,” *Symmetry* **16** (2024) no.8, 1078 doi:10.3390/sym16081078
- [7] R. Grazi, D. S. Shaikh, M. Sassetti, N. T. Ziani and D. Ferraro, “Controlling Energy Storage Crossing Quantum Phase Transitions in an Integrable Spin Quantum Battery,” *Phys. Rev. Lett.* **133** (2024) no.19, 197001 doi:10.1103/PhysRevLett.133.197001
- [8] N. Goldenfeld, “Lectures on Phase Transitions and the Renormalization Group,” Addison–Wesley, Reading, MA, (1992).

- [9] P. W. Anderson, "More Is Different," *Science* **177** (1972) no.4047, 393-396 doi:10.1126/science.177.4047.393.
- [10] X. G. Wen, "Quantum Field Theory of Many-Body Systems: From the Origin of Sound to an Origin of Light and Electrons," Oxford University Press, (2004).
- [11] L. D. Landau, "The Theory of a Fermi Liquid," *J. Exp. Theor. Phys.* **30** (1956), 1058 doi:10.1016/b978-0-08-010586-4.50095-x
- [12] L. D. Landau, "Oscillations in a Fermi Liquid," *Sov. Phys. JETP* **5** (1957), 101-108 doi:10.1016/b978-0-08-010586-4.50096-1
- [13] L. D. Landau, "On the Theory of the Fermi Liquid," *J. Exp. Theor. Phys.* **35** (1958), 97 doi:10.1016/b978-0-08-010586-4.50100-0
- [14] V. L. Ginzburg and L. D. Landau, "On the Theory of superconductivity," *Zh. Eksp. Teor. Fiz.* **20** (1950), 1064-1082 doi:10.1016/b978-0-08-010586-4.50078-x
- [15] M. Kardar, "Statistical Physics of Fields," Cambridge University Press, Cambridge, UK (2007) doi:10.1017/CBO9780511815881
- [16] K. G. Wilson, "Renormalization group and critical phenomena. 1. Renormalization group and the Kadanoff scaling picture," *Phys. Rev. B* **4** (1971), 3174-3183 doi:10.1103/PhysRevB.4.3174
- [17] K. G. Wilson, "Renormalization group and critical phenomena. 2. Phase space cell analysis of critical behavior," *Phys. Rev. B* **4** (1971), 3184-3205 doi:10.1103/PhysRevB.4.3184
- [18] Y. Nambu, "Quasiparticles and Gauge Invariance in the Theory of Superconductivity," *Phys. Rev.* **117** (1960), 648-663 doi:10.1103/PhysRev.117.648
- [19] J. Goldstone, "Field Theories with Superconductor Solutions," *Nuovo Cim.* **19** (1961), 154-164 doi:10.1007/BF02812722
- [20] A. J. Beekman, L. Rademaker and J. van Wezel, "An Introduction to Spontaneous Symmetry Breaking," *SciPost Phys. Lect. Notes* **11** (2019), 1 doi:10.21468/SciPostPhysLectNotes.11
- [21] J. Goldstone, A. Salam and S. Weinberg, "Broken Symmetries," *Phys. Rev.* **127** (1962), 965-970 doi:10.1103/PhysRev.127.965
- [22] S. Sachdev, "Quantum Phase Transitions," Cambridge University Press, 2011,

- ISBN 978-0-511-97376-5 doi:10.1017/cbo9780511973765.
- [23] P. Pfeuty, "The one-dimensional Ising model with a transverse field," *Annals Phys.* **57** (1970) no.1, 79-90 doi:10.1016/0003-4916(70)90270-8
- [24] M. Greiner, O. Mandel, T. Esslinger, T. W. Hänsch and I. Bloch, "Quantum phase transition from a superfluid to a Mott insulator in a gas of ultracold atoms," *Nature* **415** (2002), 39-44 doi:10.1038/415039a
- [25] J. E. Hoffman, E. W. Hudson, K. M. Lang, V. Madhavan, H. Eisaki, S. Uchida and J. C. Seamus Davis, "A four unit cell periodic pattern of quasi-particle states surrounding vortex cores in $\text{Bi}_2\text{Sr}_2\text{CaCu}_2\text{O}_{8+d}$," *Science* **295** (2002), 466-469 doi:10.1126/science.1066974
- [26] P. W. Anderson, "Plasmons, Gauge Invariance, and Mass," *Phys. Rev.* **130** (1963), 439-442 doi:10.1103/PhysRev.130.439
- [27] P. W. Higgs, "Broken Symmetries and the Masses of Gauge Bosons," *Phys. Rev. Lett.* **13** (1964), 508-509 doi:10.1103/PhysRevLett.13.508
- [28] K. von Klitzing, G. Dorda and M. Pepper, "New method for high accuracy determination of the fine structure constant based on quantized Hall resistance," *Phys. Rev. Lett.* **45** (1980), 494-497 doi:10.1103/PhysRevLett.45.494
- [29] D. J. Thouless, M. Kohmoto, M. P. Nightingale and M. den Nijs, "Quantized Hall Conductance in a Two-Dimensional Periodic Potential," *Phys. Rev. Lett.* **49** (1982), 405-408 doi:10.1103/PhysRevLett.49.405
- [30] D. C. Tsui, H. L. Stormer and A. C. Gossard, "Two-dimensional magneto-transport in the extreme quantum limit," *Phys. Rev. Lett.* **48** (1982), 1559-1562 doi:10.1103/PhysRevLett.48.1559
- [31] R. B. Laughlin, "Anomalous quantum Hall effect: An Incompressible quantum fluid with fractionally charged excitations," *Phys. Rev. Lett.* **50** (1983), 1395 doi:10.1103/PhysRevLett.50.1395
- [32] D. Arovas, J. R. Schrieffer and F. Wilczek, "Fractional Statistics and the Quantum Hall Effect," *Phys. Rev. Lett.* **53** (1984), 722-723 doi:10.1103/PhysRevLett.53.722
- [33] B. I. Halperin, "Statistics of quasiparticles and the hierarchy of fractional quantized Hall states," *Phys. Rev. Lett.* **52** (1984), 1583-1586 [erratum: *Phys. Rev. Lett.* **52** (1984), 2390] doi:10.1103/PhysRevLett.52.1583

- [34] G. V. Dunne, "Aspects of Chern-Simons theory," Contribution to: Les Houches Summer School in Theoretical Physics, Session 69: Topological Aspects of Low-dimensional Systems, 7-31 July 1998. Les Houches, France [arXiv:hep-th/9902115 [hep-th]].
- [35] S. S. Chern and J. Simons, "Characteristic forms and geometric invariants," *Annals Math.* **99** (1974), 48-69 doi:10.2307/1971013
- [36] A. S. Schwarz, "The Partition Function of Degenerate Quadratic Functional and Ray-Singer Invariants," *Lett. Math. Phys.* **2** (1978), 247-252 doi:10.1007/BF00406412
- [37] E. Witten, "Quantum Field Theory and the Jones Polynomial," *Commun. Math. Phys.* **121** (1989), 351-399 doi:10.1007/BF01217730
- [38] E. H. Fradkin, "Field Theories of Condensed Matter Physics," *Front. Phys.* **82** (2013), 1-852 Cambridge Univ. Press, 2013, ISBN 978-0-521-76444-5, 978-1-107-30214-3.
- [39] S. C. Zhang, T. H. Hansson and S. Kivelson, "An effective field theory model for the fractional quantum hall effect," *Phys. Rev. Lett.* **62** (1988), 82-85 doi:10.1103/PhysRevLett.62.82
- [40] D. Tong, "Lectures on the Quantum Hall Effect," <http://www.damtp.cam.ac.uk/user/tong/qhe.html> [arXiv:1606.06687 [hep-th]].
- [41] X. G. Wen, "Vacuum Degeneracy of Chiral Spin States in Compactified Space," *Phys. Rev. B* **40** (1989), 7387-7390 doi:10.1103/PhysRevB.40.7387
- [42] X. G. Wen, "Topological Order in Rigid States," *Int. J. Mod. Phys. B* **4** (1990), 239 doi:10.1142/S0217979290000139
- [43] X. G. Wen, "Chiral Luttinger Liquid and the Edge Excitations in the Fractional Quantum Hall States," *Phys. Rev. B* **41** (1990), 12838-12844 doi:10.1103/PhysRevB.41.12838
- [44] X. G. Wen and Q. Niu, "Ground-state degeneracy of the FQH states in the presence of random potential and on high-genus Riemann surfaces," *Phys. Rev. B* **41**, 9377 (1990).
- [45] A. Y. Kitaev, "Fault tolerant quantum computation by anyons," *Annals Phys.* **303** (2003), 2-30 doi:10.1016/S0003-4916(02)00018-0

- [46] X. G. Wen, "Quantum orders and symmetric spin liquids," *Phys. Rev. B* **65** (2002), 165113 doi:10.1103/PhysRevB.65.165113
- [47] M. A. Levin and X. G. Wen, "String net condensation: A Physical mechanism for topological phases," *Phys. Rev. B* **71** (2005), 045110 doi:10.1103/PhysRevB.71.045110
- [48] M. A. Levin and X. G. Wen, "Colloquium: Photons and electrons as emergent phenomena," *Rev. Mod. Phys.* **77** (2005), 871-879 doi:10.1103/RevModPhys.77.871
- [49] F. Franchini, "An introduction to integrable techniques for one-dimensional quantum systems," *Lect. Notes Phys.* **940** (2017), pp. Springer, 2017, doi:10.1007/978-3-319-48487-7
- [50] S. M. Giampaolo, F. B. Ramos and F. Franchini, "The Frustration of being Odd: Universal Area Law violation in local systems," *J. Phys. Comm.* **3** (2019) no.8, 081001 doi:10.1088/2399-6528/ab3ab3
- [51] J. J. Dong, P. Li and Q. H. Chen, "The A-Cycle Problem for the Transverse Ising Ring," *J. Stat. Mech.* **2016** (2016) 113102
- [52] J. J. Dong and P. Li, "The A-Cycle Problem in XY Model with Ring Frustration," *Mod. Phys. Lett. B* **31** (2017) no. 06, 1750061
- [53] V. Marić, S. M. Giampaolo and F. Franchini, "Quantum Phase Transition induced by Topological Frustration," *Commun. Phys.* **3** (2020), 220 doi:10.1038/s42005-020-00486-z
- [54] M. Vojta, "Quantum phase transitions," *Rept. Prog. Phys.* **66** (2003), 2069–2110
- [55] L. Néel, "Propriétés magnétiques des ferrites; ferrimagnétisme," *Ann. Phys. (Paris)* **17** (1932), 5–105aa
- [56] G. Torre, J. Odavić, P. Fromholz, S. M. Giampaolo and F. Franchini, "Long-range entanglement and topological excitations," *SciPost Phys. Core* **7** (2024), 050 doi:10.21468/SciPostPhysCore.7.3.050
- [57] V. Marić, S. M. Giampaolo, D. Kuić and F. Franchini, "The frustration of being odd: how boundary conditions can destroy local order," *New J. Phys.* **22** (2020) no.8, 083024 doi:10.1088/1367-2630/aba064
- [58] V. Marić, S. M. Giampaolo and F. Franchini, "Fate of local order in topo-

- logically frustrated spin chains,” *Phys. Rev. B* **105** (2022) no.6, 064408 doi:10.1103/PhysRevB.105.064408
- [59] V. Marić, G. Torre, F. Franchini and S. M. Giampaolo, “Topological Frustration can modify the nature of a Quantum Phase Transition,” *SciPost Phys.* **12** (2022) no.2, 075 doi:10.21468/SciPostPhys.12.2.075
- [60] M. Pretko, “Subdimensional Particle Structure of Higher Rank U(1) Spin Liquids,” *Phys. Rev. B* **95**, no.11, 115139 (2017) doi:10.1103/PhysRevB.95.115139.
- [61] R. M. Nandkishore and M. Hermele, “Fractons,” *Ann. Rev. Condensed Matter Phys.* **10**, 295-313 (2019) doi:10.1146/annurev-conmatphys-031218-013604.
- [62] M. Pretko, X. Chen and Y. You, “Fracton Phases of Matter,” *Int. J. Mod. Phys. A* **35** (2020) no.06, 2030003 doi:10.1142/S0217751X20300033.
- [63] A. Gromov and L. Radzihovsky, “Colloquium: Fracton matter,” *Rev. Mod. Phys.* **96** (2024) no.1, 011001 doi:10.1103/RevModPhys.96.011001.
- [64] W. Shirley, K. Slagle and X. Chen, “Foliated fracton order from gauging subsystem symmetries,” *SciPost Phys.* **6** (2019) no.4, 041 doi:10.21468/SciPostPhys.6.4.041.
- [65] C. Chamon, “Quantum Glassiness in Strongly Correlated Clean Systems: An Example of Topological Overprotection”, *Phys. Rev. Lett.* **94** (2005) 040402 doi.org/10.1103/PhysRevLett.94.04040.
- [66] S. Vijay, J. Haah and L. Fu, “A New Kind of Topological Quantum Order: A Dimensional Hierarchy of Quasiparticles Built from Stationary Excitations,” *Phys. Rev. B* **92** (2015) no.23, 235136 doi:10.1103/PhysRevB.92.235136.
- [67] S. Vijay, J. Haah and L. Fu, “Fracton Topological Order, Generalized Lattice Gauge Theory and Duality,” *Phys. Rev. B* **94** (2016) no.23, 235157 doi:10.1103/PhysRevB.94.235157.
- [68] J. Haah, “Local stabilizer codes in three dimensions without string logical operators,” *Phys. Rev. A* **83** (2011) no.4, 042330 doi:10.1103/physreva.83.042330
- [69] A. Rasmussen, Y.-Z. You and C. Xu, “Stable Gapless Bose Liquid Phases without any Symmetry,” doi:10.48550/arXiv.1601.08235 [arXiv:1601.08235v1 [cond-mat.str-el]].
- [70] A. Blasi and N. Maggiore, “The theory of symmetric tensor field: from

- fractons to gravitons and back,” *Phys. Lett. B C* **833**, 137304 (2022) doi:10.1016/j.physletb.2022.137304.
- [71] E. Bertolini, A. Blasi, A. Damonte and N. Maggiore, “Gauging Fractons and Linearized Gravity,” *Symmetry* **15** (2023) no.4, 945 doi:10.3390/sym15040945.
- [72] D. Dalmazi and R. R. L. d. Santos, “The dimensional reduction of linearized spin-2 theories invariant under transverse diffeomorphisms,” *Eur. Phys. J. C* **81** (2021) no.6, 547 doi:10.1140/epjc/s10052-021-09297-0.
- [73] K. Hinterbichler, “Theoretical Aspects of Massive Gravity,” *Rev. Mod. Phys.* **84** (2012), 671-710 doi:10.1103/RevModPhys.84.671.
- [74] E. Bertolini and N. Maggiore, “Maxwell theory of fractons,” *Phys. Rev. D* **106**, no.12, 125008 (2022) doi:10.1103/PhysRevD.106.125008.
- [75] D. Birmingham, M. Blau, M. Rakowski and G. Thompson, “Topological field theory,” *Phys. Rept.* **209** (1991), 129-340 doi:10.1016/0370-1573(91)90117-5.
- [76] Y. You, T. Devakul, S. L. Sondhi and F. J. Burnell, “Fractonic Chern-Simons and BF theories,” *Phys. Rev. Res.* **2** (2020) no.2, 023249 doi:10.1103/PhysRevResearch.2.023249.
- [77] A. Prem, M. Pretko and R. Nandkishore, “Emergent Phases of Fractonic Matter,” *Phys. Rev. B* **97** (2018) no.8, 085116 doi:10.1103/PhysRevB.97.085116.
- [78] Y. You, F. J. Burnell and T. L. Hughes, “Multipolar Topological Field Theories: Bridging Higher Order Topological Insulators and Fractons,” *Phys. Rev. B* **103** (2021) no.24, 245128 doi:10.1103/PhysRevB.103.245128.
- [79] X. Huang, “A Chern-Simons theory for dipole symmetry,” *SciPost Phys.* **15**, no.4, 153 (2023) doi:10.21468/SciPostPhys.15.4.153.
- [80] H. T. Lam, J. H. Han and Y. You, “Topological dipole insulator,” *SciPost Phys.* **17**, no.5, 137 (2024) doi:10.21468/SciPostPhys.17.5.137.
- [81] W. Heisenberg, “Zur Theorie des Ferromagnetismus,” *Z. Phys.* **49** (1928) no.9-10, 619-636 doi:10.1007/BF01328601
- [82] H. Bethe, “On the theory of metals. 1. Eigenvalues and eigenfunctions for the linear atomic chain,” *Z. Phys.* **71** (1931), 205-226 doi:10.1007/BF01341708
- [83] T. Holstein and H. Primakoff, “Field dependence of the intrinsic do-

- main magnetization of a ferromagnet," *Phys. Rev.* **58** (1940), 1098-1113 doi:10.1103/PhysRev.58.1098
- [84] F. Bloch, "Zur Theorie des Ferromagnetismus," *Z. Phys.* **61** (1930), 206–219 doi:10.1007/BF01339661
- [85] P. W. Anderson, "An Approximate Quantum Theory of the Antiferromagnetic Ground State," *Phys. Rev.* **86** (1952) no.5, 694 doi:10.1103/PhysRev.86.694
- [86] F. D. M. Haldane, "Nonlinear field theory of large spin Heisenberg antiferromagnets. Semiclassically quantized solitons of the one-dimensional easy Axis Neel state," *Phys. Rev. Lett.* **50** (1983), 1153-1156 doi:10.1103/PhysRevLett.50.1153
- [87] F. D. M. Haldane, "Continuum dynamics of the 1-D Heisenberg antiferromagnetic identification with the O(3) nonlinear sigma model," *Phys. Lett. A* **93** (1983), 464-468 doi:10.1016/0375-9601(83)90631-X
- [88] E. H. Lieb, T. Schultz and D. Mattis, "Two soluble models of an antiferromagnetic chain," *Annals Phys.* **16** (1961), 407-466 doi:10.1016/0003-4916(61)90115-4
- [89] S. Katsura, "Statistical Mechanics of the Anisotropic Linear Heisenberg Model," *Phys. Rev.* **127** (1962), 1508–1518 doi:10.1103/PhysRev.127.1508
- [90] Th. Niemeijer, "Some Exact Calculations on a Chain of Spins 1/2," *Physica* **36** (1967), 377–419
- [91] Th. Niemeijer, "Some Exact Calculations on a Chain of Spins II," *Physica* **39** (1968), 313–326
- [92] P. Jordan and E. P. Wigner, "About the Pauli exclusion principle," *Z. Phys.* **47** (1928), 631-651 doi:10.1007/BF01331938
- [93] E. Barouch, B. M. McCoy and M. Dresden, "Statistical Mechanics of the XY Model. I," *Phys. Rev. A* **2** (1970) no.3, 1075 doi:10.1103/PhysRevA.2.1075
- [94] A. De Pasquale and P. Facchi, "XY model on the circle: diagonalization, spectrum, and forerunners of the quantum phase transition," *Phys. Rev. A* **80** (2009), 032102 doi:10.1103/PhysRevA.80.032102
- [95] N. D. Mermin and H. Wagner, "Absence of ferromagnetism or antiferromagnetism in one-dimensional or two-dimensional isotropic Heisenberg models," *Phys. Rev. Lett.* **17** (1966), 1133-1136 doi:10.1103/PhysRevLett.17.1133

- [96] I. Affleck, "Field Theory Methods and Quantum Critical Phenomena," Les Houches Summer School in Theoretical Physics: Fields, Strings, Critical Phenomena, Print-88-0765 (BRITISH COLUMBIA).
- [97] S. R. Coleman, "There are no Goldstone bosons in two-dimensions," *Commun. Math. Phys.* **31** (1973), 259-264 doi:10.1007/BF01646487
- [98] L. D. Landau and E. M. Lifshitz, "Statistical Physics, Part 1," Butterworth-Heinemann, 1980, ISBN 978-0-7506-3372-7
- [99] B. Damski and M. M. Rams, "Exact results for fidelity susceptibility of the quantum Ising model: The interplay between parity, system size, and magnetic field," *J. Phys. A* **47** (2014), 025303 doi:10.1088/1751-8113/47/2/025303
- [100] A. B. Zamolodchikov, "Irreversibility of the Flux of the Renormalization Group in a 2D Field Theory," *JETP Lett.* **43** (1986), 730-732
- [101] J. Polchinski, "Scale and Conformal Invariance in Quantum Field Theory," *Nucl. Phys. B* **303** (1988), 226-236 doi:10.1016/0550-3213(88)90179-4
- [102] H. W. J. Bloete, J. L. Cardy and M. P. Nightingale, "Conformal Invariance, the Central Charge, and Universal Finite Size Amplitudes at Criticality," *Phys. Rev. Lett.* **56** (1986), 742-745 doi:10.1103/PhysRevLett.56.742
- [103] I. Affleck, "Universal Term in the Free Energy at a Critical Point and the Conformal Anomaly," *Phys. Rev. Lett.* **56** (1986), 746-748 doi:10.1103/PhysRevLett.56.746
- [104] P. Calabrese and J. Cardy, "Entanglement entropy and conformal field theory," *J. Phys. A* **42** (2009), 504005 doi:10.1088/1751-8113/42/50/504005
- [105] J. Fuchs, I. Runkel and C. Schweigert, "TFT construction of RCFT correlators 1. Partition functions," *Nucl. Phys. B* **646** (2002), 353-497 doi:10.1016/S0550-3213(02)00744-7
- [106] E. Barouch and B. M. McCoy, "Statistical Mechanics of the XY Model. II. Spin-Correlation Functions," *Phys. Rev. A* **3** (1971) no.2, 786 doi:10.1103/PhysRevA.3.786
- [107] L. G. Molinari, "Notes on Wick's theorem in many-body theory," (2017) [arXiv:1710.09248 [math-ph]].
- [108] T. T. Wu, "Theory of Toeplitz Determinants and the Spin Correlations of the

- Two-Dimensional Ising Model. I," *Phys. Rev.* **149** (1966), 380–401
- [109] B. M. McCoy and T. T. Wu, "Theory of Toeplitz Determinants and the Spin Correlations of the Two-Dimensional Ising Model. II," *Phys. Rev.* **155** (1967), 438-452 doi:10.1103/PhysRev.155.438
- [110] H. Cheng and T. T. Wu, "Theory of Toeplitz Determinants and the Spin Correlations of the Two-Dimensional Ising Model. III," *Phys. Rev.* **164** (1967), 719-735 doi:10.1103/PhysRev.164.719
- [111] B. M. McCoy and T. T. Wu, "Theory of Toeplitz Determinants and the Spin Correlations of the Two-Dimensional Ising Model. IV," *Phys. Rev.* **162** (1967), 436–475
- [112] B. M. McCoy and T. T. Wu, "Theory of Toeplitz Determinants and the Spin Correlations of the Two-Dimensional Ising Model. V," *Phys. Rev.* **174** (1968), 546-559 doi:10.1103/PhysRev.174.546
- [113] V. Marić and F. Franchini, "Asymptotic behavior of Toeplitz determinants with a delta function singularity," *J. Phys. A* **54** (2020) no.2, 025201 doi:10.1088/1751-8121/abcd55
- [114] N. Shannon, T. Momoi and P. Sindzingre, "Nematic order in square lattice frustrated ferromagnets," *Phys. Rev. Lett.* **96** (2006), 027213 doi:10.1103/PhysRevLett.96.027213
- [115] S. M. Giampaolo and B. C. Hiesmayr, "Topological and nematic ordered phases in many-body cluster-Ising models," *Phys. Rev. A* **92** (2015), 012306 doi:10.1103/PhysRevA.92.012306
- [116] E. Witten, "Fermion Path Integrals And Topological Phases," *Rev. Mod. Phys.* **88** (2016) no.3, 035001 doi:10.1103/RevModPhys.88.035001
- [117] J. Vannimenus and G. Toulouse, "Theory of the frustration effect. II. Ising spins on a square lattice," *J. Phys. C* **10** (1977), L537–L542
- [118] C. Lacroix, P. Mendels and F. Mila (eds.), "Introduction to Frustrated Magnetism: Materials, Experiments, Theory," Springer Series in Solid-State Sciences, Vol. 164 (2011).
- [119] G. G. Cabrera and R. Jullien, "Universality of Finite-Size Scaling: Role of the Boundary Conditions," *Phys. Rev. Lett.* **57** (1986), 393–396

- [120] G. G. Cabrera and R. Jullien, "Role of boundary conditions in the finite-size Ising model," *Phys. Rev. B* **35** (1987), 7062–7072
- [121] M. N. Barber and M. E. Cates, "Effect of boundary conditions on the finite-size transverse Ising model," *Phys. Rev. B* **36** (1987), 2024–2029
- [122] M. Campostrini, A. Pelissetto and E. Vicari, "Quantum transitions driven by one-bond defects in quantum Ising rings," *Phys. Rev. E* **91** (2015), 042123
- [123] M. Campostrini, A. Pelissetto and E. Vicari, "Quantum Ising chains with boundary fields," *J. Stat. Mech.* **1511** (2015) no.11, P11015 doi:10.1088/1742-5468/2015/11/P11015
- [124] J. J. Dong, Z. Y. Zheng and P. Li, "Rigorous proof for the nonlocal correlation function in the transverse Ising model with ring frustration," *Phys. Rev. E* **97** (2018), 012133 doi:10.1103/PhysRevE.97.012133
- [125] G. Torre, V. Marić, D. Kuić, F. Franchini and S. M. Giampaolo, "Odd thermodynamic limit for the Loschmidt echo," *Phys. Rev. B* **105** (2022) no.18, 184424 doi:10.1103/PhysRevB.105.184424
- [126] G. Torre, V. Marić, F. Franchini and S. M. Giampaolo, "Effects of defects in the XY chain with frustrated boundary conditions," *Phys. Rev. B* **103** (2021) no.1, 014429 doi:10.1103/PhysRevB.103.014429
- [127] V. Marić, F. Franchini, D. Kuić and S. M. Giampaolo, "Resilience of the topological phases to frustration," *Sci. Rep.* **11** (2021) no.1, 6508 doi:10.1038/s41598-021-86009-4
- [128] A. G. Catalano, D. Brtan, F. Franchini and S. M. Giampaolo, "Simulating continuous symmetry models with discrete ones," *Phys. Rev. B* **106** (2022) no.12, 125145 doi:10.1103/PhysRevB.106.125145
- [129] J. Odavić, T. Haug, G. Torre, A. Hamma, F. Franchini and S. M. Giampaolo, "Complexity of frustration: A new source of non-local non-stabilizerness," *SciPost Phys.* **15** (2023) no.4, 131 doi:10.21468/SciPostPhys.15.4.131
- [130] R. Moessner, "Magnets with strong geometric frustration," *Can. J. Phys.* **79** (2001), 1283–1294 doi:10.1139/p01-113
- [131] V. Maric, "Topologically Frustrated Quantum Spin Chains,"

- [132] A. G. Catalano, C. Dağ, G. Torre, S. M. Giampaolo and F. Franchini, “Experimental preparation of W states through many-body physics on a quantum simulator,” [arXiv:2510.17974 [quant-ph]].
- [133] H. Tasaki, “Physics and Mathematics of Quantum Many-Body Systems,” 2020, doi:10.1007/978-3-030-41265-4
- [134] C. Wei, V. V. Mkhitarian and T. A. Sedrakyan, “Unveiling chiral states in the XXZ chain: finite-size scaling probing symmetry-enriched $c = 1$ conformal field theories,” JHEP **06** (2024), 125 doi:10.1007/JHEP06(2024)125
- [135] P. W. Anderson, “Ground state of a magnetic impurity in a metal,” Phys. Rev. **164** (1967), 352–359 doi:10.1103/PhysRev.164.352
- [136] P. W. Anderson, “Infrared Catastrophe in Fermi Gases with Local Scattering Potentials,” Phys. Rev. Lett. **18** (1967), 1049–1051 doi:10.1103/PhysRevLett.18.1049
- [137] H. Sevinçli, “Quartic dispersion, strong singularity, magnetic instability, and unique thermoelectric properties in two-dimensional hexagonal lattices of group-VA elements,” Nano Lett. **17** (2017), 2589–2595 doi:10.1021/acs.nanolett.7b00366
- [138] C. M. de Sterke, A. F. J. Runge, D. D. Hudson and A. Blanco-Redondo, “Pure-quartic solitons and their generalizations—Theory and experiments,” APL Photonics **6** (2021), 091101 doi:10.1063/5.0059525
- [139] H. Triki, A. Pan and Q. Zhou, “Pure-quartic solitons in presence of weak nonlocality,” Phys. Lett. A **459** (2023), 128608 doi:10.1016/j.physleta.2022.128608
- [140] M. Olshanii, S. Choi, V. Dunjko, A. E. Feiguin, H. Perrin, J. Ruhl and D. Aveline, “Three-dimensional Gross-Pitaevskii solitary waves in optical lattices: stabilization using the artificial quartic kinetic energy induced by lattice shaking,” Phys. Lett. A **380** (2016), 177–181 doi:10.1016/j.physleta.2015.10.042
- [141] M. Abramowitz and I. A. Stegun (eds.), “Handbook of Mathematical Functions with Formulas, Graphs, and Mathematical Tables,” ninth Dover printing, tenth GPO printing, Dover Publications, New York (1964).
- [142] S. Porta, F. M. Gambetta, N. Traverso Ziani, D. M. Kennes, M. Sasseti and F. Cavaliere, “Nonmonotonic response and light-cone freezing in fermionic systems under quantum quenches from gapless to gapped or partially gapped states,” Phys. Rev. B **97** (2018), 035433 doi:10.1103/PhysRevB.97.035433

- [143] E. S. Hewitt and R. E. Hewitt, “The Gibbs–Wilbraham phenomenon: An episode in Fourier analysis,” *Arch. Hist. Exact Sci.* **21** (1979), 129–160 doi:10.1007/BF00330404
- [144] D. Gottlieb and C. W. Shu, “On the Gibbs phenomenon and its resolution,” *SIAM Rev.* **39** (1997), 644–668 doi:10.1137/S0036144596301390
- [145] A. Zee, “Quantum Hall fluids,” *Lect. Notes Phys.* **456** (1995), 99–153 doi:10.1007/BFb0113369.
- [146] A. Blasi, A. Braggio, M. Carrega, D. Ferraro, N. Maggiore and N. Magnoli, “Non-Abelian BF theory for 2+1 dimensional topological states of matter,” *New J. Phys.* **14** (2012), 013060 doi:10.1088/1367-2630/14/1/013060.
- [147] M. Z. Hasan and C. L. Kane, “Topological Insulators,” *Rev. Mod. Phys.* **82** (2010), 3045 doi:10.1103/RevModPhys.82.3045.
- [148] G. Y. Cho and J. E. Moore, “Topological BF field theory description of topological insulators,” *Annals Phys.* **326** (2011), 1515–1535 doi:10.1016/j.aop.2010.12.011.
- [149] M. Pretko, “Generalized Electromagnetism of Subdimensional Particles: A Spin Liquid Story,” *Phys. Rev. B* **96** (2017) no.3, 035119 doi:10.1103/PhysRevB.96.035119.
- [150] N. Seiberg and S. H. Shao, “Exotic $U(1)$ Symmetries, Duality, and Fractons in 3+1-Dimensional Quantum Field Theory,” *SciPost Phys.* **9** (2020) no.4, 046 doi:10.21468/SciPostPhys.9.4.046.
- [151] N. Seiberg and S. H. Shao, “Exotic \mathbb{Z}_N symmetries, duality, and fractons in 3+1-dimensional quantum field theory,” *SciPost Phys.* **10** (2021) no.1, 003 doi:10.21468/SciPostPhys.10.1.003.
- [152] N. Seiberg and S. H. Shao, “Exotic Symmetries, Duality, and Fractons in 2+1-Dimensional Quantum Field Theory,” *SciPost Phys.* **10** (2021) no.2, 027 doi:10.21468/SciPostPhys.10.2.027.
- [153] M. Pretko and L. Radzihovsky, “Fracton-Elasticity Duality,” *Phys. Rev. Lett.* **120** (2018) no.19, 195301 doi:10.1103/PhysRevLett.120.195301.
- [154] A. Gromov, “Chiral Topological Elasticity and Fracton Order,” *Phys. Rev. Lett.* **122** (2019) no.7, 076403 doi:10.1103/PhysRevLett.122.076403.

- [155] A. Gromov, A. Lucas and R. M. Nandkishore, “Fracton hydrodynamics,” *Phys. Rev. Res.* **2** (2020) no.3, 033124 doi:10.1103/PhysRevResearch.2.033124.
- [156] D. Doshi and A. Gromov, “Vortices as fractons,” *Commun Phys* **4**, 44 (2021) doi:10.1038/s42005-021-00540-4.
- [157] K. T. Grosvenor, C. Hoyos, F. Peña-Benítez and P. Surówka, “Hydrodynamics of ideal fracton fluids,” *Phys. Rev. Res.* **3** (2021) no.4, 043186 doi:10.1103/PhysRevResearch.3.043186.
- [158] A. Głódkowski, F. Peña-Benítez and P. Surówka, “Hydrodynamics of dipole-conserving fluids,” *Phys. Rev. E* **107**, no.3, 034142 (2023) doi:10.1103/PhysRevE.107.034142.
- [159] M. Pretko, “Emergent gravity of fractons: Mach’s principle revisited,” *Phys. Rev. D* **96**, no.2, 024051 (2017) doi:10.1103/PhysRevD.96.024051.
- [160] E. Afxonidis, A. Caddeo, C. Hoyos and D. Musso, “Fracton gravity from spacetime dipole symmetry,” *Phys. Rev. D* **109** (2024) no.6, 065013 doi:10.1103/PhysRevD.109.065013
- [161] D. Bulmash and M. Barkeshli, “The Higgs Mechanism in Higher-Rank Symmetric $U(1)$ Gauge Theories,” *Phys. Rev. B* **97** (2018) no.23, 235112 doi:10.1103/PhysRevB.97.235112.
- [162] H. Ma, M. Hermele and X. Chen, “Fracton topological order from the Higgs and partial-confinement mechanisms of rank-two gauge theory,” *Phys. Rev. B* **98** (2018) no.3, 035111 doi:10.1103/PhysRevB.98.035111.
- [163] E. Bertolini, N. Maggiore and G. Palumbo, “Covariant fracton gauge theory with boundary,” *Phys. Rev. D* **108**, no.2, 025009 (2023) doi:10.1103/PhysRevD.108.025009..
- [164] A. Prem, J. Haah and R. Nandkishore, “Glassy quantum dynamics in translation invariant fracton models,” *Phys. Rev. B* **95** (2017) no.15, 155133 doi:10.1103/PhysRevB.95.155133
- [165] S. Bravyi, B. Leemhuis and B. M. Terhal, “Topological order in an exactly solvable 3D spin model,” *Annals Phys.* **326** (2011) no.4, 839-866 doi:10.1016/j.aop.2010.11.002
- [166] A. M. Polyakov, “Compact Gauge Fields and the Infrared Catastrophe,” *Phys.*

- Lett. B **59** (1975), 82-84 doi:10.1016/0370-2693(75)90162-8
- [167] M. Pretko, "Higher-Spin Witten Effect and Two-Dimensional Fracton Phases," Phys. Rev. B **96**, no.12, 125151 (2017) doi:10.1103/PhysRevB.96.125151.
- [168] S. Deser, R. Jackiw and S. Templeton, "Topologically Massive Gauge Theories," Annals Phys. **140**, 372-411 (1982) [erratum: Annals Phys. **185**, 406 (1988)] doi:10.1016/0003-4916(82)90164-6.
- [169] S. Deser, R. Jackiw and S. Templeton, "Three-Dimensional Massive Gauge Theories," Phys. Rev. Lett. **48**, 975-978 (1982) doi:10.1103/PhysRevLett.48.975.
- [170] D. Bailin and A. Love, "Introduction to Gauge Field Theory," Graduate Student Series in Physics, Institute of Physics Publishing, Bristol, UK (1986).
- [171] N. Nakanishi, "Covariant Quantization of the Electromagnetic Field in the Landau Gauge," Prog. Theor. Phys. **35** (1966), 1111-1116 doi:10.1143/PTP.35.1111.
- [172] B. Lautrup, "Canonical Quantum Electrodynamics In Covariant Gauges," Kong. Dan. Vid. Sel. Mat. Fys. Med. **35**, no. 11 (1967).
- [173] L. Alvarez-Gaume, J. M. F. Labastida and A. V. Ramallo, "A Note on Perturbative Chern-Simons Theory," Nucl. Phys. B **334**, 103-124 (1990) doi:10.1016/0550-3213(90)90658-Z.
- [174] P. Di Francesco, P. Mathieu and D. Senechal, "Conformal Field Theory," Springer-Verlag, 1997, ISBN 978-0-387-94785-3, 978-1-4612-7475-9 doi:10.1007/978-1-4612-2256-9
- [175] K. Slagle and Y. B. Kim, "Quantum Field Theory of X-Cube Fracton Topological Order and Robust Degeneracy from Geometry," Phys. Rev. B **96** (2017) no.19, 195139 doi:10.1103/PhysRevB.96.195139.
- [176] X. Ma, W. Shirley, M. Cheng, M. Levin, J. McGreevy and X. Chen, "Fractonic order in infinite-component Chern-Simons gauge theories," Phys. Rev. B **105** (2022) no.19, 195124 doi:10.1103/PhysRevB.105.195124.
- [177] X. Chen, H. T. Lam and X. Ma, "Ground State Degeneracy of Infinite-Component Chern-Simons-Maxwell Theories," [arXiv:2306.00291 [cond-mat.str-el]].
- [178] A. Gromov, "Towards classification of Fracton phases: the multipole algebra," Phys. Rev. X **9**, no.3, 031035 (2019) doi:10.1103/PhysRevX.9.031035.

- [179] Raab, Roger E., and Owen L. de Lange, "Multipole Theory in Electromagnetism: Classical, quantum, and symmetry aspects, with applications", International Series of Monographs on Physics (Oxford, 2004; online edn, Oxford Academic, 1 Sept. 2007), ISBN: 9780198567271 doi.org/10.1093/acprof:oso/9780198567271.001.0001
- [180] A. Blasi and R. Collina, "Finiteness of the Chern-Simons Model in Perturbation Theory," Nucl. Phys. B **345**, 472-492 (1990) doi:10.1016/0550-3213(90)90397-V.
- [181] F. Delduc, C. Lucchesi, O. Piguet and S. P. Sorella, "Exact Scale Invariance of the Chern-Simons Theory in the Landau Gauge," Nucl. Phys. B **346**, 313-328 (1990) doi:10.1016/0550-3213(90)90283-J.
- [182] E. Bertolini, A. Blasi and N. Maggiore, "Quasi-topological fractons: a 3D dipolar gauge theory," Eur. Phys. J. C **85**, no.1, 68 (2025) doi:10.1140/epjc/s10052-025-13821-x.
- [183] T. H. Hansson, V. Oganesyan and S. L. Sondhi, "Superconductors are topologically ordered," Annals Phys. **313** (2004) no.2, 497-538 doi:10.1016/j.aop.2004.05.006.
- [184] J. H. Han, "Dipolar background field theory and dipolar braiding statistics," Phys. Rev. B **109** (2024) no.23, 235127 doi:10.1103/PhysRevB.109.235127.
- [185] Y. T. Oh, J. Kim, E. G. Moon and J. H. Han, "Rank-2 toric code in two dimensions," Phys. Rev. B **105**, no.4, 045128 (2022) doi:10.1103/PhysRevB.105.045128.
- [186] Y. T. Oh, J. Kim and J. H. Han, "Effective field theory of dipolar braiding statistics in two dimensions," Phys. Rev. B **106**, no.15, 155150 (2022) doi:10.1103/PhysRevB.106.155150.
- [187] S. D. Pace and X. G. Wen, "Position-dependent excitations and UV/IR mixing in the ZN rank-2 toric code and its low-energy effective field theory," Phys. Rev. B **106** (2022) no.4, 045145 doi:10.1103/PhysRevB.106.045145.
- [188] Y. T. Oh, S. D. Pace, J. H. Han, Y. You and H. Y. Lee, "Aspects of ZN rank-2 gauge theory in (2+1) dimensions: Construction schemes, holonomies, and sublattice one-form symmetries," Phys. Rev. B **107** (2023) no.15, 155151 doi:10.1103/PhysRevB.107.155151.
- [189] H. Ebisu, M. Honda and T. Nakanishi, "Foliated field theories and multipole sym-

- metries," *Phys. Rev. B* **109** (2024) no.16, 165112 doi:10.1103/PhysRevB.109.165112.
- [190] T. Meng, "Coupled-wire constructions: a Luttinger liquid approach to topology," *Eur. Phys. J. ST* **229** (2020) no.4, 527-543 doi:10.1140/epjst/e2019-900095-5.
- [191] E. Bertolini, E. Lui and N. Maggiore, "Quasi-topological mass generation for 3D linearized gravity," *Phys. Rev. D* **112**, 044035 (2025) doi:10.1103/db71-jwd2
- [192] C. Itzykson and J. B. Zuber, "Quantum Field Theory," McGraw-Hill, 1980, ISBN 978-0-486-44568-7
- [193] S. M. Carroll, "Spacetime and Geometry: An Introduction to General Relativity," Cambridge University Press, 2019, ISBN 978-0-8053-8732-2, 978-1-108-48839-6, 978-1-108-77555-7 doi:10.1017/9781108770385
- [194] P. Sikivie, "Experimental Tests of the Invisible Axion," *Phys. Rev. Lett.* **51** (1983), 1415-1417 [erratum: *Phys. Rev. Lett.* **52** (1984), 695] doi:10.1103/PhysRevLett.51.1415.
- [195] F. Wilczek, "Two Applications of Axion Electrodynamics," *Phys. Rev. Lett.* **58** (1987), 1799 doi:10.1103/PhysRevLett.58.1799.
- [196] G. Rosenberg and M. Franz, "Witten effect in a crystalline topological insulator," *Phys. Rev. B* **82** (2010), 035105 doi:10.1103/PhysRevB.82.035105.
- [197] A. Chatzistavrakidis, G. Karagiannis and P. Schupp, "Torsion-induced gravitational θ term and gravitoelectromagnetism," *Eur. Phys. J. C* **80** (2020) no.11, 1034 doi:10.1140/epjc/s10052-020-08600-9.
- [198] A. G. Catalano, S. M. Giampaolo, O. Morsch, V. Giovannetti and F. Franchini, "Frustrating Quantum Batteries," *PRX Quantum* **5** (2024) no.3, 030319 doi:10.1103/PRXQuantum.5.030319
- [199] A. Amoretti, A. Braggio, G. Caruso, N. Maggiore and N. Magnoli, "Introduction of a boundary in topological field theories," *Phys. Rev. D* **90** (2014) no.12, 125006 doi:10.1103/PhysRevD.90.125006.
- [200] N. Maggiore, "Holographic reduction of Maxwell-Chern-Simons theory," *Eur. Phys. J. Plus* **133** (2018) no.7, 281 doi:10.1140/epjp/i2018-12130-y.
- [201] N. Maggiore, "From Chern-Simons to Tomonaga-Luttinger," *Int. J. Mod. Phys. A* **33** (2018) no.02, 1850013 doi:10.1142/S0217751X18500136.

- [202] E. Bertolini, G. Gambuti and N. Maggiore, “Notes from the bulk: Metric dependence of the edge states of Chern-Simons theory,” *Phys. Rev. D* **104**, no.10, 105011 (2021) doi:10.1103/PhysRevD.104.105011
- [203] E. Bertolini, F. Fecit and N. Maggiore, “Topological BF Description of 2D Accelerated Chiral Edge Modes,” *Symmetry* **14** (2022) no.4, 675 doi:10.3390/sym14040675.
- [204] K. Slagle, “Foliated Quantum Field Theory of Fracton Order,” *Phys. Rev. Lett.* **126** (2021) no.10, 101603 doi:10.1103/PhysRevLett.126.101603.
- [205] A. Amoretti, A. Braggio, G. Caruso, N. Maggiore and N. Magnoli, “3+1D Massless Weyl spinors from bosonic scalar-tensor duality,” *Adv. High Energy Phys.* **2014**, 635286 (2014) doi:10.1155/2014/635286
- [206] A. Blasi and N. Maggiore, “Massive gravity and Fierz-Pauli theory,” *Eur. Phys. J. C* **77**, no.9, 614 (2017) doi:10.1140/epjc/s10052-017-5205-y
- [207] A. Blasi and N. Maggiore, “Massive deformations of rank-2 symmetric tensor theory (a.k.a. BRS characterization of Fierz–Pauli massive gravity),” *Class. Quant. Grav.* **34**, no.1, 015005 (2017) doi:10.1088/1361-6382/34/1/015005
- [208] G. Gambuti and N. Maggiore, “Fierz–Pauli theory reloaded: from a theory of a symmetric tensor field to linearized massive gravity,” *Eur. Phys. J. C* **81**, no.2, 171 (2021) doi:10.1140/epjc/s10052-021-08962-8
- [209] G. Gambuti and N. Maggiore, “A note on harmonic gauge(s) in massive gravity,” *Phys. Lett. B* **807**, 135530 (2020) doi:10.1016/j.physletb.2020.135530
- [210] C. Turner, “Dualities in 2+1 Dimensions,” *PoS Modave2018*, 001 (2019) doi:10.22323/1.349.0001.
- [211] S. Weinberg, “The Quantum theory of fields. Vol. 1: Foundations,” Cambridge University Press, 2005, ISBN 978-0-521-67053-1, 978-0-511-25204-4 doi:10.1017/CBO9781139644167
- [212] C. W. Misner, K. S. Thorne and J. A. Wheeler, “Gravitation,” W. H. Freeman, 1973, ISBN 978-0-7167-0344-0, 978-0-691-17779-3.
- [213] D. Tong, “Lectures on General Relativity,” <http://www.damtp.cam.ac.uk/user/tong/gr.html>.

- [214] S.R. de Groot and L.G. Suttorp, "The relativistic energy-moment tensor in polarized media: VI. The difference between the energy-moment tensors in the presence and in the absence of external fields" *Physica* **39**, 1 (1968), 77-83 doi:10.1016/0031-8914(68)90048-7.
- [215] R. Medina and J. Stephany, "The energy-moment tensor of electromagnetic fields in matter," [arXiv:1703.02109 [physics.class-ph]].
- [216] I. H. Brevik, I. H. Brevik, M. M. Chaichian and M. M. Chaichian, "Axion electrodynamics: Energy-moment tensor and possibilities for experimental tests," *Int. J. Mod. Phys. A* **37** (2022) no.24, 2250151 [erratum: *Int. J. Mod. Phys. A* **37** (2022) no.36, 2250151] doi:10.1142/S0217751X22501512.
- [217] A. Sekine and K. Nomura, "Axion Electrodynamics in Topological Materials," *J. Appl. Phys.* **129** (2021) no.14, 141101 doi:10.1063/5.0038804.

List of figures

1.1.	Ground state configurations of the classical antiferromagnetic Ising chain with periodic boundary conditions. For even N , the ground state is doubly degenerate and spanned by the two Néel state (a). For odd N case, the ground state is $2N$ -fold degenerate and spanned by the kink states (b), characterized by the presence of two nearest-neighbour spin which are ferromagnetically aligned.	10
1.2.	Subdimensional quasiparticles. Figure taken from [64].	11
2.1.	Plot of the dispersion relation $\epsilon(q)$ as a function of $q \in [-\pi, \pi]$ for $h = 1.5$ and different values of the anisotropy parameter: $\gamma = 0$ (blue), $\gamma = 0.5$ (orange), $\gamma = 1$ (green), $\gamma = 1.5$ (red) and $\gamma = 2$ (purple). . . .	39
2.2.	Curves (in blue) where $E_0^+ = E_0^-$, <i>i.e.</i> where $ GS^\pm\rangle$ are degenerate, for different values of the chain length: $N = 8$ (a), $N = 9$ (b), $N = 10$ (c) and $N = 11$ (d).	40
2.3.	Plot of the dispersion relation $\epsilon(q)$ as a function of $q \in [-\pi, \pi]$ for $h = 0.5$ and different values of the anisotropy parameter: $\gamma = 0$ (blue), $\gamma = 0.5$ (orange), $\gamma = 1$ (green), $\gamma = 1.5$ (red) and $\gamma = 2$ (purple). . . .	44
2.4.	Plot of the dispersion relation $\epsilon(q)$ as a function of $q \in [-\pi, \pi]$ for $h = 1$ and different values of the anisotropy parameter: $\gamma = 0$ (blue), $\gamma = 0.5$ (orange), $\gamma = 1$ (green), $\gamma = 1.5$ (red) and $\gamma = 2$ (purple).	45

- 2.5. Phase diagram of the ferromagnetic XY chain with PBC in the region $h, \gamma \geq 0$. Red lines indicate the quantum critical lines ($h = 1$ and $\gamma = 0$ for $0 \leq h \leq 1$), where the system undergoes second-order quantum phase transitions. The dashed green line corresponds to the transverse-field Ising chain ($\gamma = 1$), while the dashed blue curve denotes the circle $h^2 + \gamma^2 = 1$, along which the ground state is exactly doubly degenerate even at finite size. 46
- 3.1. Plot of the dispersion relation $\epsilon(q)$ as a function of $q \in [-\pi, \pi]$ for $h = 0.5$ and different values of γ : $\gamma = 0$ (black), $\gamma = 0.25$ (blue), $\gamma = 0.5$ (green), $\gamma = \gamma^*(0.5) = \sqrt{2}/2$ (red) and $\gamma = 0.75$ (orange). 60
- 3.2. Plot of $\frac{\partial \Delta E}{\partial \gamma}$ as a function of γ for different values of h : $h = 0.25$ (black), $h = 0.5$ (blue) and $h = 0.75$ (red). 64
- 3.3. Plot of $\frac{\partial^2 E(h, \gamma; N)}{\partial \gamma^2}$ as a function of $\gamma/\gamma^*(h)$ for three different values of $\delta\gamma$: $\delta\gamma = 0.25\delta k$ (black), $\delta\gamma = 0.5\delta k$ (green dashed), $\delta\gamma = 0.75\delta k$ (red dotted). Here, $h = 0.1$ and $N = 50001$ 66
- 3.4. Plot of $\frac{\partial^2 E(h, \gamma; N)}{\partial \gamma^2}$ as a function of $\gamma/\gamma^*(h)$ for different values of h : $h = 0.1$ (black), $h = 0.3$ (blue), $h = 0.5$ (red). The top left inset shows a zoom centered about the abrupt jump. Here $N = 10001$ and note that the curves have been offset in order to vertically align the center of the jump region. 67
- 3.5. Panel (a): Plot of $\Delta\gamma/\sqrt{1-h}$ (green dots) and of the function $2\pi/N$ (red line) as a function of N . Panel (b): plot of $\Delta\frac{\partial^2 E}{\partial \gamma^2}\Big|_{\gamma^*(h)}$ (green dots) and of the fitting function $c_1 + c_2 N$ as a function of N . Here, $h = 0.1$ and the fitting parameters have been found to be $c_1 \approx 39.97$ and $c_2 \approx 6.79 \cdot 10^{-11}$. 68
- 3.6. Plots of $\frac{\partial^2 E(h, \gamma; N)}{\partial \gamma^2}$ as a function of $\gamma/\gamma^*(h)$ (black solid line) and of the extrapolating functions $\varphi_-(\gamma)$ (red dashed line) and $\varphi_+(\gamma)$ (blue dashed line). Here, $h = 0.1$ and $N = 10001$ 69
- 3.7. Plots of the numerically evaluated gap $\Delta\frac{\partial^2 E}{\partial \gamma^2}\Big|_{\gamma^*(h)}$ (defined by Eq. (3.44)) as a function of h (green dots) and of the analytical result $4/h$. Here, $N = 100001$ 70

- 3.8. Zero temperature phase diagram of the frustrated XY chain in the thermodynamic limit. The blue (red) bold lines represent the first (second) order boundary QPT induced by the imposition of FBC. The empty circle at (1,0) stands for the absence of boundary quantum phase transitions and the filled circle at (0,1) indicates the presence of a first order boundary quantum phase transition. 71
- 4.1. Operators appearing in the X-cube Hamiltonian (4.1). Figure taken from [164]. 75
- 4.2. When a membrane operator $\hat{\mathcal{M}}$, built as a product of σ_i^z operators (red lines), acts on the ground state, it creates four fractons (blue cubes). The notation $\mathbf{e}^{(0)}$ indicates that each excitation is a 0-dimensional object. Figure taken from [164]. 77
- 4.3. A fracton (blue cube) can be moved, but doing so necessarily creates two additional excitations, each carrying a finite energy cost. The red line represents a z-Pauli operator. Figure taken from [164]. 77
- 4.4. A pair of adjacent fractons (blue cubes) can be moved freely by applying strings of z-Pauli operators (red lines) whose links lie in the plane containing the intersection of the two cube excitations. The notation $\mathbf{e}^{(2)}$ reminds us that such an object is able to move only within a 2-dimensional manifold (a plane) without creating additional excitations. Figure taken from [164]. 78
- 4.5. Dictionary of the fracton-elasticity duality. Figure taken from [153]. . . 104

List of tables

3.1. Classification of b-QPT by order and dispersion relation in the XY quantum spin chain with FBC.	71
--	----